To the Graduate Council:

I am submitting herewith a dissertation written by David Kent Hylbert entitled "Development of Geological Structural Criteria for Predicting Unstable Mine Roof Rocks." I recommend that it be accepted in partial fulfillment of the requirements for the degree of Doctor of Philosophy, with a major in Geology.

Otto C. Kopp

Otto C. Kopp, Major Professor

We have read this dissertation
and recommend its acceptance:

Russell J. Lewis

Samuel Biggs

Harry J. Kleper

Accepted for the Council:

Hilton A. Smith

Vice Chancellor
Graduate Studies and Research

Thesis
76b
.H955
cop. 2

DEVELOPMENT OF GEOLOGICAL STRUCTURAL CRITERIA FOR PREDICTING UNSTABLE MINE ROOF ROCKS

A Dissertation

Presented for the

Doctor of Philosophy

Degree

The University of Tennessee, Knoxville

David Kent Hylbert

December 1976

1303793

ACKNOWLEDGEMENTS

Research on coal mine roof falls was completed with the help and cooperation of many individuals. The writer is especially indebted to Mr. Norman Yarborough, President of the Eastover Mining Company and his staff for permission and assistance in conducting research in the Bailey Creek and Highsplint mines. Special thanks are also directed to Mr. Cloyd McDowell and Mr. Bernard Holcolm of the Harlan County Coal Operators' Association for information and assistance throughout the project.

The members of the dissertation committee, Dr. Otto C. Kopp, Chairman, Dr. Harry J. Klepser, Dr. Garrett Briggs and Dr. Russell Lewis are thanked for their assistance and suggestions.

Financial assistance for the study was provided through Contract HO133018 with the United States Bureau of Mines. The Bureau of Research and Development and Appalachian Coal Mine Research Institute at Morehead State University also assisted in the study.

The writer is also indebted to his two field assistants, Mr. Brian Grothaus and Mr. Thomas McLoughlin, students in the Geoscience Department at Morehead State University, to Mr. Allan Lake for assistance with photographs, and to Dr. David Muse of the Morehead State University Mathematics Department for assisting with statistical analysis and computer programming.

Acknowledgement is made for the use of x-ray laboratory facilities at Eastern Kentucky University and the University of Kentucky.

Finally, the writer expresses appreciation to his wife, Shirley, for her assistance and encouragement in the completion of this dissertation.

ABSTRACT

This study was designed to investigate the cause of roof falls in room-and-pillar coal mines and to determine geologic methods for predicting unstable roof conditions. The study area was located in Harlan County, Kentucky and the Bailey Creek and Highsplint mines were selected for study. The Bailey Creek mine operates in the Harlan coal bed and the Highsplint mine operates in the Darby coal bed, about 200 feet higher stratigraphically. Both coal beds are in the Mingo Formation of the Breathitt Group of Pennsylvanian age, deposited in a fluvio-deltaic environment.

The mines are drift mines and correlations were made laterally between surface outcrops and within the mines using lithologic and trend analysis criteria as follows:

1. Lithologic criteria involved comparing changes in roof strata. Outcrop studies showed that the strata are cyclic or repetitious vertically. Five vertical sequences were recognized and correlations made with roof falls. Results indicated that roof falls are associated with zones of weakness within or between vertical cycles. These zones include rider coal seams, carbonized plant debris on bedding planes, thin-bedded brittle rocks, cross-bedding and zones of poor sandstone cementation. Abrupt lateral facies changes occur. In-mine studies were also conducted. In the Highsplint mine, 91 measured rib and coal sections provided the basis for a roof classification in four categories or conditions: Conditions A and B (Laminated Shale), Condition C

(Rolling Sandstone with Shale in Pockets) and Condition D (Zone of Major Sandstone Roll(s)). A structure contour map of the Darby coal bed, and isopach maps of the Darby coal bed and immediate roof rocks were used to project axial trends of the sandstone roof.

2. Trend analysis studies were conducted to investigate cross-bedding, channel trough axes and sole marks. Computer programs were used to analyze the data, and a comparison between surface trough axes and sandstone roll axes means within the Highsplint mine indicated a discrepancy of about 35°. Computer programs were used to analyze jointing, coal cleat, and "slips" (slickensides). The program groups into 4- or 6-sets. The mean directions of the four joint sets for the area are: Set I - N65°E to N75°E, Set II - N27°W to N15°W, Set III - N25°E to N32°E and Set IV - N65°W to N58°W. Surface joints were compared with surface drainage segments and with joints, "slips," and sandstone rolls inside the mines. A direct relationship between joint and "slip" frequency and direction with sandstone roll trends was found. Correlations between surface joints and joint-controlled roof falls underground were not found in areas of the mines under overburden in excess of 600 feet.

Studies were made of samples obtained from ten NX cores taken from the roof in the Highsplint mine, on both sides of a roof-fall zone, to investigate trends. Petrographic methods were used to evaluate composition and texture for 27 thin-sections of the sandstone roof. Correlation between cores showed that the roof-fall zone represented a marginal position between sand-filled channels. Twelve shale and

siltstone core samples from the immediate roof were studied using x-ray diffraction. The dominant clay minerals include illite, chlorite and kaolinite. Sharpness ratios (10A illite peak), and the chlorite 14A peak height were compared between cores.

Studies at the Bailey Creek mine indicated that roof falls involving the main roof were related to cross-bedding in a sandstone channel. Failure was caused by the heading direction being driven subparallel to the channel direction and to the strike of cross-bedded sandstones filling the channel. Monitoring of the mine from April, 1976 to September, 1976 indicated improved conditions when the heading direction was changed to avoid both the channel direction and frequent joint directions.

TABLE OF CONTENTS

SECTION		PAGE
I.	INTRODUCTION	1
	General Discussion	1
	Scope of Work	2
	Selection of Study Area	3
	Location of Study Area	5
	Regional Structure	8
	Stratigraphy	10
	Topography	16
	The Eastern Kentucky Coal Field	18
	The Upper Cumberland River Coal District	18
II.	STRATIGRAPHIC RELATIONSHIPS OF THE MINGO FORMATION	23
	Objectives	23
	Physical Features	23
	Lithologies	25
	Shales	25
	Underclays	26
	Sandstones	26
	Sandstone Bedding	28
	Sandstone Cross-Bedding	28
	Large-Scale Trough Cross-Bedding	31
	Large-Scale Tabular Cross-Bedding	31
	Small-Scale Trough Cross-Bedding	35

SECTION PAGE

Longitudinal Cross-Bedding 35
Climbing-Ripple Lamination 35
Horizontal Bedding 37
Parallel Lamination 37
Graded Bedding 40
Representative Sedimentation Units 40
Conclusions and Recommendations 50
Lateral Changes in Lithology 50
III. ROOF COMPOSITION AND TREND ANALYSIS - HIGHSPLINT MINE . . 54
Roof Classification 54
Roof Condition A (Laminated Shale) 54
Roof Condition B (Laminated Shale) 57
Roof Condition C (Rolling Sandstone with Shale in Pockets) 57
Roof Condition D [Zone of Major Sandstone Roll(s)] . . . 62
Roof Composition Map 65
Structure Contour Map 67
Isopach Map-Darby Coal Bed and Claystone/Coal Rash . . 69
Immediate Roof Isopach Map 72
Sandstone Trough - Axis Projection Map 74
Relationship of Roof Type and Thickness to Roof Falls 76
Conclusions 80
IV. THE BAILEY CREEK MINE 82

SECTION PAGE

General Relationships 82
Investigations in the Mine 82
Joint Observations 85
Mine Progress and Recommendations 91
Geologic Conditions and Roof Control 92
Comparison - Bailey Creek and Highsplint Mines . . . 94
V. PALEOGEOGRAPHY AND ENVIRONMENT OF DEPOSITION 97
Source Area and Sediment Transport Direction 97
Possible Environmental Models 103
Floodbasin Environment 103
Interdistributary Bay Environment 108
VI. CROSS-BEDDING AND PALEOCURRENT STUDIES 112
Objectives 112
Field Procedure 115
Analysis of Cross-Bedding Data 116
Paleocurrent Analysis - Computer Program 116
Geologic Evaluation of Cross-Bedding 124
Method of Analysis 127
Application of Method 127
Cross-Bed Analysis - Conclusions 130
VII. JOINTS AND COAL CLEAT 135
Joints in the Study Area 135
Previous Studies in the Area 139

SECTION PAGE

Initial Analysis of Surface Rock Joints 140
Computer Analysis of Joints 143
Unimodal and Bimodal Programs 144
Strain Model Program 144
Independent Mean Program 152
Simulated Data Program 153
Drainage Analysis 158
Comparison of 4-Set and 6-Set Joints 158
Regional Joint Map 162
Comparison of Surface and Subsurface Joints 165
Conclusions and Recommendations 168
VIII. CORE DRILLING AND CORE ANALYSIS - 004 SECTION, HIGHSPLINT MINE 170
Correlation of Core Sections 175
Correlation of Sandstone Cores 177
Interpretation of Correlations 185
Petrography 188
Composition 188
Framework Grains 188
Matrix 194
Heavy Minerals 194
Sandstone Classification 194
Thin-Section Textural Studies 196
Procedures Used 197

SECTION PAGE

Difficulties 198
Statistical Measures Used 198
Application of Textural Studies to 004 Section 203
Clay Mineralogy 205
Purpose and Scope 205
X-ray Studies 205
Identification Procedures 207
Illite 207
Kaolinite 210
Chlorite 210
Clay Mineral Index Studies 212
Indexes Used 212
Analysis of Sharpness Ratio Values 214
Texture Comparisons 217
Possible Causes of Observed Clay Mineral Trends . . 219
Evidence for Detrital Mica 221
Evidence for Diagenetic Changes 223
Chlorite Peak Heights 225
Conclusions 226
IX. SUMMARY AND CONCLUSIONS 227
Summary of Findings 227
Recommendations for Future Studies 230

SECTION PAGE

SELECTED REFERENCES 232

APPENDIXES 240

Appendix A 241
Appendix B 242
Appendix C 247
Appendix D 250

VITA 267

LIST OF TABLES

TABLE		PAGE
1.	Categories of Roof-Fall Studies	6
2.	Pennsylvanian Correlations - Kentucky and Virginia	12
3.	Correlation of Coal Beds - Hazard, Southwestern and Upper Cumberland Reserve Districts	21
4.	Analysis of the Darby and Harlan Coal Beds, Harlan Subdistrict	22
5.	Cross-Bedding Analysis - Unimodal Program	120
6.	Trough Axes Analysis - Unimodal Program	120
7.	Cross-Bedding Frequency Distributions by Locality	122
8.	Cross-Bedding Frequency Distributions (Totals)	123
9.	Sole Marks - Surface Outcrops	133
10.	Parting Lineation - Surface Outcrops	133
11.	Total Variances Associated with Strain Program	150
12.	Regional Surface Joints - Comparison of Strain and Independent Mean Programs - 6-Set Model	154
13.	Regional Surface Joints - Comparison of Strain and Independent Mean Programs - 4-Set Model	155
14.	Total Surface Joints	156
15.	Simulated Joint Data	156
16.	Mineral Composition in Volume Percent of Sandstone Thin-Sections	189
17.	Thin-Section Point-Counting Data	200
18.	Comparison of Sample U-2-2 Diffraction Data with Analyzed Samples of Illite, Chlorite and Kaolinite	208

TABLE PAGE

19. Shale/Siltstone Scale of Texture 213

20. Major Element Analyses by Atomic Absorption 218

21. Summary of Illite Sharpness Ratios and Chlorite Peak Heights Compared with Rock Texture 220

22. Summary of Elemental Abundances Compared with Rock Texture 220

23. Sharpness Ratio Determinations from <2μm Elutriated Samples (Not Heat Treated) 222

24. Sharpness Ratio Determinations from <2μm Elutriated Samples (Heat Treated to 600°C for 1 Hour) 222

B1. English-metric Length Conversion 242

B2. Comparison of Quantitative Terms for Layered Rocks 242

B3. Measured Rib Sections - Highsplint Mine 243

B4. Underground Mapping - Checklist 245

LIST OF FIGURES

FIGURE		PAGE
1.	Detail of Immediate Roof Overlying the Darby Coal in the Highsplint Mine	4
2.	Map of Study Area Showing Location of Bailey Creek Mine and Highsplint Mine	7
3.	Geology and Structure of the Cumberland Overthrust Block After Harris	9
4.	The Mingo Formation Showing the Stratigraphic Position of Harlan and Darby Coal Beds and Lithologic Description of Associated Strata	13
5.	General Stratigraphy at the Highsplint and Bailey Creek Mines	14
6.	Entrance of Bailey Creek Mine	15
7.	Terrain Drawing of Harlan County, Kentucky and Outline of Study Area	17
8.	Kentucky Coal Fields and Reserve District	19
9.	Brookside Stratigraphic Section	24
10.	Close-Up of Siderite and Shale Clasts Interbedded in Sandstone Immediately Overlying the Darby Coal Bed at Highsplint	27
11.	Block Diagrams of Tabular and Trough Cross-Bedding Together with Reference System and Nomenclature of Cross-Bedded Units	29
12.	Large-Scale Trough Cross-Bedding in Lower Part of Cycle 12, Brookside Section	32
13.	"Fining-Upward" Sequence in Unit 6, Brookside Section	33
14.	Trough Cross-Stratification Exposed on Darby Strip Bench	34
15.	Longitudinal Cross-Bedding Exposed on Base of Sandstone Roll, New 004 Section, Highsplint Mine	36
16.	Horizontal Bedding Exposed on Darby Strip Bench, Highsplint Mine	38

17. View of Roof-Fall Zone in the Old 004 Section, Highsplint Mine 39

18. Representative Sedimentation Unit - Section A 41

19. Representative Sedimentation Unit - Section B 42

20. Representative Sedimentation Unit - Section C 43

21. Representative Sedimentation Unit - Section D 44

22. Representative Sedimentation Unit - Section E 45

23. "Fining-Upward" Sequence in Bailey Creek Mine Characteristic of Channel-Fill Sandstones 48

24. Stratigraphic Sequence Immediately Above the Darby Coal Seam at the Bailey Creek Mine 49

25. Kettlebottom in Roof in Bailey Creek Mine 51

26. Photographic Mosaic of Rolling Sandstone 52

27. "Slip" Expressed as Small Reverse Fault in Immediate Roof Shale 55

28. Roof Condition A 56

29. Roof Condition B 58

30. Roof Condition C 59

31. View of Rolling Sandstone Roof in the Old 004 Section, Highsplint Mine 60

32. View of Roof-Fall Zone in the Old 004 Section, Highsplint Mine 61

33. Roof Condition D 63

34. Erosional Contact Between Laminated Immediate Roof Shale and Overlying Sandstone Roll Indicated by Abrupt Truncation of Horizontal Shale 64

35. Roof Composition Map, Highsplint Mine 66

36. Structure Contour Map Drawn on the Base of the Darby Coal Bed, Highsplint Mine 68

37. Isopach Map of Darby Coal Bed, Highsplint Mine 70

38. Isopach Map of Claystone/Coal Rash, Highsplint Mine 71

39. Isopach Map of Immediate Roof Rocks in the Highsplint Mine 73

40. Sandstone Axis Projection Map 75

41. Profile of 003 Section, Highsplint Mine 77

42. Photographic Mosaic of Shale "Horseback" 79

43. Bailey Creek Mine Map Showing Probable Position of Sand-Filled Channels and Projected 4-set Joint Means 83

44. Well Defined Erosional Contact Between Roof Rocks and Channel in the Bailey Creek Mine 84

45. Dipping Roof Rocks in the Bailey Creek Mine 86

46. Sandstone Body Between Harlan Coal Bed and Rider Seam at Brookside, Kentucky 87

47. Four-mode Independent Mean Program Circular Histograms of Surface Joints and Underground Joints at Bailey Creek Mine 88

48. View of Weathered Joint Surface in Roof-Fall Area Four Breaks Inside the Bailey Creek Mine 89

49. Traces of Weathered Joints in Roof-Fall Area Four Breaks Inside the Bailey Creek Mine 90

50. General View of Roof-Fall Area in the Left 001 Section, Bailey Creek Mine 93

51. Tectonic Setting of Kentucky and Adjacent States During the Carboniferous 98

52. Map of Kentucky and Surrounding States Showing Axial Trends of the Dunkard, Pocahontas and Warrior Basins 99

53. Photographic Mosaic of Symmetrical Shale-Filled Trough . . . 102

54. Current Crescent on Base of Sandstone Roof Roll in New 004 Section, Highsplint Mine 104

55. Current Scour and Tool Marks Preserved on Base of Sandstone Roof in the Highsplint Darby Mine 105

56. Radiographs of Core Sections Showing Sandstone with Included Coal Lenses in A and Graded Bedding in Lag in B and C 106

57. Crevasse Splays Deposited During Flood in Floodbasin of the Brahmaputra River 107

58. Interdistributary Bay Model as Proposed by Elliott 109

59. Field Localities for Cross-Bed Data 114

60. Circular Histograms for Cross-Bedding by Locality 117

61. Main Types of Azimuthal Roses 126

62. Possible Misleading Cross-Bed Distributions A Through D . . . 126

63. Cross-Bedding Histograms by Locality 132

64. Field Localities for Rock Jointing Data 136

65. Entrance to Highsplint Mine 138

66. A. Joint Grouping by Sets with 90° Separation. B. Underground Coal Cleat. C. Total Surface Joints and D. Total Underground Joints 141

67. Circular Diagram of Systematic and Nonsystematic Joint Groupings 142

68. Idealized Geometric Relationships Between the Principal Stresses and Fractures 145

69. Orientation of the Strain Ellipsoid to the Middlesboro Syncline 147

70. Computer Program Models 148

71. Simulated Data Analysis by Independent Mean Program 157

72. Clover Fork Drainage System and Regions A, B and C For Computer Analysis 159

73. Four-Mode Independent Mean Program Circular Histograms For Drainage Regions A, B and C 160

74. Four-Mode Independent Mean Program Circular Histograms of A. Total Harlan Surface Joints B. Total Darby Surface Joints C. Total Surface Drainage and D. Total Surface Joints in Ten Degree Intervals 161

75. Projections of 4-Mode Strain Program Means Across Study Area from Station Localities 163

76. Highsplint Area 4-mode Independent Mean Program Circular Histograms of A. Surface Joints B. "Slips" in Highsplint Darby Mine C. Joints in Highsplint Darby Mine and D. Sandstone Trough Axes in Highsplint Darby Mine 166

77. Core-Drilling Apparatus 171

78. Core-Drilling Equipment Used in 004 Section, Highsplint Mine 172

79. Index Map of Core Drilling Site in the Old 004 Section, Highsplint Mine 173

80. Profile of Cores in Drilling Site, Old 004 Section, Highsplint Mine 174

81. Graph of Total Shale Thickness and Laminated Shale Thickness in 004 Section 176

82. Core Analyses Graphs for Cores 1, 2 and 3 178

83. Core Analyses Graphs for Cores 4 and 5 179

84. Core Analyses Graphs for Cores 6 and 7 180

85. Core Analyses Graphs for Cores 8 and 10 181

86. Core Analyses Graphs for Core 9 182

87. Radiographs of Core Sections Showing Cross-Laminated Sandstone in A and B. Laminated Shale with Ironstone Bands in C 184

88. Large Crystal of Plagioclase Feldspar with Albite and Carlsbad Twinning Together with Other Feldspar Grains Showing Replacement by Sericite 191

89. Interlocking Crystals of Untwinned Feldspar and Quartz with Straight Contacts Indicating Pressure Solutioning . . . 191

90. Relatively Finer, More Heterogeneous Texture in Core 1. . . . 192

91. Relatively Coarser, More Homogeneous Texture in Core 2 . . . 192

92. A. Sandstone Classification Scheme Modified from Dott. B. Arenite Triangel Showing Plot of Feldspar-Quartz-Rock Fragment Components of Samples from Table 16 195

93. Cumulative Frequency Curve for Sample 3-13 and Sample Calculations 202

94. Graph of Arithmetic Mean Grain Diameter Averages and Graph of Mean Graphic Standard Deviation Averages for Cores in the 004 Section, Highsplint Mine 204

95. Location of Shale and Siltstone Samples for Clay Mineral Analyses in Cores from 004 Section, Highsplint Mine 206

96. Diffraction Patterns of Sample U-2-2 Showing A. Effects of Glycolation and Heat Treatment and B. Effects of KCl and Acid Treatment 211

97. Sharpness Ratio Values Plotted for <4μm Smear and Elutriated Samples and <2μm Elutriated Samples 215

98. Chlorite Peak Height Plots and Elemental Abundances 216

A1. Location Map of Highsplint Mine Showing Coordinate System for Rib Sections and Coal Sections 241

I. INTRODUCTION

General Discussion

Roof falls in underground coal mines continue to be the major cause of injury to miners. In many cases, roof falls can be attributed to improper roof support measures. However, as mining operations advance, the condition of the roof beyond the working face cannot normally be anticipated. As a result, unexpected changes in roof conditions are often encountered that result in roof falls before preventative measures can be taken.

Changes in roof conditions can often be attributed to geologic relationships of rocks overlying coal seams. Abrupt changes in roof-rock lithology or structure, both vertically and laterally, may be encountered. Compounding the problem is the fact that many of the lithologic and structural aspects of roof rocks are interrelated in a complex manner making it difficult to anticipate where problem areas will be encountered as mining progresses.

This study approached the problem of unstable roof conditions by considering the rocks overlying coal seams from a geologic standpoint. The primary objectives were to identify compositional and structural features of roof rocks that contribute to roof falls, and to establish directional trends of these rocks, both within the mines and at surface exposures, so that problem areas could be anticipated in advance of mining.

This report is written using United States Bureau of Mines format. The units of measure are English, except for metric usage in classification schemes or microscope work. A metric-English conversion chart for linear measure is included in Appendix B (Table 1, Appendix B) for the convenience of the reader.

Scope of Work

The United States Bureau of Mines has conducted research devoted to coal mine health and safety for many years. At the present time the Bureau conducts in-house research and also awards contracts to private industry, consulting firms and educational institutions for health and safety related projects. This study was the outgrowth of such a Bureau of Mines contract with Morehead State University, Morehead, Kentucky. The study was originally submitted to the Bureau as an unsolicited proposal by the author.

The original contract was for a two-year period from January 19, 1973 through January 19, 1975. However, based on results during that time, the contract was extended to May 23, 1977. The contract extension provided for the refinement of geologic predictive techniques and allowed time to conduct a roof monitoring program to further test the effectiveness of these techniques. The effectiveness of predictive techniques developed to date and reported here must be considered somewhat tentative pending further refinement and testing as monitoring preceeds.

Selection of Study Area

Pursuant to contract objectives, discussions were held with personnel of the Kentucky Department of Mines and Minerals and the Kentucky Geological Survey in order to locate a suitable study area. As a result of these discussions, visits were made to several mines in eastern Kentucky. An examination of the Bailey Creek (known as Bailey's Creek locally) and Highsplint mines, operated by the Eastover Mining Company, Brookside, Kentucky, appeared to offer the best possibilities for a geologic study based on the following criteria:

1. Both mines have experienced difficulty in roof control. Relatively large roof falls in the mines enhance a geologic study by exposing strata above the coal. The immediate roof (Figure 1) is exposed in large areas of the Highsplint mine as a result of mining operations, so that strata above the Darby coal bed could be studied within the mine. The mines had been developed to a large enough extent so that possible trends within the mines could be traced.

2. The roof rocks in both mines are characterized by abrupt lateral lithofacies changes, so that studies of roof conditions under varying rock types were possible.

3. Because many roof falls are associated with areas of lateral lithofacies changes in the roof rocks, the possibility of predicting unstable areas in advance of mining was relatively favorable.

4. The roof rocks are jointed in many areas of the mines so joint studies were possible.

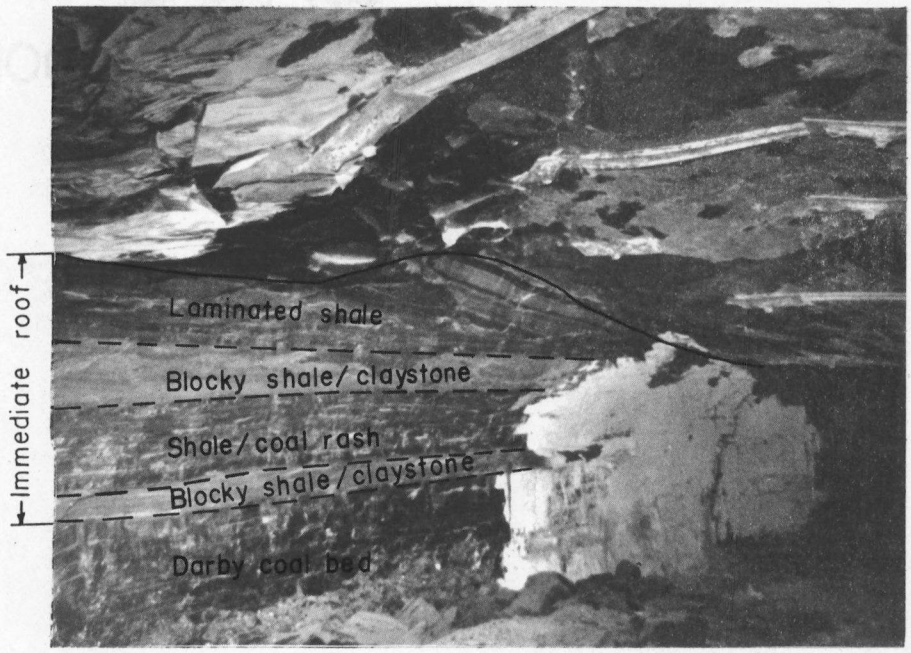

FIGURE 1. - Detail of immediate roof overlying the Darby coal in the Highsplint mine. Also shown is a closeup of N60°E trending sandstone roll shown on page 60. Note contact between sandstone roll and laminated shale is partly compactional. Location is old 004 Section. Roof-bolt plates are about 12 inches long for scale.

5. Both mines are "drift mines" located above major drainage. Even though surface outcrops are limited, one of the major objectives of the study—that of lateral correlation of in-mine and outcrop trends established at the same stratigraphic position—was possible.

6. Comparable mining methods are used in both mines. All mining is by the room-and-pillar method, and mining is done by continuous mining machines. Rooms, or crosscuts, are normally spaced on 80-to 100 foot centers, with entries and rooms usually 20 feet wide. Conventional roof bolts three to eight feet long, spaced on approximate four foot centers are used in most places for roof support. In unstable roof areas, bolts are supplemented by cross-collars or straps, or by timbering. Reasonably consistent mining methods, then, greatly reduce possible operationally induced factors in roof falls.

By considering contract objectives with roof conditions at the Bailey Creek and Highsplint mines, it was evident that these mines were well suited for geologic studies. Table 1 shows the categories of studies that were conducted at these mines.

Location of Study Area

The Bailey Creek and Highsplint mines investigated in this study are located in Harlan County, Kentucky along tributaries of the Clover Fork of the Cumberland River (Figure 2). The study area is represented by parts of the Louellen, Kentucky; Nolansburg, Kentucky: Evarts, Kentucky; and Pennington Gap, Kentucky—Virginia 7-1/2 minute topographic quadrangles. Geologic maps have also been completed through a statewide

TABLE 1. - Categories of roof-fall studies

A. Structural Studies

1. Joints
   a. "Slips" or slickensided planes
   b. Joints formed by differential compaction, tectonic forces and/or by stream unloading
   c. Coal cleat

2. Faults
   a. Effects of Pine Mountain thrust fault

B. Stratigraphic Studies

1. Studies of rock types and bedding characteristics and their relationship to roof stability

2. Studies of vertical and lateral changes in rock types

3. Studies of primary sedimentary structures and associated fossils

4. Consideration of depositional environments

C. Trend Analyses

1. Computer analysis of paleocurrent data

2. Computer analysis of jointing

D. Compositional Studies

1. Physical properties of roof rocks
   a. Apparent reaction to stress
   b. Relationship of composition of roof rocks to joint frequency

2. Mineralogy (coarse fraction)
   a. Identification of minerals in coarse fraction
   b. Changes in texture vertically and laterally in roof rocks

3. Clay mineralogy
   a. Identification of dominant clay minerals
   b. Changes in composition and/or structure of clay minerals vertically and laterally in roof rocks

4. Elemental analysis
   a. Changes in major elemental abundances of roof shales vertically and laterally in roof rocks

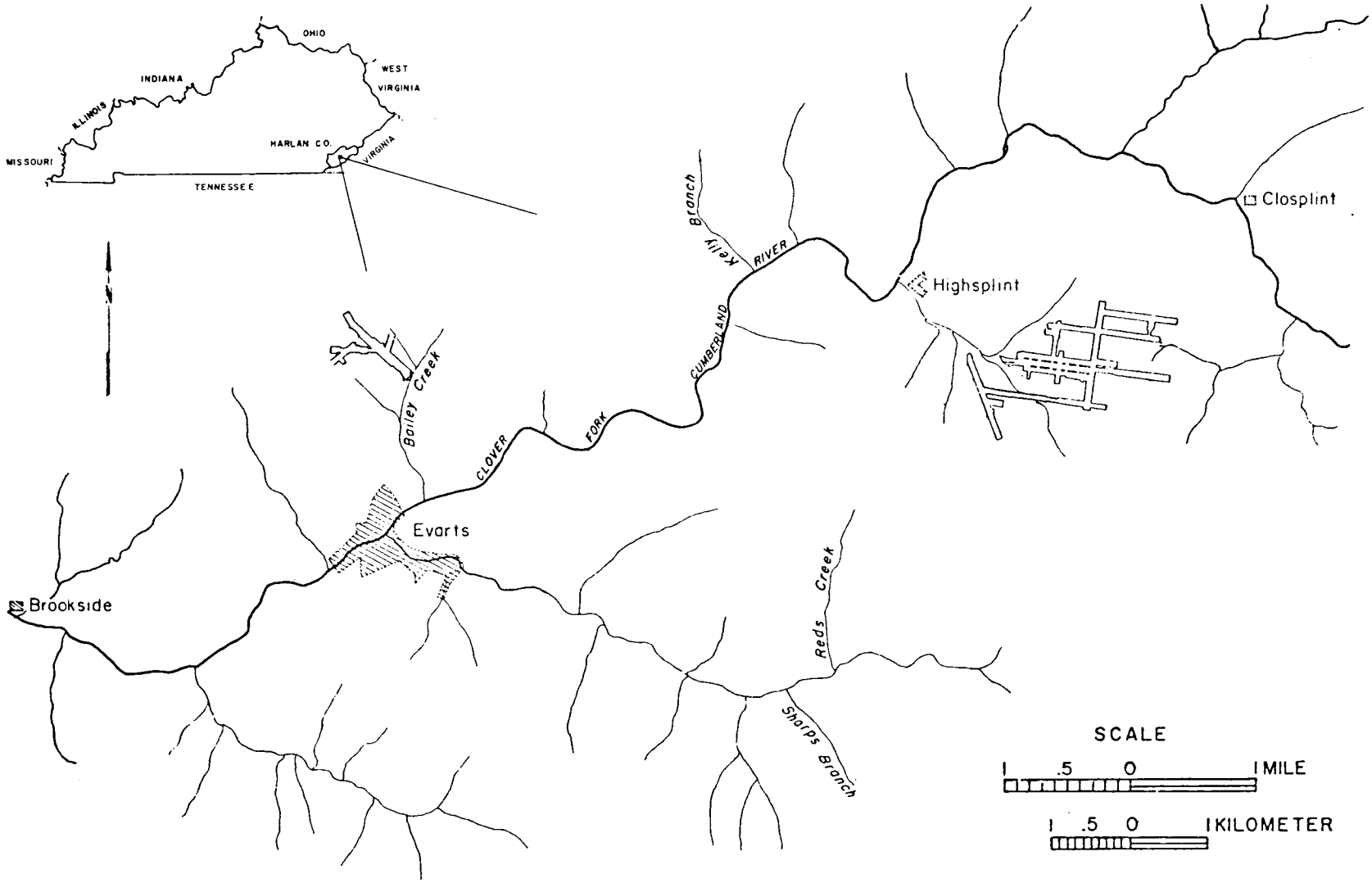

FIGURE 2. - Map of study area showing location of Bailey Creek mine and Highsplint mine.

geologic mapping program conducted jointly by the United States Geological Survey and Kentucky Geological Survey using the above 7-1/2 minute topographic maps as a base (15, 32, 56, 77).

Regional Structure

On a regional scale, the study area represents a rather small part of a unique structural region described as the Cumberland overthrust block (86). The Cumberland overthrust block is about 125 miles long and about 25 miles wide, occurring in parts of Kentucky, Tennessee and Virginia (Figure 3). It is bounded on the northwest by the Pine Mountain thrust fault, on the southwest by the Jacksboro fault, on the southeast by the Hunter Valley-Wallen Valley thrust fault and on the northeast by the Russell Fork fault. The Jacksboro and Russell Fork faults are tear faults that mark the northeast and southwest boundaries of the overthrust block. Lengthwise, the Cumberland overthrust block is divided into two major structural features, the Powell Valley anticline on the southeast and the Middlesboro syncline on the northwest.

Studies dealing with the nature and origin of the Cumberland overthrust block have been pursued by several geologists over the years. According to Rodgers (68), the first report of the structure was apparently made by J. M. Safford in 1869 in a volume entitled The Geology of Tennessee. The Russell Fork fault was first recognized by Wentworth (86), who also described the Pine Mountain fault. However, Wentworth apparently assumed that at Pine Mountain the Pine Mountain fault extended at a sharp angle toward the southeast into the basement. Butts (7), in

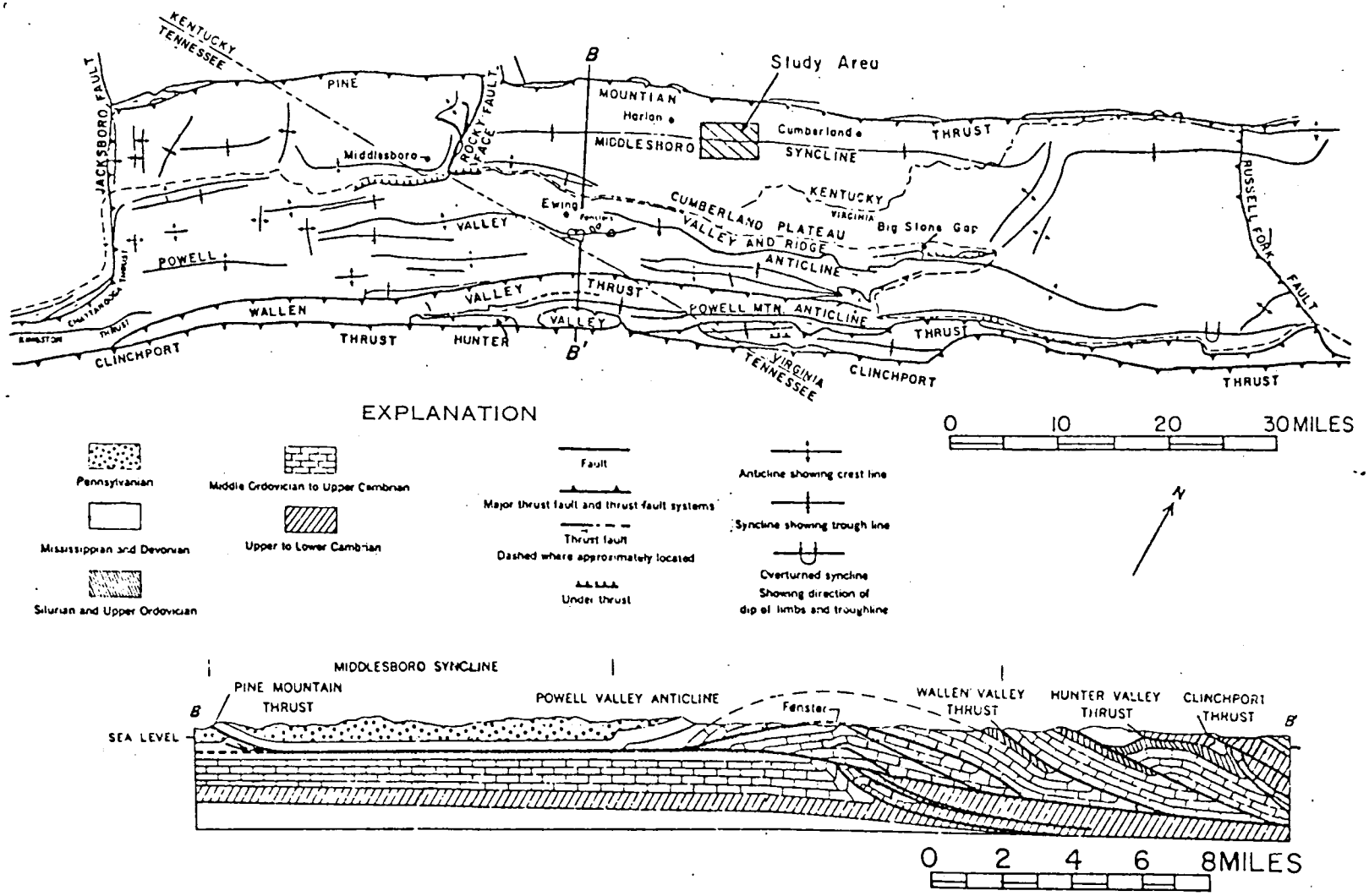

FIGURE 3. - Geology and structure of the Cumberland overthrust block after Harris (35).

his study of the fensters (windows) on the crest of the Powell Valley anticline near Ewing and Rose Hill, Virginia, is credited for demonstrating that the Pine Mountain fault is actually a bedding-plane thrust. Butts' interpretation of the Pine Mountain fault was confirmed by Rich (66), who elaborated on the nature and origin of the Cumberland overthrust block and associated structures. More recently, Miller and Fuller (55) and Miller and Brosge (54) discussed the detailed geology of many of the fensters and surrounding areas in the overthrust block. The possibility of involvement of basement rocks in the origin of the Cumberland overthrust block has also been considered (36).

Reference to the cross section (B-B') in Figure 3, page 9, shows that the Pine Mountain fault is present in Early and Middle Cambrian shales (Rome and Conasauga) in Tennessee, but toward the northwest cuts upward through competent strata to the incompetent Chattanooga Shale of Devonian-Mississippian age beneath the Middlesboro syncline.

Studies have indicated that horizontal displacement of the overthrust block toward the northwest was not uniform, but that the southwest end of the block had been displaced about nine miles, whereas displacement of the northeast end was only about two miles (54).

Stratigraphy

Pennsylvanian-age rocks associated with the Cumberland overthrust block were first divided into named units in a report on the Big Stone Gap Coal Field of Virginia and Kentucky (8). These units included the following: Harlan Sandstone, Wise Formation, Gladeville Sandstone, Norton Formation and Lee Conglomerate.

While this nomenclature is currently in general use in the Virginia coal fields, only the Lee Conglomerate (now Lee Formation) is recognized in Kentucky (53). Table 2, modified from the stratigraphic column of the Pennington Gap Geologic Quadrangle, shows equivalent formation names in current use in Virginia and Kentucky (56).

Except for the marine Kendrick Shale of Jillson (42); and a member of the Wise Formation, known as the Magoffin Beds of Morse (57), the entire sequence of Pennsylvanian age rocks is composed essentially of sandstones, siltstones, shales and coal beds. Most of these rocks are apparently marginal marine to nonmarine. The composite thickness of these Pennsylvanian clastics is in excess of 5,000 feet locally (43).

This study focused attention on only a small part of the total thickness of the Pennsylvanian age rocks exposed in the Middlesboro syncline area. Both the Harlan and Darby coal beds are part of the Mingo Formation (Figure 4), and these studies were essentially limited to strata immediately overlying these seams. Figure 5 shows the general roof rock sequence over the Harlan coal bed at the Bailey Creek mine and over the Darby coal bed at the Highsplint mine. Figure 6 shows the entrance of the Bailey Creek mine and Figure 1, page 4, shows the immediate and main sandstone roof in the Highsplint mine. Although situated in the Middlesboro syncline with essentially flat-lying rocks, the dip of the rocks in the immediate vicinity of the Bailey Creek mine is about 140 feet per mile to the southeast. The dip of the rocks at the Highsplint mine is about 60 feet per mile toward the northwest because of a local structural high trending northwest-southeast in the Little Black Mountain area immediately east of the mine.

TABLE 2. - Pennsylvanian correlations - Kentucky and Virginia *

SYSTEM	GROUP	Kentucky	Virginia
PENNSYLVANIAN	BREATHITT	Bryson Formation ?	Harlan Formation
		Hignite Formation	Wise Formation
		Catron Formation	
		Mingo Formation	
		Hance Formation	Gladeville Sandstone
			Norton Formation
		Lee Formation (Not exposed in the Pennington Gap Quad.)	Lee Formation

* [Modified from Miller and Roen (56)]

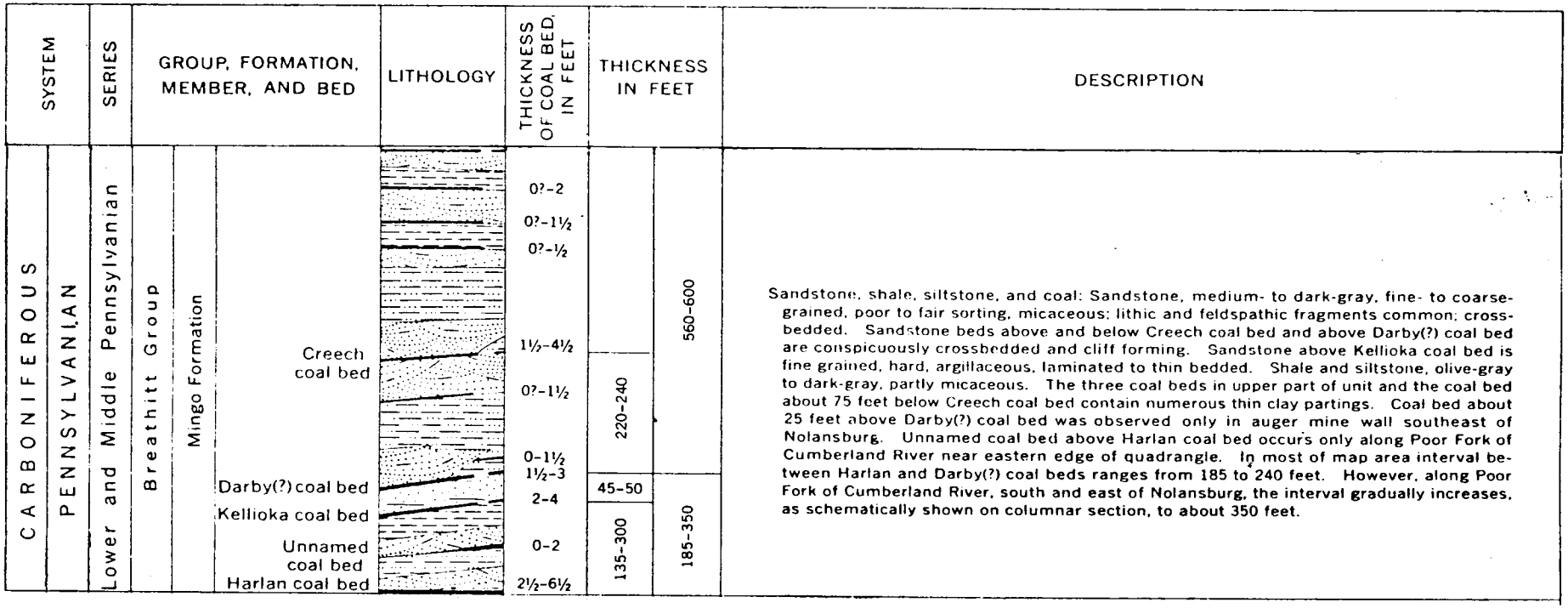

FIGURE 4. - The Mingo Formation showing the stratigraphic position of Harlan and Darby coal beds and lithologic description of associated strata [from Csejtsey (15)].

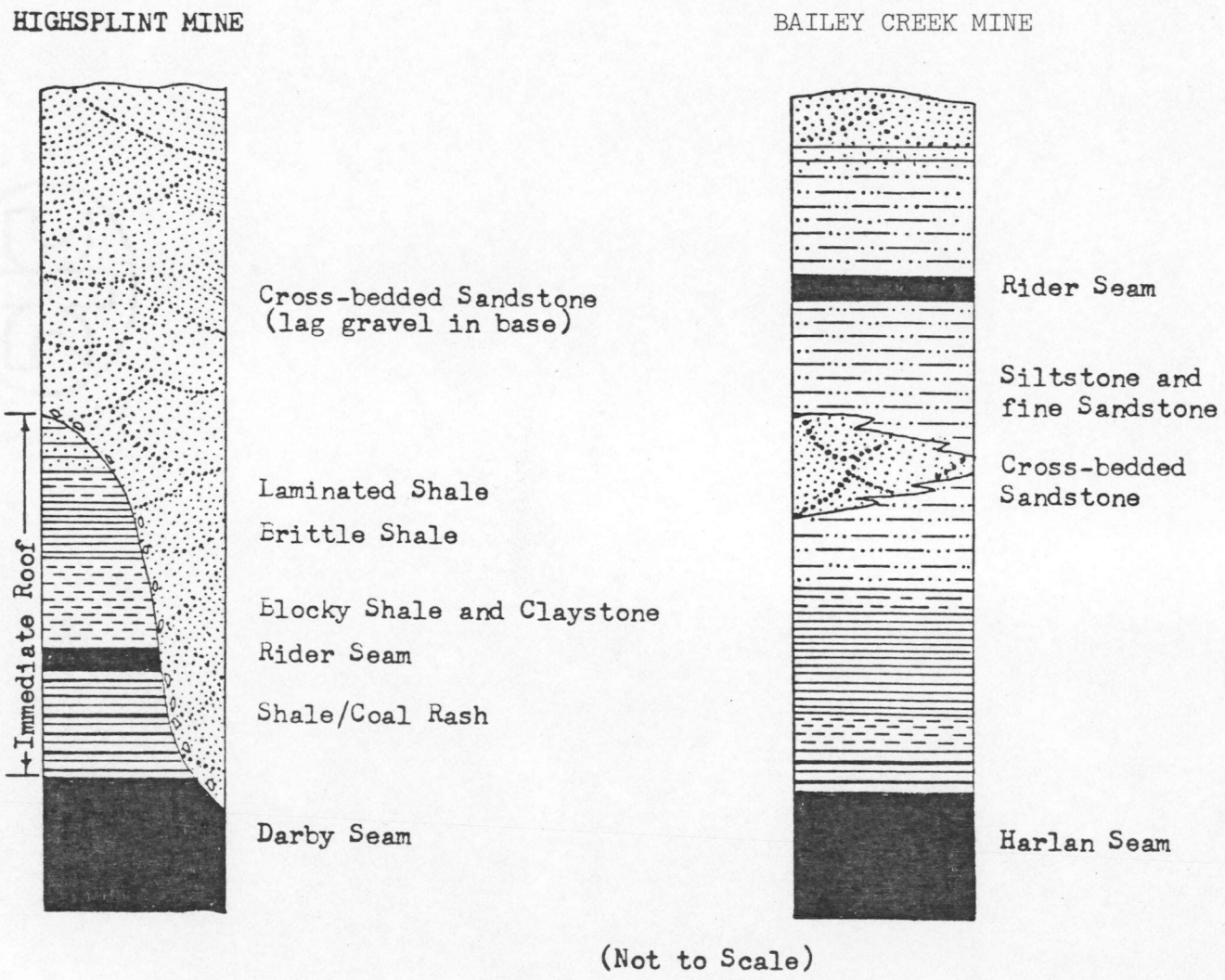

FIGURE 5. - General stratigraphy at the Highsplint and Bailey Creek mines.



FIGURE 6. - Entrance of Bailey Creek mine. Note coarsening-upward sequence between Harlan coal bed and overlying rider seam as indicated by ledges of fine-grained sandstone beneath rider seam.

Topography

The Middlesboro syncline, which includes the study area, is bounded on the northwest by Pine Mountain. Northwest-facing Pine Mountain is a homoclinal mountain capped by the resistant Lee Formation of Pennsylvanian age. The southeast side of the syncline is bounded by a similar homoclinal mountain, known as Cumberland Mountain, which is also capped by the Lee Formation.

Physiographically, the synclinal area between the two ridges is a maturely dissected part of the Cumberland Plateau of the type that is responsible for the terrain's being called "mountains" rather than "plateau" (79). Dissection by stream erosion has resulted in deep valleys, with very little flat valley bottoms remaining, and elongate narrow ridgetops. The most notable of the erosional mountains in the synclinal area is Black Mountain (Big Black Mountain). Its elevation at "The Double", near Benham, is 4,150 feet and is the highest point in Kentucky. Commonly, the relief of the area is from 1,000 feet to as much as 3,000 feet (Figure 7).

Because mines in the area are drift mines situated above major drainage lines and operating in essentially flat-lying strata, extreme changes in overburden thickness and stresses generated by overburden pressure can be expected within short horizontal distances.

Overburden thickness over the Bailey Creek mine in Big Black Mountain is as much as 1,200 feet. The Highsplint Darby mine, in Little Black Mountain, operates under as much as 1,500 feet of overburden.

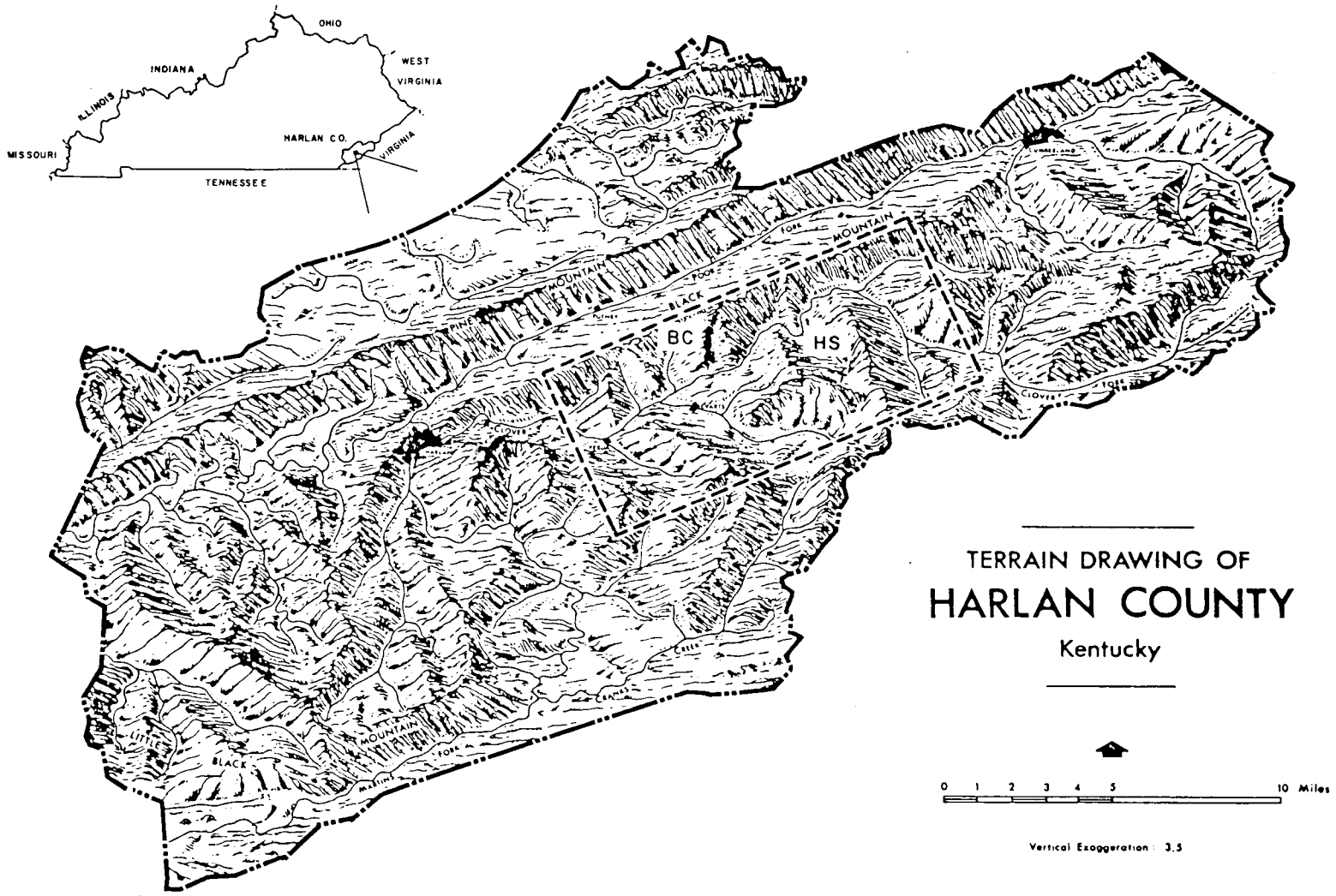

FIGURE 7. - Terrain drawing of Harlan County, Kentucky and outline of study area [Modified after Yarbrough (90)]. Highsplint mine (HS) and Bailey Creek mine (BC) also indicated.

The Eastern Kentucky Coal Field

The Darby and Highsplint mines are included in the Appalachian Coal Region and more specifically in the Eastern Kentucky Coal Field (Figure 8). In turn, the Eastern Kentucky Coal Field, which includes some 10,270 square miles in 31 counties, has been divided into six reserve districts (40).

In the past, the Eastern Kentucky Coal Field had been divided essentially into major drainage areas, such as the Cumberland River drainage or the Licking River drainage, because the drainage area determined the transportation routes and outlined in a general way the mining districts (40). Later, as transportation methods improved, drainage areas became less important, and coal districts were named more often for the major towns within the district. Examples of this method of classification include the Harlan-Benham, Hazard and Corbin districts. The current method of coal district classification is based almost entirely on county lines in eastern Kentucky. The only exception is the Upper Cumberland River Reserve District, which includes the study area.

The Upper Cumberland River Coal District

The Upper Cumberland River Reserve District includes parts of Harlan, Whitney, Letcher and Bell counties. Harlan and parts of Bell and Letcher counties form the eastern part of the district (Harlan Subdistrict), which is geologically separated from the Middlesboro area (Middlesboro Subdistrict) to the west by the fault-produced Rocky Face Mountain, (Figure 3, page 9).

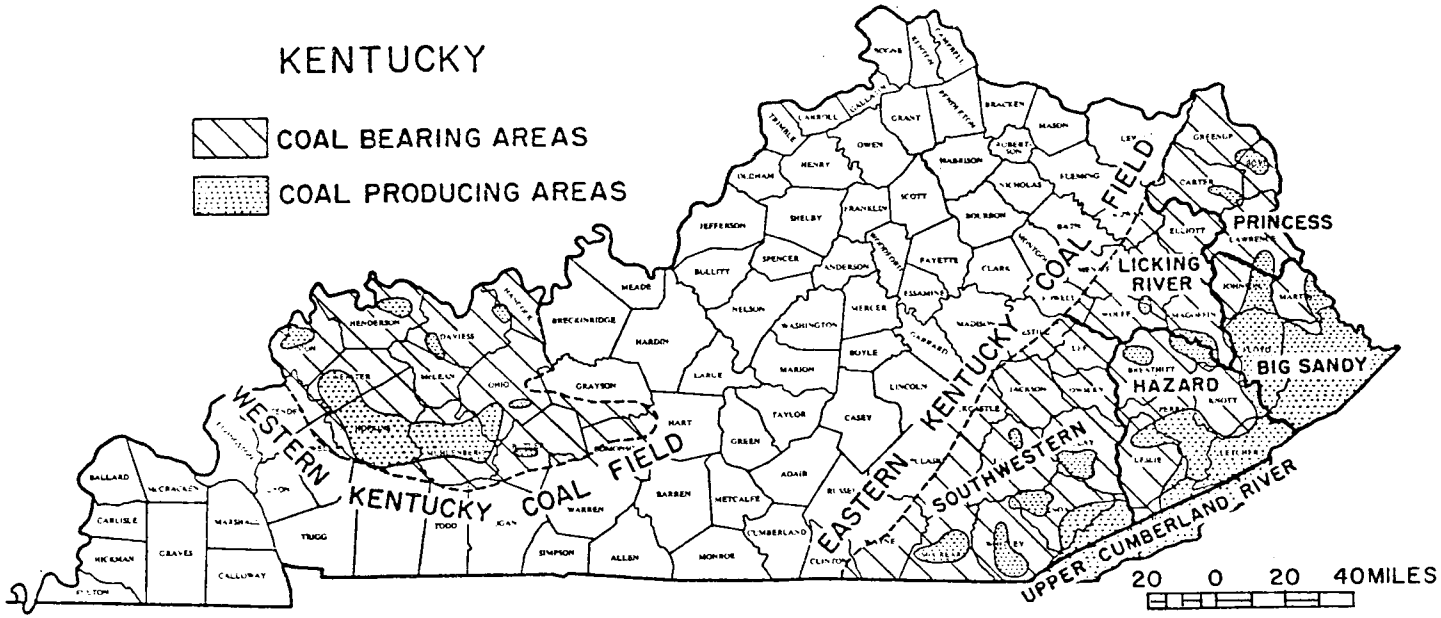

FIGURE 8. - Kentucky coal fields and reserve district [After Smith and McGrain (72)].

Within the Harlan Subdistrict, there are 16 coal beds for which reserves have been calculated. Of these 16 coal beds, the most important ones include the Imboden, Harlan, Darby, Wallins (Fire Clay) and Highsplint in ascending stratigraphic order (72).

Detailed geologic mapping in eastern Kentucky by the Kentucky Mapping Program has indicated that many of the coal beds, known by various names locally, are probably correlative. Table 3 shows equivalent names for major coal beds between the Upper Cumberland Reserve District and the adjacent Southwestern and Hazard Reserve Districts.

The coals of the Eastern Kentucky Coal Field are generally ranked as high volatile B to high volatile A bituminous coal and are commonly banded or splint. Both the Harlan and Darby coals, investigated in this study, are classed as high volatile A bituminous rank. Table 4 compares analyses of the two coals.

The Harlan and Darby coal beds are variable in thickness in the study area; the Harlan ranges from about 36 to as much as 48 inches thick at the Bailey Creek mine; the Darby coal bed at Highsplint is more variable, ranging in thickness from about 30 inches to as much as 50 inches.

TABLE 3. - Correlation of coal beds - Hazard, Southwestern, and Upper Cumberland Reserve Districts*

HAZARD	SOUTHWESTERN	UPPER CUMBERLAND	
		HARLAN	MIDDLESBORO
Hazard No. 7 coal bed	Hazard No. 7 coal bed	High Splint coal bed	Red Spring coal bed
Fire Clay coal bed	Fire Clay coal bed	Wallins (Fire Clay) coal bed	Poplar Lick coal bed
Upper Elkhorn No. 3 coal bed	Jellico or Straight Creek coal bed	Darby or "C" coal bed	Mingo or "Mason" coal bed
Upper Elkhorn No. 1 coal bed	Blue Gem coal bed	Harlan, "B" or Hance coal bed	
Lower Elkhorn coal bed	Bacon Creek coal bed	Imboden coal bed	

* [Modified after Huddle and others (40)]

TABLE 4. - Analysis of the Darby and Harlan coal beds, Harlan Subdistrict*

Harlan Coal Bed[1]		Darby Coal Bed[2]	
		Low	High
Moisture (Percent)	2.6	2.5	3.6
Volatile Matter (Percent)	36.7	34.6	37.5
Fixed Carbon (Percent)	57.2	54.3	58.8
Ash (Percent)	3.5	2.4	6.0
Sulfur (Percent)	.8	.5	1.1
Calorific Value (BTU)	14,130	13,640	14,590

[1]Based on a composite of six mine samples from a single mine near Chevrolet, Harlan County.

[2]Based on a composite of 17 mine samples from mines near Benham, Kenvir, Liggett and Lynch, Harlan County.

*[From Huddle and others (40)]

II. STRATIGRAPHIC RELATIONSHIPS OF THE MINGO FORMATION

Objectives

The purpose of this part of the study was to consider the coal-bearing strata of the Mingo Formation with the following objectives in mind:

1. To describe the physical characteristics of the rocks. Physical features include rock type or lithology, bedding characteristics, and nature of bounding surfaces.

2. To consider properties inherent in the rocks that provide evidence of paleocurrent direction.

3. To consider changes from one lithology to another, both vertically and laterally. Also of importance were repetitions or cycles of lithologies.

4. To evaluate the above aspects of the rocks with roof stability conditions in the Highsplint and Bailey Creek mines in order to determine what lithologic conditions contributed to roof falls.

Physical Features

Figure 9 is a measured stratigraphic section of the Mingo Formation at Brookside, Kentucky where strata from the Harlan coal bed upward to the Creech coal bed are exposed. The Brookside stratigraphic section was used as a reference section for comparison with other observation sites in the study area (see discussion, page 112). The following lithologic and sedimentary characteristics of that part of the Mingo

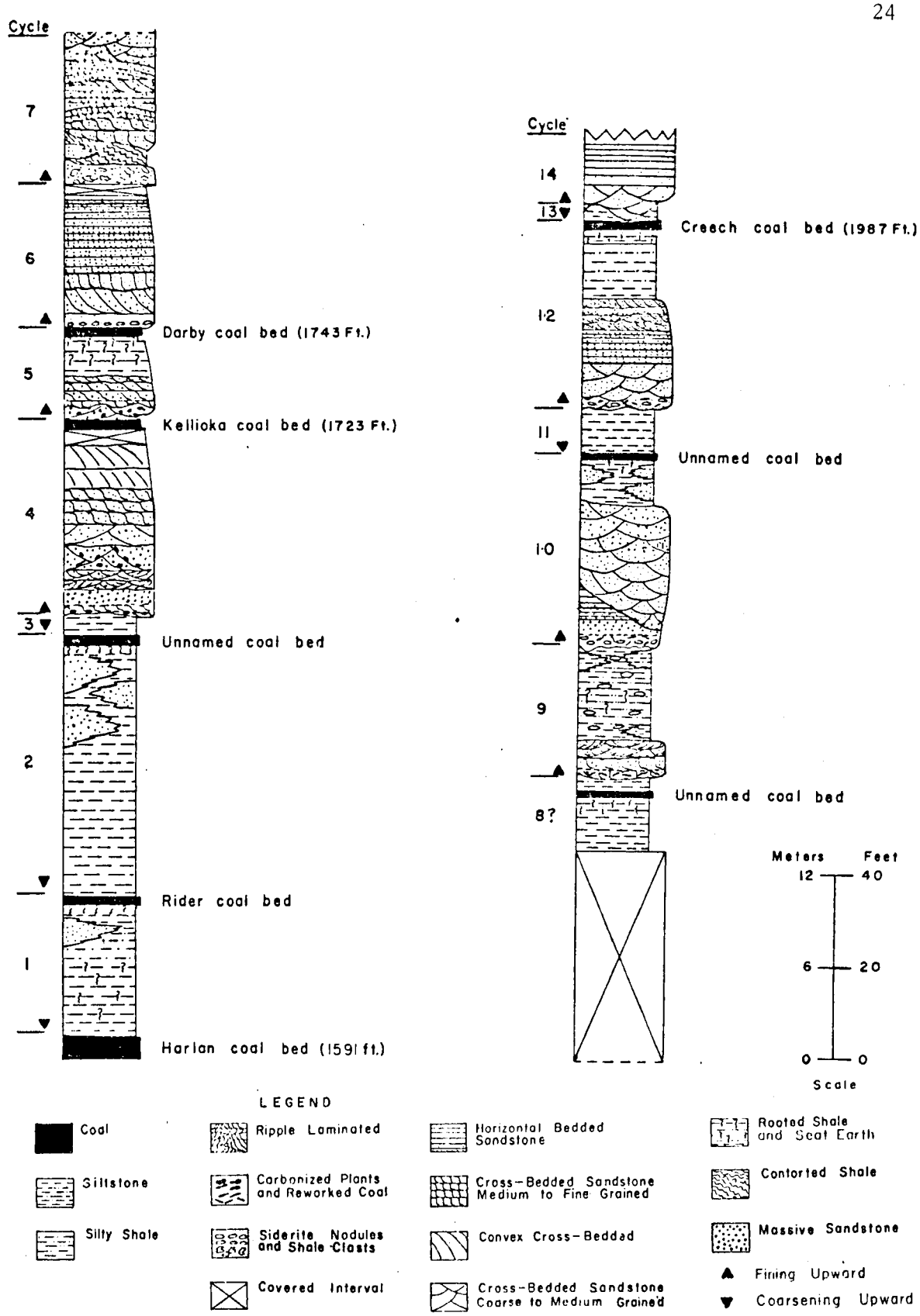

FIGURE 9. - Brookside stratigraphic section. Numbers refer to coarsening upward and fining upward cycles. See page 136 for location.

Formation between the Harlan and Creech coal beds are the result of a compilation of data from all outcrops studied, in addition to observations in the mines studied.

Lithologies

The dominant lithologies of the Mingo Formation under consideration are sandstones and shales. Siltstones, underclays (seat earths) and coal beds are subordinate.

Shales

Shales, where observed fresh in the mines, are usually light-to dark gray; the degree of darkness being proportional to the amount of incorporated carbonaceous material. On the outcrop, shales weather light- to medium brown and are usually stained with iron oxides. Figure 1, page 4 is representative of the commonly observed shale types. Laminated shales, shown in Figure 1, page 4, are arranged in roughly parallel layers 0.25 inch to as much as one inch thick. The laminae are differentiated on the basis of color (light and dark) and texture (some layers may be more silty). In fact, laminated shales locally are properly designated as siltstones on the basis of texture. Lenses and continuous thin layers of ironstone that parallel bedding are common. Laminated shales may be interbedded with fine-grained sandstones with irregular, wavy or undulating contacts. On exposure, laminated shales weather into thin layers.

Claystone, also shown in Figure 1, page 4, is also referred to as blocky shale because of its blocky fracture in the mines. It is commonly light-to medium gray when fresh and often contains numerous slickensided surfaces. Claystone weathers light-to dark brown and on exposure becomes more shaly in character.

Underclays

Underclays, also referred to as seat earths, are commonly light-to medium gray both fresh and weathered. The underclays beneath the Harlan and Darby coal beds are shaly, micaceous, dense and hard. Locally, they become plastic when wet. All underclays observed contained plant rootlets.

Sandstones

Sandstones are essentially gray to white when fresh, weather light-to medium brown and are usually stained with iron oxide. They are mostly fine-to medium grained and are moderately-to well sorted. The basal portion of a sandstone unit commonly contains zones of ironstone, shale or siltstone nodules and clasts as much as 0.5 inch in diameter (Figure 10). These basal "lag gravels" are arranged in thin, discontinuous layers concentrated in elliptical pods as much as three feet in length. They commonly are scattered along cross-beds in the lower part of the sandstone units.

Figure 9, page 24, shows that the lithologies discussed above are cyclic or repetitious. Two dominant types of cycles are indicated. The

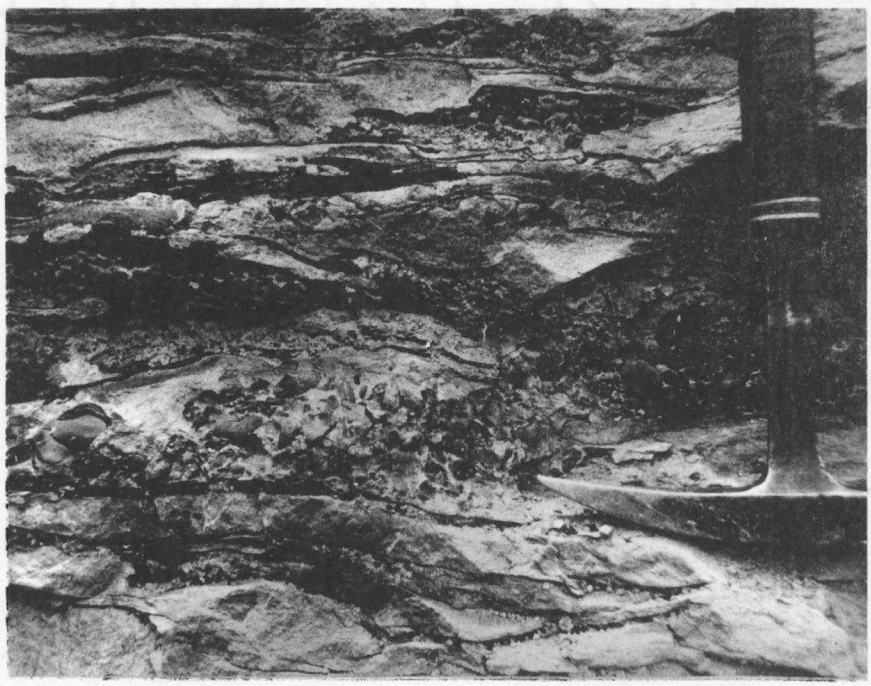

FIGURE 10. - Close-up of siderite and shale clasts interbedded in sandstone immediately overlying the Darby coal bed at Highsplint. Hammer for scale.

fining-upward cycle is characterized by relatively coarser grained sandstone that contains "lag gravel" in the basal part. Cross-bedding is usually large scale and trough cross-beds dominate. The sandstone bedding becomes thinner and flattens upward. The sandstones are overlain by siltstone and rooted underclays.

The coarsening-upward cycle begins with shale. The shales are overlain by siltstone and sandstone with rooted underclay and a coal bed at the top of the sequence. In many cases the cycles are incomplete. Duff and others (21) discussed the significance of sedimentary cycles in terms of sedimentary environments.

Sandstone Bedding

Sandstone Cross-Bedding

A cross-bed can be defined as a single layer, or a single sedimentation unit consisting of internal foreset laminae inclined to the principal surface of sedimentation. This sedimentation unit is separated from adjacent layers by a surface of nondeposition, erosion or abrupt change in character (65). Although the definition of cross-bedding is apparently simple, the description and classification of the great number of possible variations is very complex. However, there are two general categories of cross-bedding (shown in Figure 11), which are differentiated on the basis of their lower contacts and the shape of the cross-beds. Tabular cross-beds are essentially tabular shaped with planar contacts, whereas trough cross-beds have curved basal contacts.

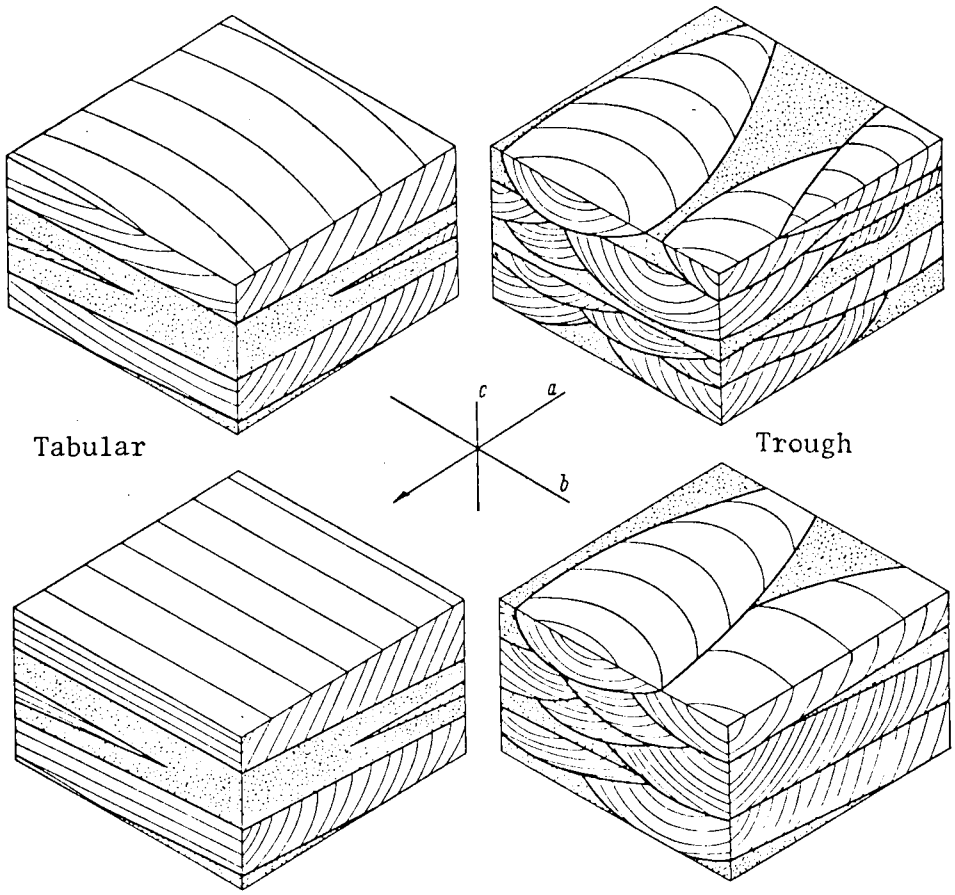

[after Potter and Pettijohn (62)]

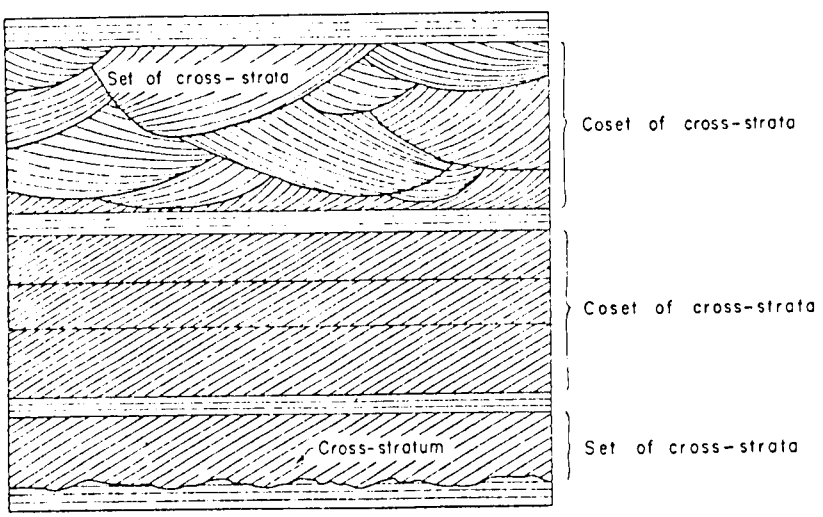

[after McKee and Weir (50)]

FIGURE 11. - Block diagrams of tabular and trough cross-bedding together with reference system (top) and nomenclature of cross-bedded units (bottom).

Other terminology applied to cross-beds is shown in the bottom diagram of Figure 11. According to McKee and Weir (50), a set consists of a "group of essentially conformable strata or cross-strata, separated from other sedimentary units by surfaces of erosion, nondeposition, or abrupt change in character." A coset was defined as "a sedimentary unit made up of two or more sets of cross-strata separated from other strata or cross-strata by original surfaces of erosion, nondeposition or abrupt change in character."

The axes a, b, and c (Figure 11, top) are used to indicate possible planes of reference. If the transporting medium that deposited the cross-beds flowed parallel to the a axis, then the a - c section would provide a longitudinal view of the beds. Likewise, the b - c section provides a cross-sectional view of the beds. Some cross-beds may be exposed on a horizontal surface, in which case the a - b section is the reference section.

According to Potter and Pettijohn (62), the distinction between tabular and trough cross-bedding depends on the extent to which the structure is exposed in three dimensions and on the size of the cross-bedded layers. Almost all of the surface exposures in the study area were vertical, showing the a - c or b - c sections, or oblique views of these sections.

Table B2, Appendix B, shows a comparison of quantitative terms for stratification and cross-stratification (50). Thickness values listed for horizontal beds were used in this study. However, because thickness values for cross-beds in Table B2, Appendix B, pertain to each

cross-stratum, cross-stratification units (sets) were described in terms of large-scale and small-scale (1). Following this practice, cosets in which the set thickness is less than two inches (5 cm) were classed as small-scale, and those in which the set thickness is greater than two inches were classed as large-scale.

Large-Scale Trough Cross-Bedding

Large-scale trough cross-bedding is especially evident in medium-grained sandstones, and where ironstone zones are found. In the vertical b - c section, especially normal to the maximum dip direction into the trough, sets are commonly wedge shaped and discordant at the base (Figure 12). The thickness of sets in a coset is commonly three feet to five feet, and the dip of cross-stratification often decreases upward (see Figure 13). Figure 14 shows large-scale trough cross-bedding that is lithologically heterogeneous. Note that the limbs of the trough at this locality are conformable.

Large-Scale Tabular Cross-Bedding

This type of cross-bedding is commonly associated with basal siderite zones as solitary sets (six inches to as much as three feet) and in fine- and medium-grained sandstones (especially the basal portions). The lower bounding surface of the set is discordant and can often be traced several hundred feet. The upper bounding surface is either discordant or the set appears to grade without an apparent discontinuity vertically into a massive sandstone unit, perhaps because of weathering. The sets are recognizable only in the vertical a - c section. For this reason tabular



FIGURE 12. - Large-scale trough cross-bedding in lower part of cycle 12, Brookside section. (See Figure 9, page 24)

Old Council Tree
Bond

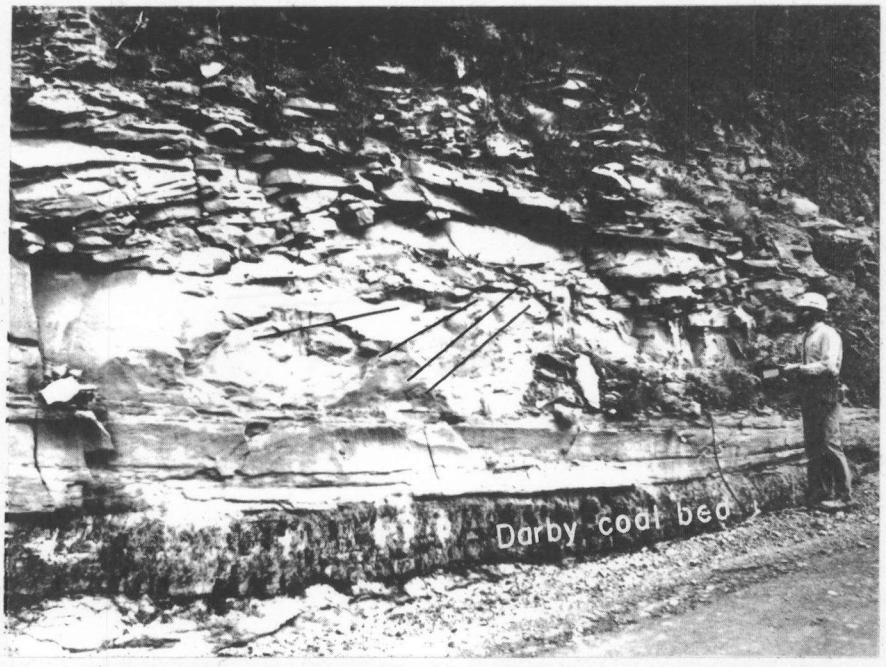

FIGURE 13. - "Fining-upward" sequence in unit 6, Brookside section. Note decrease in cross-bed thickness and degree of dip upward.

Old Council Tree Bond

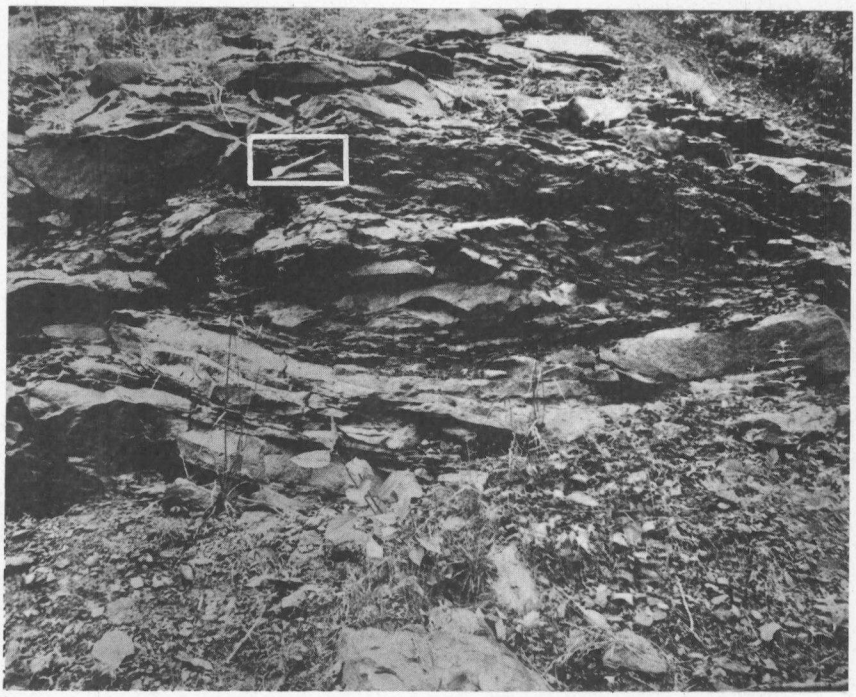

FIGURE 14. - Trough cross-stratification exposed on Darby strip bench. Location designated as P_3 on page 75. Chisel is about ten inches long for scale.

cross-bedding may be confused with trough cross-stratification if the vertical b - c section is not visible. While most large-scale tabular cross-stratification was composed of cross-strata that were planar or convex-downward, some with convex-upward cross-strata were observed at Brookside, Kentucky and the Darby strip bench at Highsplint.

Small-Scale Trough Cross-Bedding

Cross-bedding of this type is composed of cosets in which individual sets are less than two inches (5 cm) thick. This type of cross-bedding is common in fine sandstones or siltstones, and usually is associated with thinner-bedded units. In the vertical b - c section the sets are often trough-like.

Longitudinal Cross-Bedding

Longitudinal cross-bedding is considered here because of its presence in sandstone "rolls" in the new 004 Section of the Highsplint mine. Figure 15 shows cross-beds striking parallel to the roll axis. The cross-beds were not exposed in cross section, but are apparently large-scale.

Climbing-Ripple Lamination

Climbing-ripple lamination was observed at only one locality on the Darby strip bench at Highsplint in fine-grained sandstone. Climbing ripples are formed by the preservation of migrating ripples by rapid simultaneous deposition of suspended sediment (65).

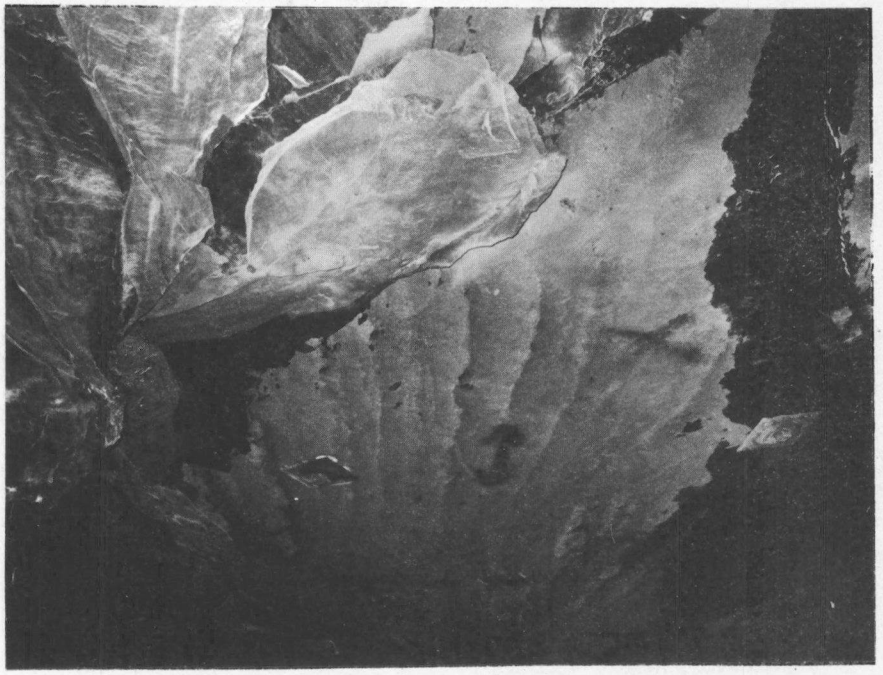

FIGURE 15. - Longitudinal cross-bedding exposed on base of sandstone roll, new 004 Section, Highsplint mine (location designation S-13 on page 241). Arrow (12 inches long) painted on roof is parallel to strike of cross-beds and axis of roll.

Horizontal Bedding

Horizontal bedding is common in fine-and medium-grained sandstones of the Mingo Formation and in ironstone zones. It also is common in siltstones. Bedding thicknesses of horizontally-bedded sandstones may be as little as one half inch thick and as much as four feet. However, many apparently thick-bedded sandstones in fresh exposures are found to weather to thinner beds when traced laterally, so individual bed thickness may be masked in fresh exposures.

Horizontal beds can often be traced several tens of feet along the outcrop (Figure 16). Also, they are commonly associated with "cut and fill" large-scale cross-bedding. In this association, horizontal beds are lenticular and laterally discontinuous. Horizontal bedding commonly overlies or underlies single sets or cosets of cross-bedded units. Upper and lower bounding surfaces may be erosional or gradational. Bedding planes are usually marked by thin shale partings, slight textural or color changes between beds, or evidence of disconformity such as ripple-marked surfaces.

In roof-fall areas in the mines, abundant carbonized plant material was often observed on bedding surfaces (Figure 17).

Parallel Lamination

Parallel lamination was observed in both the Highsplint and the Bailey Creek mines. The rocks are essentially laminated shale and siltstone. When interbedded with ripple-laminated, fine-grained sandstone,

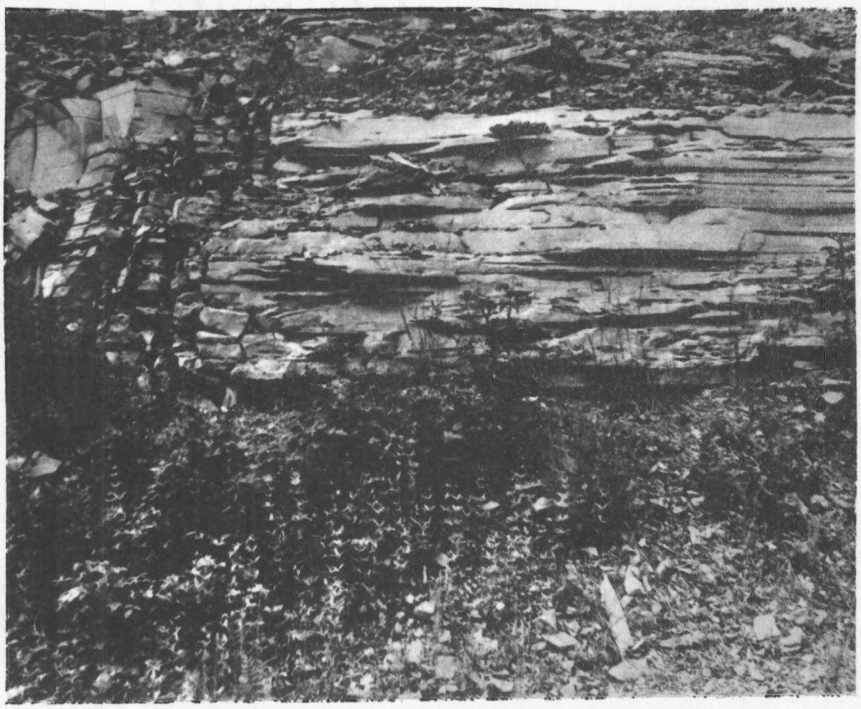

FIGURE 16. - Horizontal bedding exposed on Darby strip bench, Highsplint mine (designated P_2, page 75). Height of outcrop about six feet.



FIGURE 17. - View of roof-fall zone in the old 004 Section, Highsplint mine. Note thick laminated shale on the left. Roof fall extends upward into sandstone with abundant plant material on bedding surfaces. See page 173 for location of photo P_2. Roof-bolt plates are about 12 inches long for scale.

various terminology has been applied; notably wavy, lenticular or flaser, depending on the shale-to-sand ratio. All are associated with sand ripples migrating across a muddy substrata (65).

Graded Bedding

Radiographs of core samples from the 004 Section, Highsplint mine suggest that the coarser sandstone/lithic fraction is graded. Graded beds in the cores studied are cyclic and relatively thin (maximum of ten inches) suggesting relatively minor fluctuations in regimen (see discussion, Section V).

Representative Sedimentation Units

Figures 18, 19, 20, 21 and 22 illustrate representative sedimentary sequences that were observed in surface outcrops at the Highsplint, Bailey Creek and Brookside localities. They are believed to represent one or more cycles of deposition. In this respect, these sedimentary cycles are of importance in roof stability.

A review of the literature indicates that discontinuities in roof rocks contribute to roof falls (48, 59, 88). Discontinuities may be caused by planes of weakness, jointing, faults or a rider coal seam. Evaluation of roof falls in the present study supports this view. However, several of the larger falls extended upward beyond the immediate roof shales and include as much as ten feet or more. These falls may be caused in part by subtle discontinuities. These discontinuities appear to be related to cyclic deposition of roof strata and represent vertical

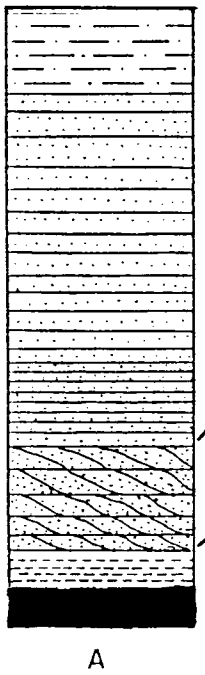

	OBSERVED FACTS	INTERPRETATION
4	Light-to medium gray sandstone, fine-to medium grained, becomes shaly upward.	Probably vertical accretion deposits or splays.
3	Light-to medium gray sandstone, fine-to medium grained.	Probably vertical accretion deposits or splays.
2	Light-to dark gray shale/siltstone.	Vertical accretion deposit from overbank floods.
1	Bituminous coal.	Coal-forming backswamp/marsh deposit.

(Not to Scale)

FIGURE 18. - Representative sedimentation unit - Section A. See Figure 9, page 24, for legend.

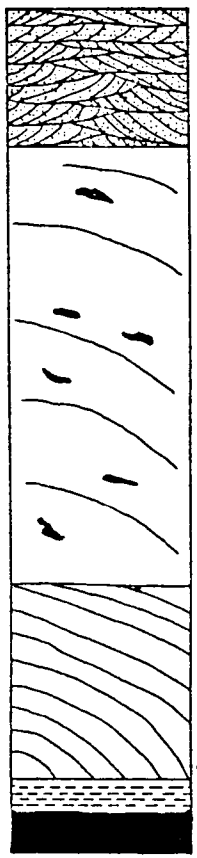

	OBSERVED FACTS	INTERPRETATION
4	Light gray fine sandstone. Ripple laminated. Small-scale cut and fill.	Probably vertical accretion deposit. Levee, swale-fill or backswamp.
3	Light-to medium gray, fine-to medium grained sandstone, massive, but weathers in convex cross-beds. Contains Carbonized plant material. Becomes thicker bedded upward.	Probably formed by migration of river mouth bars to form lake-interdistributary bay fill.
2	Light to dary gray shale/silt-stone.	Vertical accretion deposit from overbank floods.
1	Bituminous coal.	Coal-forming backswamp/marsh deposit.

(Not to Scale)

FIGURE 19. - Representative sedimentation unit - Section B. See Figure 9, page 24, for legend.

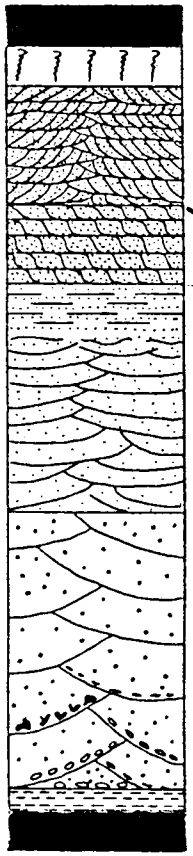

OBSERVED FACTS	INTERPRETATION
Seat earth and bituminous coal.	Coal-forming backswamp/marsh deposit.
Siltstone and fine grained sandstone. Ripple laminated. Parallel and wavy lamination. Rooted.	Probably vertical accretion deposit. Levee, swale-fill or backswamp.
Light gray, fine-to medium grained sandstone. Small-to medium scale cross-beds.	Probably lateral accretion deposits formed during lower stage of stream flow on point bars. Deposition from bedload and/or suspension.
Light gray, coarse-to medium grained sandstone, lag at base and scattered upward. Trough cross-bedding (Large to medium scale). Horizontal bedding locally.	Channel deposit probably formed in deepest part of meandering channel by lateral accretion.
Light to dark gray shale/siltstone. Laminated with ironstone bands and nodules upward.	Vertical accretion deposit from overbank floods. Thick units may include coarsening-upward crevasse splay or lake-interdistributary bay fill upward.
Bituminous coal.	Coal-forming backswamp/marsh deposit.

(Not to Scale)

FIGURE 20. - Representative sedimentation unit - Section C. See Figure 9, page 24, for legend.

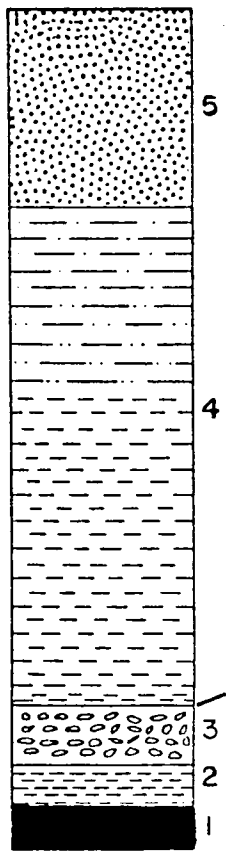

	OBSERVED FACTS	INTERPRETATION
5	Light gray, massive-to thick bedded sandstone. Cross-bedded laterally, medium-to coarse grained.	Probably channel deposit formed by lateral accretion.
4	Light-to medium gray shale grading upward into silty shale.	Probably formed as sedimentation in abandoned channel. Symmetrical channel shape is preserved. (100 feet wide and about 10 feet deep as indicated by units 3 and 4).
3	"lag gravel" conglomerate.	Channel deposit probably indicating high velocity.
2	Light-to dark gray shale/siltstone	Vertical accretion deposit from overbank floods.
1	Bituminous coal.	Coal-forming backswamp/marsh deposit.

(Not to Scale)

FIGURE 21. - Representative sedimentation unit - Section D. See Figure 9, page 24, for legend.

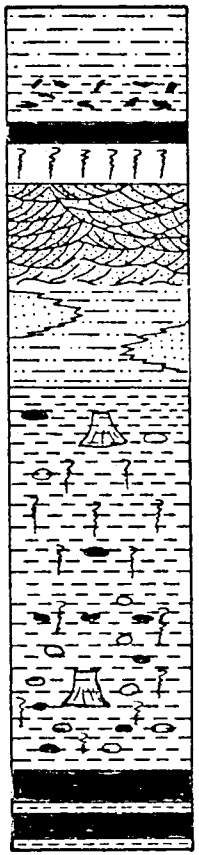

	OBSERVED FACTS	INTERPRETATION
5	Seat earth and bituminous coal.	Coal-forming backswamp/marsh deposit.
4	Light gray fine sandstone. Ripple laminated. Small-scale cut and fill.	Probably vertical accretion deposit. Levee, swale-fill or backswamp.
3	Light-to dark gray silty shale, laminated. Wavy bedded with fine sandstone locally.	Vertical accretion deposit from overbank floods or crevasse splays.
2	Medium-to dark gray shale, rooted with standing stumps (kettle-bottoms). Contains ironstone and siliceous nodules.	Probably backswamp and/or marsh deposit. Possibly inundated to form lake and/or bay.
1	Bituminous coal.	Coal-forming backswamp/marsh deposit.

E

(Not to Scale).

FIGURE 22. - Representative sedimentation unit - Section E. See Figure 9, page 24, for legend.

changes in rock texture, admixtures of plant or lithic fragments, or changes in bedding thickness and/or attitude. No vertical scale is indicated on the generalized profiles, but vertical height for complete cycles may range from about ten feet for Figure 18 to as much as 40 feet in Figure 20.

Beginning with Figure 18, representing conditions in parts of the Highsplint mine, roof falls involving several parts of the sequence have been observed. In this case, the immediate roof shales are directly overlain by cross-laminated sandstones characterized by bedding surfaces separated by carbonized plant debris. Figure 17, page 39, shows a roof fall involving units 3 and 4.

The height of roof falls appears, in fact, to be partly dependent on the length of roof bolt used or depth of penetration into the roof. If conventional bolts are anchored in unit 3, separation of the roof may occur between units 3 and 4. Longer conventional or resin bolts, extending into unit 4, either stabilize the roof or the roof separates higher than the bolt length, perhaps between unit 4 and the overlying unit.

Several possible roof separation zones are present in Figure 19, page 42. Again depending on roof-bolt length, the most likely zone for roof falls using shorter bolts is between the thinner- and thicker-bedded parts of unit 3. The second most likely zone is between units 3 and 4.

Figure 20, page 43, actually represents a "complete" cycle from one major coal to another and may involve as much as 30 feet or more of strata (Figure 9, page 24). No falls extending upward this high were observed.

However, falls involving the lower units have been noted at Highsplint. The stability of unit 3 depends largely on the degree of cementation and textural considerations related to admixtures of gravel and plant debris. Stability of this type of roof also is related to mine layout. Large-scale trough cross-beds are very unstable if the heading direction (in room-and-pillar mines) approximates the trough axis direction. This relationship is discussed in detail in Section VI.

Roof falls have also been observed at Highsplint involving separation between units of differing cross-bed thicknesses as in unit 3. Exposures of the roof above falls extending to the upper part of unit 3 or lower part of unit 4 are often covered with carbonized plant debris. Current ripple marks on bedding surfaces are often exposed on thin-bedded rocks representing the upper part of unit 3 or the lower part of unit 4 (see Figure 23).

Figure 21, page 44, is probably a local sequence and was only seen on the Darby strip bench at Bailey Creek. The outcrop is shown in Figure 24 and no roof falls specifically involving this type of sequence have been observed.

Figure 22, page 45, representing a coarsening-upward sequence capped by a rider coal seam, is taken from parts of the Bailey Creek mine adjacent to sand-filled channels (see discussion, page 92). The largest roof falls observed have involved separation at the rider coal seam (between units 4 and 5). Smaller roof falls are related to trough cross-beds occurring in units 2, 3 and/or 4. Kettlebottoms or plant fossil casts occur frequently in unit 2. Mine personnel reported that

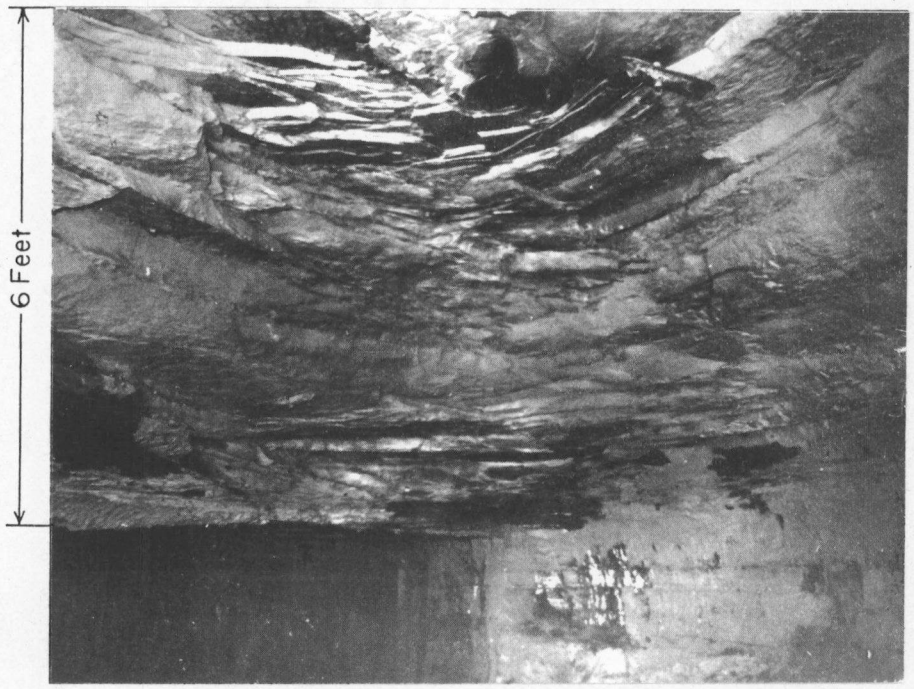

FIGURE 23. - "Fining-upward" sequence in Bailey Creek mine characteristic of channel-fill sandstones. Location is in roof-fall area BP_3 (see discussion, page 83).

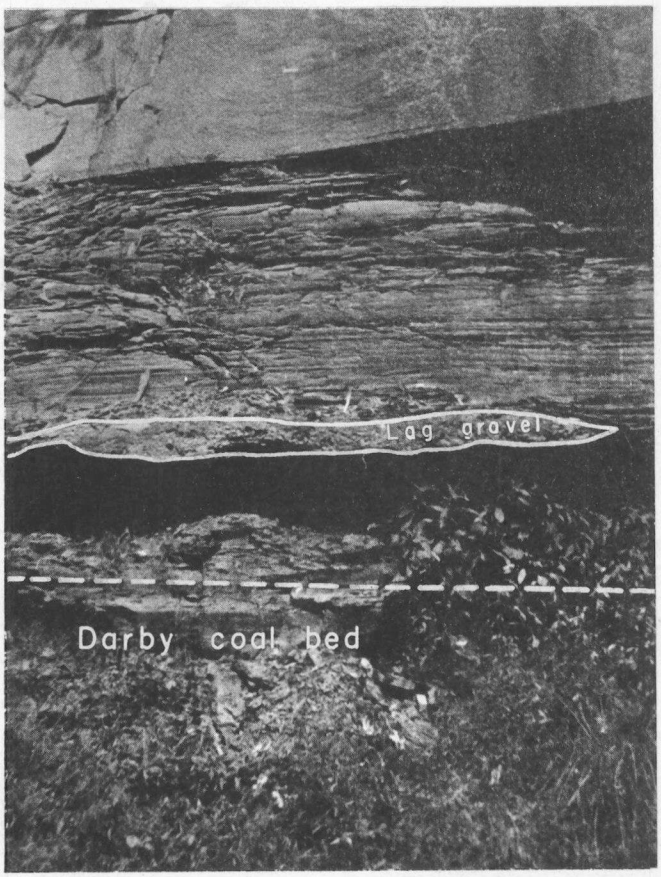

FIGURE 24. - Stratigraphic sequence immediately above the Darby coal seam at the Bailey Creek mine. "Lag gravel" is overlain directly by platy shale in a symmetrical trough about 100 feet wide. Height of outcrop about ten feet.

the lowermost section of a kettlebottom often falls when exposed in the roof, but the fall of an entire kettlebottom had not been observed, except in a large roof fall (Figure 25).

Conclusions and Recommendations

The relationship between sedimentary cycles and roof falls appears to involve zones of weakness that separate easily because of lithologic and/or bedding characteristics. It would not be an easy matter to anticipate abrupt cyclic changes in the roof as mining progresses. However, this study has shown comparable cycles between surface exposures and unstable roof conditions underground. Recommended procedures in the evaluation of sedimentary cycles would involve, first of all, the study of characteristic cycles from surface exposures and/or surface drill core data. Secondly, as mining progresses, evaluation can be made by test drilling using a roof bolting machine and examination of roof-fall areas.

Lateral Changes in Lithology

The discussion of sedimentary sequences considered discontinuities in roof strata that contribute to roof instability because of vertical changes in rock character. Of considerable importance also is the change from one lithology to a distinctly different lithology laterally. These facies changes are often difficult to anticipate as mining advances. Figure 26 illustrates such a lateral change. The rolling sandstone in the center and left side of the mosaic is representative of the vertical

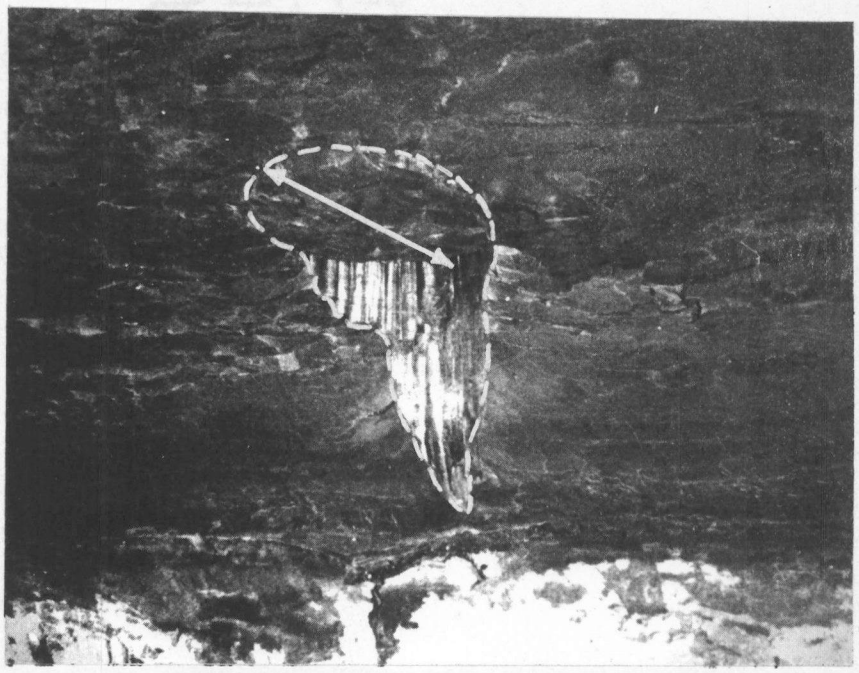

FIGURE 25. - Kettlebottom in roof in Bailey Creek mine. Note slickensided surface exposed where part of the kettlebottom has fallen. Diameter about two feet. Location designated on page 83 as BC_7.

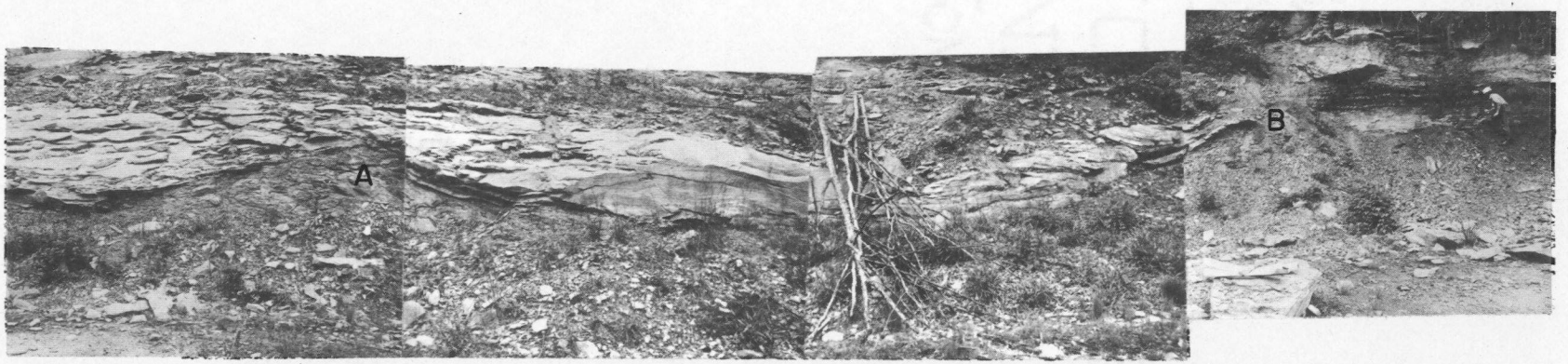

FIGURE 26. - Photographic mosaic of rolling sandstone. Note local thickening of shale at left (A) and abrupt sandstone-shale facies change at right (B). Location is Darby strip bench (designated P_1 on page 75).

sequence shown in Figure 20, page 43. However, the sequence on the extreme right is representative of the vertical sequence in Figure 22, page 45. Note the abrupt change between each sequence.

Studies in the Highsplint mine indicated that roof falls frequently occur in zones of facies change. These relationships are discussed in Section III.

III. ROOF COMPOSITION AND TREND ANALYSIS - HIGHSPLINT MINE

Roof Classification

An analysis of data indicated that the mine sections surveyed were characterized by several dominant immediate roof conditions. These conditions are representative of the entire Highsplint mine. Figure 1, page 4 and Figure 5, page 14, show the stratigraphic section of the immediate roof at Highsplint, which includes shale, shale/coal rash and siltstone. Variations in roof conditions may be summarized as follows:

Roof Condition A (Laminated Shale)

Attempts to hold the immediate roof shales are met with considerable difficulty because of discontinuities that disrupt the rocks. Perhaps the most detrimental are planar surfaces in the laminated or banded shales. While all "slips" are slickensided, rocks on either side of some have not been displaced appreciably. Hence, these "slips" may be classed as joints. However, apparent displacement of strata across other "slips" indicates that they should be considered faults as shown in Figure 27. "Slips" are sometimes observed cutting diagonally across the entire thickness of laminated shales, as on the right half of Figure 28. Because cross straps are used in the mine with conventional roof bolts on four-foot centers, it is sometimes possible in local areas to hold the laminated shales. Although not proven, success in this case is likely due to low "slip" frequency combined with an even bedding contact with the main sandstone roof above.

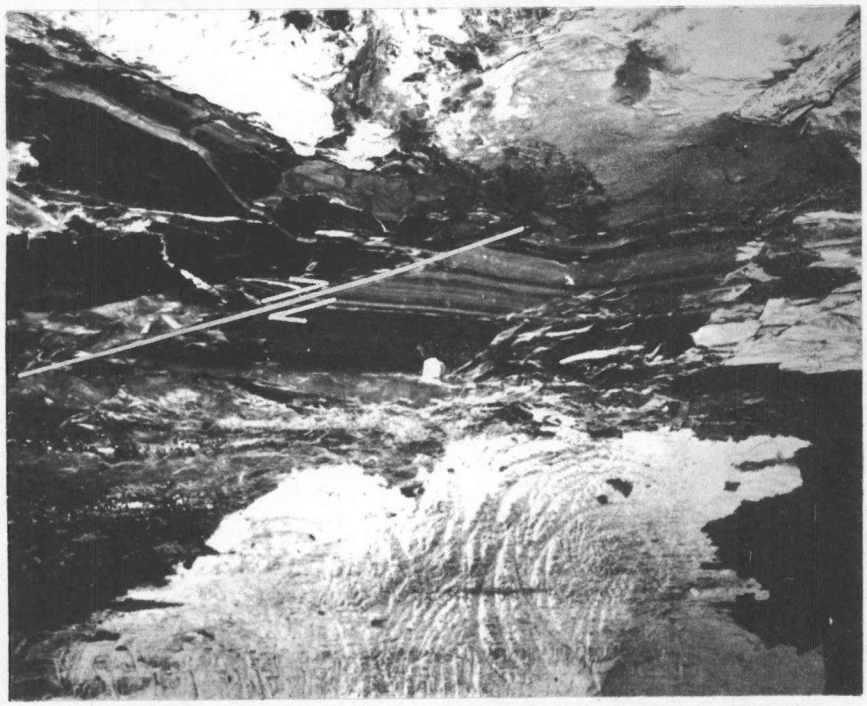

FIGURE 27. - "Slip" expressed as small reverse fault in immediate roof shale. Apparent stratigraphic separation (vertical displacement) about 12 inches. Location is old 004 Section, Highsplint mine.

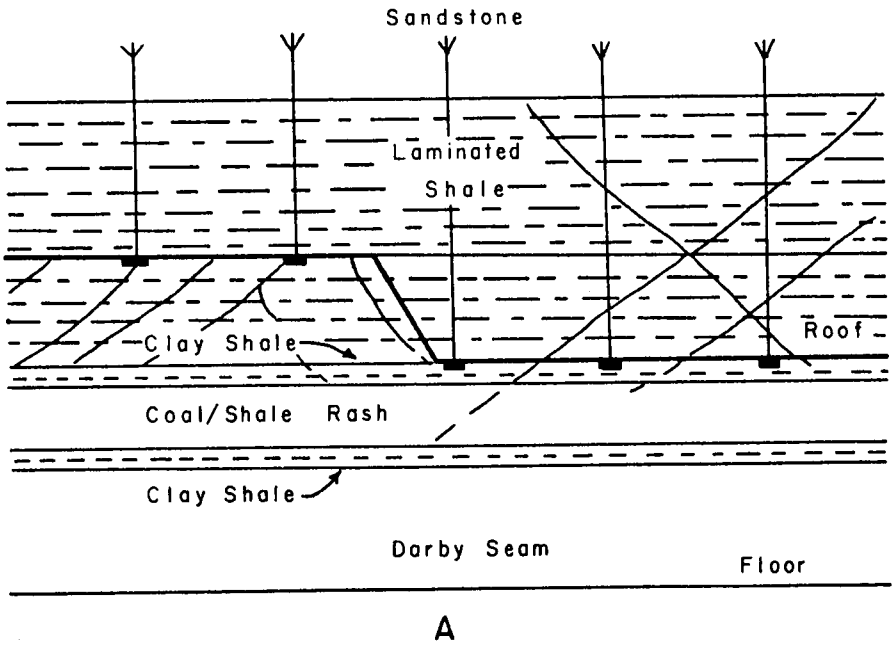

FIGURE 28. - Roof condition A. See text for explanation.

A somewhat different situation is present in the left half of Figure 28. "Slip" frequency in this case is greater in the basal part of the laminated shale. With this situation only the upper part of the immediate roof can be held.

Nonslickensided joints may also cause discontinuities in the laminated shales discussed above.

Roof Condition B (Laminated Shale)

Roof Condition B is similar to Roof Condition A in that laminated shales are involved. However, Roof Condition B indicates a situation in which a "slip" orientation is parallel to a bedding surface in the laminated shale. Horizontal "slips" show evidence of lateral movement in the shales by "crush zones" of chippy shale one half inch to one inch wide. It is apparently not possible to hold the laminated shale beneath a "slip" surface because the roof falls before bolts can be installed (Figure 29).

Roof Condition C (Rolling Sandstone with Shale in Pockets)

Represents a roof control problem associated with an uneven contact between the immediate roof shales and major sandstone roof above (Figure 30). (See also Figure 31). The contact may be partly erosional as evidenced by "reworked" sandstone containing carbonized plant debris and lithic fragments, or partly compactional resulting in shale "squeezes" (Figure 32). Both erosion and compaction form horsebacks in the roof. Numerous "slips" are usually generated in the immediate roof

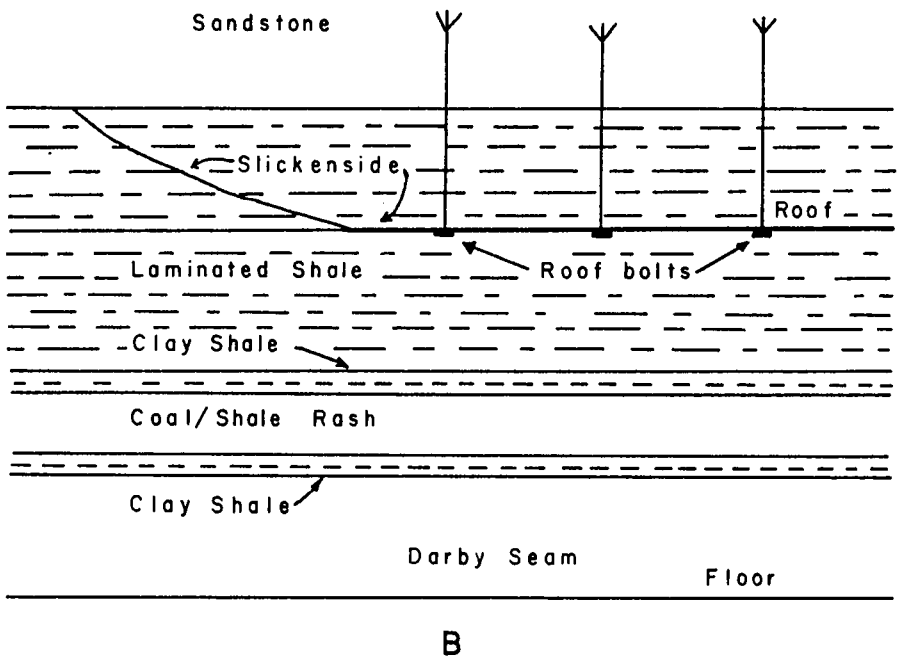

FIGURE 29. - Roof condition B. See text for explanation.

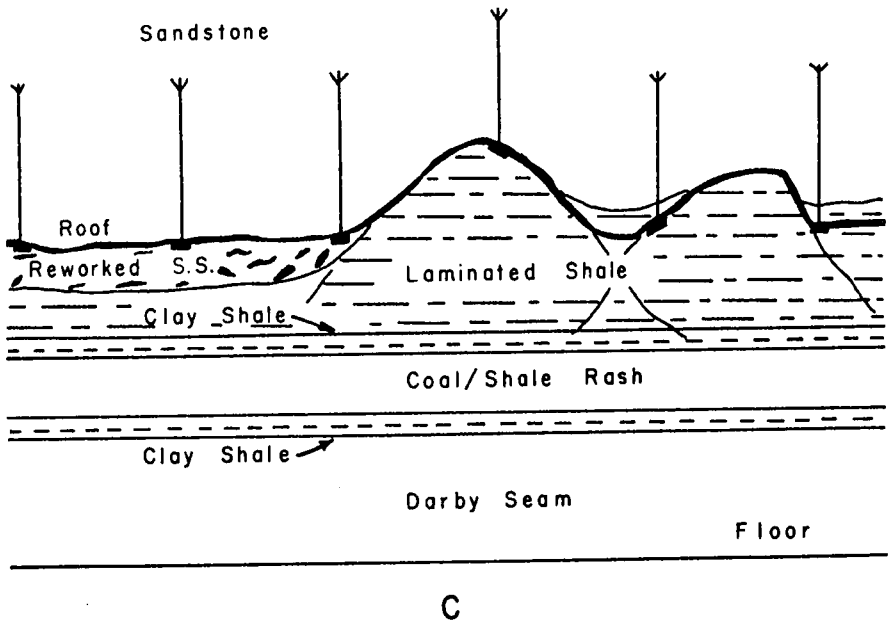

FIGURE 30. - Roof condition C. See text for explanation.

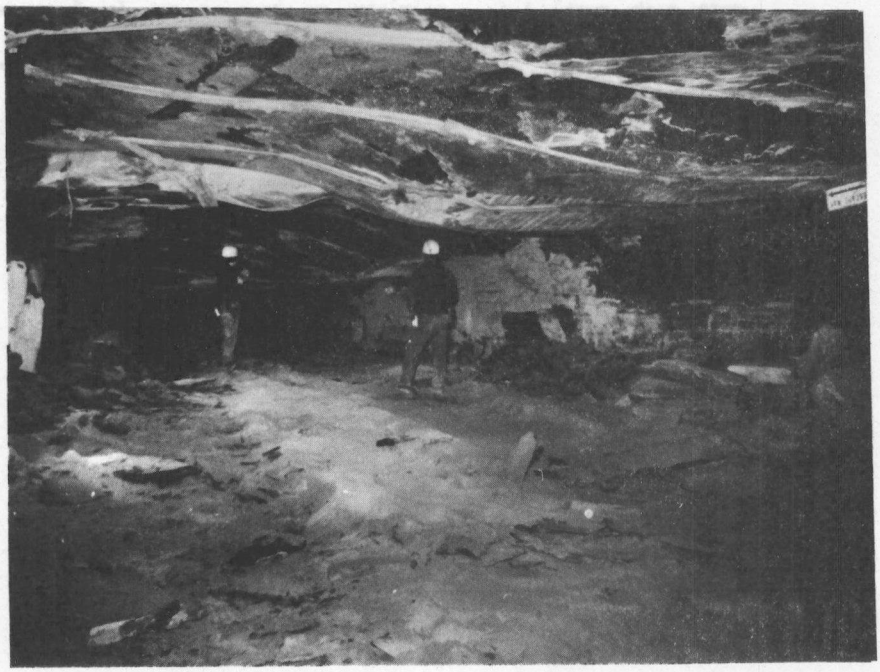

FIGURE 31. - View of rolling sandstone roof in the old 004 Section, Highsplint mine (location coordinates 0-15 Figure A1, Appendix A). (Roof condition C)



FIGURE 32. - View of roof-fall zone in the old 004 Section, Highsplint mine. Note contorted laminated shale unit with black "slips" or slickensided surfaces between sandstone rolls. (Location coordinates 0-15 on Figure A1, Appendix A). Roof bolt plates are about 12 inches long for scale. (Roof condition C)

shales beneath rolling sandstone roof causing difficulty in roof support. However, some shales may be held between sandstone rolls in narrow zones or pockets.

Roof Condition D [Zone of Major Sandstone Roll(s)]

This is actually an exaggeration of Roof Condition C and represents a sandstone roll that usually occurs marginal to an area of rolling sandstone roof (Figure 33).

According to Williamson (89), downward projections of the main roof, usually consisting of sandstone or conglomerate, may be classified into two categories. The first, washouts, are those areas of seams where the coal has been entirely or partly removed by erosion. Washes, wants, dumb-faults, stone dikes and horses are other terms applied to washouts. The second category of downward projection of clastic sediments is referred to as a roof roll or simple washout (also rock roll or nip). Roof rolls differ from washouts in that the roof roll may only replace the upper layers of the coal bed, or may be separated from the coal bed by immediate roof strata (64).

Major sandstone rolls in the Highsplint mine occur in an area of major erosion of the underlying shales during or shortly after deposition of the roof rocks, or represent sand deposition in a topographic low. Erosion is indicated by the abrupt truncation of the shales against the sides of the roll (Figure 34). However, in some cases, marginal shales are highly disrupted and contorted and bend down under the sandstone. This situation probably represents soft-sediment slumping and/or

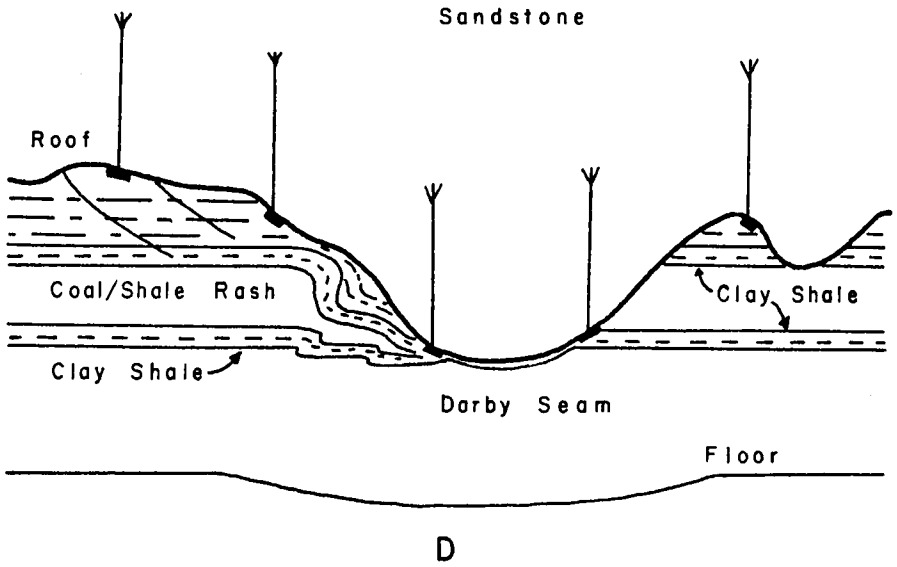

FIGURE 33. - Roof condition D. See text for explanation.

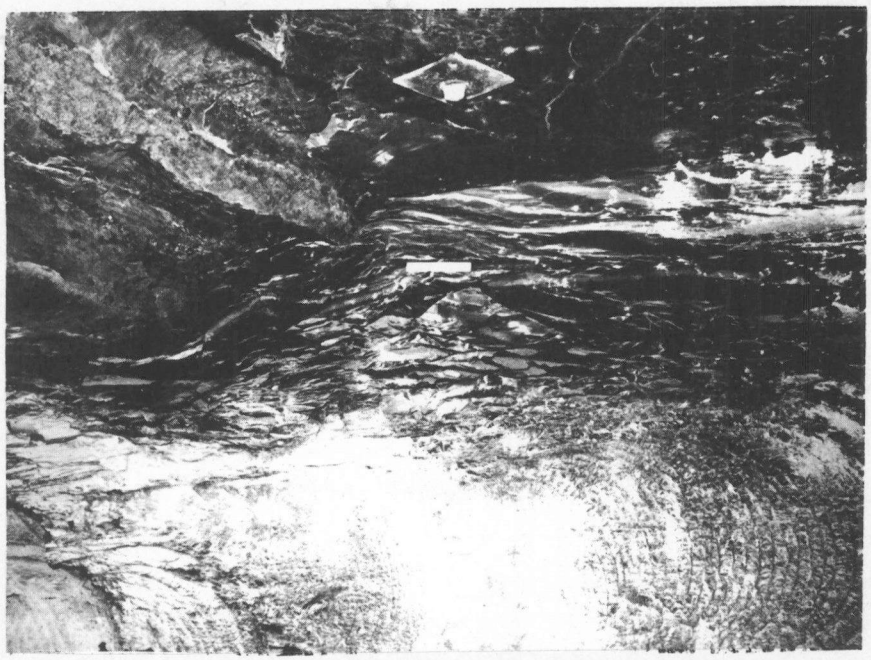

FIGURE 34. - Erosional contact between laminated immediate roof shale and overlying sandstone roll indicated by abrupt truncation of horizontal shale. Note "slips" in shale in contact with the sandstone conforming to the base of the roll and striking parallel to the roll. "Slips" extend to position of six inch scale. Location is new 004 Section, Highsplint mine. Coordinates 5-12 on Figure A1, Appendix A. (Roof condition D)

compaction during sedimentation. In areas of major sandstone rolls the immediate roof is not generally supported. In fact, the roll usually extends down to the top of the coal. The sandstone rolls fit the description of washouts except that in this area of the mine, erosion did not extend below the top of the coal. Also, where sandstone rolls occur, the underlying coal and mine floor may dip under the roll. The major rolls are usually relatively narrow (30 feet to 80 feet), but evidence indicates that the linear trend of individual rolls or zones of rolls may extend for several hundreds of feet. The major rolls on outcrop appear to mark the axes of sand-filled channels and/or swales, some as much as 30 feet thick.

The best roof conditions in the survey area appear to include areas where the immediate roof shales are thin and are overlain by homogeneous sandstone with a relatively even basal contact.

Roof Composition Map

Figure 35 shows the Highsplint mine mapped on the basis of roof composition according to the classification scheme developed in this study. Control for lateral boundaries parallel to headings was based on traverses made through the mine supplemented by measured rib sections (see Figure A1, Appendix A, and Table B3, Appendix B). Areas on the map indicated as inferred were not accessible for a variety of reasons such as unsafe roof conditions, water flooding or possible insufficient air in abandoned areas. However, such areas were tentatively mapped on the basis of discussions with mine personnel who had worked in these areas,

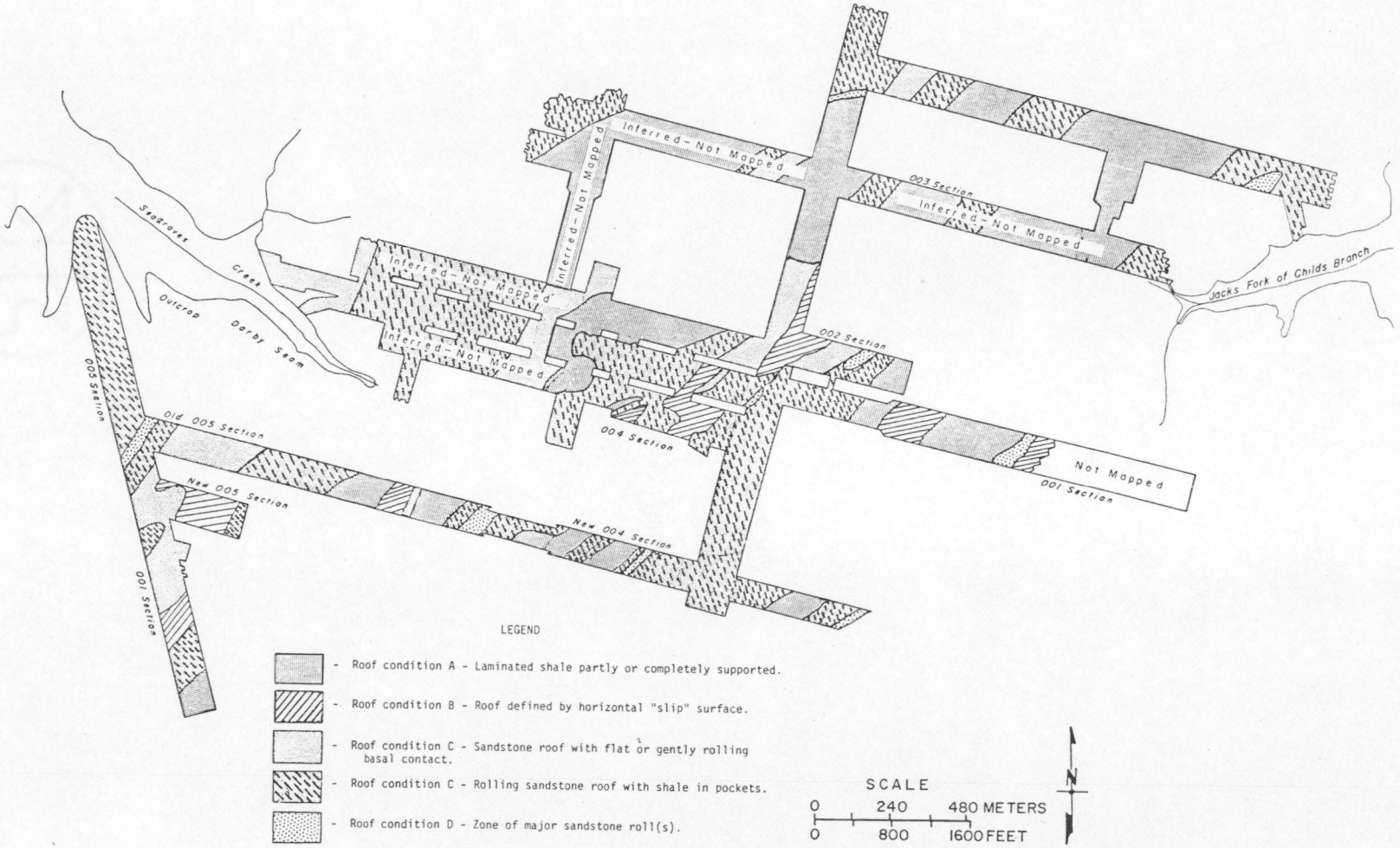

FIGURE 35. - Roof composition map, Highsplint mine.

together with boundary projections from adjacent mapped areas. Control across individual headings was based on traverses across headings together with the projected trends established by mapped sandstone roll bodies.

Structure Contour Map

As a normal procedure, engineering surveys are made as mining progresses and floor elevations are generally determined at every third crosscut using transit and stadia rod. For example, if the crosscuts are established on 80-foot centers, then an elevation point is determined at intervals of 240 feet. This spacing provides excellent control for drawing structure contours on the base of the coal being mined. Figure 36, which shows structure contours drawn on the roof composition map as a base, was prepared using elevations provided by Eastover Mining Company.

The resulting map indicates the following:

1. The strike of the rocks in the mine are generally NE-SW, which coincides reasonably well with the NE-SW regional structure. The dip of the rocks is toward the northwest.

2. A structural low is evident in the central part of the mine. Elevations near the center of the structural low are at about 1,665 feet.

3. The strike of the rocks in the mine generally coincides with sandstone trough axes and in some cases the floor dips under a sandstone roll forming a linear trough that parallels the sandstone roll axes. Also roof-rock composition and thickness comparisons (see discussion, page 72) suggest that the thickest shale roof areas coincide with the structural low discussed above and also in the relatively level area

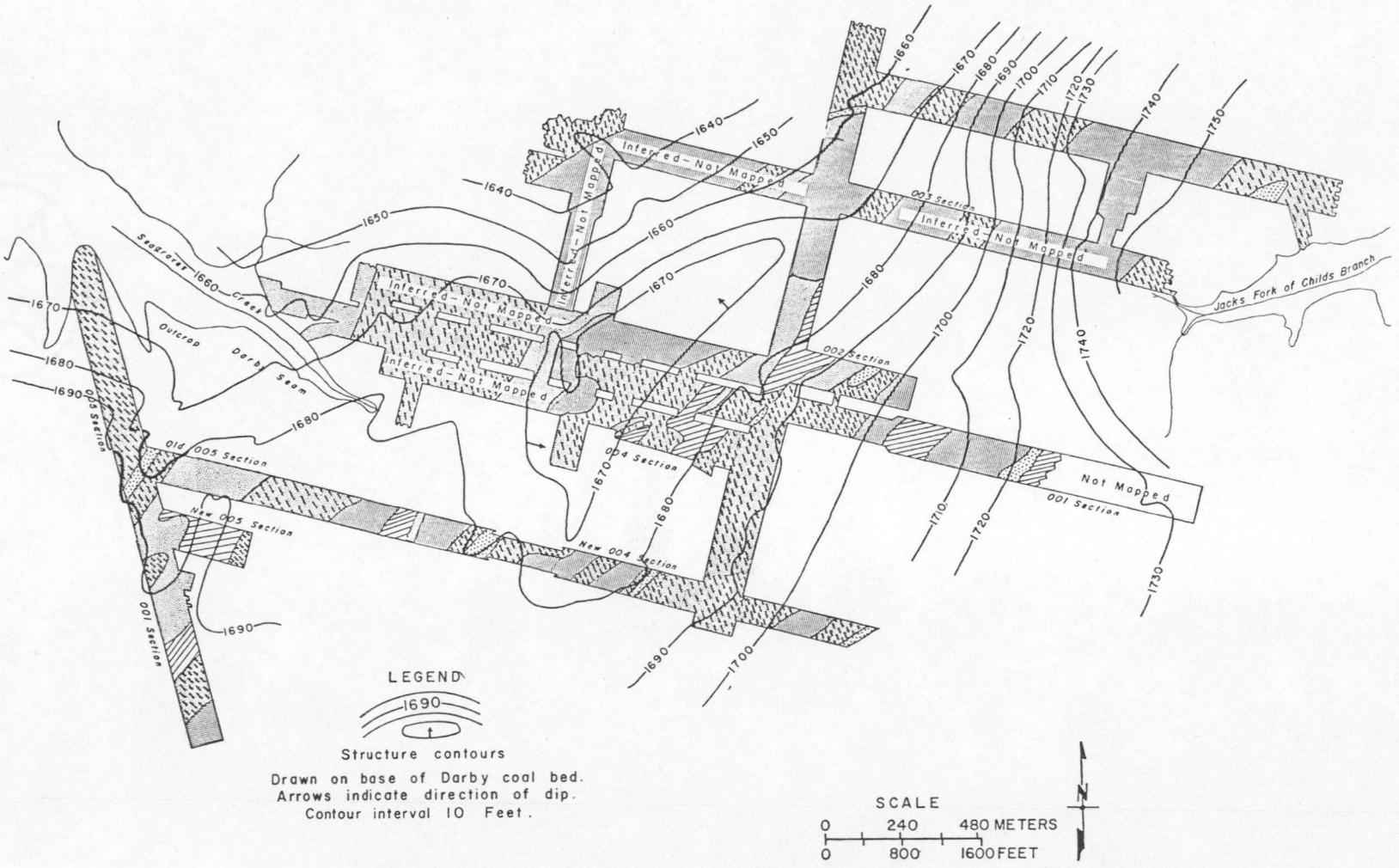

FIGURE 36. - Structure contour map drawn on the base of the Darby coal bed, Highsplint mine.

immediately west of the Not Mapped area (001 Section) in the vicinity of the 1700 and 1720 contours. Although perhaps coincidental, this evidence suggests that the structure contours reflect not only the local and regional structure, but also topographic conditions during deposition.

Isopach Map - Darby Coal Bed and Claystone/Coal Rash

Figure 37 is an isopach map of the Darby coal bed. The 87 data points for its preparation are partly from measured rib sections and partly from coal sections supplied by Eastover Mining Company (see Figure A1, Appendix A). The Darby coal bed is relatively uniform in thickness, generally ranging from about 26 inches to as much as 48 inches. Locally, however, the Darby has been observed to be only about seven inches thick under sandstone troughs. The isopach map (Figure 37) indicates only a general relationship to the roof composition map used as a base. However, slightly greater coal thickness appears to coincide with areas of relatively thick immediate roof shales.

Figure 38 is an isopach map of the claystone and coal rash portion of the immediate roof based on 93 data points from measured rib sections and data from Eastover coal sections (see Figure A1, Appendix A). The relationships indicated by the Darby coal bed isopach map are also shown by the claystone/coal rash map. Generally, areas of the mine with thicker claystone/coal rash thickness coincide with shale roof conditions and greater Darby coal bed thicknesses.

The relationship of areas of thicker coal (Figure 37) and areas of thicker claystone/coal rash (Figure 38) coinciding with areas of thicker

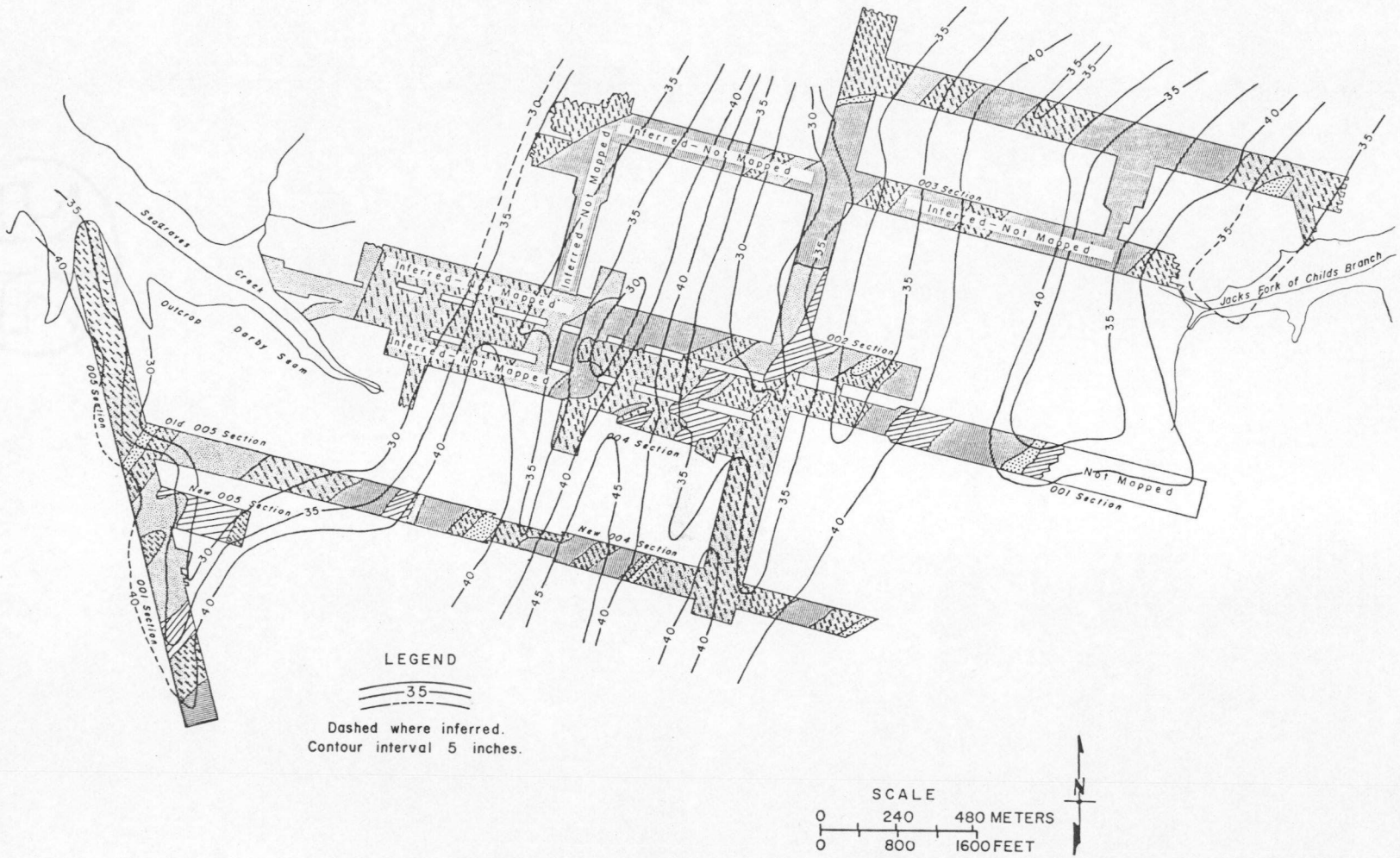

FIGURE 37. - Isopach map of Darby coal bed, Highsplint mine. Roof composition map used as base.

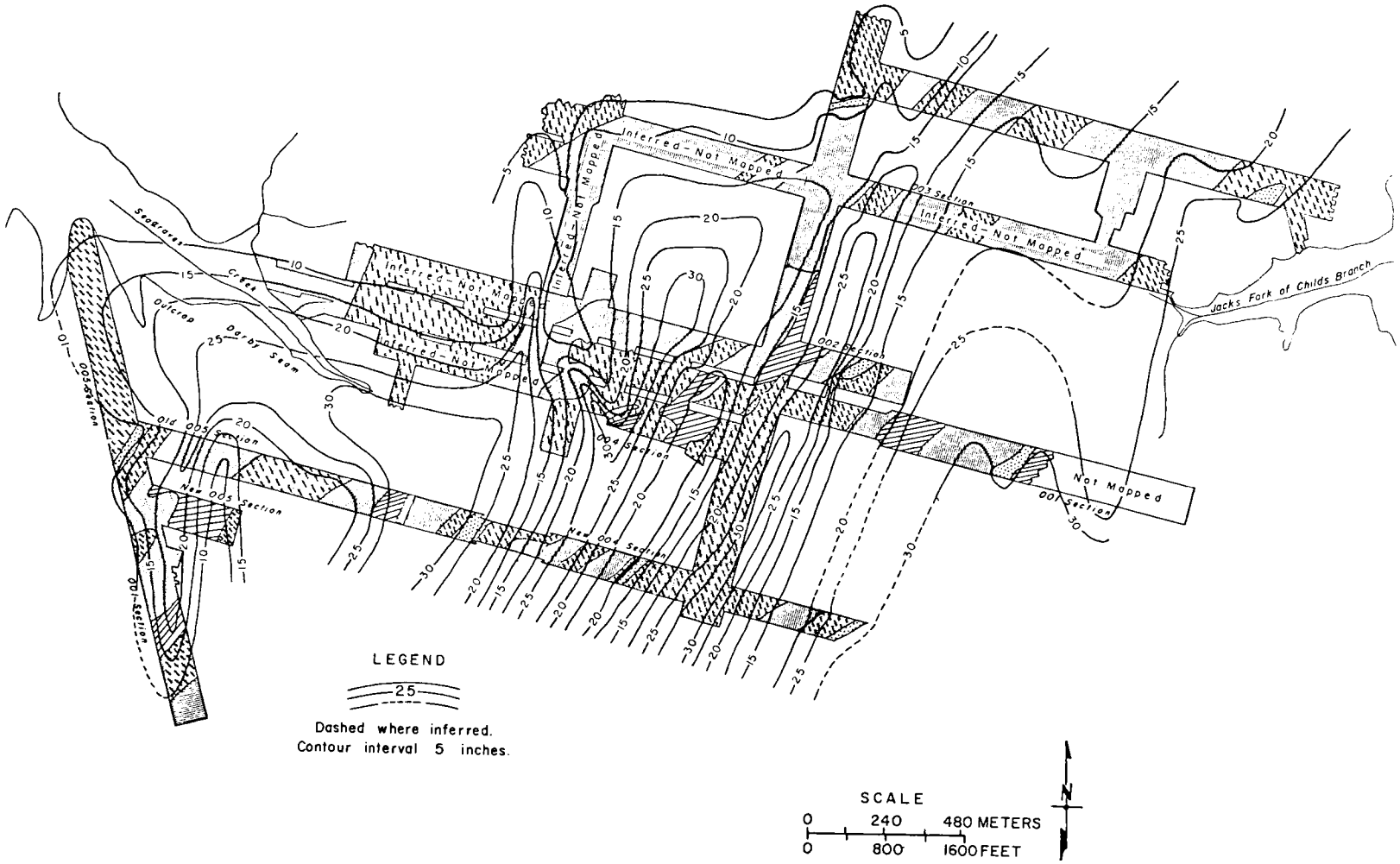

FIGURE 38. - Isopach map of claystone/coal rash, Highsplint mine. Roof composition map used as base.

total immediate roof shales suggests that these areas were topographic "lows" during deposition and were more favorable accumulation sites for peat and mud. (See discussion, page 80).

Immediate Roof Isopach Map

The total immediate roof thickness from the top of the Darby coal seam upward to the main sandstone roof (see Figure 1, page 4) was determined from measured rib sections (locations shown in Figure A1, Appendix A, and values indicated in Table B3, Appendix B). Immediate roof units include claystone, coal rash, and laminated shale. Table B3, Appendix B also indicates whether the main roof was sandstone or shale. In some instances, it was necessary to estimate the shale thickness to the main sandstone roof. Estimated shale thickness was based on roof bolt length. Company policy for conventional bolting is to use roof bolts long enough to anchor in at least two feet of sandstone. Thus, if four-foot bolts were used in an area, it was assumed that the shale thickness was two feet.

The immediate roof isopach map (Figure 39) was prepared using an isopach interval of 20 inches, and trend interpretation was based on several sandstone roll axes. The thickness isopachs are shown drawn on the roof composition map as a base, allowing comparisons of immediate roof thickness to be made with the composition map as follows:

1. There is generally good agreement between areas of relatively thick immediate roof and shale-roof areas in the mine. Conversely, thin immediate roof areas are reflected by sandstone rolls. In fact, lateral

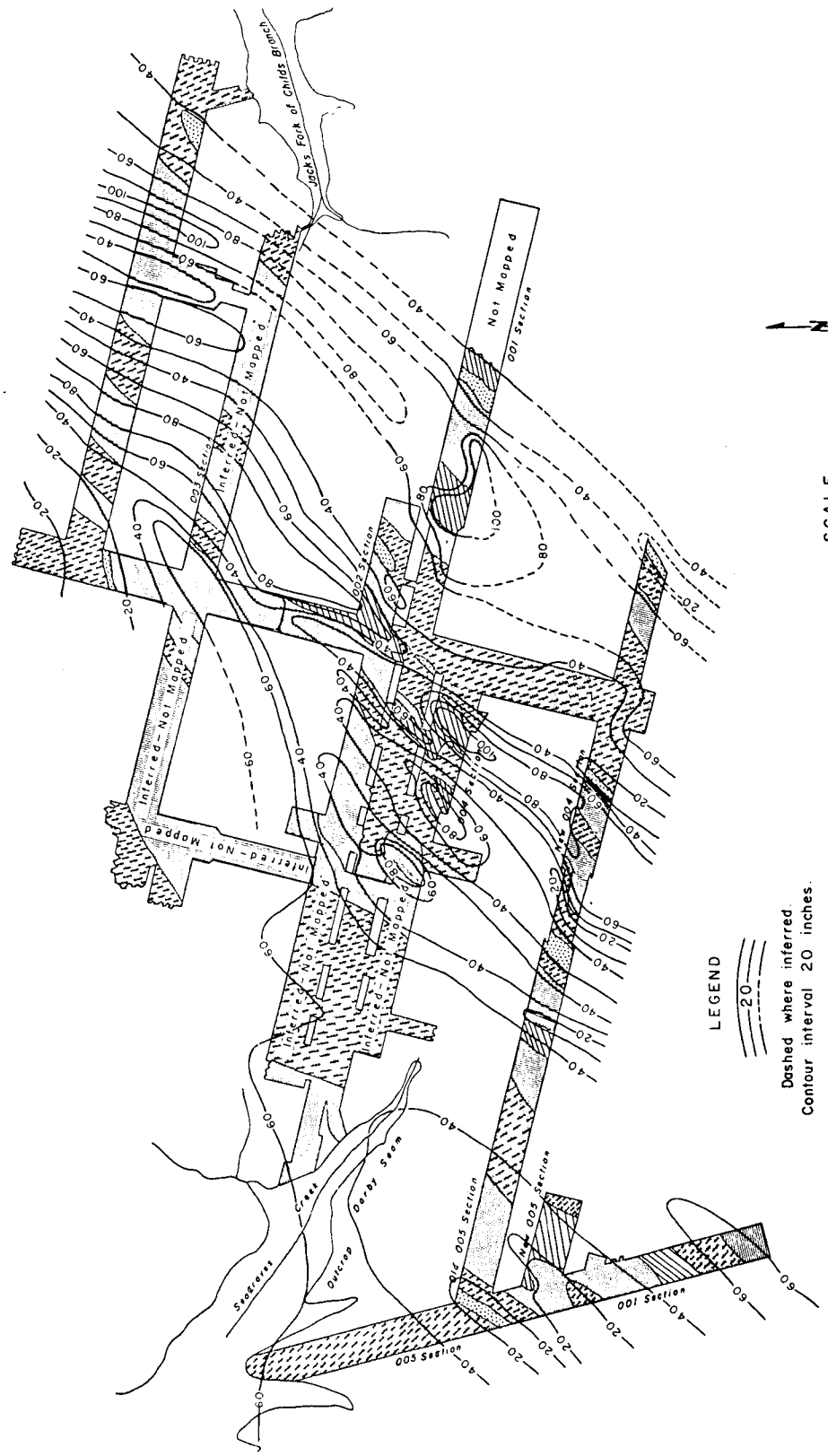

FIGURE 39. - Isopach map of immediate roof rocks in the Highsplint mine. Roof composition map used as base.

changes from thick to thin immediate roof areas are usually in the order—shale (Roof Condition A or B), to rolling sandstone roof with shale in pockets (Roof Condition C), to major sandstone rolls (Roof Condition D).

2. By combining immediate roof isopach lines on the roof composition map it is possible to project specific roof-rock types from one section of the mine to another.

Sandstone Trough-Axis Projection Map

In order to extend projections of roof composition using isopach data, Figure 40 was constructed. First, sandstone trough axes were plotted through relatively thin immediate roof areas using isopach data as a guide. It was found that by arbitrarily omitting all isopach contours of less than 60 inches, the roof composition map was essentially divided into two types. For thickness values of less than 60 inches the roof is composed almost entirely of major sandstone rolls (Roof Condition D, Figure 33, page 63) and gently rolling to rolling sandstone with shale in pockets (Roof Condition C). The remaining areas, greater than 60 inches, coincide essentially with shale roof rocks (Roof Conditions A and B).

It should be noted from Figure 40, showing only isopach lines of 60 inches or greater, that almost all sandstone trough axes were mapped in areas of the mine where the immediate roof is less than 60 inches in thickness. However, several axes are included in areas where the

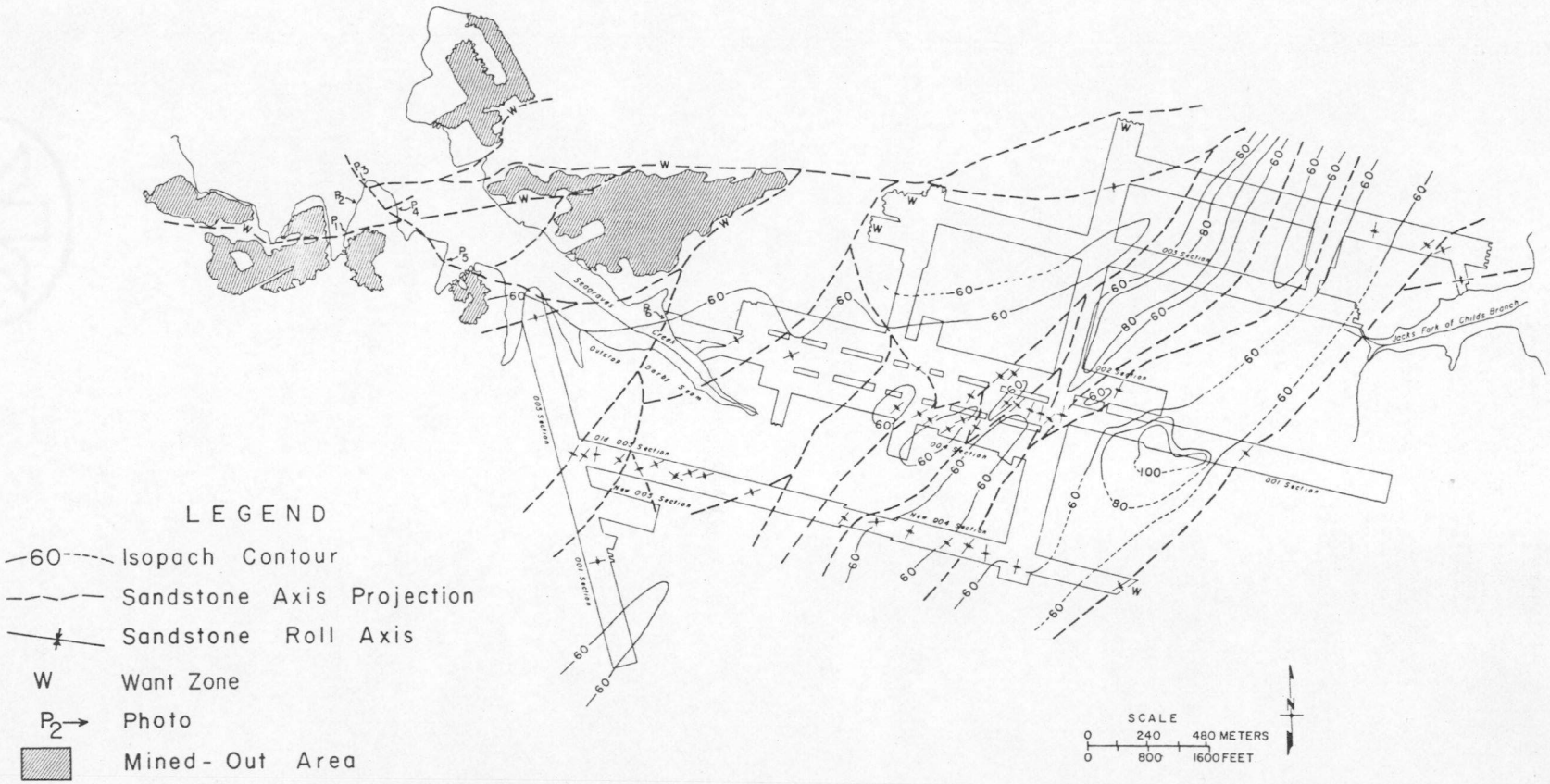

FIGURE 40. - Sandstone axis projection map. Also shown are areas enclosed by isopach lines where the immediate roof is greater than 60 inches thick.

immediate roof thickness exceeds 60 inches in thickness. This relationship is especially evident in the old 004 Section of the mine. Here the sandstone rolls are essentially the result of differential compaction, and are not erosional.

Also included in Figure 40 are sandstone trough axes projections along Seagraves Creek. These projections are based on two sources of data. First, the areas labeled W are want zones or washouts representing major sandstone rolls that were encountered during mining and were large enough to curtail advancement. Some of the want zones were in abandoned works, and their locations were verified by discussions with mining personnel. Also, data for trough axes were obtained from surface outcrop exposures along Seagraves Creek and areas marginal to the mine entrances of the Highsplint Darby mine. Outcrop data included cross-bedding and trough axes position and trend (location Darby A). From these data, sandstone axial trends were plotted. The resulting axial trend projections along Seagraves Creek are in good agreement with those plotted in underground mapping in the Highsplint mine. (See discussion, page 134).

Relationship of Roof Type and Thickness to Roof Falls

In order to evaluate the interrelationships between the structure contour, roof composition and isopach maps discussed above, a profile of the 003 Section was prepared (Figure 41). The 003 Section is representative of roof conditions found in the remainder of the mine because all roof categories are present. Also, roof conditions range from

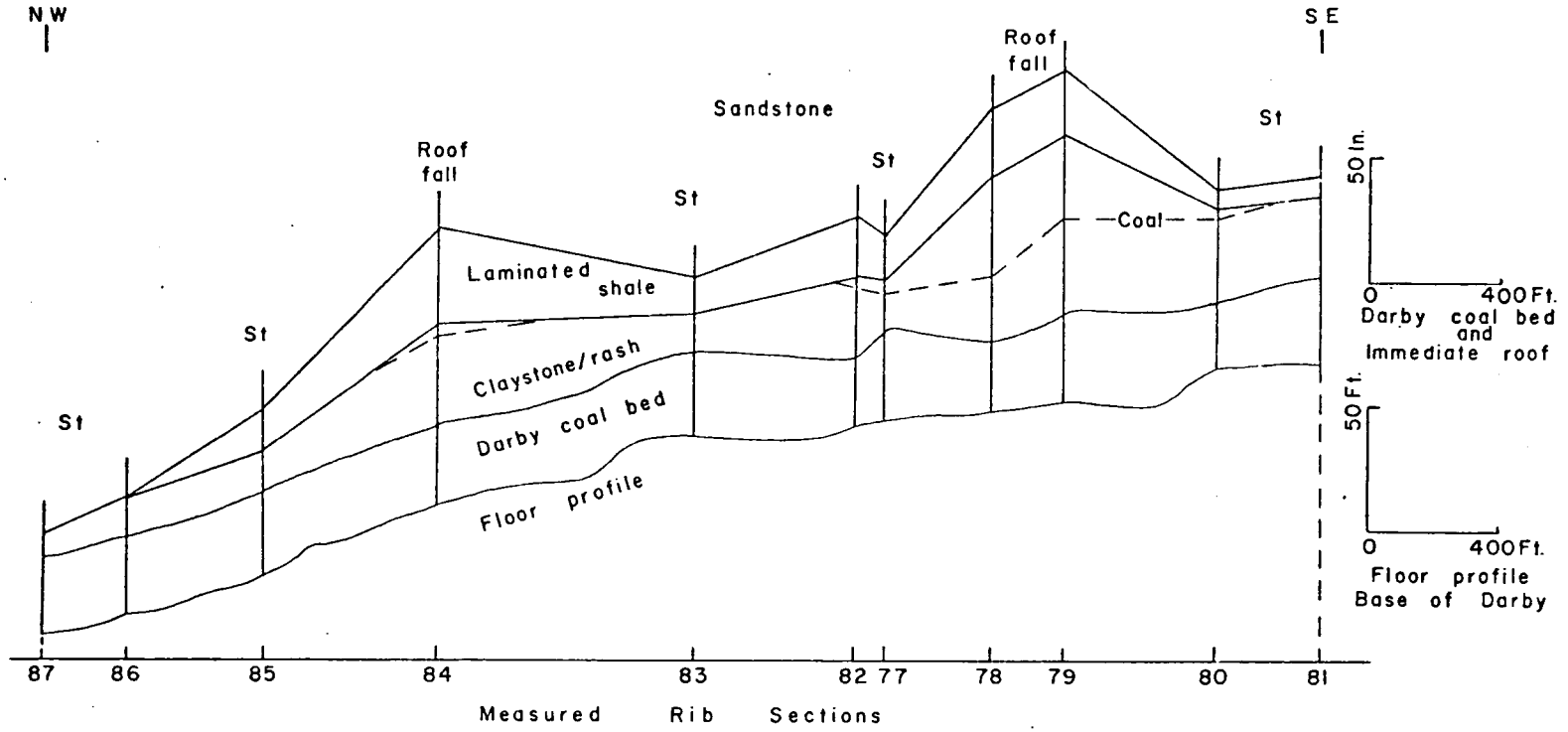

FIGURE 41. - Profile of 003 Section, Highsplint mine. St represents sandstone trough positions. Note that two different vertical scales are used to emphasize details of immediate roof and compare Darby coal bed to floor profile.

"good" to "bad", so comparisons could be made as to roof stability versus roof-rock conditions.

The profile was prepared as follows: First, the profile of the base of the Darby coal bed was drawn from mine map elevations using a vertical scale of one inch to 50 feet. Eleven rib sections, 77 through 87, were measured upward from the base of the Darby coal bed and plotted using a scale of one inch to 50 inches in order to emphasize details (location map, Figure A1, Appendix A). Using the same procedure as was used in preparing the immediate roof isopach map (Figure 39, page 73), the thickness to the main sandstone roof was estimated from roof-bolt length for about half of the measured sections. No estimate was needed for sections 86, 87, 79, 80, 81 and 84 because the main roof was visible.

Evaluation of the resulting profile section (Figure 41) indicates the following:

1. The floor profile is variable. The floor steepens appreciably between sections 85 and 83, becomes more level and rolling between sections 83 and 80 and steepens rather abruptly just northwest of section 80. (See structure contour map, Figure 36, page 68).

2. Total immediate roof thickness increases abruptly and coincides with flexures in the floor just northwest of section 83 and again just northwest of section 80. Both of these areas of thick immediate roof are "bad roof" zones, where roof falls extend upward to the main roof.

A comparison of the roof-fall zones shown in the 003 Section profile (Figure 41) with Figure 42 indicates that these areas are evident on the outcrop.

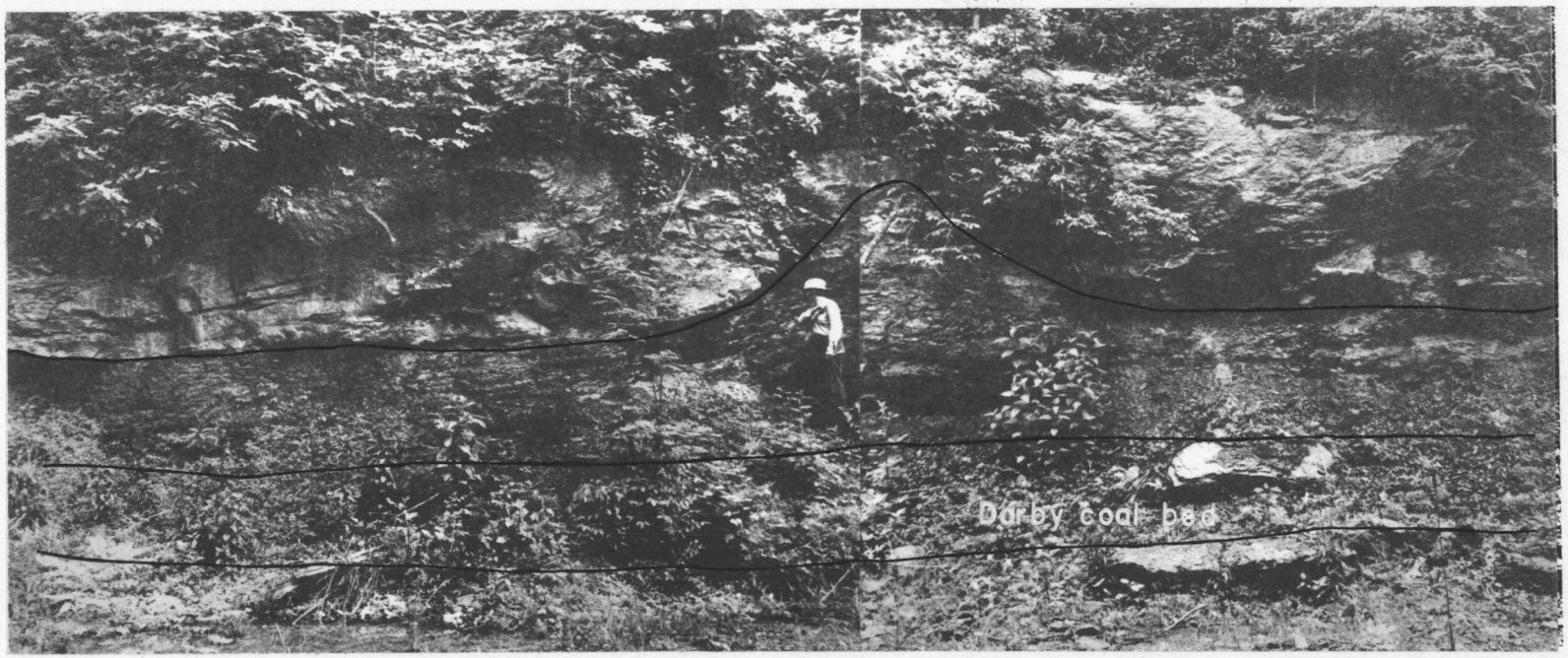

FIGURE 42. - Photographic mosaic of shale "horseback." Location is Darby strip bench at Highsplint mine (designated P_5 on Figure 39, page 75).

discontinuities in rock.

- rock
- planes of weakness
- jointing
- faults
- cleavage

3. Noticeable thickening of the Darby coal bed occurs in section 79, coinciding with thick immediate roof shales, and also topographic "lows" in the floor profile.

4. The claystone and coal rash portion of the immediate roof thickness coincides with laminated shale thicknesses. This suggests the genetic relationship discussed previously. This relationship is indicated also by the presence of the thin rider coal bed in areas of greater immediate roof thickness.

5. Areas indicated as St. in Figure 41, page 77, are sandstone trough axes (see also Figure 40, page 75). Roof conditions in these areas are generally good, especially in the vicinity of section 87. However, southeast of section 81 some difficulty with holding the immediate roof shales was noted (Roof Condition C).

Conclusions

Analysis of the profile indicates two areas of rather abrupt thickening of the immediate roof flanked on both sides by sandstone troughs. Beginning with section 77, the main sandstone roof becomes progressively lower (with the exception of section 84) until it locally rests on the Darby coal bed in the vicinity of section 87. Also, the want area just northwest of section 87 indicates that sandstone partly or entirely replaces the Darby.

The lateral relationship of immediate roof thickness and main sandstone roof trends discussed above can be detected in most of the other parts of the mine.

An effective mapping program in an underground mine is difficult, especially where drill core information is limited. Apparently insignificant information may be found later to contribute greatly to an understanding of roof control and general mining conditions. During the course of this study, the kinds of in-mine information that are useful have been identified. As a result, Table B4, Appendix B, was prepared as a proposed "checklist" for underground mapping. Not all of the information on the checklist is appropriate in every case, and specific mines with different roof lithologies may require different treatments. Also, the primary objective of the study, the amount of supporting information available, and the time available for mapping would partly determine the amount of detail desired.

IV. THE BAILEY CREEK MINE

General Relationships

Figure 2, page 7, shows the location of the Bailey Creek mine. The general stratigraphic relationships are shown in Figure 5, page 14 and Figure 6, page 15.

The holding characteristics of the roof in the Bailey Creek mine are unique. For the first 2,000 feet into the mine (Figure 43), the roof is generally stable except for two roof falls that are apparently joint controlled (localities BP_5, BP_6, and BP_7). Along the No. 1 heading of N50°W, however, five large falls have occurred (Figure 43). All of these falls occurred in the headings, and most falls included strata up to the rider seam above the Harlan coal bed.

Investigations in the Mine

During roof-fall investigations in the Bailey Creek mine, it was observed that the vertical stratigraphic interval between the Harlan coal bed and the overlying rider seam differed from the interval at the mine entrance. First, the interval was thicker than that observed at the mine entrance (20 feet as opposed to 12 feet). Secondly, the interval was largely occupied by sandstone instead of shale and siltstone. Also, abrupt erosional contacts were noted in the roof rocks in several fall areas (Figure 44).

These areas were tentatively identified as narrow, sand-filled channels. Further, the strike of the cross-beds of the channels was

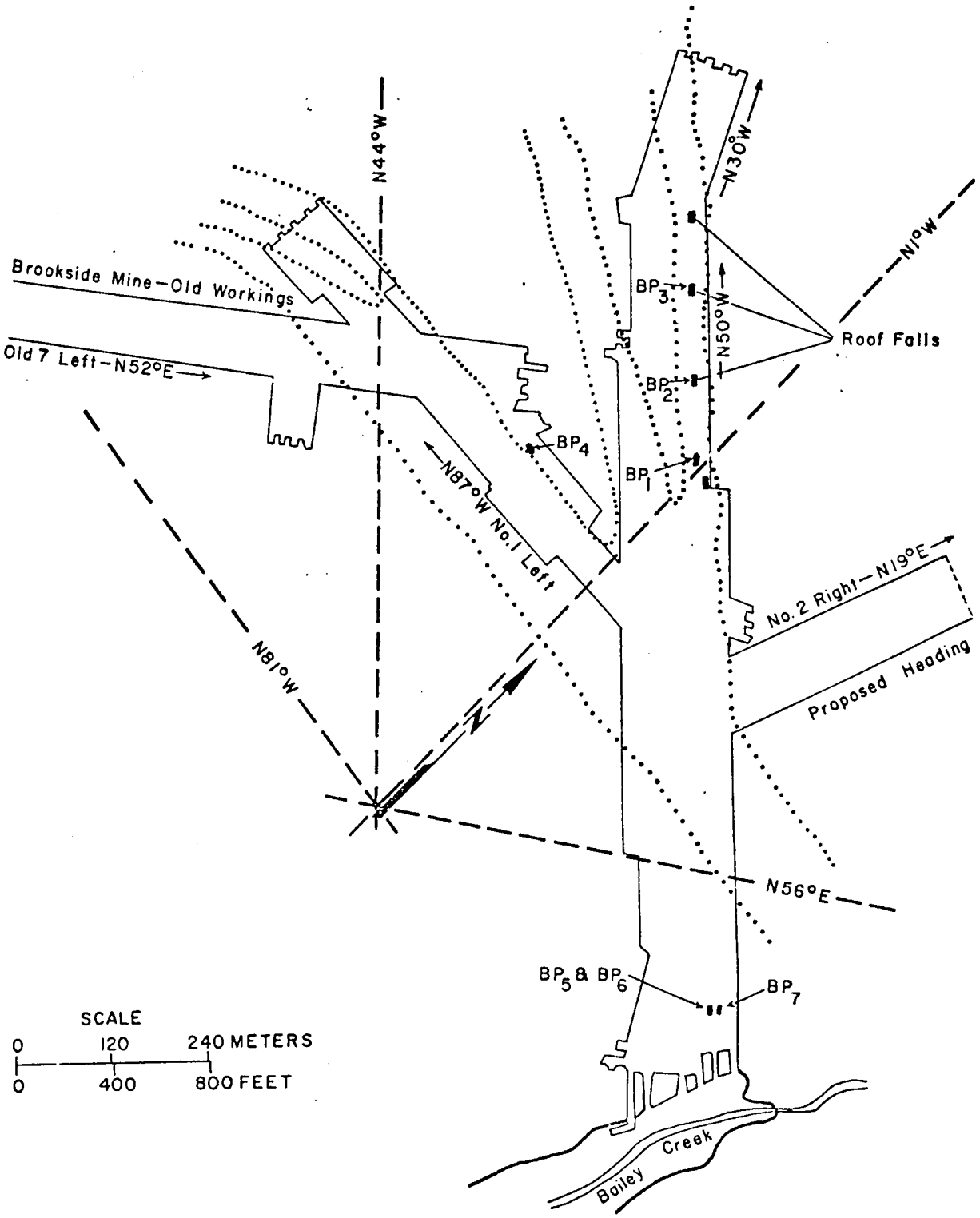

FIGURE 43 - Bailey Creek mine map showing probable position of sand-filled channels (dotted lines) and projected 4-set joint means (dashed lines). Also shown are photograph locations (BP_1).

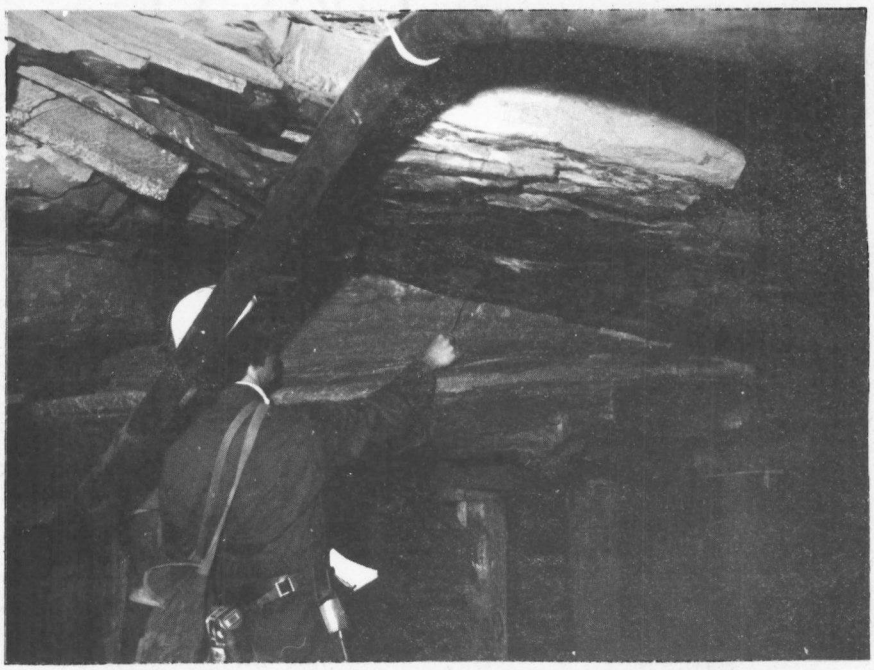

FIGURE 44. - Well defined erosional contact between immediate roof rocks (horizontal) and channel in the Bailey Creek mine. Location designated as BP_1 in Figure 43.

subparallel to the heading of N50°W to about N80°W (Figures 43 and 45). The channel trend was also substantiated by current-directional features (flute casts) on the base of the sandstone.

Because surface outcrop exposures are very limited at the Bailey Creek mine, the Harlan-rider seam interval was studied at Brookside (Figure 2, page 7). At that locality, sand-filled channels were observed overlying the Harlan coal bed, confirming the presence of channels (Figure 46).

Joint Observations

Figure 47 shows a comparison between circular histograms of surface joints at locality Darby E (see discussion, page 162) and composite joint observations taken during underground mapping in the Bailey Creek mine. Surface joints indicate a major northeast joint set (mean N50°E), and two other less frequent sets toward the northwest (N40°W and N70°W).

The N50°E joint set coincides with the face cleat inside the mine (mean N61°E) and the N40°W set parallels the coal butt cleat (mean N36°W). These trends were also observed within the mine. However, the N1°W mean joint set observed underground is reflected in only one observation on the surface. This is likely due to the fact that only 15 joint observations were possible at locality Darby E because of the poor exposure. With a few surface observations, however, it was possible to delineate dominant joint trends within the mine from surface observations.

Reference to Figures 48 and 49 shows strong evidence of joint controlled roof falls in the Bailey Creek mine. The location of the falls



FIGURE 45. - Dipping roof rocks in the Bailey Creek mine. Trend of entry (N50°W) subparallel to strike of roof rocks. supporting roof beam about 20 feet long. Location designated as BP_2 in Figure 43.

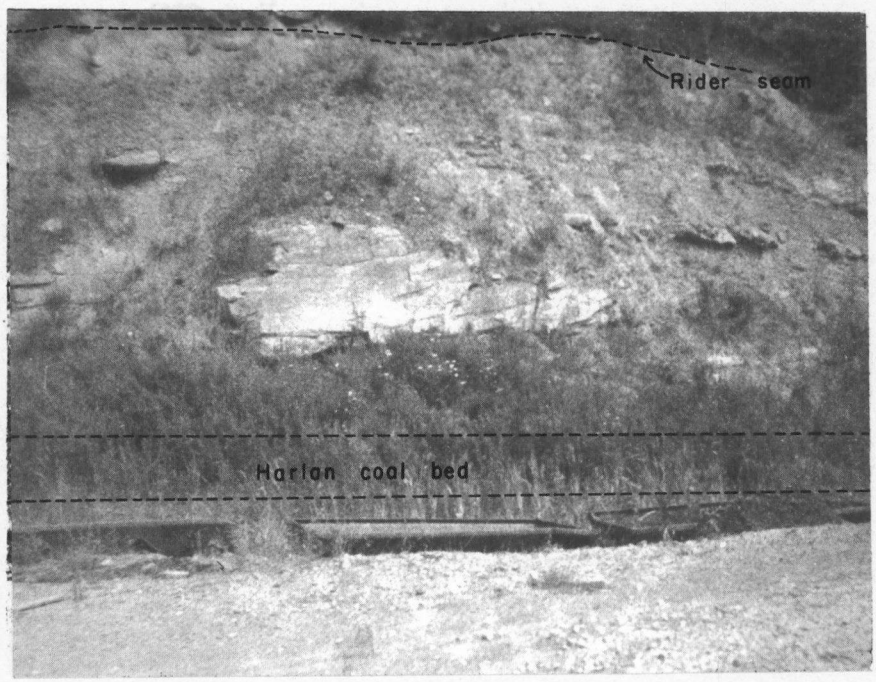

FIGURE 46. - Sandstone body between Harlan coal bed and rider seam at Brookside, Kentucky. Coal cars are about 12 feet long for scale.

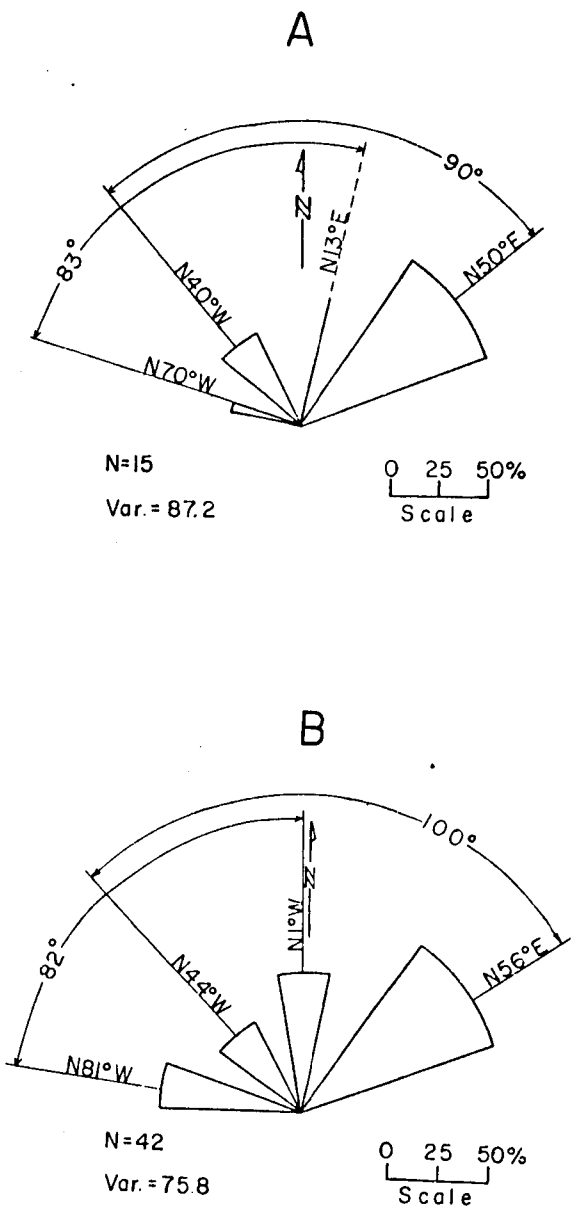

FIGURE 47. - Four mode Independent Mean program circular histograms (A) of surface joints (location Darby E) and underground joints at Bailey Creek mine (B).

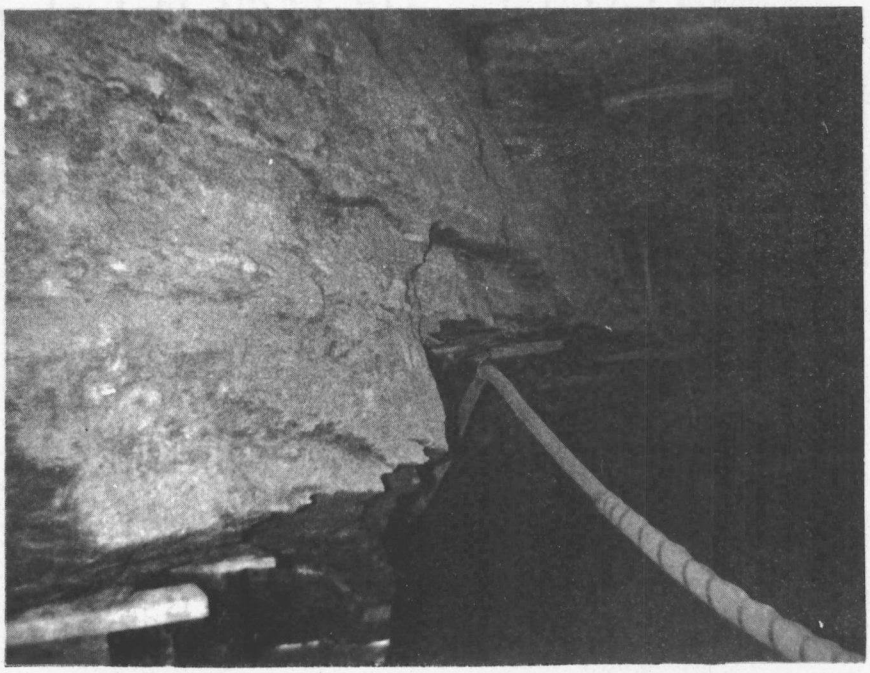

FIGURE 48. - View of weathered joint surface in roof-fall area four breaks inside the Bailey Creek mine. Location is BP_5 in Figure 43, page 83. Height of joint surface about four feet.

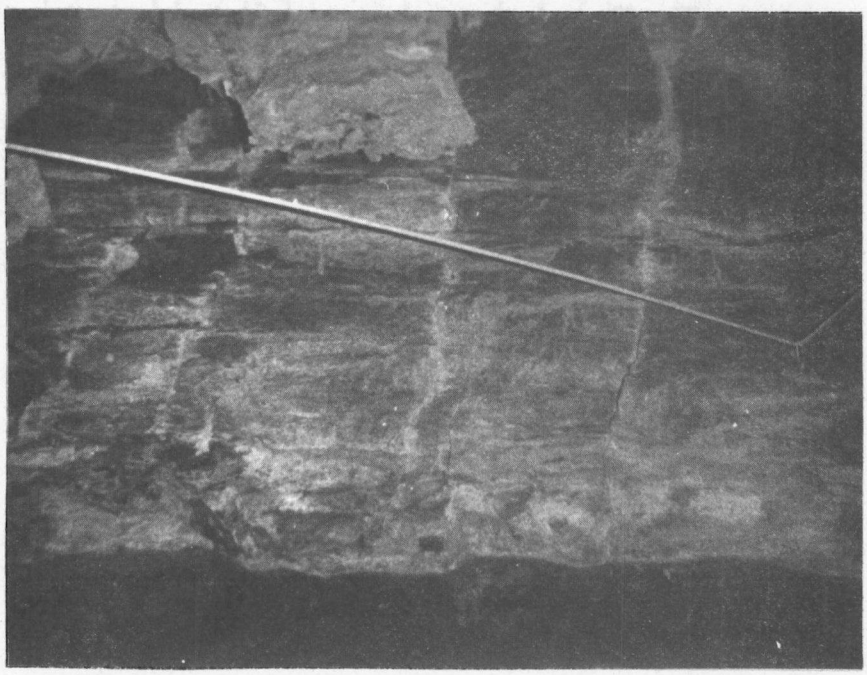

FIGURE 49. - Traces of weathered joints in roof-fall area four breaks inside the Bailey Creek mine. Joints are spaced about one foot to three feet apart. Location BP_6 in Figure 43, page 83.

is shown in Figure 43, page 83. The falls are bounded by weathered joint surfaces, and the overburden thickness at these fall sites is about 200 feet. No examples of weathered joints were observed in other parts of the mine under a greater thickness of overburden.

In order to relate underground jointing to the mine layout, the histogram mean directions in Figure 47, page 88, are shown superimposed over the mine outline in Figure 43, page 83.

Mine Progress and Recommendations

Just as this study began, attempts were made to turn the mine heading in a more favorable direction. Figure 43, page 83, shows that the heading changed from N50°W to N30°W. Roof conditions improved somewhat, but at the same time a resin bolting program was initiated as the heading was turned and it could not be determined if the improved roof conditions reflected resin bolting or the change in heading direction relative to channel trends.

Based on observations in this study, recommendations were made to the company to avoid the N30°W to N80°W directions for headings, and a heading of about N15°W to N20°W was recommended.

However, it was necessary for the company to drive a heading of N87°W (Left No. 1) in order to intersect the Brookside heading and retrieve mining equipment blocked by falls (Figure 43, page 83). Roof conditions along this heading have gradually deteriorated and present roof stability is probably due largely to resin bolting.

Because of the desire on the company's part to turn a northeast heading (Right No. 1), recommendations were made to drive in a direction of N20°E. This direction avoids joint sets (Figure 43, page 83), and will hopefully avoid channels in the roof. It is likely that under considerable overburden (+600 feet), driving headings parallel to channels is likely to be more detrimental than driving parallel to jointing (26). At the time of this writing, mining has just begun along this heading with stable roof conditions reported.

Geologic Conditions and Roof Control

The rocks adjacent to ancient stream channels are characteristic of shallow water cyclic deposition of laminated shales with increasing amounts of fine-to medium-grained sandstones upward (Figure 50). The shales contain some very large fossil tree trunks. These kettlebottoms, as much as four feet in diameter, were observed in the roof and in roof-fall debris (Figure 25, page 51) and casts of plant fossils 20 feet in length and four feet in diameter are preserved in the roof at the top of roof-fall areas.

Physically, the roof rocks are dense and brittle. The thin-bedded nature of the sandstones provides poor anchorage for roof bolts, especially when interbedded with shale. Also, the presence of the rider coal seam eight feet to ten feet above the Harlan coal bed contributes greatly to roof instability. Conventional roof bolts used in the Left No. 1 heading are four feet and/or five feet in length, spaced on approximate four foot centers. Better roof control might be possible if

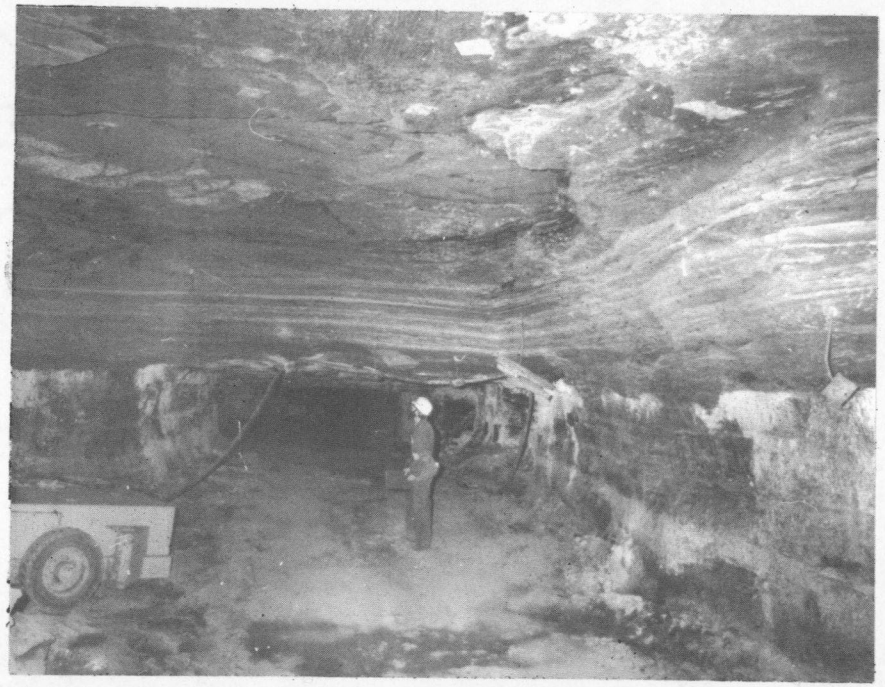

FIGURE 50. - General view of roof-fall area in the Left 001 Section, Bailey Creek mine. Note interbeds of thin sandstone and laminated shale. Location is BP_4 in Figure 43, page 83.

bolts long enough to extend above the rider seam were used. However, the Harlan coal bed is less than 50 inches thick in the mine which prohibits using longer bolts.

The use of resin roof bolts has undoubtedly contributed to roof stability. Even in areas of the mine showing roof sags and shear zones between the roof and rib (cutters), resin bolts apparently provide superior anchorage compared to conventional bolts.

Heading directions that parallel channel directions in the mine are very unstable. The cross-bedded nature of the channel-fill sandstone and the dip of cross-beds into the mine entry are important contributing factors in roof falls. Wang (82) studied the effects of cross-bedding in roof material structurally. He concluded that, in general, high tensile stresses occur in the midspan of the roof in hard roof material. This relationship appears valid in the Bailey Creek mine because of the presence of roof sags in areas of channel-fills.

Comparison - Bailey Creek and Highsplint Mines

A comparison of the Highsplint Darby mine and the Bailey Creek mine indicated the following major differences:

1. Thickness of immediate roof: The immediate roof rocks of the Bailey Creek mine are, in general, thicker. Shales and siltstones occupy the interval from the Harlan coal bed to the overlying rider seam, which ranges from 12 feet to 20 feet above the Harlan coal bed. However, immediate roof siltstones and shales overlying the Darby coal bed ranges from 0 to as much as 15 feet.

2. Abundance of kettlebottoms: While kettlebottoms were observed in both mines, especially in areas of thicker immediate roof rocks, they are more frequent and larger at Bailey Creek.

3. Development of "slips": Slickensided surfaces were rarely observed at Bailey Creek, but were frequently observed at Highsplint. If slickensides are caused by differential compaction of sediment because of loading, then deposition of the main roof sandstones at Highsplint must have been relatively rapid while the immediate roof sediments were only partly indurated in places. Where observed, contacts between channel sandstones and underlying immediate roof rocks in the Bailey Creek mine were always sharp and erosional.

4. Relationship of roof falls: Because of the differing lithologic relationships at the two mines, the nature of roof falls observed may be contrasted.

Roof falls at the Highsplint mine may be considered in two categories: those involving the immediate roof and those involving the basal part (perhaps 15 feet) of the main sandstone roof. Immediate roof rocks cut by diagonal "slips" are very common, and horizontal "slips" cause the roof to fall during mining operations. Available evidence strongly supports the conclusion that "slips" developed parallel to sandstone rolls in the overlying sandstone, so the immediate roof in areas of rolling roof is relatively unstable. Roof falls involving the basal part of the main sandstone appear to be related to cyclic sedimentation and discontinuities caused by internal sandstone structures. Jointing in the main sandstone roof did not appear to be a major contributing factor in roof instability.

Roof falls in the Bailey Creek mine, however, are caused by narrow channels and associated cross-beds that dip into the entries, coupled with the discontinuity caused by the rider coal seam. High overburden stress acting on these rocks was indicated by roof sags and "cutters". Joint-controlled rock falls were also observed in the mine under overburden of about 200 feet.

V. PALEOGEOGRAPHY AND ENVIRONMENT OF DEPOSITION

Source Area and Sediment Transport Direction

Figure 51 shows the tectonic setting of Kentucky and surrounding states during the Carboniferous, and Figure 52 shows that the study area in southeastern Kentucky is included in the Pocahontas basin as a part of the Appalachian geosyncline (27). The Pocahontas basin was a linear basin, intermittently subsiding to the southeast, that extended northeast-southwest across West Virginia and adjacent areas of Kentucky before swinging farther south paralleling the trend of the Kentucky dome and eastern Kentucky syncline (3).

Recent studies of Carboniferous clastic deposition within the areas of eastern Kentucky, West Virginia and southern Ohio have suggested a general northwest transport direction with a source area to the east and southeast (19, 24, 27, 51). Also, the same authors have invoked a fluvio-deltaic system that prograded toward the northwest.

Within the general framework of the fluvio-deltaic system, several subenvironments have been recognized. Beginning at or near the source area, these include essentially the alluvial valley and alluvial plain or delta plain extending to the sea. Each depositional environment is characterized by unique assemblages of lithologic and biologic features, many of which are transitional between environments. Based on data obtained in this study, it is concluded that the Mingo Formation was deposited as a dominantly prograding sequence of clastics generally toward the west, southwest and northwest. Deposition is postulated as

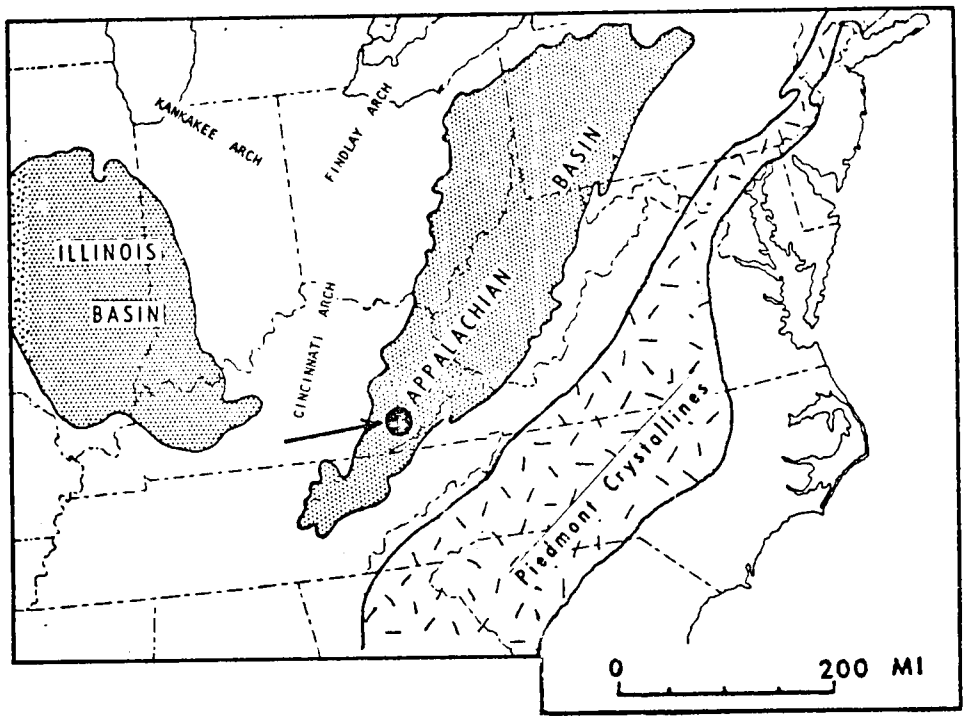

FIGURE 51. - Tectonic setting of Kentucky and adjacent states during the Carboniferous [after Meckel (51)].

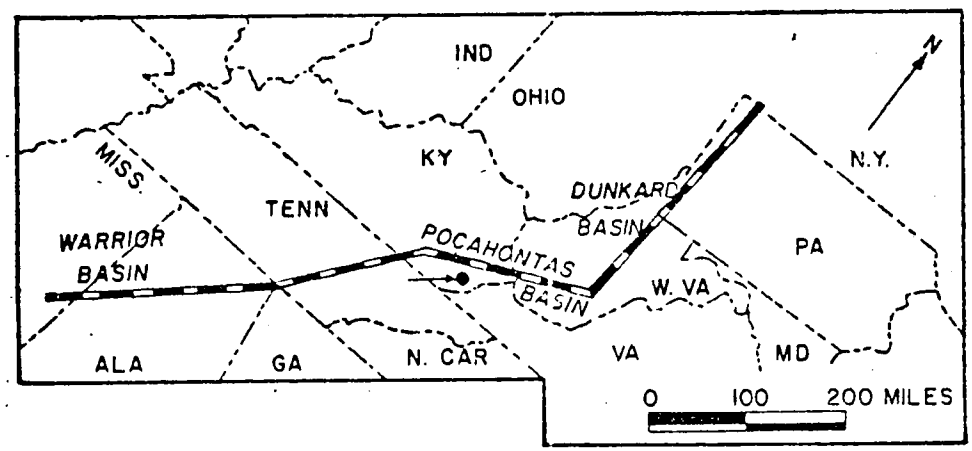

FIGURE 52. - Map of Kentucky and surrounding states showing axial trends of the Dunkard, Pocahontas and Warrior Basins [after Ferm (27)].

taking place on an alluvial plain. The alluvial plain environment probably includes deposition taking place on river floodplains or a deltaic lobe or series of lobes. The entire sequence from the Harlan upward to the Creech coal beds may include a combination of these environments. However, because of the absence of definite marine zones in the study area, it is assumed that deposition of the sediments took place dominantly in a fresh-water environment.

In a fluvial environment, meandering streams flanked by backswamp or marsh environments is strongly suggested. A fluvial interpretation is supported by cross-bedding analysis which indicates an essentially unimodal direction.

Reference to Table 4, page 22, shows that the sulfur content of both the Harlan and Darby coal beds is very low (0.8% to 1.1% for the analyses given). Cheek and Donaldson (12) reviewed studies comparing the sulfur content of coals overlain by marine versus nonmarine roof rock and noted that low sulfur coal is likely to be overlain by nonmarine roof rocks.

Thin-section studies indicated that the sands are immature because of the apparent low degree of grain rounding and the high percentage of feldspar (8% - 12%), which would suggest a relatively short transport distance (29). However, except for poorly sorted basal sandstone "lag gravels," the sandstones are generally moderately to well sorted. The combination of immature sands and good sorting suggests streams with sufficient flow rate to effectively winnow the finer sediments (41). That the streams were meandering and/or braided is indicated by fining-upward sequences. It is likely that a meandering river system dominated because

of the presence of point bars (Figure 20, page 43), abandoned channels (Figure 53 and Figure 24, page 49), and also by the presence of abundant overbank material (73). The sharp basal contacts of the larger sandstone bodies, together with sharp and/or transitional (interfingering) lateral contacts with a general upward widening or "winged" shape has been used as evidence for an aggrading stream that became more meandering during later stages (27).

If the evidence for a meandering river system is valid, then it is likely that such a system would be flanked by a system of levees. This view is also supported by the ripple laminated and rooted zones at the top of the fining-upward sequences, characteristic of levee deposits (2, 49).

The backswamp area appears to have been largely a reducing environment as indicated by the presence of pyrite and siderite in the shales and basal sandstones (33). Periodic influx of fine-grained sediment is suggested by the development of coal/shale rash and shale partings in the coal. Times of at least partial emergence are indicated by rooted zones and kettlebottoms (tree stumps) in the shales immediately overlying the coals. Inundation of parts of the coal-forming swamp or marsh is suggested by laminated shales and siltstones containing burrows and occasional ostracods in the immediate roof rocks. However, the lack of mudcracks and little evidence of oxidizing conditions indicate little subaerial exposure.

In an environmental setting of meandering rivers flanked by low-lying swamps or marshes, sudden influxes of sediment during flooding is

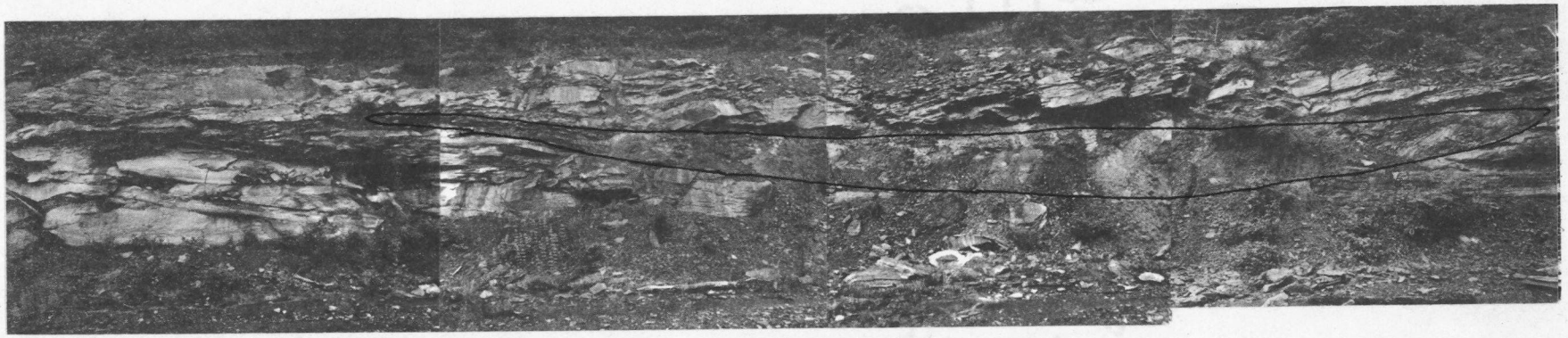

FIGURE 53. - Photographic mosaic of symmetrical shale-filled trough. Location is Darby strip bench, Highsplint mine (designated as P_4 on Figure 39, page 75). Size of outlined trough about 80 feet wide and 10 feet thick.

likely through crevasses in the levees. Scour surfaces and sole marks on the base of sandstone rolls (Figures 54 and 55) together with crude graded bedding (Figure 56) supports this view (14, 23, 75).

Reference to Figures 18 through 22, pages 41 through 45 shows representative sedimentary sequences observed in the study area. The right-hand column is an environmental interpretation based on a postulated fluvial system.

Possible Environmental Models

The following discussion suggests two possible environmental settings that may have prevailed during deposition of the strata in the study area. These models are suggested because both provide reasonable present-day analogs to the sedimentary characteristics observed. Still more important is that both models provide possible explanations for the presence of elongate narrow sandstone bodies observed in the Highsplint and Bailey Creek mines.

Floodbasin Environment

A possible comparison to the environment is the present-day Brahmaputra River. The river is characterized by periodic flooding and the transport of large volumes of relatively fine-grained sediment. The Brahmaputra River, studied in detail by Coleman (14), has a braided pattern because of instability caused by large sediment volume.

Figure 57 shows a present-day environmental setting that may characterize the Highsplint and Bailey Creek mines. The aggrading



FIGURE 54. - Current crescent on base of sandstone roof roll in new 004 Section, Highsplint mine. Note cross-bedding expressed as linear trends parallel to current flow shown by arrow.



FIGURE 55. - Current scour and tool marks preserved on base of sandstone roof in the Highsplint Darby mine. (Location coordinates R-12 on Figure A1, Appendix A. Probable current direction (SW) indicated by arrow.

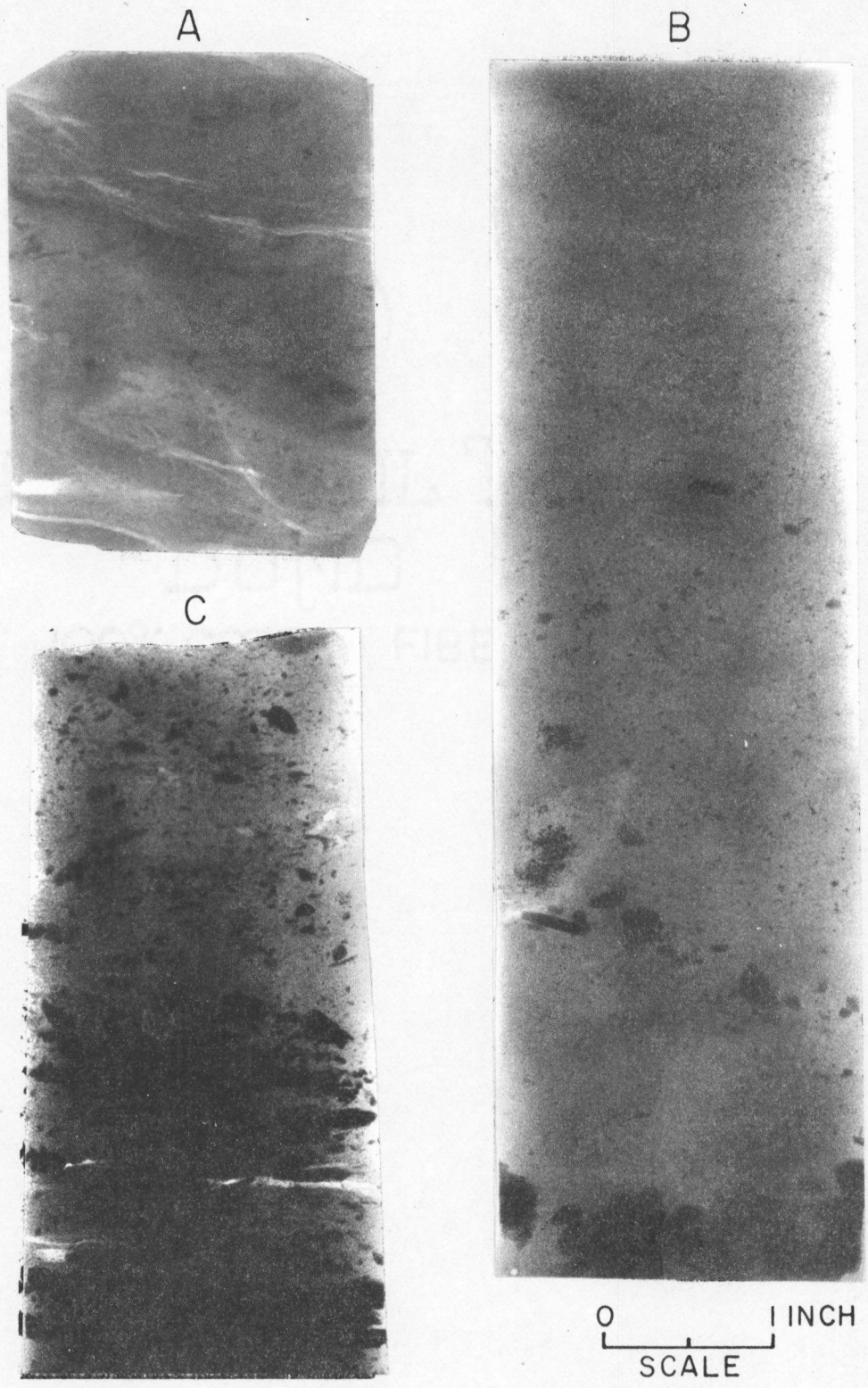

FIGURE 56. - Radiographs of core sections showing sandstone with included coal lenses in A (S-4-10) and graded bedding in lag in B (S-4-4) and C (S-4-12). Samples are cores from 004 Section, Highsplint mine.

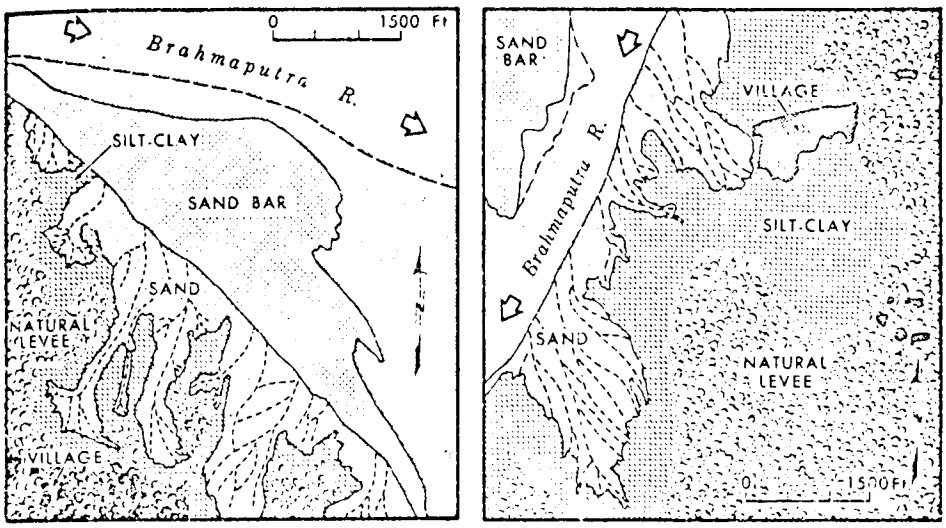

FIGURE 57. - Crevasse splays deposited during flood in the floodbasin of the Brahmaputra River [after Coleman . (14)].

Brahmaputra River has built a levee system. During flooding, the levee is breached by floodwaters through channels that rapidly spread outward into the floodbasin. These floodbasin areas, known as beels in East Pakistan, are accumulation sites for peat, and may be inundated by as much as 8 to 12 feet of water during floods. The resulting anastomosing pattern of channels cutting the levee and spreading outward into the floodbasin is comparable to channel patterns found in the sediments in the Highsplint Darby mine, (Figure 40, page 75).

Interdistributary Bay Environment

An environmental model somewhat similar to the preceeding example, except that it involves deposition on a delta lobe, is the interdistributary bay environment (23).

As defined by Elliott (23), the interdistributary bay is an area between deltaic distributaries, irrespective of whether the bays are open to the sea, or partially or entirely closed, and includes coastal lakes and basins. Present-day bays are generally shallow water bodies (3 to 15 feet average depth) and may be fresh, brackish or marine. Because the bays are often extensively vegetated, they may also be considered sites of peat accumulation.

Figure 58 is a sequence of events leading to the filling of an interdistributary bay as envisioned by Elliott (23). In phase I a recently initiated distributary contributes mud to the bay by sheet overbank floods. In phase II an alluvial ridge (levee) had developed. Flood waters are now channelled through the levee forming a crevasse splay

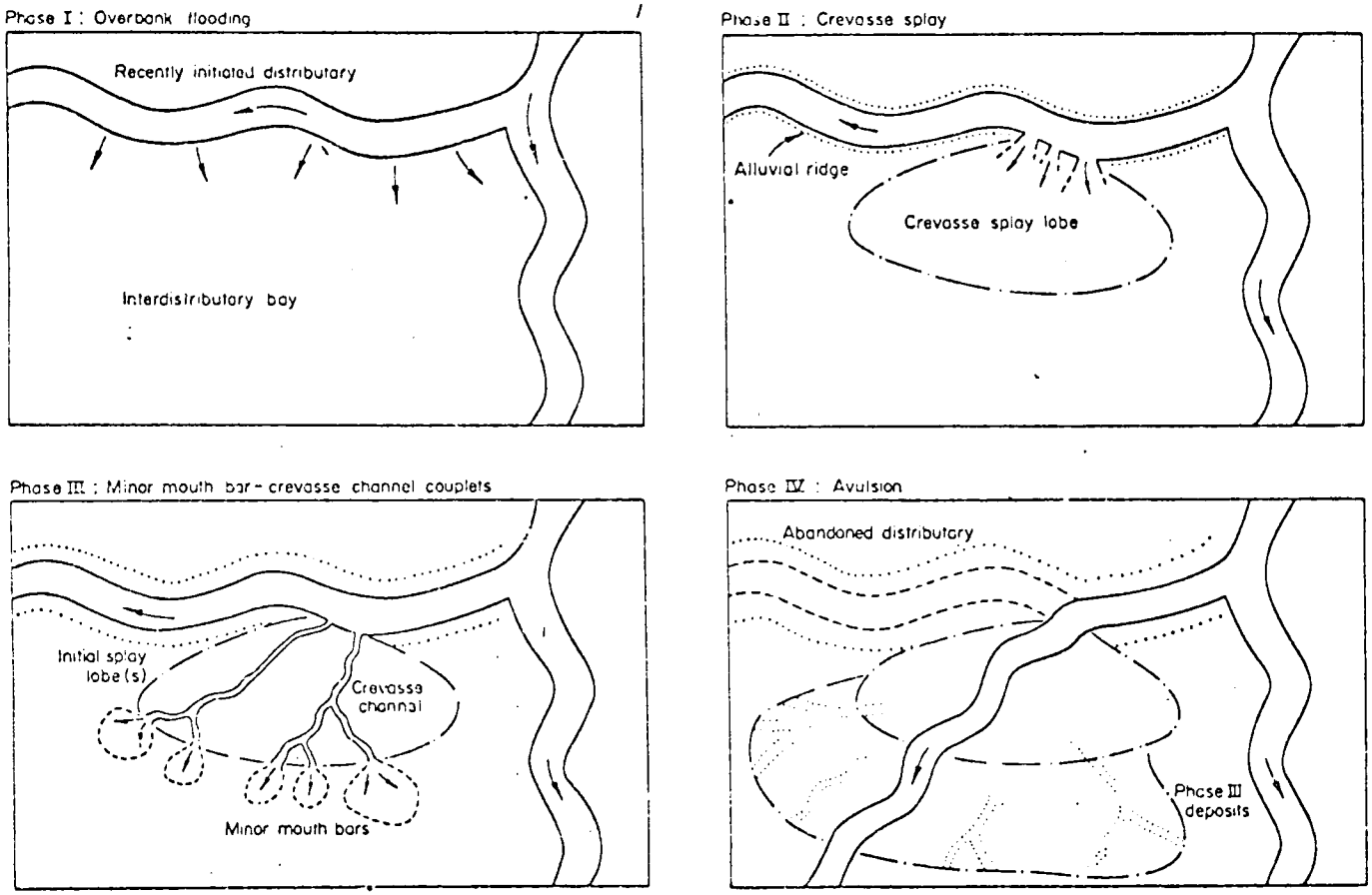

FIGURE 58. - Interdistributary bay model as proposed by Elliott. (23)

lobe. Phase III is characterized by continued bay filling by channelized flow in crevasse channels. At the edge of the splay lobes minor mouth bars are deposited in the bay. Phase IV involves avulsion (abandonment) of the major distributary. Avulsion is caused by continued vertical accretion of the levee in phase III causing an increase in gradient of the crevasse channels. Avulsion in phase IV results in the distributary channel cutting downward through the previously deposited bay-fill sequence. This produces an erosional base and fining-upward sequence.

The interdistributary bay model is similar in many respects to the Brahmaputra floodbasin example. It is interesting to note that the depth of water in present-day delta lakes and interdistributary bays (3 to 15 feet) and the depth of water in the Brahmaputra flood basin (8 to 12 feet) are comparable. Considering ancient bay-fill sequences, Ferm (27) suggested that the thickness of the bay-fill sequence between rooted seat earths represents the maximum depth of the open-water body that was filled. The interval of the immediate roof shales between coals in the Harlan and Darby mines approximates this value of three feet to 15 feet (Figure 5, page 14).

The development of crevasses may have been an important process in river avulsion. Also, the development of crevasse splay lobes and minor mouth bars followed by the prograding crevasse channel deposits into inundated backswamp/marsh areas may explain coarsening-upward sequences and the development of sandstone rolls.

Alternatively, it is known that floodbasins contain networks of small channels that are partly inherited from older drainage systems (28).

These channels have the role of conducting water from an active meander belt into the floodbasin during flooding and on the falling stage draining back into the active channel the flow ponded in basins (2). This network of channels may explain the relationship of the mine floor forming a topographic low paralleling sandstone rolls. The original topographic configuration of the swamp would direct the flow into and out of the drainage basin and concentrate deposition into topographic lows. A similar explanation has been used, where evidence of marine influence is present, to explain parallelism in undulating floor and mine roof rolls as formed by tidal channels in a tidal flat environment (67).

VI. CROSS-BEDDING AND PALEOCURRENT STUDIES

Objectives

A review of paleocurrent studies applied to ancient sandstone bodies, as summarized by Potter and Pettijohn (62), shows that much work has been done in an attempt to reconstruct eolian or aqueous current patterns responsible for sand body deposition. The basic objective of these studies has been to interpret the trends of sandstone bodies and, in turn, make inferences concerning the conditions that existed at the time of deposition.

The delineation of sandstone body trends applied to underground mine layout and design is of considerable importance from both an economic and safety standpoint. It has been observed by Wier (88), Williamson (89), Raistrick and Marshall (64) and others that roof falls are likely to occur in areas marginal to sandstone rolls. Also, "washouts" associated with partial or total erosion of the coal may hinder or stop mining operations entirely.

Observations in the Highsplint mine early in the study indicated that the roof sandstone rolls were linear (Figure 1, page 4). Furthermore, the trends appeared fairly consistent in a northeast-southwest direction, with only a few trending in a northwest-southeast direction.

Mapping sandstone roll trends in the mine and projecting roll trends over short distances from one working section to another has been successful in most cases (Figure 40, page 75). However, an important consideration of sandstone projections involves premining considerations

or projecting sandstone trends into an existing mine from surface outcrop information.

In order to investigate the possibility of determining probable in-mine roof roll conditions and trends from outcrop information, a surface mapping program was conducted. The mapping program attempted to satisfy five major goals:

1. To determine what relationships exist between cross-bedding directions and sand body trends.

2. To determine what cross-bedding parameters best characterize the measured data.

3. To examine associated paleocurrent directional features for comparison with cross-bedding results.

4. To gather data that would provide insight into possible depositional environments of the roof strata.

5. To sample both the Darby and Harlan stratigraphic horizons to determine if paleocurrent directions were comparable over the vertical stratigraphic interval of about 200 feet that separates them.

In order to carry out these objectives surface mapping of rocks immediately overlying the Darby coal bed was concentrated in the area of the Highsplint mine (Figure 59, Location Darby A). In addition, directional features were determined from surface exposures for both the Darby and Harlan roof sandstones that included surface mine benches, road cuts, railroad cuts and areas prepared ("faced up") for underground operations in the study area (Figure 59). Attempts at devising an areal sampling plan using a grid system largely failed due to the scarcity of

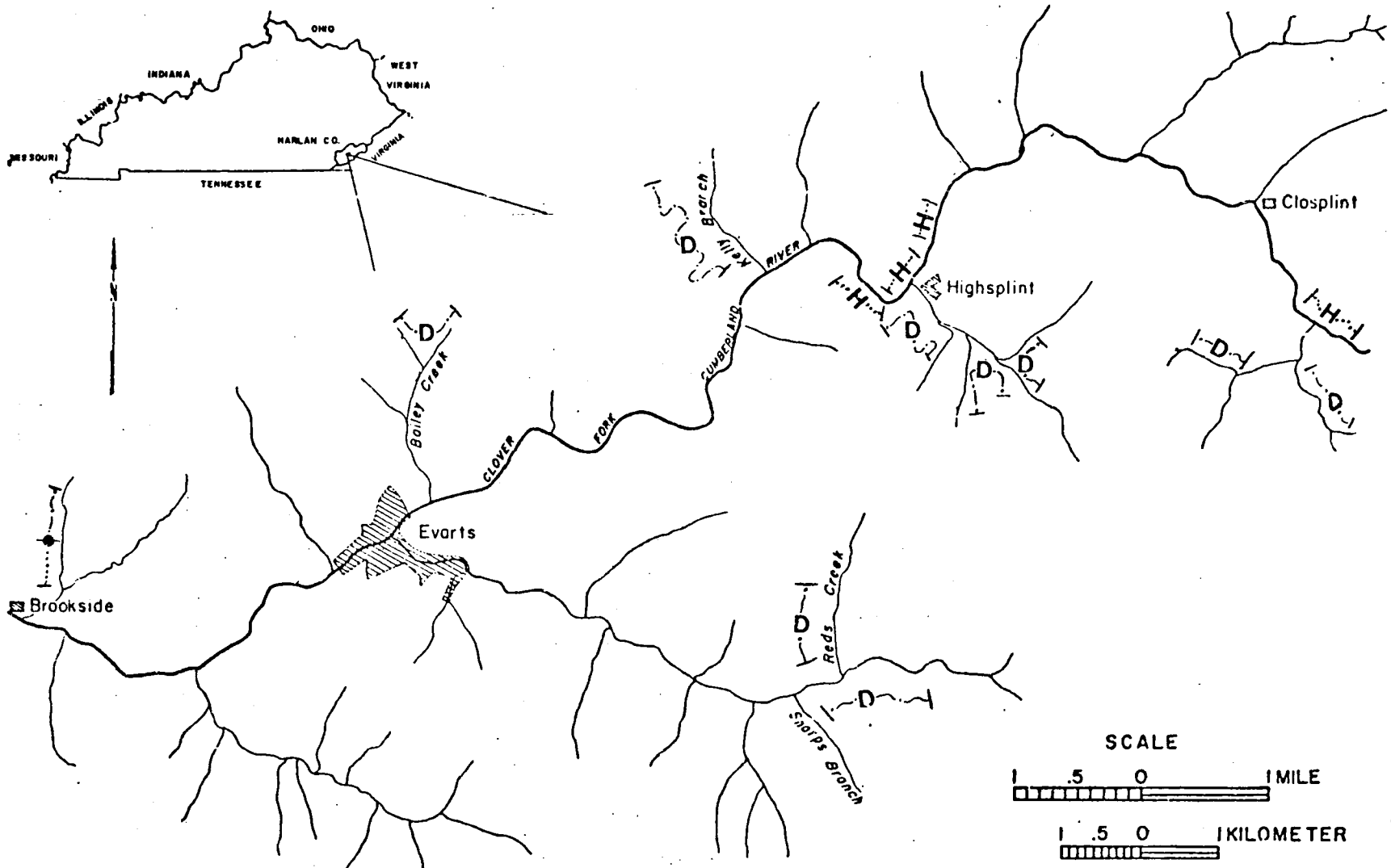

FIGURE 59. - Field localities for cross-bed data. Broken line indicates traverse. D designates Darby coal bed horizon and H designates Harlan coal bed horizon.

outcrops and the rugged nature of the terrain. Surface outcrop sampling was restricted to strata immediately overlying the Darby and Harlan coal seams, generally being limited to about 20 feet vertically over the coal seams. With this restriction, observations were actually made at all known outcrops.

Field Procedure

A Brunton compass was used to determine the strike and dip angle of cross-bedding as well as the dip direction. In practice, it was found that a clipboard with a sheet of paper taped to the top was useful in taking cross-bed readings. The clipboard was placed on the cross-bed and the strike and dip of the board was recorded. This method provided greater accuracy because it "smoothed" the bedding surface, provided a means of projecting the bedding surface outward and assured taking a true dip angle. For analysis, on a 360° basis, the azimuth of the dip direction was determined as 90° from the strike in the dip direction. Because the rocks are essentially flat lying, no correction for tilted strata was necessary. When possible, the probable type of cross-beds were noted (trough, planar), as well as the nature of contacts (tangential, sharp).

At each locality, associated directional features were also recorded. These included sandstone trough axes and sole marks, together with rare parting lineations, and plant fossil orientations. The relative apparent abundance of types of directional features was undoubtedly due to the nature of the outcrops. Most exposures were vertical, so cross-bedding and trough axes were more evident than features normally preserved on bedding planes.

A total of 108 cross-bed observations were taken for the Darby roof rocks from four localities and a total of 60 cross-bed observations were taken for the Harlan roof rocks from three localities for a combined total of 168 observations.

Analysis of Cross-Bedding Data

The most common method of analysis of directional data is to plot the data on a circular frequency histogram or rose diagram (18). Figure 60 illustrates this type of diagram in which the rose represents the cross-bed dip azimuth distribution on a 360° basis and the length of each petal represents the relative frequency for observations within a given angular range. If the distribution is obviously unimodal and data are clustered within a 180° range the arithmetic mean may be calculated (62). However, when observations are dispersed or polymodal distributions are suspected, special methods of analysis are needed.

Paleocurrent Analysis - Computer Program

In the early stages of the study it was decided that a computer program was needed for the following reasons:

1. Computer programs are often used as a method of systematic data analysis, especially when dealing with large numbers of observations. In many mining areas, limited outcrops make it difficult to obtain large numbers of observations, and it was felt that computer analysis would provide the most systematic method of analysis for both large and small sample sizes.

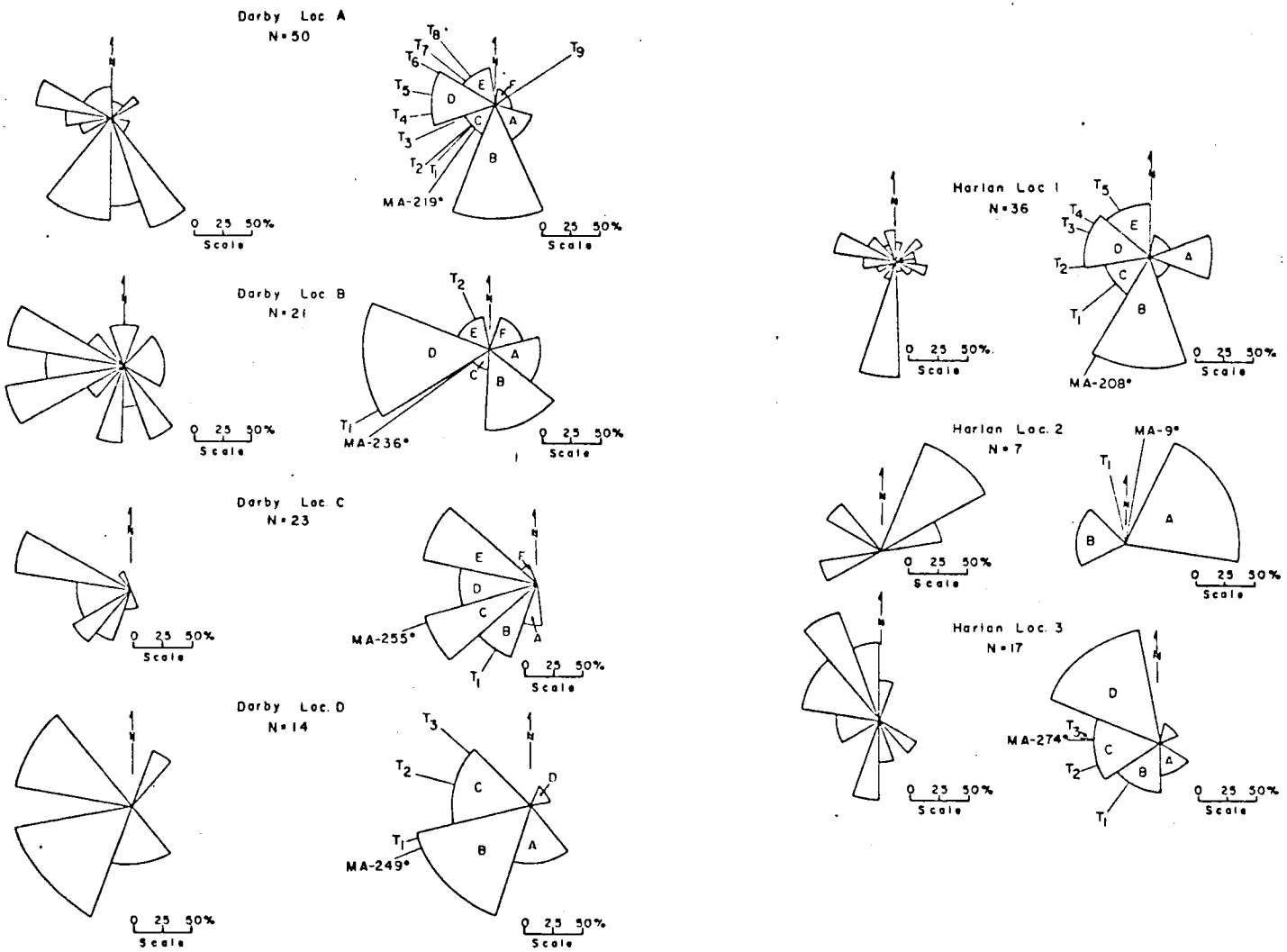

FIGURE 60. - Circular histograms for cross-bedding by locality. Left columns are drawn in ten degree intervals. Right columns are computer analyzed for comparison. Unimodal mean azimuths (MA) also indicated.

2. As discussed by Curray (16), the major problem in the analysis of circular data is that it is not open-ended. It is necessary to choose an origin in order to divide the circular distribution into a linear frequency curve. The problem is especially difficult in the determination of class boundaries in bimodal and/or polymodal distributions. A procedure based on minimum variance criteria, even with small sample sizes, requires a great number of trial calculations and the computer is very useful in this respect.

The computer program discussed in Appendix D was used to calculate the following major statistics for cross-bedding and associated sedimentary data:

1. Azimuth of vector resultant.
2. Mean azimuth.
3. Variance (around both the vector resultant and mean azimuth).
4. Vector magnitude.
5. Cross-bedding frequency distributions by locality.

In addition, several statistical tests were used.

1. Tukey's Chi-square statistic.
2. Chi-square statistic.
3. Goodness of fit statistic.
4. Raleigh significance level.

These statistics were designed to satisfy the requirements for analyzing orientation data according to Curray (16) as follows:

1. To obtain a measure of central tendency or a preferred orientation direction that is independent of origin.

2. To obtain a measure of dispersion independent of origin.

3. To test the statistical significance of results against a model of randomness.

4. To utilize a model distribution from which deviations can be tested.

Two methods were used to obtain a measure of central tendency of the data, both of which are independent of origin. The azimuth of the vector resultant is derived by treating each observation as a vector. The north-south and east-west components of each observation are computed to derive the vector resultant. The mean azimuth, however, is calculated using minimum variance criteria (Appendix D). Table 5 shows individual sample localities and combined cross-bedding data together with associated azimuths and calculated variances. A comparison between the azimuth of the vector resultant and mean azimuth shows that in most cases they coincide reasonably well. Note, however, that the variance associated with the mean azimuth is consistently lower than the variance associated with the vector resultant. In fact, the smaller the difference between the variances the closer the vector resultant agrees with the mean azimuth. At Locality Darby C, both the variances and the values for the mean azimuth and vector resultant coincide. It seems reasonable to conclude, then, that the mean azimuth gives a better indication of the center of the data than the vector resultant. Table 6 shows a similar analysis of trough axes.

The variance associated with the mean azimuth can be used, for comparative purposes, to indicate the dispersion about the center of the data. Also, the standard deviation, or square root of the variance, may

TABLE 5. - Cross-bedding analysis - Unimodal Program

Location	Number	Vector Resultant (degrees)	Mean Azimuth (degrees)	Variance (VR)	Variance (MA)	Standard Deviation (degrees) (MA)
Darby A	50	207	219	5894	5757	75.9
Darby B	21	242	236	8188	8155	90.3
Darby C	23	255	255	1523	1523	39.0
Darby D	14	244	249	3913	3879	62.3
Harlan 1	36	210	208	8292	8288	91.0
Harlan 2	7	21	9	3849	3687	60.7
Harlan 3	17	289	274	5287	5058	71.1
Total Darby	108	237	236	5142	5140	71.7
Total Harlan	60	272	276	8697	8682	93.2
Combined Harlan and Darby	168	243	250	6552	6511	80.7

TABLE 6. - Trough axes analysis - Unimodal Program

Location	Number	Mean Azimuth (degrees)	Variance (MA)	Standard Deviation (degrees)
Total Darby	15	275	1492	38.6
Total Harlan	8	271	1118	33.4
Combined Harlan and Darby	23	274	1308	36.1
Darby A	10	277	1436	37.9
Sandstone roll trends, Highsplint mine	55	243	1679	41.0

be used to indicate dispersion. Assuming a normal distribution, slightly over two-thirds (68.2%) of observations will fall within one standard deviation on either side of the mean value. Approximately 95% of all observations are included within two standard deviations, and more than 99% are covered by the interval lying three standard deviations on both sides of the mean (17).

An indication of the data distribution was established by the use of the frequency distribution procedure outlined in Appendix D and shown in Tables 7 and 8. The frequency distributions were used in drawing circular histograms shown in Figure 60, page 117.

Histograms were drawn by using the interval column to plot the range for each class. The length of the petal for each class interval was determined by recalculating the observation frequencies to 100 to derive a percent value.

In addition to providing an indication of the distribution of the data, the frequency distribution was used as a basis for testing the uniform randomness of the data within the range in which the data were observed. Tukey's Chi-square statistic (Appendix D) was used for cross-bedding data as a possible indication of a unimodal versus polymodal distribution on a 360° basis.

In order to test bidirectional data such as trough axes and parting lineation on a 180° basis, the Chi-square statistic was used (Appendix D).

The normality assumption was also tested using the normal goodness of fit procedure (Appendix D).

While attempts at using the Tukey's Chi-square, normal goodness of fit statistical tests were made, the results are not reported here

TABLE 7. - Cross-bedding frequency distributions by locality

Sample Designation	No.	Interval		Frequency
		Lower	Upper	
Darby A	50	5.5	54.8	2
		54.8	104.1	2
		104.1	153.4	6
		153.4	202.6	19
		202.6	251.9	5
		251.9	301.2	10
		301.2	350.5	6
Darby B	21	16.5	71.8	2
		71.8	127.2	3
		127.2	182.5	5
		182.5	237.8	1
		237.8	293.2	8
		293.2	348.5	2
Darby C	23	174.5	202.0	2
		202.0	229.5	4
		229.5	257.0	6
		257.0	284.5	4
		284.5	312.0	6
		312.0	339.5	1
Darby D	14	21.5	80.3	1
		80.3	139.1	0
		139.1	197.9	3
		197.9	256.7	6
		256.7	315.5	4
Harlan 1	36	9.5	59.5	2
		59.5	109.5	6
		109.5	159.5	2
		159.5	209.5	11
		209.5	259.5	4
		259.5	309.5	6
		309.5	359.5	5
Harlan 2	7	24.5	97.3	5
		97.3	107.0	0
		170.0	242.8	0
		242.8	315.5	2
Harlan 3	17	11.5	68.0	1
		68.0	124.5	0
		124.5	181.0	2
		181.0	237.5	3
		237.5	294.0	4
		294.0	350.5	7

TABLE 8. - Cross-bedding frequency distributions (totals)

Sample Designation	No.	Interval		Frequency
		Lower	Upper	
Total Darby	108	5.5	48.6	5
		48.6	91.8	4
		91.8	134.9	2
		134.9	178.0	20
		178.0	221.1	24
		221.1	264.3	18
		264.3	307.4	28
		307.4	350.5	11
Total Harlan	60	9.5	59.5	7
		59.5	109.5	7
		109.5	159.5	3
		159.5	209.5	15
		209.5	259.5	6
		259.5	309.5	11
		309.5	359.5	11
Combined Darby and Harlan Crossbedding	168	5.5	44.8	10
		44.8	85.2	10
		84.2	123.5	6
		123.5	162.8	14
		162.8	202.2	36
		202.2	241.5	21
		241.5	280.8	25
		280.8	320.2	36
		320.2	359.5	14

because they did not give comparable results for estimation of unimodal versus polymodal cross-bedding distributions. Most statistics agree that these tests are not very powerful. (Dr. David Muse, personal communication).

If a bimodal distribution is suspected, the bimodal computer program (Appendix D) can be used. Cross-bedding was also analyzed using this method. The program is based on splitting the total observations into two samples using a minimum variance criteria. The program gives no assurance that the bimodal distribution is appropriate, but provides a systematic method of sample division.

Geologic Evaluation of Cross-Bedding

Because a major objective of the present study was to determine if sandstone trough trends coincide with trough trends encountered in underground mines, and because the statistical tests discussed previously were not conclusive, additional analysis of cross-bedding was necessary.

Many studies of cross-bedding data have demonstrated that statistical analysis of cross-beds often provides an average or mean direction that generally coincides with elongate sand trends (62). However, several recent studies dealing with trough cross-bedding have shown that local cross-bed distributions may be very misleading.

In review of published literature dealing with the azimuthal roses of paleocurrent data, Selley (71) concluded that the majority of them belong to three main groups:

1. Unimodal
2. Bimodal
   i) with mutually opposed modes (bipolar)
   ii) with mutually perpendicular modes
3. Polymodal

These main groups of azimuthal roses are shown in Figure 61. The upper series of roses (Figure 61) represent general types listed above and the lower series (A through D) (Figure 62) represent actual possibilities of cross-bed distributions that are misleading as paleocurrent indicators when compared to actual paleocurrent directions (shown by arrows).

A cursory comparison of rose diagrams of Harlan and Darby roof strata by locality (Figure 60, page 117) on a purely descriptive basis with possibilities shown in Figure 61, indicates that Darby A, Darby B and Harlan 1 distributions are polymodal, or at least bimodal, because of "dispersed" modes, especially modes D and B.

Localities Darby C and Darby D, however, appear bimodal or unimodal as is the case possibly with Harlan 3. Harlan 2 approximates a bipolar distribution.

Because trough cross-bedding occurs so frequently in the Harlan and Darby roof rocks, the method of rose diagram analysis as proposed by Dott (20) was used to analyze cross-bedding in the study area. Dott listed the following parameters to be used in the analysis of trough cross-bedding:

1. Bimodal cross-set patterns bisected by the trough axes reflect equal numbers of readings from the flanks of troughs that were filled symmetrically. This is similar to example C, Figure 62.

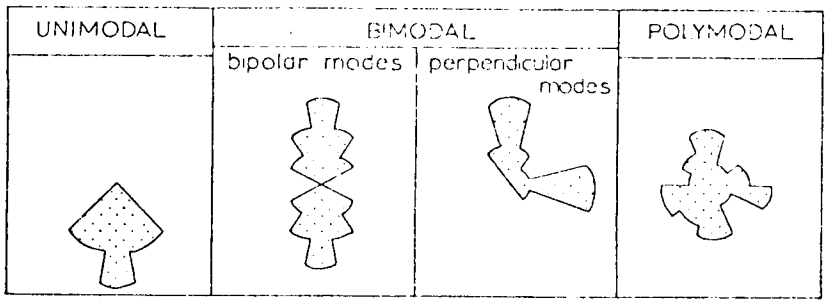

FIGURE 61. - Main types of azimuthal roses [after Selley (71)].

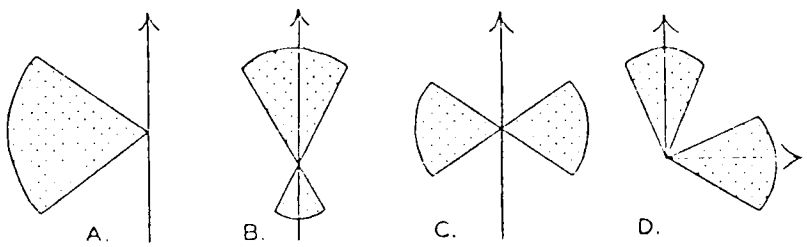

FIGURE 62. - Possible misleading cross-bed distributions A through D [after Selley (71)].

2. Asymmetrical cross-set histograms with one large lateral mode generally represent troughs filled largely from one side. This would represent possible point bar cross-bedding, and is similar to example A, Figure 62.

3. Where a single mode corresponds closely with the trough axes, it is likely that most of the laminae measured represent the trough "heads" rather than limbs. This is the ideal case in which the unimodal cross-bedding azimuth corresponds to the mean direction of the depositing current.

Method of Analysis

The criteria outlined above were applied to Harlan and Darby roof strata cross-bedding by systematically plotting the azimuths of individual cross-bed observations on either side of troughs. Thus, a single trough axis was plotted together with all cross-bed azimuths representing readings taken from the limbs on either side. This was accomplished with the use of photographic mosaics of vertical outcrop exposures at the Highsplint mine where control was better. The same procedure was used at other localities, but without the use of photographic mosaics.

Application of Method

The designation of various parts of the histogram rose as letters on Figure 60, page 117, will simplify their references. However, a "B" petal on one histogram does not necessarily imply an equivalent "B" petal on another.

Darby A - This histogram is composed of polymodal distribution with a unimodal mean azimuth of 219°. Mode A is essentially composed of foresets belonging to trough T_9 and overbank(?) deposits. Mode B may be interpreted as composed of the following cross-beds:

1. Southwest dipping beds on limb of trough T_1.
2. Southwest dipping beds on limb of trough T_2.
3. Overbank(?) or "swale-fill" deposits.
4. Lateral accretion (point bar) deposits.
5. Southeast dipping beds on troughs T_1 and T_2.

Mode C may be interpreted essentially as foreset beds of trough T_1 and T_2 and some lateral accretion beds. Mode D is interpreted as:

1. Foreset beds associated with troughs T_1 through T_6.
2. Northwest dipping limbs of troughs T_1 and T_2.

Mode E represents:

1. Foreset beds trending in a northwest direction for troughs T_7 and T_8.
2. Possible side filling of trough T_1.

Mode F represents northeast-dipping foreset beds associated with trough T_2. It is of interest to note that this trough, shown in Figure 53, page 102, is only one of two definite northeast-dipping troughs observed. The other is located on the Darby strip mine bench at Bailey Creek, (Figure 24, page 42) and both are shale filled. They probably represent abandoned channels.

Darby B - Two possible trough axes were observed at this locality. Trough T_1 is represented by cross-bed observations in Modes B, C, D and E.

Trough T_2 is represented by observations in Modes E and D. Modes F, A and part of B are possibly overbank or crevasse splay deposits, but their positive identification is uncertain. Figure 24, page 49 shows a probable abandoned channel, the direction of which coincides with an abandoned(?) easterly transport direction.

Darby C - The azimuth of the only observed trough axis at this locality was 215°. Darby C is near Darby A (see location map, Figure 59, page 114) where southwest and due west trending troughs were observed. The cross-bedding at Darby C appeared to be consistent in dip and westerly direction suggesting foreset bedding dipping parallel to the "heads" of the troughs rather than the limbs.

Darby D - This locality is the closest approximation to an "idealized" unimodal distribution observed. The arithmetic mean of the trough axes is 282° and the mean azimuth is 249°.

Harlan 1 - Trough axes for the Harlan roof strata at this locality are generally in a westerly direction. Modes C, D, and E and most of B represent foresets and side filling beds with these troughs. The high frequency of cross-beds in Mode B probably indicates similar combinations of cross-beds as those listed for Mode B for the Darby A location. Mode A probably represents overbank deposits.

Harlan 2 - Outcrops were very limited at this locality. However, the cross-beds are associated with a northwest trending trough. The rose diagram in this case reflects a greater number of observations taken from one side of the trough (Mode A).

Harlan 3 - The arithmetic mean of observed trough axes at this locality was 249°. This would suggest a dominant side-filling toward the northwest as indicated by Mode D.

Cross-Bed Analysis - Conclusions

Analyses of cross-bedding, trough axes, and related directional features from surface outcrops in the study area has resulted in the following conclusions:

1. The kind of cross-bedding is very important in the determination of paleocurrent direction. Very misleading results are possible if trough cross-bedding is not recognized. Dott (20) concluded that, once trough cross-bedding is recognized, only trough axes need be recorded. However, it was found in this study that cross-bed readings on each side of a trough often aid in the projection of the trough axis when observed in a vertical surface exposure, as well as the direction of plunge of the trough. Also, the use of photographic mosaics of at least one fairly continuous exposure, such as the strip bench at the Highsplint mine, was very useful as all observations can be plotted and later used to determine the distribution of each cross-bed on the circular histogram. By analogy, other sampling localities could then be evaluated.

2. From the geologic analysis of rose histograms, it was concluded that cross-bedding in the study area is essentially unimodal. Most bimodal histograms in Figure 60, page 117, resulted from cross-bed observations taken from opposite limbs of troughs. However, all cross-bedding histograms associated with the circular histograms were not easy

to explain. Dott (20) concluded that factors such as actual random distributions of cross-set orientations, operator errors, poor exposures, or inadequate sampling may produce polymodal patterns.

Figure 63 shows the areal distribution of cross-bedding histograms in the study area.

3. The use of the computer program to analyze cross-bedding seemed to provide a rapid and reasonable method of ordering observations and an approximation of the mean sediment transport direction, class intervals and frequencies, and variance determinations. This is shown on Figure 60, page 117, by comparing the histograms drawn from the raw data with computer analyzed histograms for each locality.

4. A comparison of sole marks (Table 9) and parting lineation (Table 10) with cross-bedding (Table 5, page 120) shows only a general agreement. Only a few observations were possible in outcrop exposures, and the local variability of these bedding plane features was considerable. Sole marks were better observed, although only locally, on the base of the main sandstone in the Highsplint and Bailey Creek mines. (See discussion, page 85).

5. The paleoslope and depositional conditions in the area appear to have remained relatively constant during deposition of the strata between the Harlan and Darby coal beds. Evidence for this conclusion is shown in the similarity of the histogram shapes in Figure 60, page 117, especially the Harlan Locality 1 and Darby Locality A. In addition, the mean azimuths are generally all in an angular range of 90° in the southwest quadrant, except for the Harlan Locality 2 histogram with only seven observations.

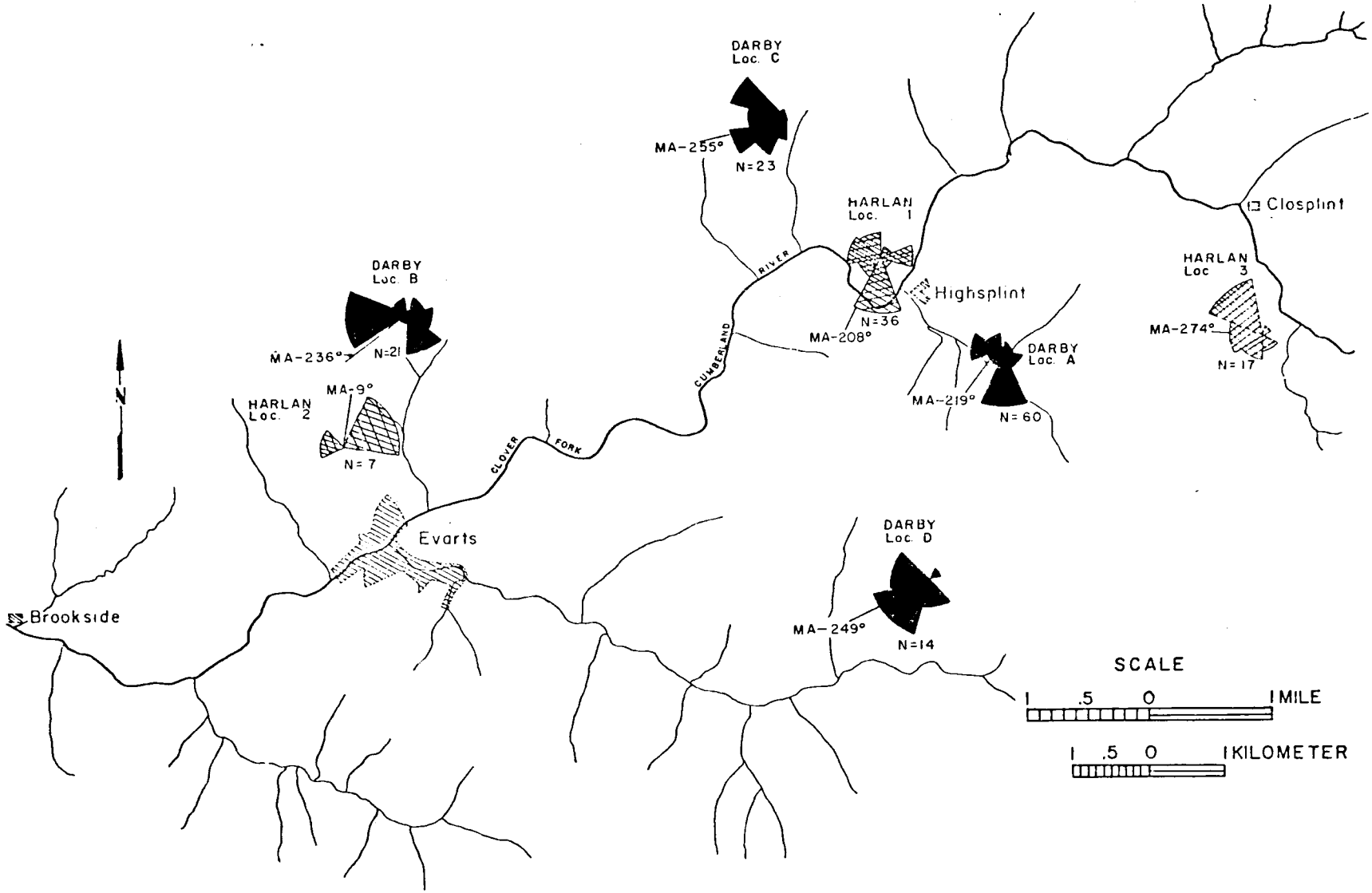

FIGURE 63. - Cross-bedding histograms by locality. Unimodal paleocurrent direction indicated by mean azimuth (MA).

TABLE 9. - Sole marks - surface outcrops

	Number	Sole mark azimuth (degrees)
Total Harlan	6	304
Total Darby	3	235
Combined Harlan and Darby	9	281

TABLE 10. - Parting lineation - surface outcrops

	Number	Parting lineation azimuth (degrees)
Total Harlan	3	245
Total Darby	4	225
Combined Harlan and Darby	7	234

The transport direction by cross-bedding analysis (Figure 63) is indirectly supported by the stratigraphic thickness or interval between the Harlan and Darby coal beds. From east to west across the study area, the interval decreases from about 300 feet to about 180 feet. This relationship suggests a source area toward the east as reflected by thickening of strata in that direction.

6. Trough axes determination in surface exposures is important to premining evaluations. It is probable that if well-defined troughs are not present in surface exposures then few problems with sandstone "rolls" or channels and the difficulties associated with them need be anticipated. However, well-defined trough cross-bedding observed in surface exposures in the vicinity of the Highsplint mine (Darby Locality A and Harlan Locality 1) correlate reasonably well with computer analyzed sandstone "rolls" within the mine. The unimodal mean azimuth for the "rolls" was 243°, with a variance of 1,679 for 55 observations (Table 6, page 122).

VII. JOINTS AND COAL CLEAT

Fractures are surfaces of secondary origin across which there has been a loss of cohesion. They occur in most igneous, metamorphic and sedimentary rock bodies, and they are commonly found in unconsolidated sediments. Fractures usually occur as sets of subparallel joint trends and sometimes have an even spacing. The fractures may break the rock up into blocks and two or more sets are common (5, 74). Coal beds also exhibit joints with relatively smooth, even surfaces known as the face or master cleat, and more irregular, discontinuous joints referred to as the butt or cross cleat. The face and butt cleats commonly intersect at an angle of nearly 90° (47).

Joint directions in coal and roof rocks have considerable influence in mining. Traditionally, mines were developed parallel to coal cleat directions due to the ease of coal extraction. Jointing in roof rocks, however, is a common cause of roof falls and mining parallel to "hill seams" or "slips" is to be avoided.

Joints in the Study Area

This study considered the analysis of surface joints in coal and roof rocks in the area between the Bailey Creek and Highsplint mines and methods were developed to correlate surface joints with those observed within the mines for predictive purposes.

Observations of rock jointing and coal cleat were made with a Brunton compass at field localities shown on Figure 64 in rocks at the

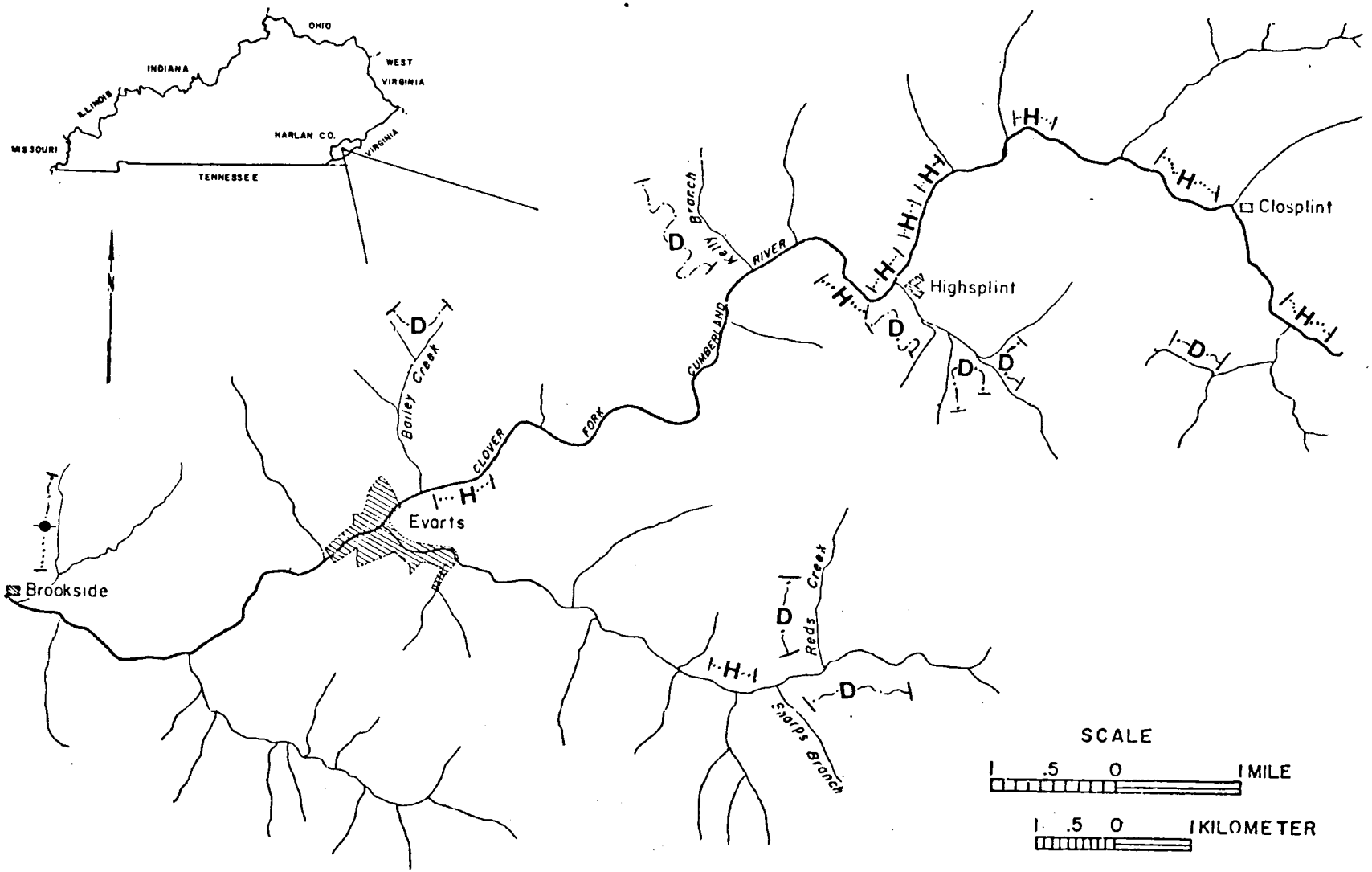

FIGURE 64. - Field localities for rock jointing data. Broken line indicates traverse. D designates Darby coal bed horizon and H designates Harlan coal bed horizon. Location of measured section at Brookside also indicated.

Harlan and Darby coal bed horizons. For comparison with surface observations, joint observations were also made in the Highsplint and Bailey Creek mines (Figure 64). Other data collected in the Highsplint mine for comparative purposes included "slip" or slickenside observations and sandstone roll trough axis observations.

Joints in surface rock exposures show the following characteristics:

1. Joints occur in all rock types studied.

2. Surface joints tend to be perpendicular to the bedding surface of the rocks, even where the major bedding surfaces are inclined. Because the rocks in the study area are essentially horizontal, the joints are vertical, or nearly so (Figure 65). Consequently, only the strike (bearing) of the joint surface was recorded during field studies.

3. Weathering of surface outcrops often causes joints to become widened and filled with clay.

4. The frequency (spacing) of joints varies considerably, but joint frequency was observed to increase with a decrease in grain size of the rocks. For example, sandstone joints may be spaced six feet to 12 feet apart, siltstone one foot to four feet and shale six inches or less.

5. All outcrops studied showed at least two or more joint sets (directions). Commonly, joint sets intersect at approximate right angles. Also, intersecting joint sets are composed of dominant sets cutting entirely through the exposed rock units and other joints. Other joints, often with curving and irregular faces, are discontinuous and terminate at the faces of dominant joints. Hodgson (39) applied the



FIGURE 65. - Entrance to Highsplint mine. (001 Section). Note nearly orthogonal joints in sandstone above entry.

terms systematic and nonsystematic, respectively, to these joints. In coal, the face cleat is an example of systematic joints and the butt cleat is nonsystematic.

Previous Studies in the Area

In an earlier study of joints in the Harlan County area, Jones (43) discussed rock joints as follows:

> Pronounced joints in the sandstones, shales and coals occur in this area. The strike of joints and cracks were measured on the surface as well as inside the various mines. The classification of two hundred joints shows the following results: 47 average N64°E; 46 average N24°W; 37 average N-S; 22 average N22°E; 35 average N65°W and 14 average E-W. The sets of joints N-S; N24°W and N22°E might be combined as one group. Those extending east and west are observed infrequently. This grouping would result in three main sets of joints and cracks; namely, N-S; N64°E and N65°W. Cleavage faces of coal range in various parts of the area from N45°E to N72°E, the average being N59°E. The faces in the mines relatively close to the steep dips flanking the Pine Mountain Fault average N65°E or approximately parallel to the strike of the fault.
>
> Butt faces are not as well defined. They frequently approximate right angles to the faces. In some of the mines the butts are very irregular. As a whole the cleavage faces parallel the Pine Mountain Fault and also the intense folding along Cumberland Mountain to the south. Cracks and joints observed inside the mines were as follows: N47°E; N50°E; N55°E; N65°E----N65°W; N85°W----N-S; N12°W; N25°E. These cracks fall in the general classification of those observed on the surface.

If the mean directions of the six sets of joints discussed by Jones and the angular relationships between sets are considered, including the east-west set, it is found that six apparant sets of joints are present with angular relationships of nearly 90°. Also, the N22°E and N24°W sets appear to form conjugate sets symmetrically disposed on either side of the north-south set.

Initial Analysis of Surface Rock Joints

A similar result in joint analysis was obtained in the present study by initially grouping surface joints into 5° and 10° intervals using a circular histogram. However, one of the most difficult problems in joint analysis using this procedure was the difficulty in determining whether two adjacent joint sets should be considered separate sets or a single set.

In order to estimate the number of joint sets present on a regional scale—i.e., the total area covered in the present study, surface joints were considered at each sampling locality. It was found that at almost all localities, at least two joint sets were present, and at several localities with more extensive exposures as many as six possible sets were observed. The angular relationship of 90° between sets, together with the distinction between systematic and nonsystematic joint sets where possible, were criteria used to establish possible sets. Figure 66 shows the results of grouping each pair of joint sets using the criteria discussed above.

In addition to the construction of preliminary joint histograms in joint analysis, a representative sample of 50 of the best defined systematic and nonsystematic surface joints was selected to consider the angular ranges of systematic and nonsystematic joints. Figure 67 shows the results of this grouping, from which the following observations may be made.

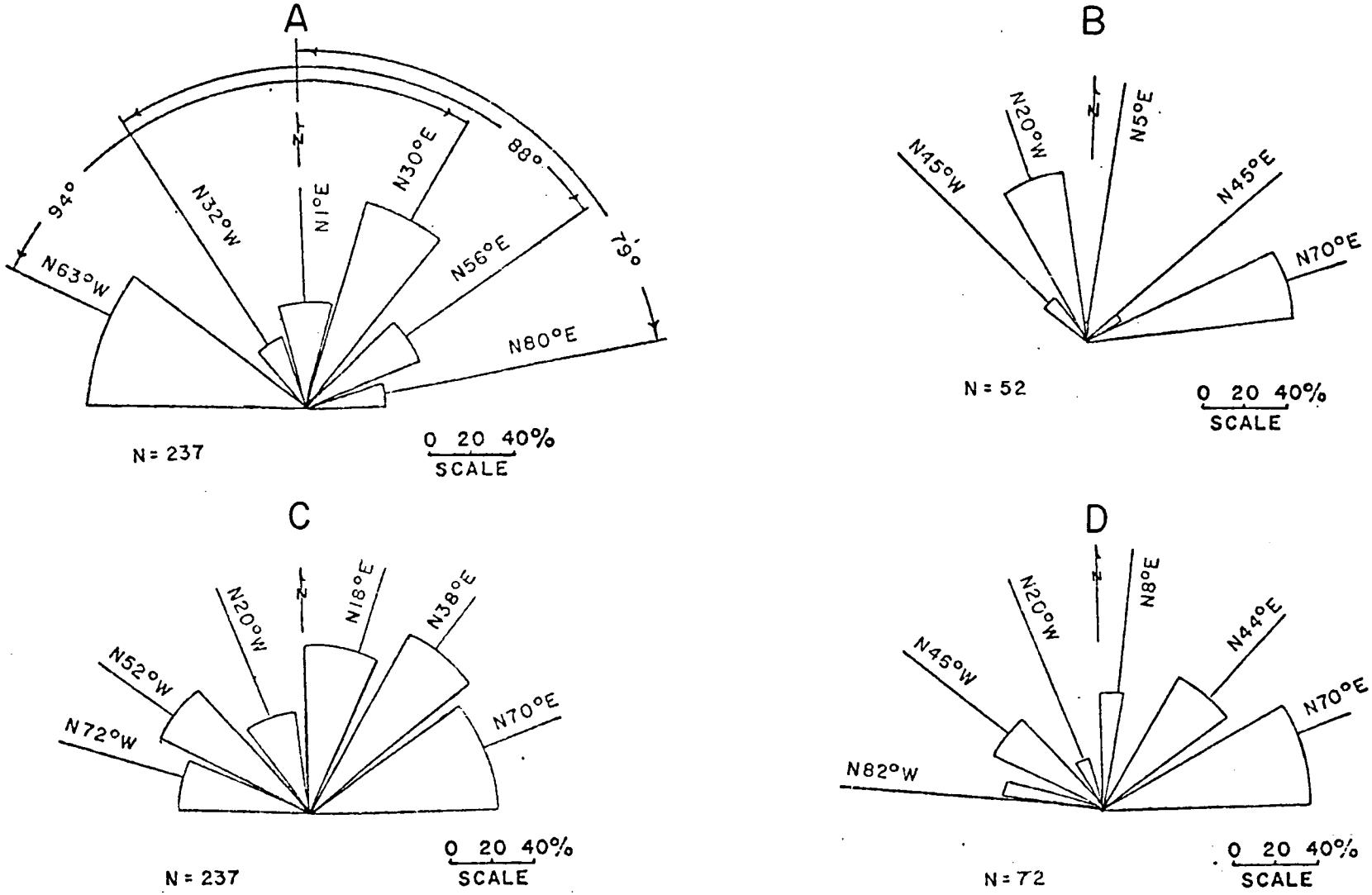

FIGURE 66. - A. Joint grouping by sets with 90° separation. B. Underground coal cleat. C. Total surface joints and D. Total underground joints (B, C and D are six-set Strain model computer program).

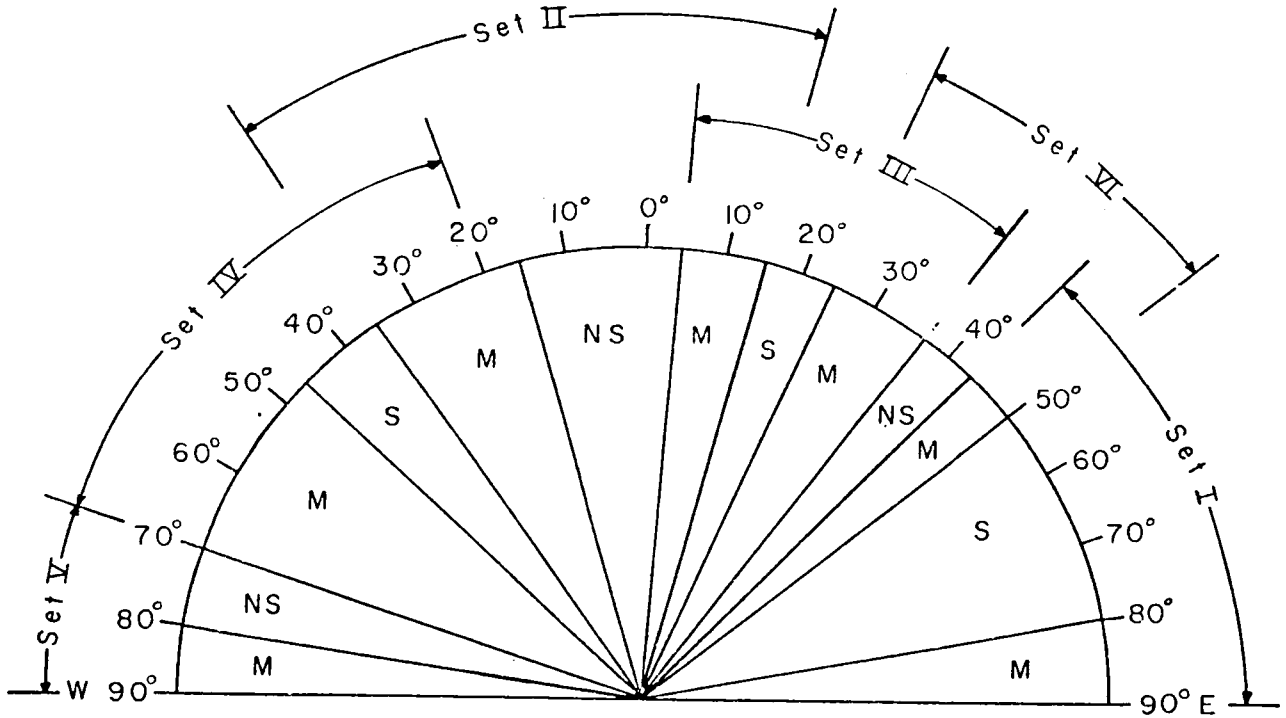

Figure 67. - Circular diagram of systematic and nonsystematic joint groupings. "Mixed" intervals, where both systematic and nonsystematic joints were observed, is designated by (M). (S) indicates systematic joint regions. (NS) indicates nonsystematic joint regions.

1. Only systematic joints were observed from N50°E to nearly N90°E. However, some nonsystematic joints are possible from perhaps N80°E to N90°E.

2. Only nonsystematic joints were observed in the range of about N15°W to N5°E, and from N70°W to N80°W. Also, only nonsystematic joints were observed from about N35°E to N45°E.

3. In the ranges from about N35°W to N48°W and N15°E to N25°E only systematic joints were noted.

4. On either side of these systematic intervals, both systematic and nonsystematic joints were observed and are designated M for mixed systematic and nonsystematic.

Keeping in mind that the surface joints considered represent joint observations over the entire study area and also observations from both the Harlan and Darby stratigraphic positions, it is likely that the areas of combined systematic and nonsystematic joints represent overlapping ranges over which adjacent systematic and nonsystematic joints occur, depending on location and stratigraphic position. After construction of Figure 67, the remaining surface joints studied appear to "fit" into the pattern shown.

Computer Analysis of Joints

In order to facilitate the analysis of joint data, several computer programs were written for the project by Dr. David Muse of the Morehead State University Mathematics Department. All of the programs were written in Fortran IV language and analyzed using an IBM 370 computer. The complete set of programs includes the following:

1. Unimodal and Bimodal Program.
2. Strain Model (4-mode and 6-mode).
3. Independent Mean Program (4-set and 6-set models).
4. Simulated Data Program.

Unimodal and Bimodal Programs

The Bimodal Program, in addition to being used for bidirectional sedimentary features, was also used for coal cleat analysis. The face and butt cleat directions generally form an angle of approximately 90°, and at least appear bimodal. The coal cleat was also analyzed using the Strain and Independent Mean Programs (Appendix D).

Strain Model Program

In considering tectonic stresses as a cause of joints, the study area provides an ideal structural setting to evaluate this concept since it is on the axis of the Middlesboro syncline immediately south of the Pine Mountain fault. This large mass of rocks has been thrust-faulted and transported toward the northwest, and tectonic forces responsible for this deformation are known to have acted toward the northwest (Figure 3, page 9).

Knowing the direction of tectonic forces makes possible the utilization of a model for grouping joint sets. Figure 68 shows the distribution of stresses as outlined by Friedman (31) that approximates the study area. The greatest principal stress axis (compressive) was horizontal and acted, in this case, toward the northwest. The

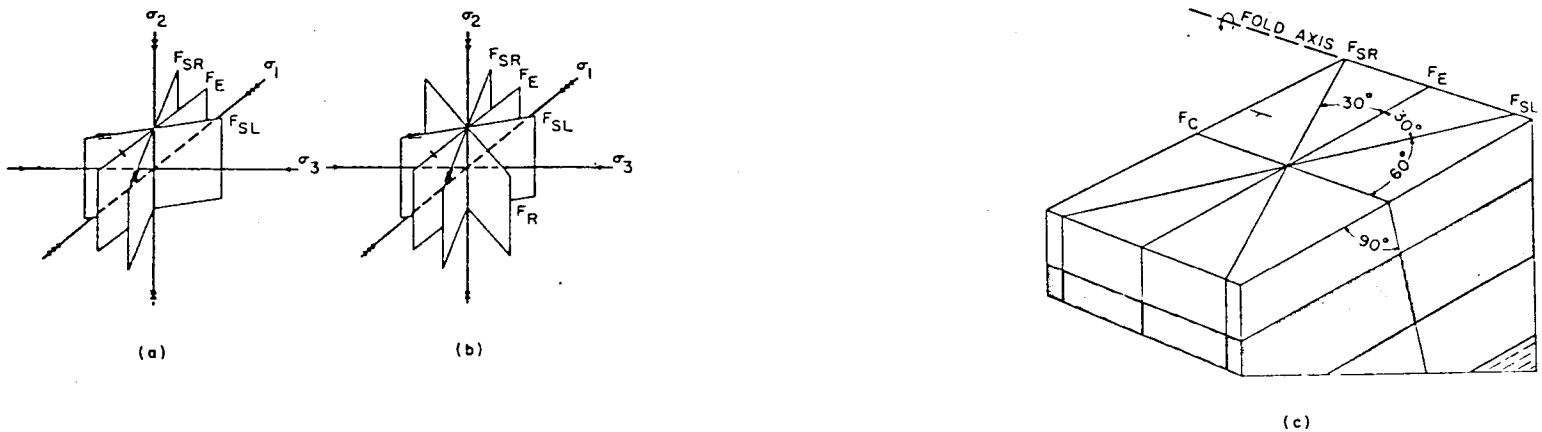

FIGURE 68. - Idealized geometric relationships between the principal stresses and fractures. A. Two shear fractures (F_{SL} and F_{SR}) are illustrated with the enclosed extension fracture (F_E). B. A relaxation fracture (F_R) is added to the configuration in A. C. An additional extension fracture (F_C) is added to the geometry in A in folded beds only. [Modified after Friedman (31)].

intermediate stress axis was vertical and the least stress axis was horizontal and at right angles to the greatest stress axis direction. In addition, two sets of shear fractures would be expected to develop at about ± 30° to the greatest stress axis (4).

The model used in this study is the strain ellipsoid (Figure 69). It is used here in the sense of being the reciprocal of the stress distribution system discussed by Friedman (31), and is an ellipsoid formed from an imaginary sphere in rocks subjected to compressive tectonic forces. Being the reciprocal of the stress axes discussed above, the greatest strain axis was parallel to the axis of the Middlesboro syncline. The intermediate axis was assumed vertical and the least strain axis paralleled the direction of known regional tectonic forces. If it is assumed that the ellipse was formed by compression parallel to the least strain axis, then four sets of joints would be expected to develop. The first set was formed parallel to the least strain axis and was tensional in origin. These joints are referred to as extension fractures. At right angles to this set is a set interpreted as forming later by release. In addition, two sets of shear fractures developed at acute angles to the least strain axis represented by θ_1 and θ_2.

In order to utilize the strain ellipsoid model (Figure 69) the 4-set Strain Program was used. Reference to Figure 70 A and B diagrammatically shows joint sets established by the program. Basically, the simplest case of the program was designed so that the greatest strain axis direction was "set". The computer was then instructed to group

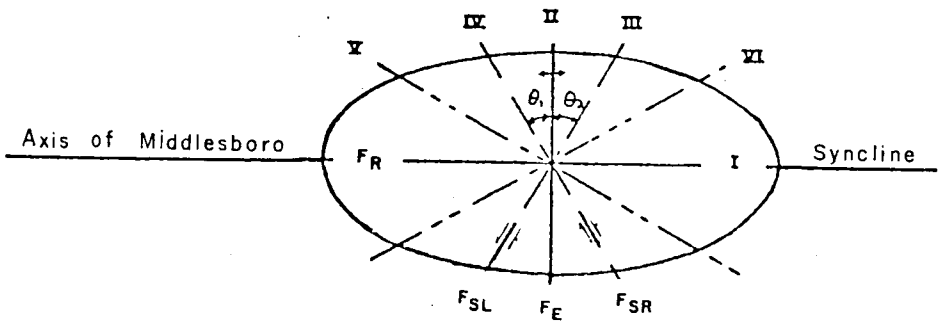

FIGURE 69. - Orientation of the strain ellipsoid to the Middlesboro Syncline. Axes of Middlesboro Syncline "fits"model in Figure 68 (C), page 145,by paralleling extension fracture (F_c) line.

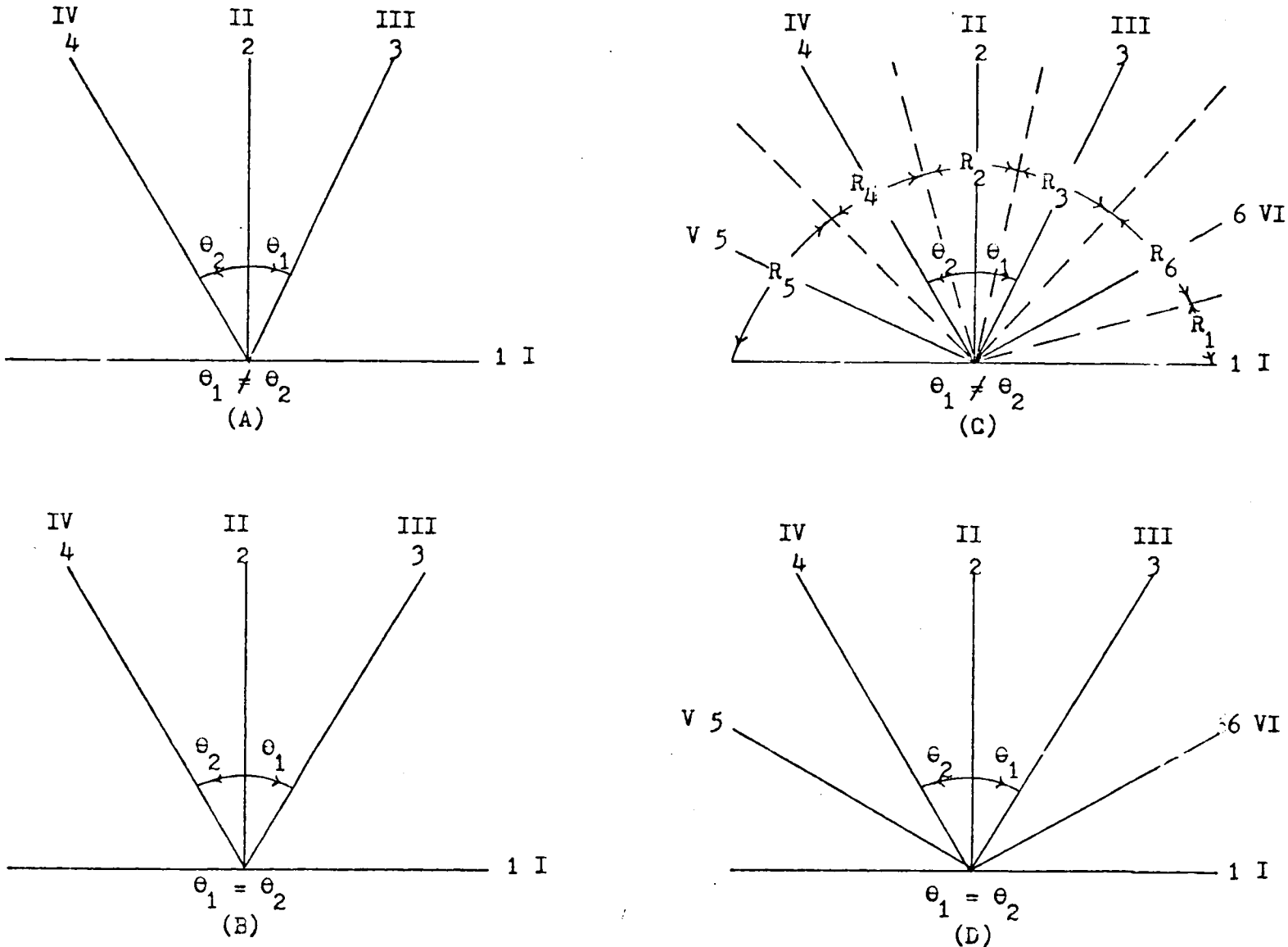

FIGURE 70. - Computer program models. (A) and (B) are 4-set models; (C) and (D) are 6-set models.

joint bearings around this axis as a mean (set I). Next, joint bearings were grouped around the least strain axis as a mean at right angles to the greatest strain axis (set II). The computer was then instructed to search both east and west of the least strain axis direction from 25° to 50° in increments of 1° until bearings were determined which yielded minimum variance. These joint set bearings, then, theoretically represent the positions of the two sets of shear fractures (sets III and IV). Specific details of the program are given in Appendix D.

The computer program also has been used to analyze a 6-set model (Figure 70 C and D). In addition to the sequence outlined in the 4-set model above, sets V and VI are determined by the establishment of a mean at 90° from sets III and IV.

Additional analyses were made to determine the most probable direction of the greatest strain axis. Geologic maps of the area indicate that the approximate directional trend of the Pine Mountain fault in the study area is from N60°E to N70°E. This trend should approximately parallel the axis of the Middlesboro syncline and the greatest strain axis direction of the strain ellipsoid. Table 11 shows several computer runs, in which the greatest strain axis was "set" at various bearings from N60°E to N80°E. The N70°E and N75°E directions produced the least variance for the 6-set model.

A comparison between total surface and underground joints according to the 6-mode N70°E program shows that joint set means are within 10° (Figure 66, page 141). Figure 66 shows the 6-set model underground coal cleat. The histogram shows the well-defined face cleat (mean N70°E)

TABLE 11. - Total variances associated with Strain Program

	Model	$\theta_1 \neq \theta_2$
N60°E	4	159.5
	6	100.4
N65°E	4	130.3
	6	76.9
N70°E	4	120.9
	6	
N75°E	4	120.9
	6	58.1
N80°E	4	130.7
	6	61.1

and butt cleat (mean N20°W). Also, the model grouping of joints may indicate that the coal cleat involves more than one set of jointing.

Assignment of joint sets to the strain ellipsoid model may be summarized as follows:

1. Of the six sets of joints, sets I, III and IV are here considered systematic (set I includes the coal face cleat and III and IV are shear fractures). Sets II, V and VI are considered nonsystematic (set II includes the coal butt cleat direction).

2. The assignment of sets III and IV as shear fractures is based on the presumed stress field that produced the Pine Mountain fault. Associated with overthrust faults are tear faults that formed when the overthrust sheet moved forward. The Jacksboro fault and the Russell Fork fault, bounding the Cumberland overthrust block, are of this type (Figure 3, page 9). Spencer (74) described other associated faults as follows:

> Tears oriented normal to the thrust and in positions which might be explained in terms of shear failure (two conjugate sets at ± 30° to the direction of transport of the thrust) of the overthrust plate are commonly found.

While no tear faults within the thrust sheet are present in the immediate area of the mines, faults of this kind may be found in the Middlesboro, Kentucky area about 30 miles to the southwest (25). Here, the trace of the Rocky Face fault follows a general north-south trend with local trends at about N45°W (Figure 3, page 9). These trends approximate the mean directions of the shear joints in the study area. Since the Middlesboro area occupies a comparable position in the thrust

sheet it is probable that similar shear stresses were present in both areas, but that greater shear stresses in the Middlesboro area produced tear faults whereas only shear fractures developed in the study area. Also, normal faults along the leading edge of the Pine Mountain fault just north of the Middlesboro area that trend approximately N20°W to N30°W give support for tensional stresses indicated in set II joints. However, it is possible that some set II joints may have formed by shearing stresses as this set is parallel to the direction of thrusting.

Independent Mean Program

Since the Strain Model Program was restricted in that set II joints were required to be "set" at a 90° angle from set I joints it was decided to devise a program that was free of any restrictions.

The Independent Mean (I.M.) Program, also based on minimum variance criteria for joint grouping and the determination of joint means, was written to accommodate either 4- or 6-sets of joints. The basic difference is that none of the joint set directions are restricted in any way. The program is written so that after ordering the data, the computer begins at N90°W. Proceeding clockwise (eastward) in 1° increments, the computer calculates minimum variances and stores tentative joint set means until all data is calculated. When the total variance is minimized, the resulting joint means and ranges are printed.

The advantage of the I.M. Program is that it is not restricted. However, it has the disadvantage of "requiring" a certain number of joints. If the 6-set program is used to analyze only five actual joint

sets, the set with the greatest variance will be divided into two sets with joint means close together. Tables 12, 13 and 14 show joints in the study area at separate localities and also combined joint data analyzed by both the I. M. and Strain Programs.

An encouraging comparison for both the I. M. and Strain Programs is shown in Tables 12, 13 and 14. Both the 4-set and 6-set models establish essentially the same means, especially for total surface joints shown in Table 14. This is an indication that both programs are comparable. Also, it is an indication that the joint grouping approximates the Strain Model for the Middlesboro syncline. It should be noted, however, that the Strain Program provides for joint analysis solely on the basis of the 90° separation between sets, even if a "tectonic" model is disregarded.

Simulated Data Program

The Simulated Data Program was written to further test both the I. M. and the Strain Programs by providing data with predetermined means. Both programs were able to analyze the data and produce comparable results (Table 15). Also, while the simulated data was generated with six separate means, Figure 71 shows how the joints were grouped with the 4-mode I. M. Program. Note that as the variances increase from top to bottom in Figure 71, the ranges increase and the 4-set program combines the two adjacent sets with minimum separation in the 6-set model.

TABLE 12. - Regional surface joints - comparison of Strain[a] and Independent Mean Programs - 6-Set Model

Location	Program	Variance	Set I	Set II	Set III	Set IV	Set V	Set VI
Harlan I &II (18)[c]	70° Strain	34.61	N70°E(4)[b]	N20°W (2)	N20°E (4)	N53°W (3)	N70°W (4)	N37°E (1)
	I.M.P.	24.08	N68°E (4)	N10°W (2)	N19°E (4)	N50°W (2)	N67°W (5)	N40°E (1)
Harlan III (75)	80° Strain	61.87	N80°E (16)	N10°W (12)	N18°E (5)	N53°W (14)	N72°W (5)	N37°E (23)
	I.M.P.	48.18	N81°E (12)	N9°W (12)	N31°E (24)[d]	N52°W (14)	N74°W (5)	N55°E (8)[d]
Harlan IV (29)	85° Strain	23.86	N85°E (0)	N5°W (2)	N22°E (10)	N49°W (5)	N68°W (9)	N41°E (3)
	I.M.P.	10.61	N40°W (2)[e]	N - S (2)	N21°E (10)	N56°W (4)[e]	N69°W (8)	N41°E (3)
Harlan V (Darby E) (15)	60° Strain	26.60	N60°E (3)	N30°W (1)	N15°E (4)	N55°W (2)	N75°W (2)	N35°E (3)
	I.M.P.	10.26	N62°E (3)	N25°W (1)	N13°E (4)	N48°W (2)	N70°W (2)	N38°E (3)
Darby A (36)	75° Strain	41.56	N75°E (4)	N15°W (3)	N25°E (11)	N40°W (1)	N65°W (9)	N50°E (8)
	I.M.P.	22.17	N77°E (4)	N11°W (3)	N29°E (9)[f]	N15°E (4)[f]	N59°W (10)	N55°E (6)
Darby B (32)	60° Strain	26.66	N60°E (5)	N30°W (2)	N19°E (5)	N55°W (5)	N71°W (8)	N35°E (7)
	I.M.P.	15.74	N59°E (5)	N18°W (2)	N18°E (5)	N60°W (8)	N73°W (5)	N36°E (7)
Darby C (21)	80° Strain	67.95	N80°E (4)	N11°W (5)	N15°E (1)	N39°W (5)	N75°W (2)	N51°E (5)
	I.M.P.	39.16	N79°E (4)	N11°W (5)	N32°W (4)[g]	N59°W (2)[g]	N82°W (1)	N48°E (5)
Darby D (12)	85° Strain	49.33	N85°E (3)	N5°W (2)	N27°E (2)	N38°W (4)	N63°W (0)	N52°E (1)
	I.M.P.	22.71	N89°E (2)[h]	N17°E (3)	N27°E (2)	N41°W (3)	N74°E (1)[h]	N50°E (1)

[a] Strain program with $\theta \neq \theta$
[b] Indicates number of observations for each joint set
[c] Indicates total observations per locality
[d] These sets included in Set I, Set II and Set VI of 80° Strain Program
[e] These sets included in Set IV and Set V of 85° Strain Program
[f] These sets included in Set III and Set VI of 75° Strain Program
[g] These sets included in Set IV and Set V of 80° Strain Program
[h] These sets included in Set I of 85° Strain Program

TABLE 13. - Regional surface joints - comparison of Strain[a] and Independent Mean Programs - 4-Set Model

Location	Program	Variance	Set I	Set II	Set III	Set IV
Harlan I & II (18)[c]	70° Strain	78.44	N70°E (4)[b]	N20°W (2)	N23°E (5)	N62°W (7)
	I.M.P.	98.48	N68°E (4)	N10°W (2)	N23°E (5)	N62°W (7)
Harlan III (75)	75° Strain	102.36	N75°E (18)	N15°W (12)	N32°E (26)	N58°W (19)
	I.M.P.	96.64	N74°E (18)	N9°W (12)	N32°E (26)	N58°W (19)
Harlan IV (29)	70° Strain	100.62	N70°E (0)	N20°W (3)	N25°E (14)	N65°W (12)
	I.M.P.	46.57	N38°E (4)[d]	N49°W (5)[d]	N16°E (11)	N68°W (9)
Harlan V (Darby E) (15)	60° Strain	122.53	N60°E (5)	N30°W (2)	N17°E (5)	N63°W (3)
	I.M.P.	87.20	N50°E (6)	N40°W (3)	N13°E (4)	N70°W (2)
Darby A (36)	65° Strain	86.42	N65°E (10)	N25°W (3)	N25°E (13)	N60°W (10)
	I.M.P.	71.22	N64°E (10)	N11°W (3)	N25°E (13)	N60°W (10)
Darby B (32)	65° Strain	73.00	N65°E (5)	N25°W (2)	N25°E (12)	N65°W (13)
	I.M.P.	59.77	N59°E (5)	N18°W (2)	N29°E (12)	N65°W (13)
Darby C (21)	80° Strain	145.52	N80°E (4)	N10°W (7)	N40°E (5)	N54°W (5)
	I.M.P.	99.44	N79°E (4)	N20°W (9)	N48°E (5)	N66°W (3)
Darby D (12)	85° Strain	79.50	N85°E (3)	N5°W (2)	N34°E (3)	N37°W (4)
	I.M.P.	65.89	N84°E (3)	N17°W (3)	N34°E (3)	N41°W (3)

[a]Strain Program with $\theta_1 \neq \theta_2$

[b]Indicates number of observations for each joint set

[c]Indicates total observations per locality

[d]Results because no joints observed N70°E

TABLE 14. - Total surface joints (n = 237)

	Variance	Set I	Set II	Set III	Set IV	Set V	Set VI
6-Mode Independent Mean Program	56.49	N73°E	N13°W	N20°E	N48°W	N67°W	N41°E
6-Mode Strain Program	58.05	N75°E	N15°W	N22°E	N48°W	N68°W	N42°E

TABLE 15. - Simulated joint data (n = 54)

	Variance	Set I	Set II	Set III	Set IV	Set V	Set VI
6-Mode Independent Mean Program	16	N69°E	N21°W	N19°E	N60°W	N69°W	N32°E
6-Mode Strain Program	16	N70°E	N20°W	N19°E	N60°W	N71°W	N30°E
4-Mode Independent Mean Program	16	N69°E	N21°W	N25°E	N65°W		
4-Mode Strain Program $\theta_1 \neq \theta_2$	16	N70°E	N20°W	N25°E	N65°W		
Actual Means		N70°E	N20°W	N20°E	N60°W	N70°W	N30°E

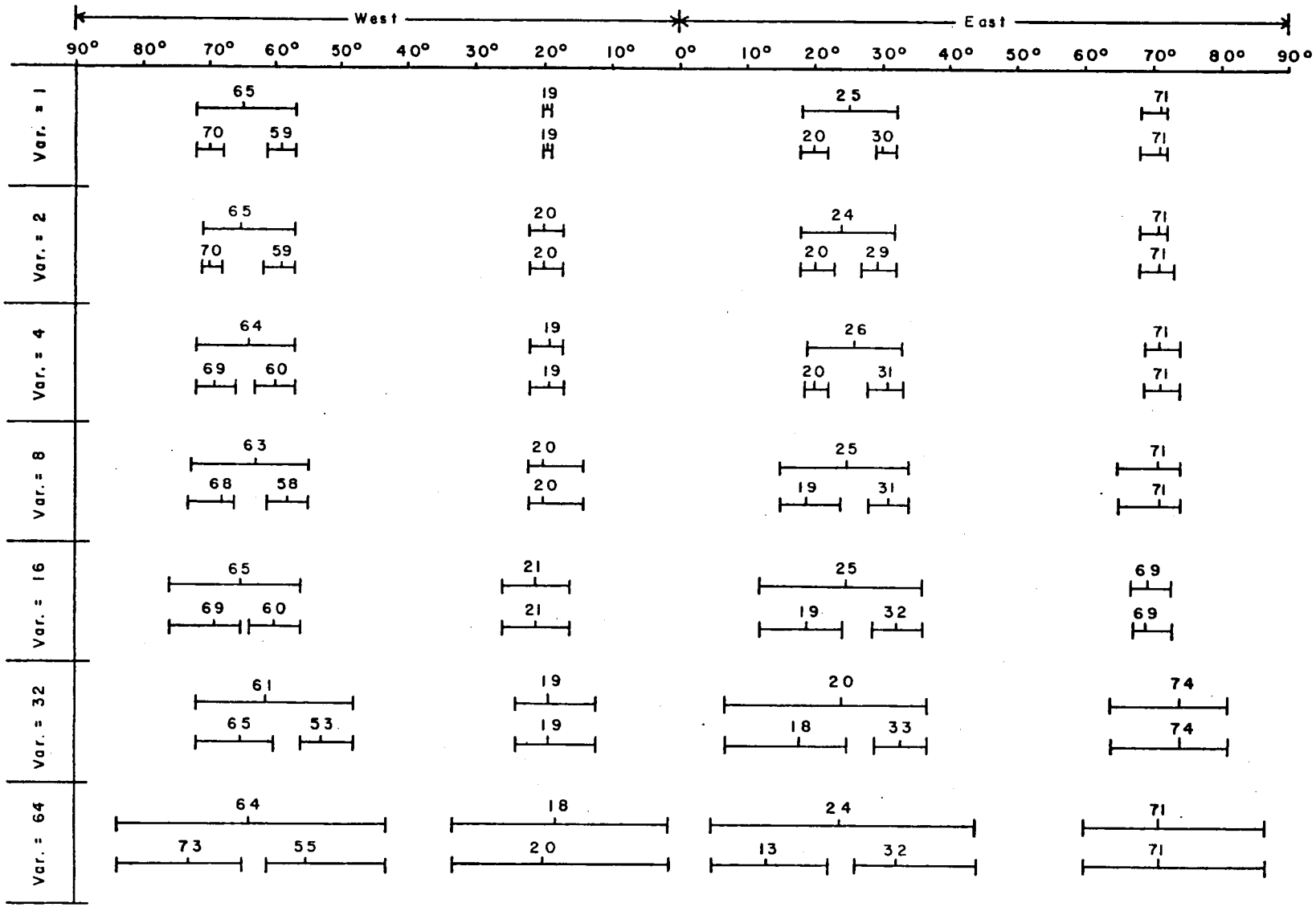

FIGURE 71. - Simulated data analysis by Independent Mean Program. Both 4-mode and 6-mode ranges and means shown. Actual means are N70°E, N30°E, N20°E, N20°W, N60°W and N70°W.

Drainage Analysis

The drainage pattern of the Clover Fork River and its tributaries within the study area was analyzed to investigate the possible correlation between the drainage pattern and joint trends.

The drainage net was divided into three regions of approximately equal size in order to compare possible east-west variations in the drainage pattern (Figure 72).

For computer analysis, parts of the streams were divided into straight-line segments on a base map (scale 1:24,000). The bearing of each segment was determined with a protractor. For frequency comparisons, the lengths of segments were weighted. All stream segments one inch long or less on the map were counted once. Longer segments were counted as multiples of one inch. The data was analyzed using the I. M. Program and the resulting circular histograms are shown in Figures 73 and 74.

The histograms of the three regions (A, B. and C) are, in general, very comparable in mean directions of sets. Also, the angular ranges between sets is approximately 90°. These facts strongly suggest that the drainage pattern is systematic in the area, and is likely controlled by jointing.

Comparison of 4-Set and 6-Set Joints

Considerable time was spent during the study in the attempt to determine whether four sets or six sets of joints are present in the study area. Preliminary analyses based on grouping joints from field

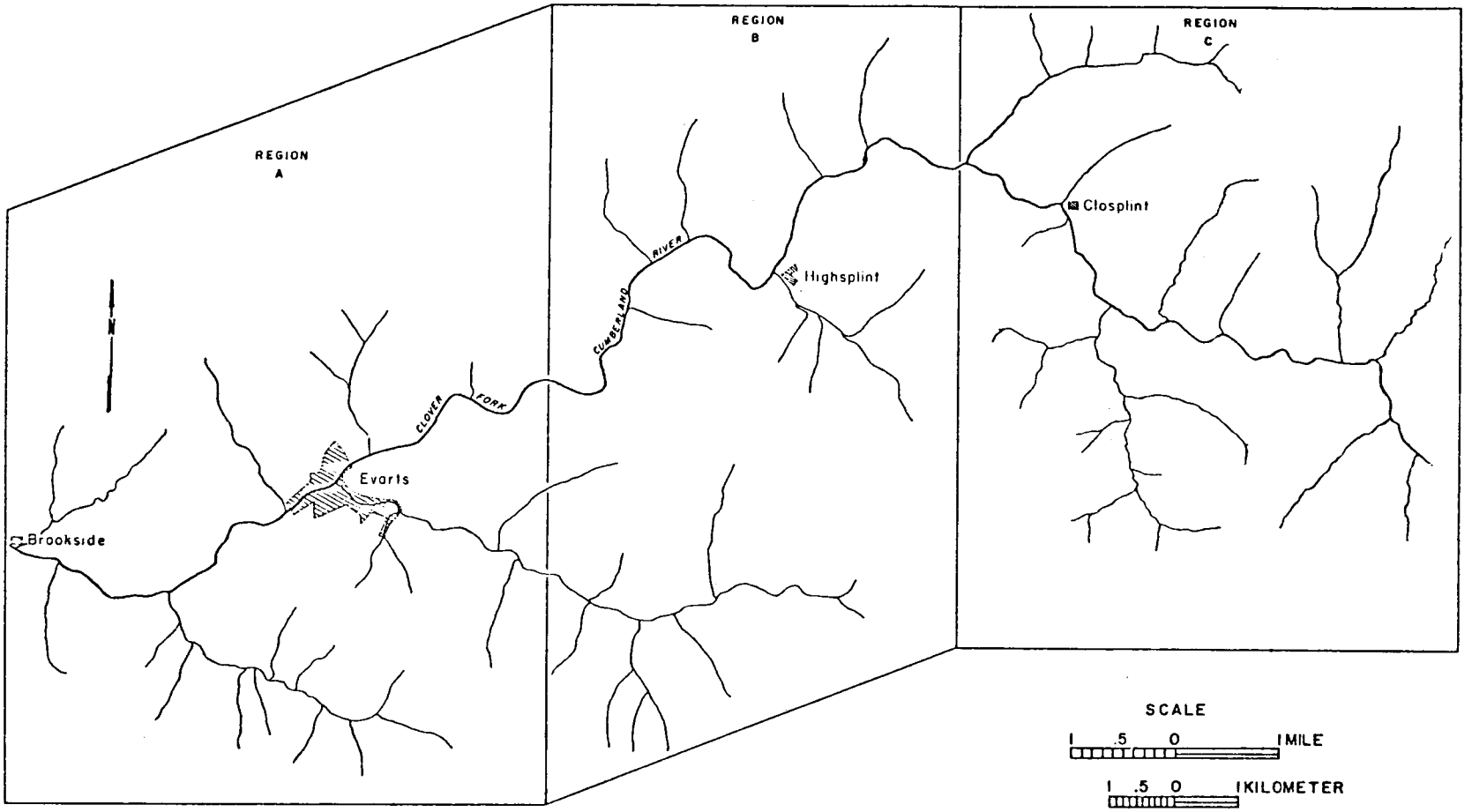

FIGURE 72. - Clover Fork drainage system and regions A, B and C for computer analysis.

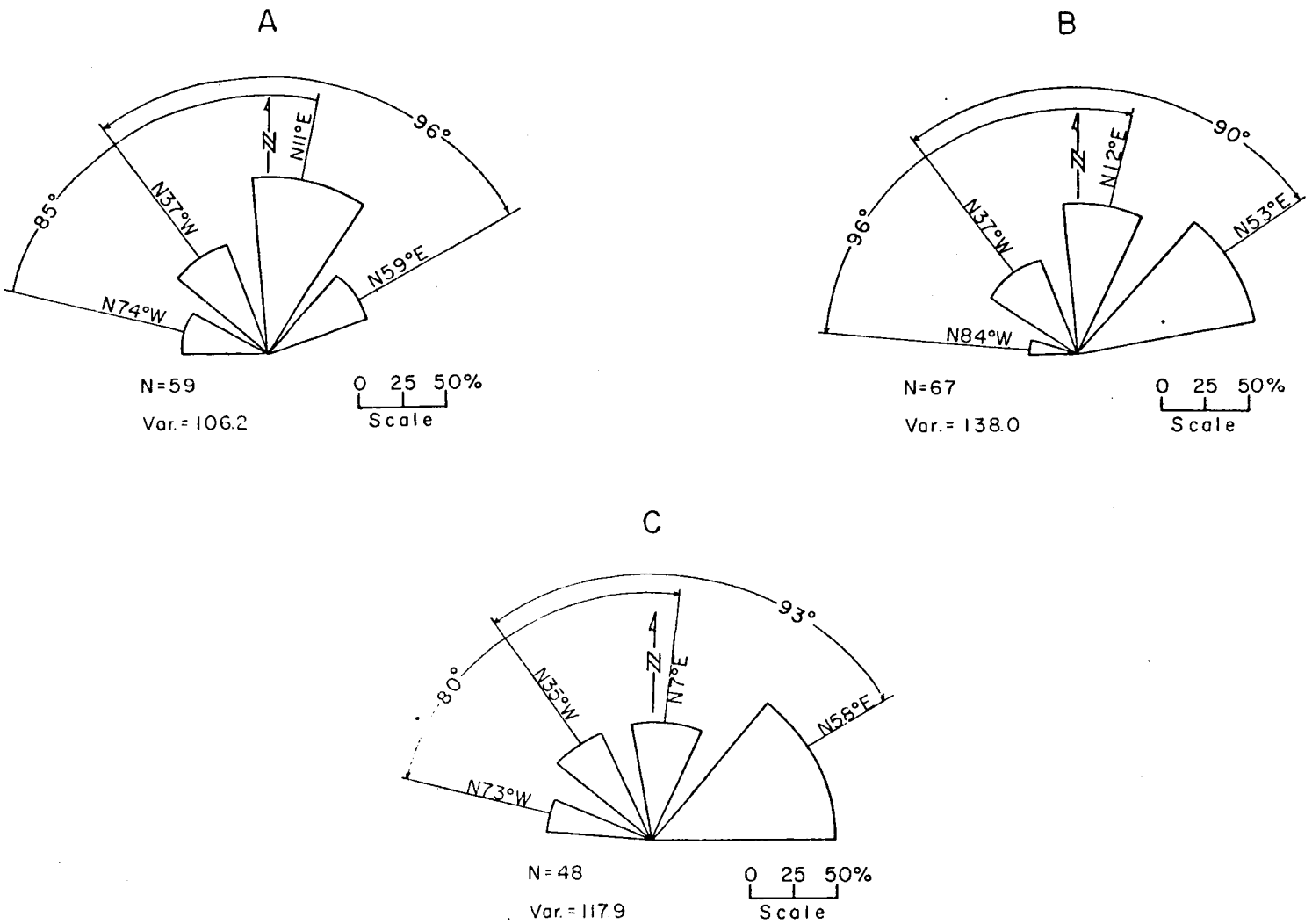

FIGURE 73. - Four-Mode Independent Mean Program (I.M.) circular histograms for drainage regions A, B and C.

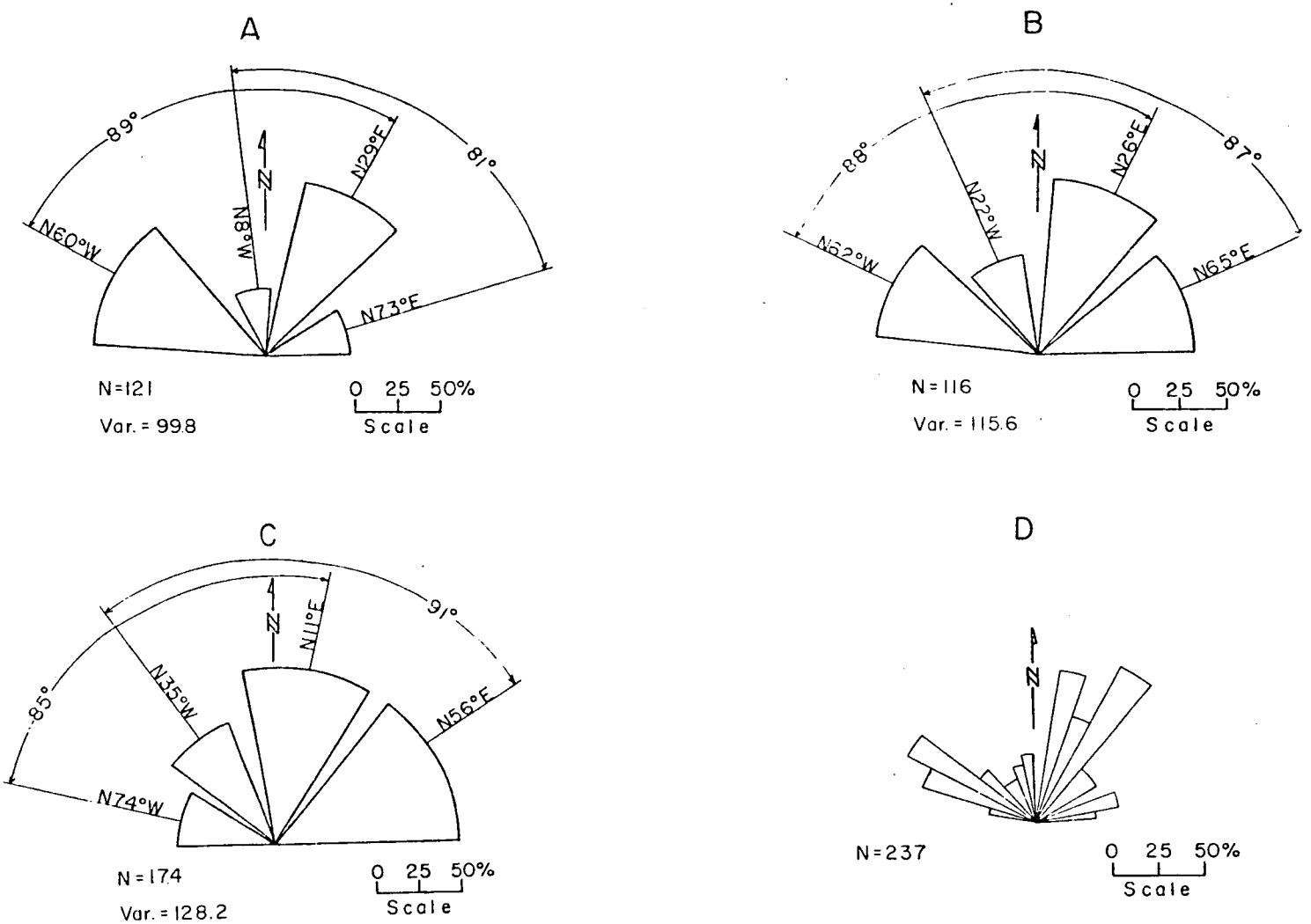

FIGURE 74. - Four-Mode Independent Mean Program circular histograms of A. Total Harlan surface joints B. Total Darby surface joints C. Total surface drainage and D. Total surface joints in ten degree intervals.

observations using 90° separation between sets indicated six sets in the study area. For all practical purposes of regional analysis, it was concluded that the 4-set model provides meaningful results, because the 4-set model shows dominant directions of jointing, which is of major importance in mine-layout and design. However, the 6-set model may be desirable to determine the means of these joint sets with greater variance in a 4-set system, or to analyze possible 6-set joint systems. Table 13, page 155, shows 4-set means and joint frequency for surface joints at each locality. The localities are shown on Figure 64, page 136.

Figure 74 shows the 4-mode Independent Mean Program used to analyze total Harlan surface joints, total Darby surface joints and total surface drainage as determined from map analysis. Also shown is a circular histogram of total surface joints drawn from raw data in 10° intervals, without regard to joint-set grouping as in Figure 66 A, page 141. The resulting histogram indicates two major modes; one toward the northwest and another toward the northeast. Also, a minor mode is indicated slightly west of north, and another nearly due east. The same general histogram patterns and relative mode frequencies are reflected in the computer-analyzed histograms of the total Harlan and Darby data (Figure 74 A and B). The total drainage histogram, however, is rather inconsistent when set ranges and set means are compared to the Harlan and Darby histograms.

Regional Joint Map

Figure 75 shows the 4-mode Strain Program joint means drawn from values obtained in Table 13, page 155 at or near each field locality

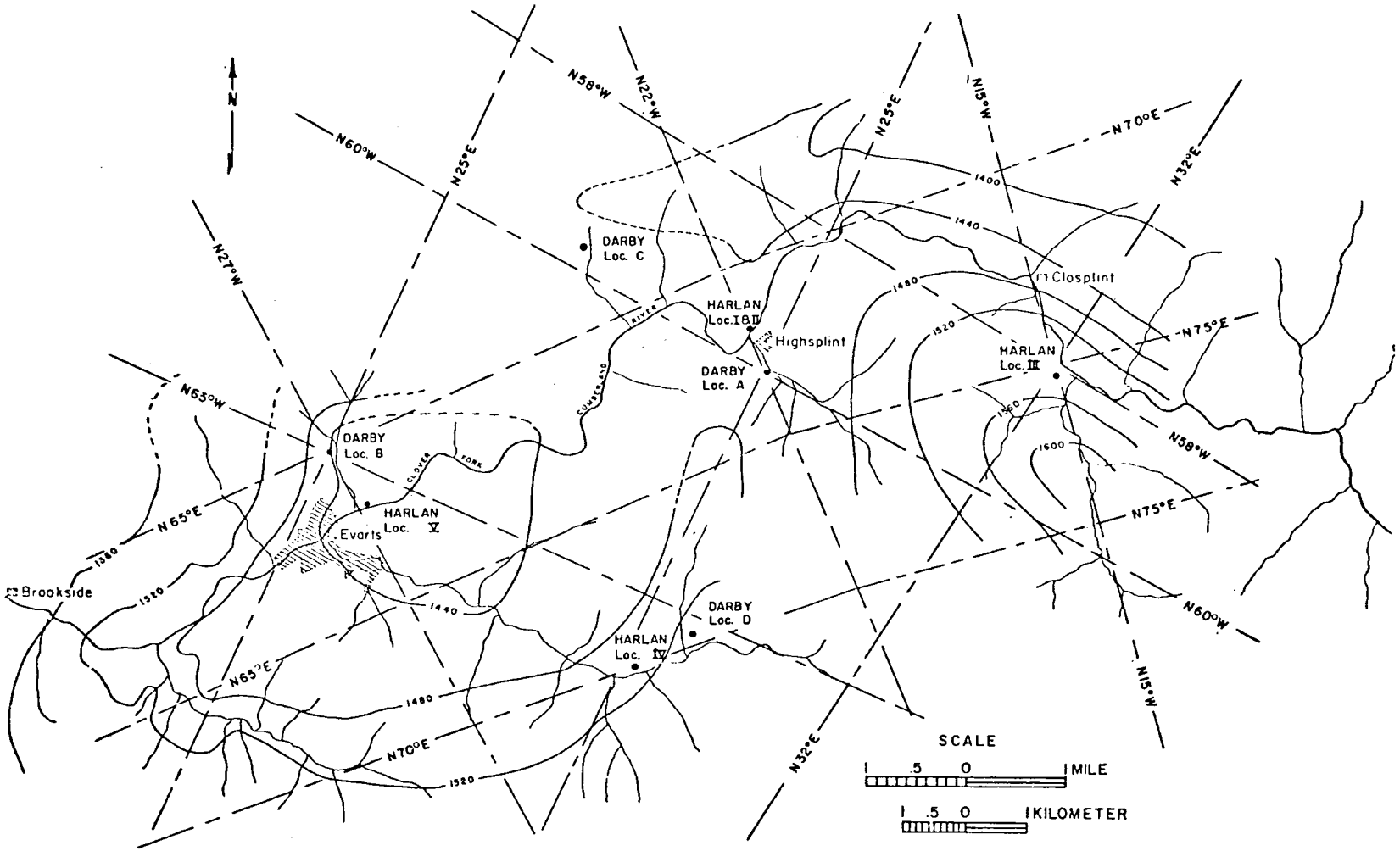

FIGURE 75. - Projections of 4-mode Strain Program means across study area from station localities. Projections superimposed on Clover Fork drainage and structure contours (from USGS geologic quandrangles).

projected so that a regional joint pattern is produced. The following observations may be made concerning the joint "overlay."

1. There is a progressive eastward swing in all joint set mean directions from west to east across the study area. Also, it is significant that the Bimodal Computer Program indicates that the coal cleat follows the same eastward shift as do the joints. The coal face cleat in the Bailey Creek mine is N61°E and the butt cleat is N36°W. At the Highsplint mine, however, the face cleat is N68°E and the butt cleat is N20°W.

2. There is little variation between joint means at the Harlan Locality I and Darby Locality A horizons at Highsplint. The same relationship holds true between Darby Locality B and the Harlan Locality V at Bailey Creek. There is a greater variation between the Harlan Locality IV and Darby Locality D, and also between the Harlan Locality I and Darby Locality C. The close relationship between two localities and a greater deviation at two others suggests that the joint patterns are probably vertically limited in variability, but that other factors such as poor exposure, sampling error or minor joints at N85°E may have caused anomalous results at Darby Locality D and Darby Locality C.

3. The resulting joint pattern appears to remain reasonably constant regardless of lithology. At Harlan Locality V joints occurred largely in shale with some interbedded sandstone. The other localities were dominantly sandstone outcrops. In fact, where joints were observed in sandstone underlain by shale, systematic joints were continuous through both sandstone and shale.

4. The close relationship between the joint pattern overlay and the drainage pattern of the Clover Fork River and its tributaries is obvious. In most cases, straight segments of the meandering drainage are parallel or subparallel to one of the projected joint means. The general path of the Clover Fork from southwest to northeast follows the swing of the N65°E joint set. Also, the frequencies of drainage segments increase toward the east from regions A through C (Figure 73, page 160).

5. Because the Clover Fork drainage system appears to be controlled at least partially by local structure, it also follows that joint sets reflect local structure. For example, at Harlan Locality III the set IV (N58°W) joint set is subparallel to the local structural high in that area and set III (N32°E) cuts across the same structure. Joint set III is subparallel to the structural low trending slightly east of due north at Harlan I and IV Localities and Darby A and D Localities. Most notable is set I (N60°E to N75°E) that follows the axis of the Middlesboro Syncline (Figure 75, page 163).

Comparison of Surface and Subsurface Joints

While the ellipsoid model shows a reasonably close correlation between surface and subsurface joints, some observations concerning the histograms in Figure 76, which compare surface and underground observations in the Highsplint area, and total data for the study area (Figure 74, page 161 and Figure 66, page 141 may be summarized as follows:

1. The major stresses that formed the Cumberland overthrust block may not have operated continuously or in a constant direction. It has

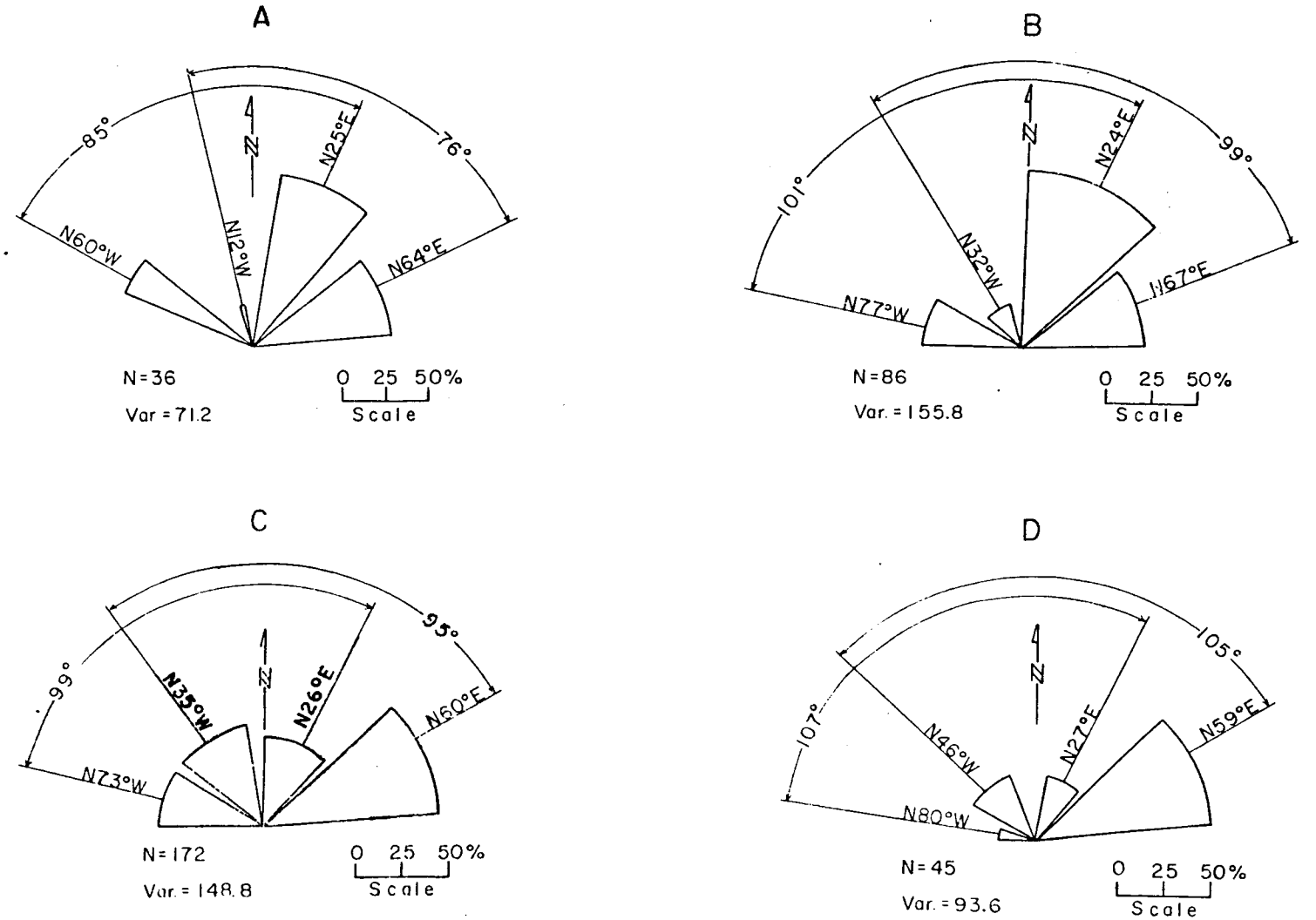

FIGURE 76. - Highsplint Area 4-mode Independent Mean Program circular histograms of A. Surface joints (location Darby A) B. "Slips" in Highsplint Darby mine C. Joints in Highsplint Derby mine and D. Sandstone trough axes in Highsplint Darby mine.

been estimated, for example, that the southwestern part of the thrust sheet moved approximately ten miles whereas the northeastern part moved only two miles (7). These effects, coupled by stresses generated by the fault moving over an uneven base, could increase the variance of observed joints and possibly generate separate sets of joints. This is a likely explanation for the arcuate trend of joints (Figure 75, page 163).

2. Observations within the mines have shown that in many cases the directions of coal cleat, joints in the roof and the linear trend of paleochannel fills correspond very closely (Figure 75). In fact, authors of several regional joint studies have concluded that many joints formed early in the rocks before deformation and are the result of a variety of causative factors that might generate stress differences. Some of these include sustained tidal effects (44), high fluid pressure in the rocks approaching the magnitude of overburden weight (70), upward propagation of fractures from older fractures (39) or warping of the sedimentary basin prior to regional folding (58).

Attempts to assign joints to the tectonic effects of the Pine Mountain thrusting versus pretectonic effects in the area were met with considerable difficulty because of coincidental factors. The axis of the depositional basin in the area, referred to as the Pocahontas basin by Ferm (27), approximates the trend of the structural axis of the Middlesboro syncline (Figure 52, page 99). As an example of the difficulty involved, the mean direction of joint set I (including the dominant coal face cleat) approximates both the strike direction of the depositional basin and also the structural axis. It is possible, then,

that this joint set initially formed prior to the Pine Mountain thrusting and was retained during and after thrusting. It is also likely that joint set I has developed both as an extension fracture and also by shearing due to changing principal stress directions during thrusting. Overprinting of joints developed during thrusting and afterward by unloading over older joints is a possible explanation for the development of six sets instead of four in the area (58). This would apply especially to sets V and VI.

Conclusions and Recommendations

Based on results of joint studies, the following conclusions and recommendations may be made:

1. Because of sampling difficulties both inside the mines and at surface exposures, it appears that computer analysis of joints based on minimum variance is desirable. Mean directions of sets provide an indication of possible zones of weakness, especially systematic joint directions. Also, it would be desirable to analyze joints on both 4-mode and 6-mode programs and compare histograms in order to evaluate joint frequency.

2. While an analysis of drainage patterns outside a "structural" area such as the Middlesboro syncline is desirable to test this method of analysis, it is logical to assume that a computer analysis of such patterns from topographic maps will give a good indication of dominant joint directions. This type of analysis might be supplemented by field checking.

3. Once dominant joint patterns are established for an area of mining, it is recommended that room and pillar entries be laid out so that headings bisect joint trends. This would allow joint trends to run diagonally across the pillars and not parallel to them.

4. It is not known with certainty how detrimental jointing is to roof conditions when compared to other geologic factors such as paleochannel trends. The impression gained from monitoring to date is that jointing in the absence of other factors is most detrimental under fairly shallow overburden. Shallow overburden would be essentially the zone of weathering and encountered most frequently near the crop line or under stream valleys, perhaps at depths of less than 600 feet (see discussion, page 85). It should be noted, however, that rock jointing and/or "slips" may accompany channel trends, kettlebottoms, and other geologically related features.

VIII. - CORE DRILLING AND CORE ANALYSIS - 004 SECTION, HIGHSPLINT MINE

In January, 1974, a series of ten NX diamond drill cores were taken from the existing roof in the 004 Section, Highsplint mine. The objective of the coring program was to study a small part of the mine in detail to supplement mine mapping and trend analysis. One major part of the study was to delineate lithologic and/or structural trends leading into a roof-fall area. However, it was not possible to adequately sample the main sandstone roof without coring. The cores provided samples that were vertically continuous and presumably unaffected by the mine atmosphere.

Core-drilling equipment consisted of the apparatus shown in Figure 77 for use with the roof-bolting machine (Figure 78). After recovery, the core sections were wrapped in polyethylene and stored in core boxes.

The location of the drilling site is in the old 004 Section of the mine, designated O-15 to P-16 in Figure A1, Appendix A. Figure 79 shows the drilling site in detail together with the locations of the core holes on either side of the roof-fall zone (roof falls shown by dashed circles).

The correlation diagram in Figure 80 shows a cross-sectional view of the cores, together with the supplemental rib sections. The existing roof coincides with the base of the cores except in the roof-fall zone where the roof has fallen to the approximate horizon indicated by the top of the roof-fall section.

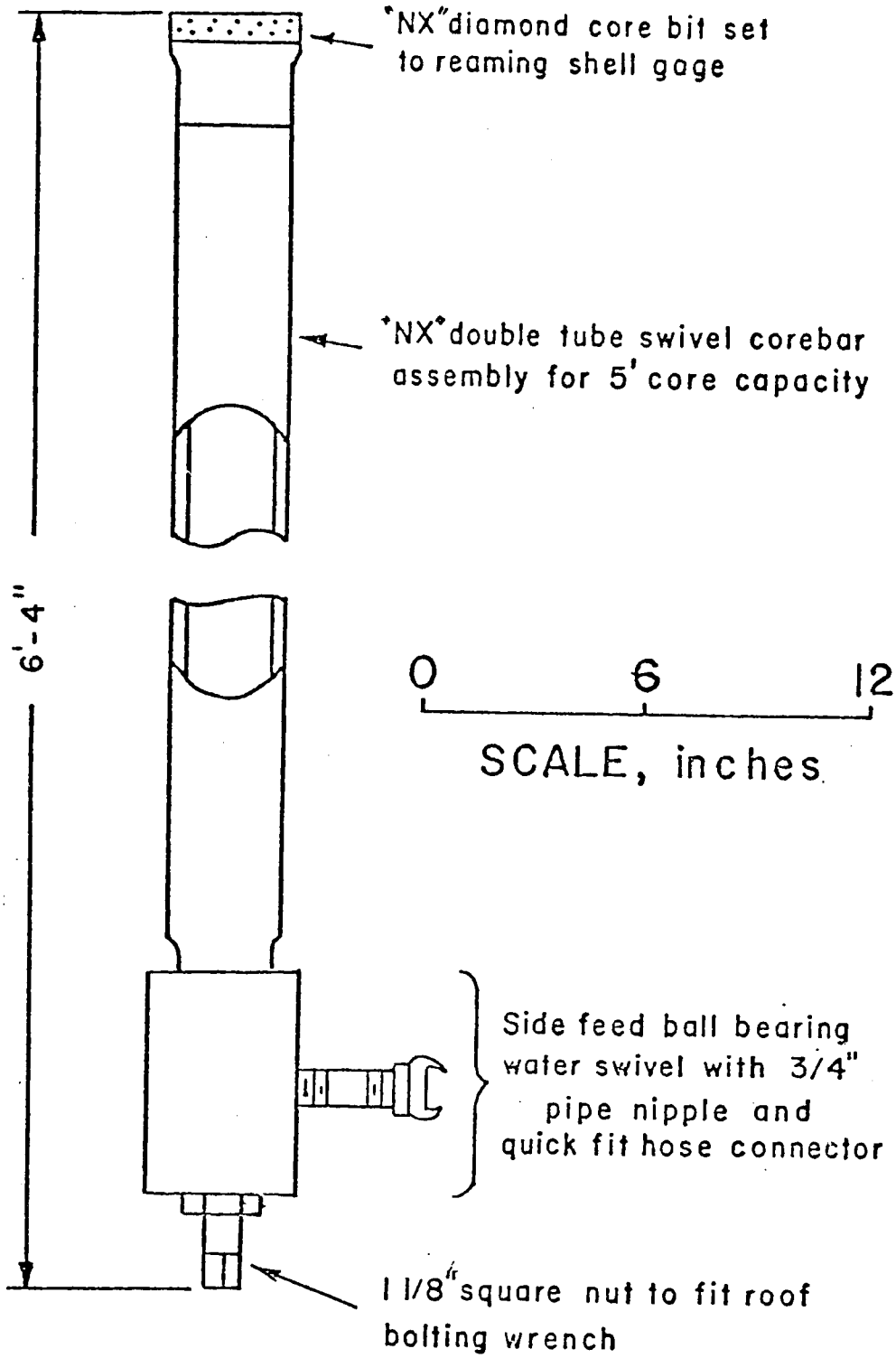

FIGURE 77. - Core-drilling apparatus (redrawn from U. S. Bureau of Mines illustration).

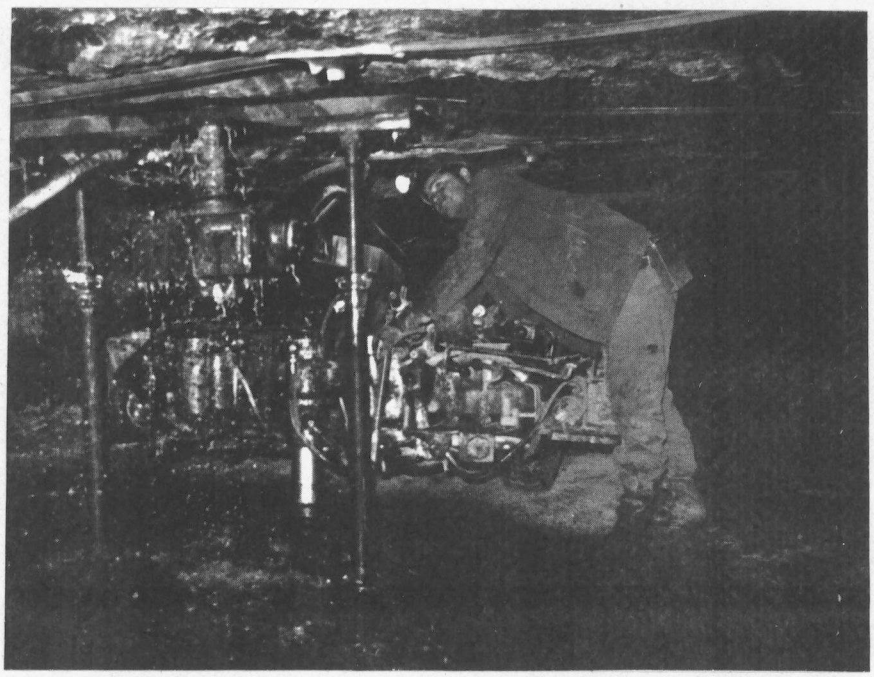

FIGURE 78. - Core-drilling equipment used in 004 Section, Highsplint mine. Note steel channel supported by jacks for control of drill steel.

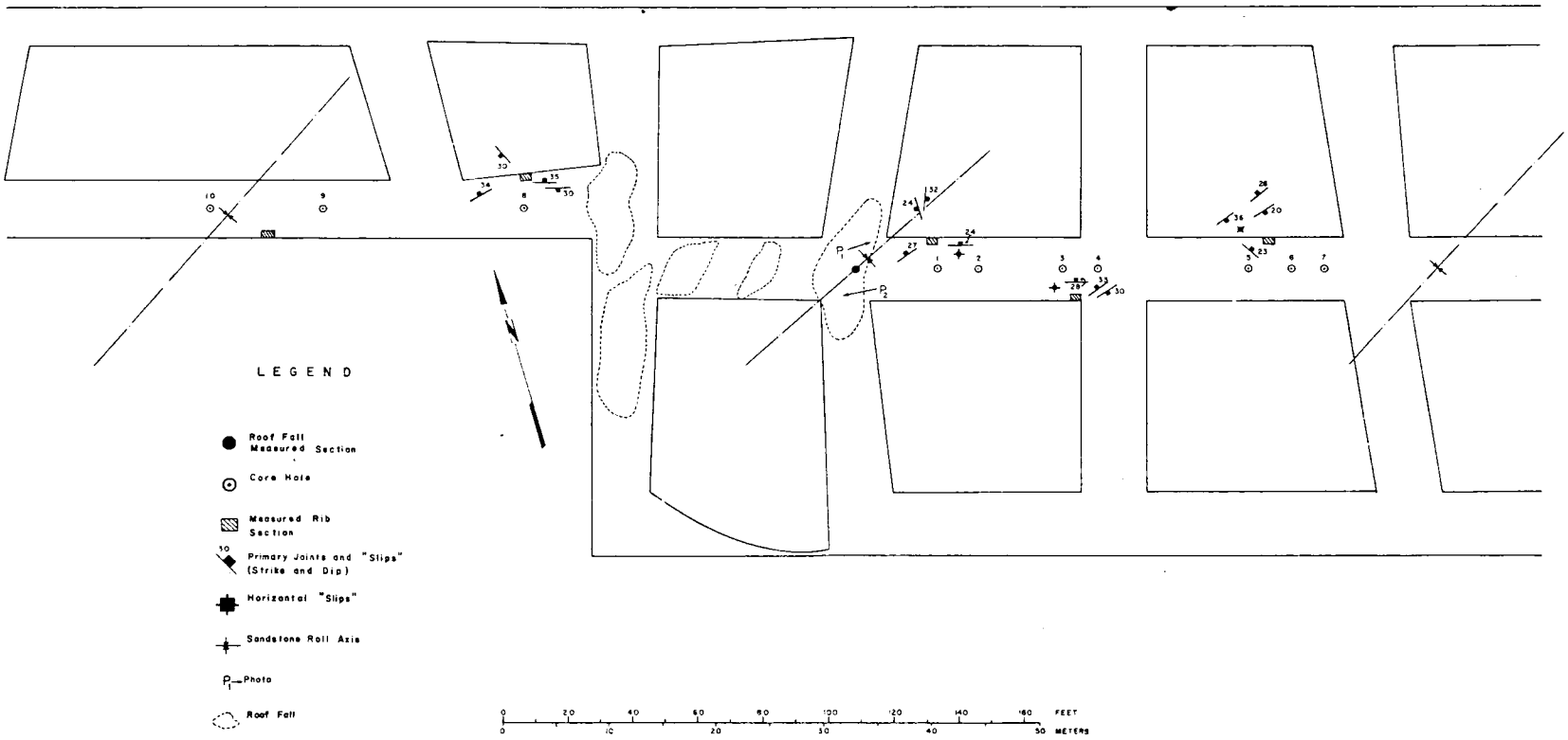

Figure 79. - Index map of core drilling site in the old 004 Section, Highsplint mine. Location coordinates 0-15 to P-16 on Location map, Figure A1, Appendix A. See Figure 80 for profile of cores.

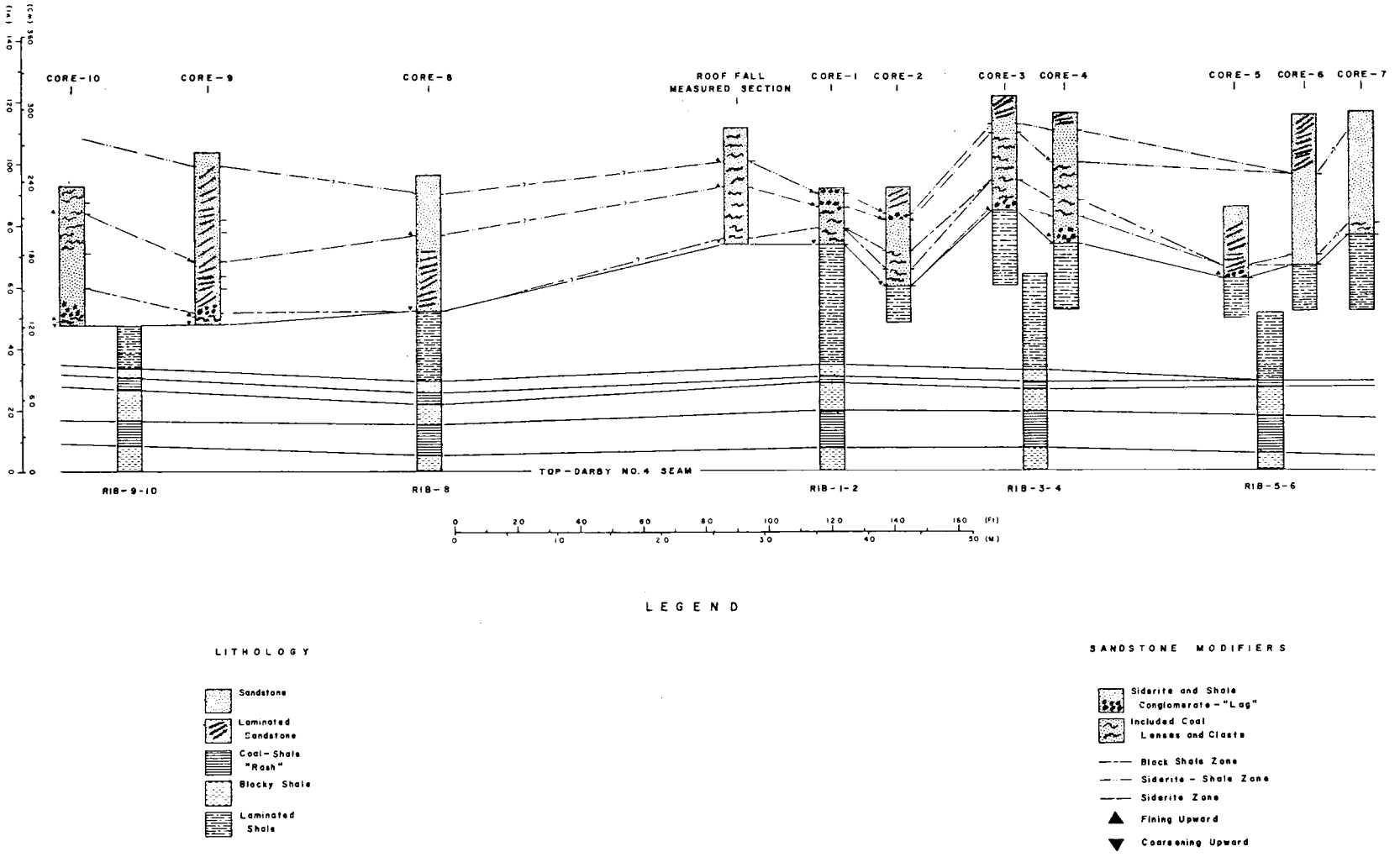

FIGURE 80. - Profile of cores in drilling site, old 004 Section, Highsplint mine. See Index Map, Figure A1, Appendix A.

Correlation of Core Sections

Correlation, or "matching" of units in the rib sections presents few problems as the shales and coal-shale "rash" zones are reasonably uniform in thickness and laterally persistent in 004 Section. An important exception is the uppermost laminated shale and siltstone unit. Figure 81 graphically shows that the variable thickness of the immediate roof is essentially due to the laminated shale unit. The solid line is a plot of the total shale thickness in inches and the dashed line is the thickness of the laminated shale unit. Of particular importance is the abrupt thickening of this unit between coreholes 2 and 3 and 1 and 8. The laminated shale in the roof-fall zone adjacent to corehole 1 is contorted and squeezed between sandstone rolls with slickensided joint surfaces or "slips" cutting diagonally downward and also curving to coincide with original bedding planes (Figure 32, page 61). Figure 79, page 173, also shows that the strike or trend of many of the joints coincide with major sandstone roll trends. The nature of the laminated shale-main sandstone roof contact indicates that the variable thickness of the laminated shale unit in the 004 Section may be due to several factors as follows:

1. Erosion of the shale before or during deposition of the overlying sand forming an uneven contact between the shale and overlying sandstone. Evidence was shown by the abrupt truncation of horizontal laminated shale against the sides of sandstone rolls (Figure 34, page 64).

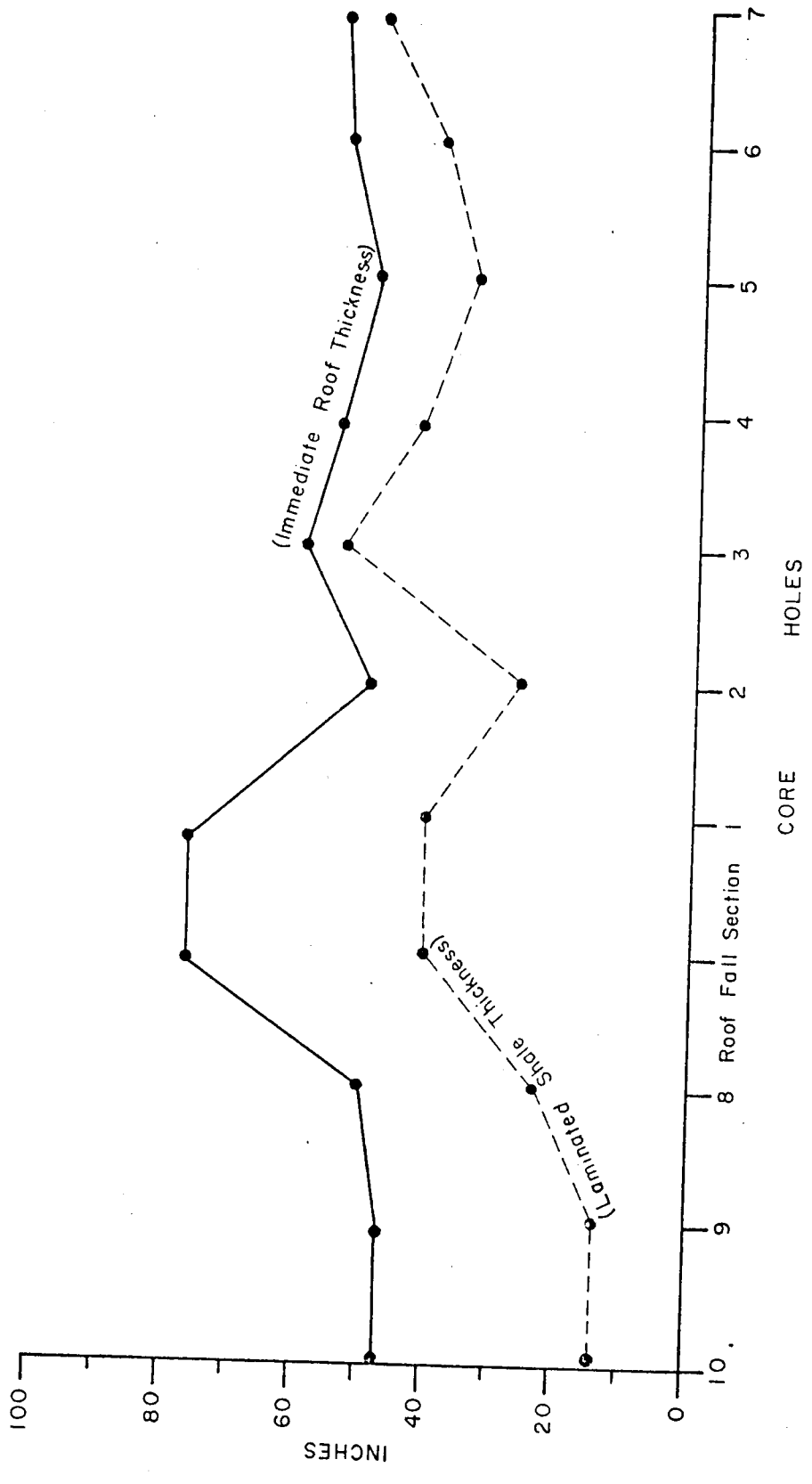

FIGURE 81. - Graph of total shale thickness (solid line) and laminated shale thickness (dashed line) in 004 Section.

2. Deposition of sand on an uneven shale surface without significant prior shale erosion. This relationship is shown by the gradational nature of the immediate-main sandstone roof contact.

3. Differential compaction or "loading" of the shale before the shale was completely lithified. "Loading" of the shale strongly suggests soft-sediment deformation and was observed in areas of the mine with relatively thick immediate roof shales. Figure 32, page 61, shows this relationship, which is evident in the 004 Section drilling site.

Correlation of Sandstone Cores

Figures 82 through 86 graphically represent the sandstone portions of the cores. The following section describes methods used to delineate vertical trends within a single core. From this information, correlations were made between cores.

Graph A is simply a plot of the sandstone bedding thickness versus height above base of sandstone. The determination of bedding planes in the core samples was generally based on the presence of plant material and concentrations of mica. Ordinarily, the cores tended to break parallel and to coincide with bedding as they were drilled. However, in horizontally laminated cores the original bedding planes were sometimes difficult to distinguish from breaks along laminae.

Graph B is a plot of the mean grain diameters of the sand-sized fraction of each core. The points enclosed by triangles represent arithmetic mean grain diameters determined by point-counting techniques of sandstone thin-sections. (See discussion, page 196). The remaining

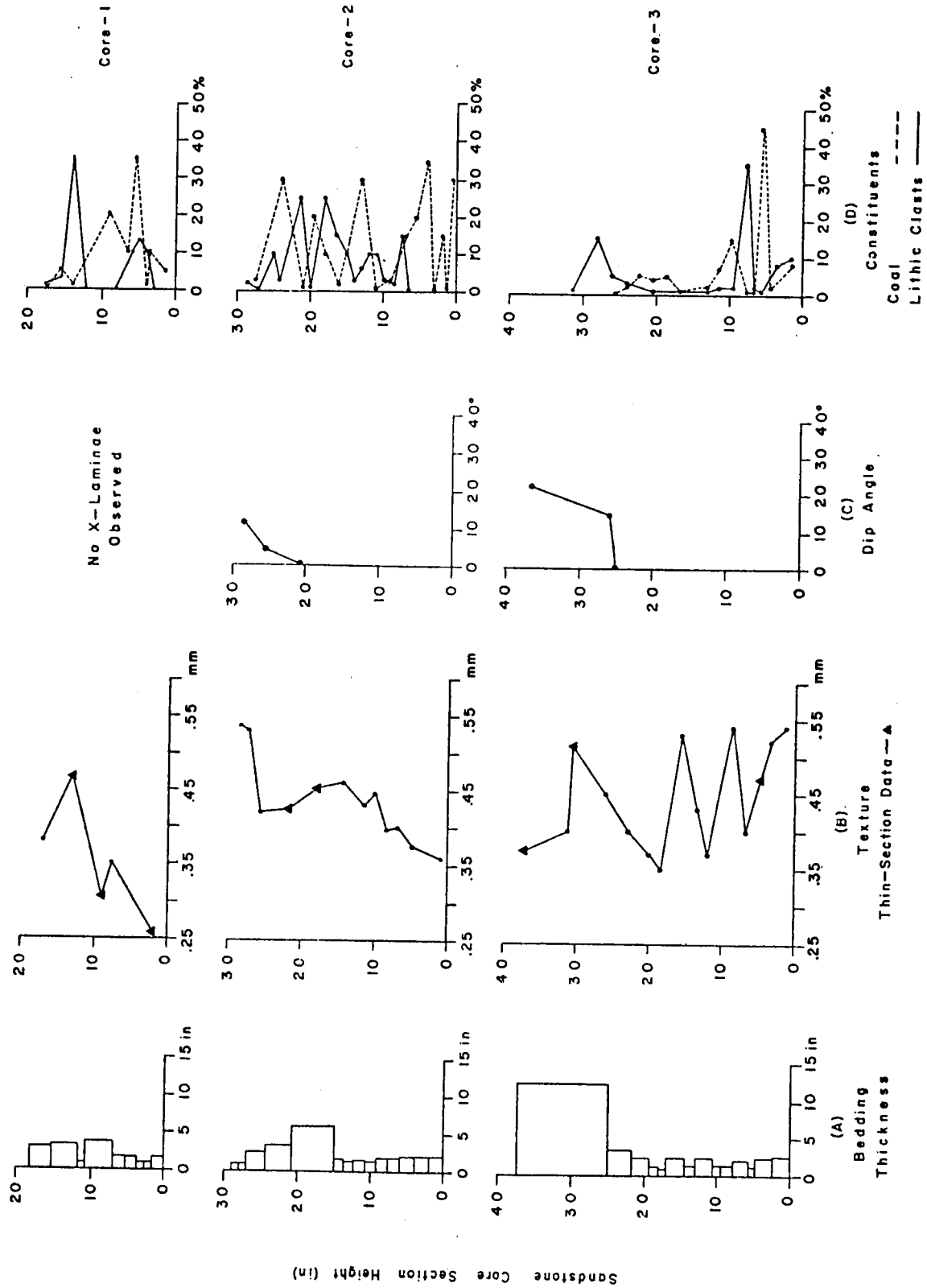

FIGURE 82. - Core analyses graphs for cores 1, 2 and 3.

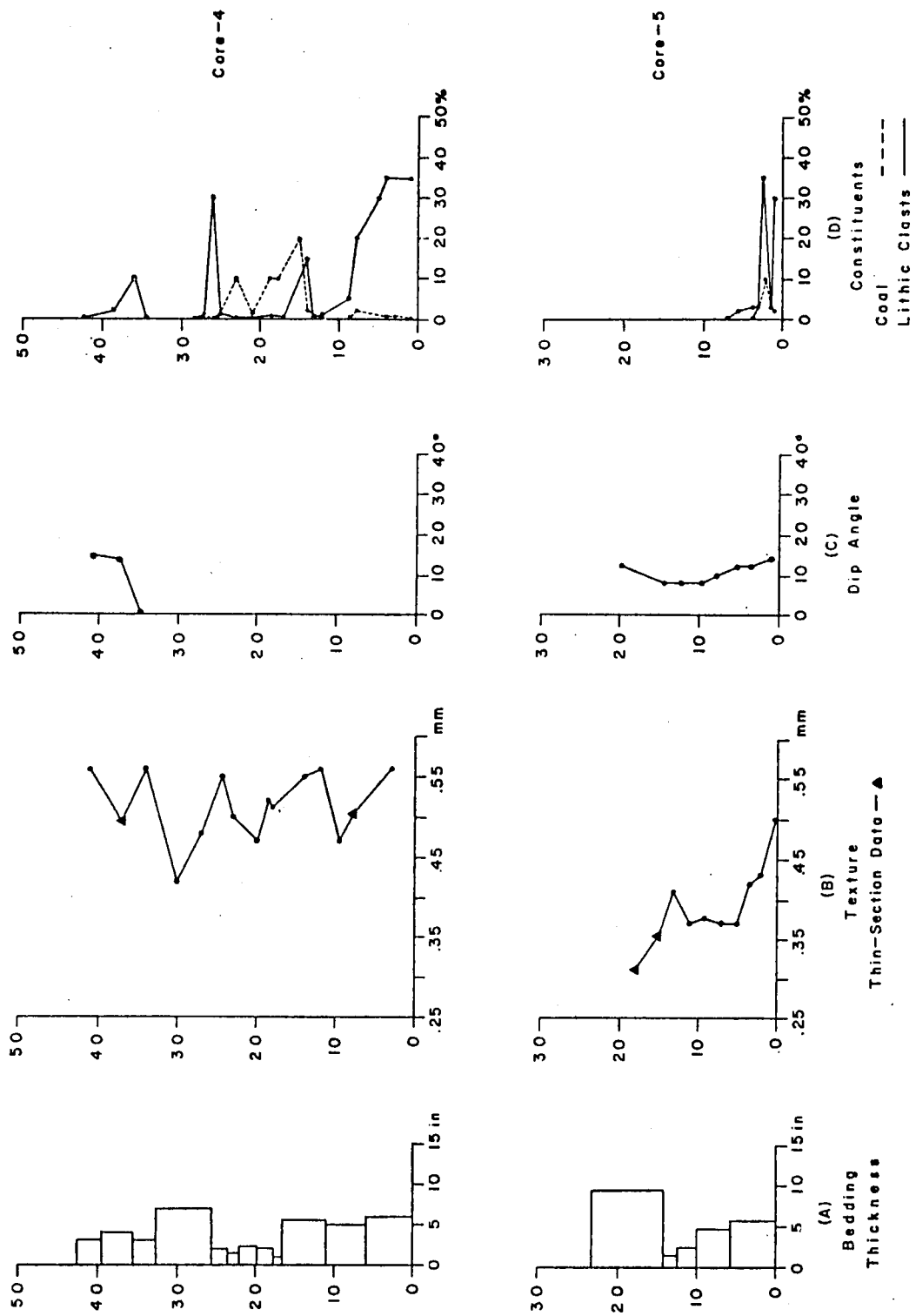

FIGURE 83. - Core analyses graphs for cores 4 and 5.

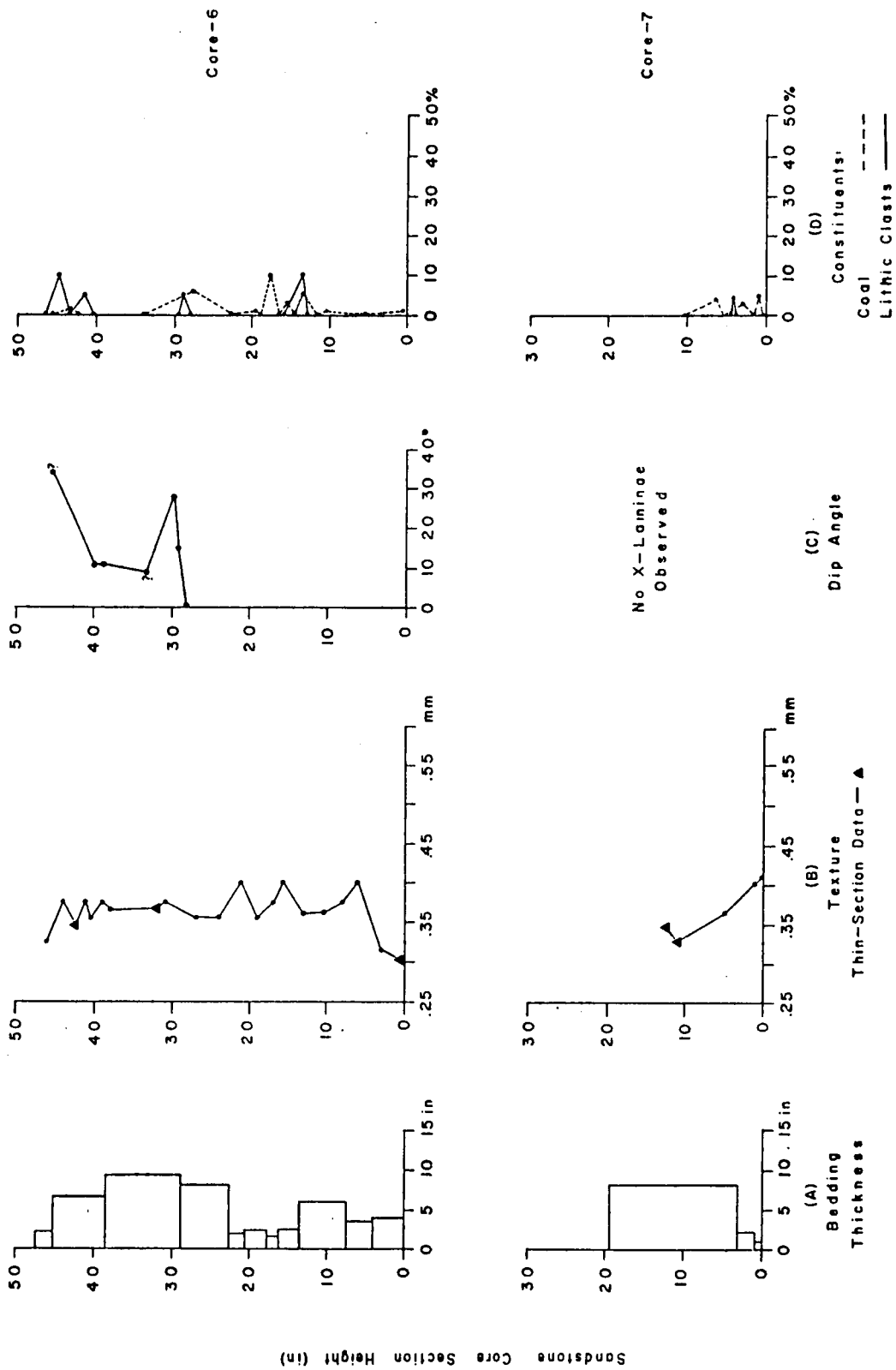

FIGURE 84. - Core analyses graphs for cores 6 and 7.

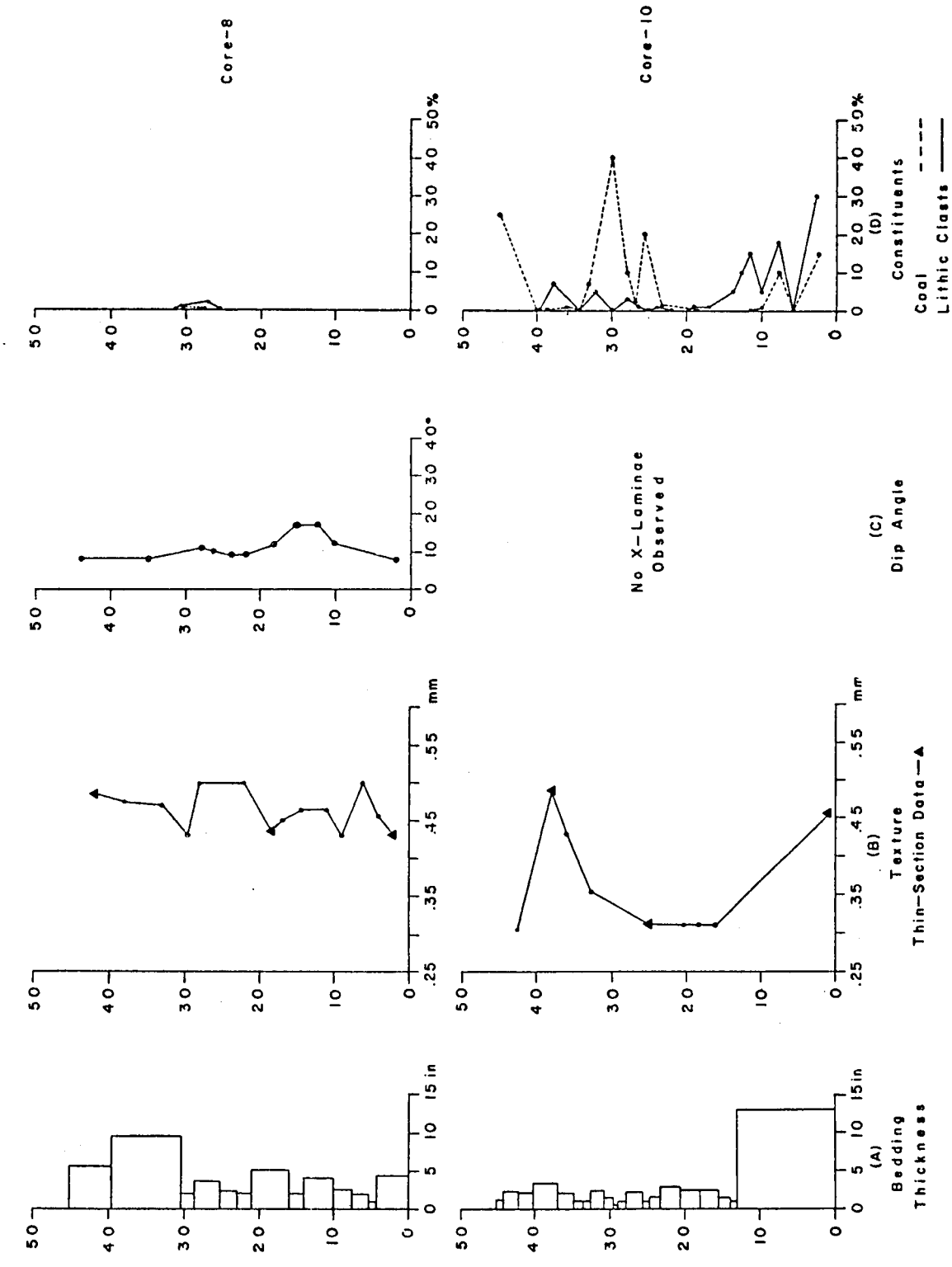

FIGURE 85. - Core analyses graphs for cores 8 and 10.

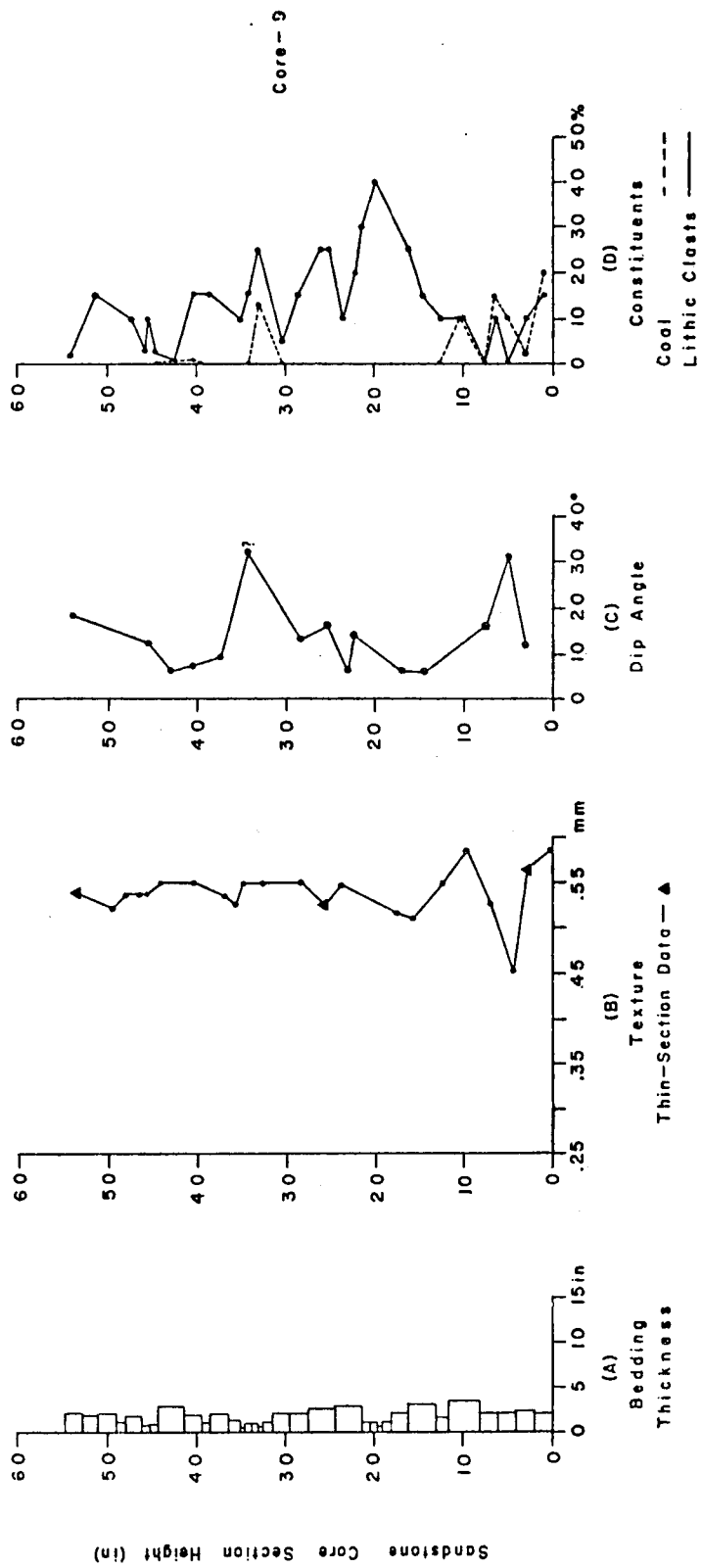

FIGURE 86. - Core analyses graphs for core 9.

points on graph B were established by visual estimates. The method used in estimating approximate textural sizes for the points was to select a suite of core samples in sequence from fine to coarse. The "unknown" core sample was classified by visual comparison and assigned a mean grain diameter value. Even though the points are estimated values, the resulting graph shows that grain size is variable vertically and appears to show cyclic trends in most cores. A comparison of the mean grain diameters of the sandstone with bedding thicknesses (graphs A and B) often shows a general correlation in that coarser grain size tends to be associated with thicker beds. Also, thicker beds tend to show a fining-upward texture from base to top. Note especially cores 4, 5, 7 and 9; also Figure 56 B and C, page 106.

Several of the cores, especially numbers 5, 6, and 8 are moderately to strongly cross-laminated in individual sets 0.1 inch to as much as 0.5 inch thick. These laminae are especially evident in radiographs, and positive prints of radiographs were used in the study of dip angles of these laminae (Figure 87).

Graph C shows maximum apparent dip angles in cross-laminated cores. The following trends may be noted:

1. The dip angles often appear cyclic upward.

2. Coarser-grained sandstones and sandstones with an associated lithic fraction tend to have laminae with relatively steeper dips.

3. Where the core is not laminated from base to top, the upper portion tends to be laminated rather than the base.

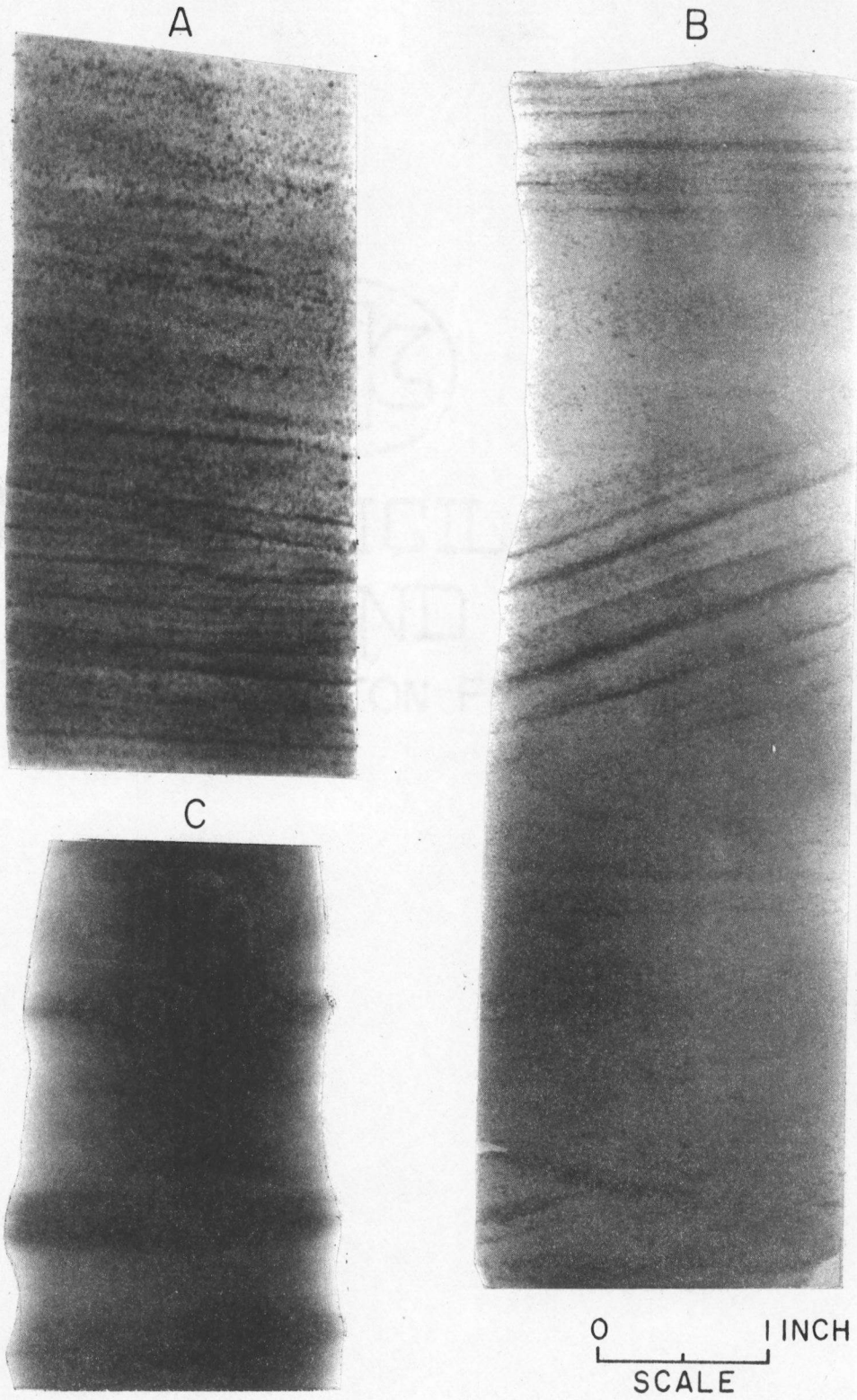

FIGURE 87. - Radiographs of core sections showing cross-laminated sandstone in A (S-8-3d) and B (S-6-5). Laminated shale with ironstone bands in C (S-7-17).

Graph D is a plot showing percentages of two common constituents of the sandstones. The first is coal that occurs as lenses, bands and fragments interlaminated with the sandstone and is shown as a dashed line. The second is the coarse lithic fraction composed of rounded, equant-to tabular-shaped siderite and claystone pebbles and angular-to subrounded shale chips (Figure 56, page 106). The lithic fraction diameters in the cores are commonly 0.1 inch to 0.2 inch, but may be as much as two inches. The percentages of both the coal and lithic fraction was based on visual estimates. Visual estimates were made by comparing core sections with published percentage diagrams (78).

By comparing the coal and lithic fraction it is evident that these fractions are cyclic and represent fluctuating depositional conditions for the sandstones. The coarse lithic fraction is associated also with the coarser sand-sized fraction (graph B) as would be expected, as well as thicker beds (graph A). Conversely, the coal fraction is commonly associated with finer-grained sandstones and thinner beds. The lithic fraction was likely formed under higher energy flow conditions whereas the coal fraction represents plant material that originally accumulated with finer sands during times of lower energy flow conditions.

Interpretation of Correlations

On the basis of sandstone core studies, tentative correlations between cores was made as shown on Figure 80, page 174. Confidence in the correlation is much higher between cores 1 through 7 because of better control due to closer core spacing. Correlation between cores 8, 9 and

10 was very tenuous as was the correlation of zones across the roof-fall area between cores 1 and 8. However, several important aspects of the correlations support the view that geologic factors have strongly contributed to the roof falls in this area as follows:

1. The occurrence of siderite pebbles or "lag gravels" is more frequent in the base of the number 3, 4 and 5 cores, with the greatest concentration in the number 4 core. The basal contact in these cores is sharp and erosional and the texture becomes finer-grained upward. The bedding becomes relatively thicker laterally from the number 1 and 2 cores toward the number 5 core (Figure 82, page 178 and Figure 83, page 179. The siderite zone is lens-shaped and is thin in the number 3 core. However, it is absent in the number 6 and 2 cores (Figure 80, page 174).

From a geologic standpoint cores 3 to 6 would likely represent at least a temporary position of erosion and deposition of coarser sediment. The thicker bedded units in the basal zone of this area also contain much less coaly material on the bedding planes and would provide more substantial anchorage for roof bolts.

2. The basal portion of cores 1 and 2 are distinctly different in that the basal contact with the underlying shale appears more gradational and the sand fraction becomes coarser-grained upward. The bedding is thin with abundant interlaminated coal. Correlation between cores 1 and 2, and 2 and 3 indicated that differential compaction of the shale is likely. The amount of compaction may locally have been as much as 30 inches. Strong evidence of compaction is indicated because the laminated shale is squeezed between minor rolls in the roof-fall area

(Figure 32, page 61). "Slips" are more numerous in the squeezed shale and horizontal "slips" are evident between bedding planes in the shale. These horizontal "slips" indicate that the shales have been subjected to horizontal stresses during loading by overlying strata. Horizontal "slips" appear as a thin "chippy" shale zone perhaps 0.5 inch wide. It is noteworthy that in nearby sections of the mine it has been possible to hold some of the immediate roof where horizontal "slips" are not present.

Evidently the sandstones in cores 1 and 2, and extending into the roof-fall area, represent deposition of sand in thinner layers on a relatively softer shale substrate along with plant material that later formed interlaminated coal with the sandstone. The thin-bedded basal portion of these sandstones would provide less stable anchorage for roof bolts, even if roof bolts extended higher into the roof. The roof-fall measured section (Figure 80, page 174) indicated that the thin-bedded sandstones became somewhat thicker-bedded upward, but then because thinner bedded at the maximum height of the fall. Figure 18, page 41 shows the relationship that roof falls extending for some distance upward into the roof likely fall to a height coinciding with a higher cycle of thin-bedded sandstones. Also, thicker laminated shale containing numerous "slips" in this area would present very unstable conditions for holding the immediate roof. (See discussion, page 54).

Petrography

Composition

A total of 46 thin-sections of the sandstone portions of the cores obtained in the 004 Section were examined petrographically. Six of the 46 thin-sections that represented lateral and vertical variations in the coring site were selected and studied in detail for sandstone composition. A point-counting stage was used to point-count grains according to Chayes' Method (11) and the results are shown in Table 16.

For the purposes of discussion, the total composition of the sandstone has been divided into two categories. The first, framework grains, includes the coarser detrital fraction composed essentially of quartz, feldspar, mica, chert(?) and rock fragments. Secondly, the matrix includes interstitial material that surrounds framework grains and may be detrital and/or authigenic (secondary).

Framework Grains

The texture of the sandstones includes a consideration of the size, shape, and arrangement of the component particles (60). The shape and arrangement is considered here. A detailed study of size relationships is considered separately. (See discussion, page 196).

In general, the shape of the grains in thin-section ranges from angular to subangular (63). The grains usually showed a parallelism to bedding or cross-laminae, especially in fine-grained sandstone sections.

TABLE 16. - Mineral composition in volume percent of sandstone thin-sections

Constituent	Sample Numbers						
	4-15	1-2	7-5	9-Top	9-16	9-25	Average
Quartz[1]	29.3	66.1	64.5	70.9	75.3	74.4	63.4
Chert(?)	.7	1.4	4.0	4.2	1.4	4.5	2.8
Feldspar	9.9	11.7	13.8	13.9	10.1	10.9	11.7
Micas	-	.5	6.0	1.1	2.5	1.2	1.9
Rock Fragments[2]	55.1	5.1	5.3	4.9	5.1	6.5	13.7
Clay[3]	4.6	15.4	6.3	4.9	5.1	1.6	6.3
Total grains counted	299	215	302	265	273	243	

[1]Includes polycrystalline quartz.

[2]Includes some possible authigenic siderite.

[3]Includes sericite and chlorite, also quartz (silt).

The framework grains in the coarser-textured sections are usually in contact separated by little matrix material and the grains do not appear to "float" in the matrix. The grain contacts, in fact, are often sutured and interpenetrating (Figures 88 and 89). Also, grains in contact are often broken and bent indicating grain deformation (Figure 90). The finer-grained sections showed that framework grains were more often not in contact because of increasing matrix content (Figures 90 and 91).

Quartz in thin-section commonly showed undulose extinction. It occurs in both monocrystalline and polycrystalline varieties. The monocrystalline grains are about the same size as feldspars and are usually embayed and corroded on the edges. The grains often interlock with straight contacts and overgrowths not in optical continuity with the enclosed grain are common. Polycrystalline varieties occur as aggregates that occur alone or may include sericite shreds.

Microcline and plagioclase feldspars were readily apparent in thin-section because of characteristic twinning. Untwinned feldspars could generally be distinguished from quartz because of crystal shape, cleavage and the relative "cloudiness" of feldspars. However, to verify the identification of untwinned feldspars staining techniques were used (6). In most thin-sections microcline and untwinned potash feldspars are at least twice as abundant as plagioclase grains. Feldspar grains showed varying degrees of alteration during weathering and/or diagenesis. The most common types are as follows:

1. Crushing - In contrast to quartz grains, feldspar grains showed a greater degree of crushing and distortion. Grains are commonly

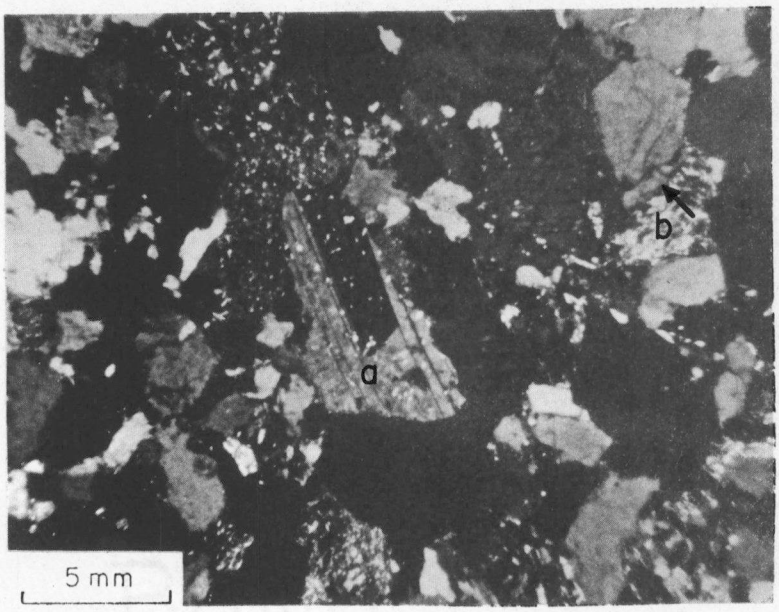

FIGURE 88. - Large crystal of plagioclase feldspar (a) with albite and Carlsbad twinning together with other feldspar grains showing replacement by sericite. Grain at right (b) is almost completely replaced except for edge shown by arrow. X-nicols (Sample 9-20)

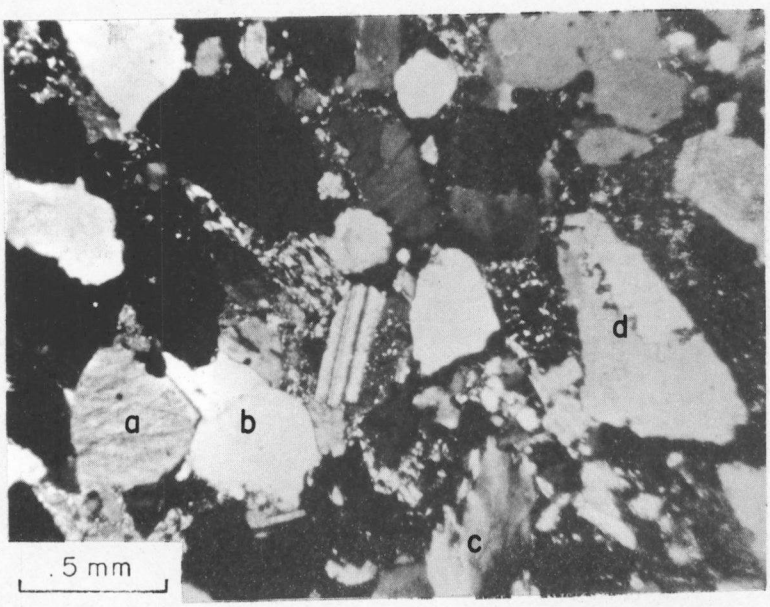

FIGURE 89. - Interlocking crystals of untwinned feldspar (a) and quartz (b) with straight contacts indicating pressure solutioning. Also shown is corroded quartz (c) and sutured quartz (d). X-nicols (Sample 10-13)

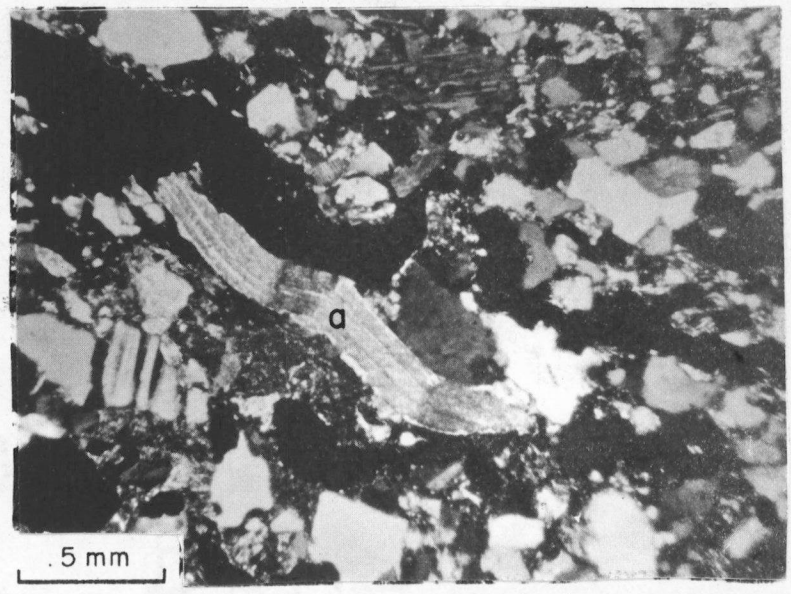

FIGURE 90. - Relatively finer, more heterogeneous texture in core 1 (old 004 Section). Dark band from upper left to lower right is coal streak. Large deformed detrital mica grain in center (a). X-nicols (Sample 1-4)

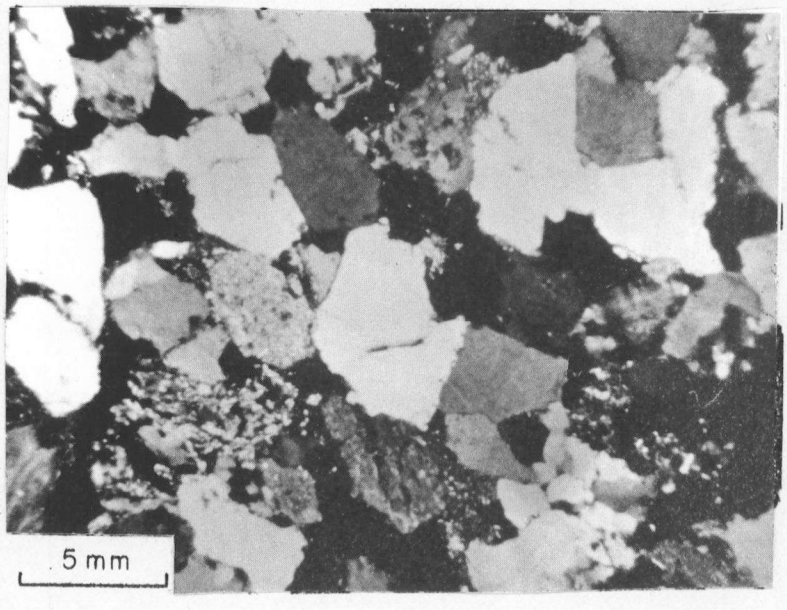

FIGURE 91. - Relatively coarser, more homogeneous texture in core 2 (old 004 Section).
X-nicols (Sample 2-4)

fractured at the point of contact with adjacent grains. Distortion is also indicated by bent and/or broken twin laminae.

2. Kaolinization (9) - Vermicular kaolinite was observed replacing about one-third of the total feldspar grain in several instances, but is probably a minor process.

3. Quartzification (9) - The result of this process is a fine aggregate of polycrystalline quartz. If the process had been complete in all cases, it would have been difficult to distinguish polycrystalline quartz from rock fragments of quartzite or chert. However, remnants of twinned feldspar often remain to verify the process. The process was extensive in sections studied.

4. Sericitization - Twinned plagioclase feldspars almost invariably showed sericite flakes scattered at random or concentrated along twin plains. In advanced stages the original feldspar was largely or completely replaced by a mass of sericite.

Alteration of feldspars appeared to be more extensive in plagioclase grains than in potash feldspars.

Rock fragments include shale and siltstone fragments, siderite clasts and chert(?) grains. Chert(?) grains observed in thin section were probably derived from siliceous nodules present in the immediate roof shales, although this was not verified. Possible metamorphic rock fragments could not be identified with certainty because of the extensive selective alteration of feldspars. Rock fragments were likely derived locally because most are not stable and all are present in the rocks immediately underlying the sandstone. Many of the softer shale fragments have been squeezed between adjacent grains forming a pseudomatrix (60).

Matrix

The matrix surrounding framework grains was found to be composed of detrital silt and clay-sized material together with authigenic material. The composition is dominantly quartz, clay minerals, chlorite, altered feldspars and sericite. The matrix content in the thin-sections studied is relatively low and ranges from 1.6% to 15.4% and averages 6.3%.

Heavy Minerals

The heavy mineral fractions of the sandstone samples were separated using tetrabromomethane (S.G. = 2.965), and grain mounts were prepared using Canada Balsam. The heavy mineral suites were limited to only a few diagnostic species. Pyrite was most abundant, occurring as encrusting masses of euhedral crystals covering detrital grains and is probably authigenic. Approximately equal numbers of tourmaline and zircon grains were observed, and most grains were moderately rounded. Some of the zircons, however, appeared only slightly rounded.

Sandstone Classification

Figure 92 (A) is a triangular sandstone classification diagram (61). The arenite triangle represents sandstones with less that 15% matrix. With quartz, feldspar and rock fragments as end members, the six thin-sections and the average for all six were plotted [Figure 92 (B)]. Since only quartz, feldspar and rock fragments were plotted, these percentages listed in Table 16, page 189, were recalculated to 100%. Also, chert(?) percentages were added to the rock fragment category for plotting,

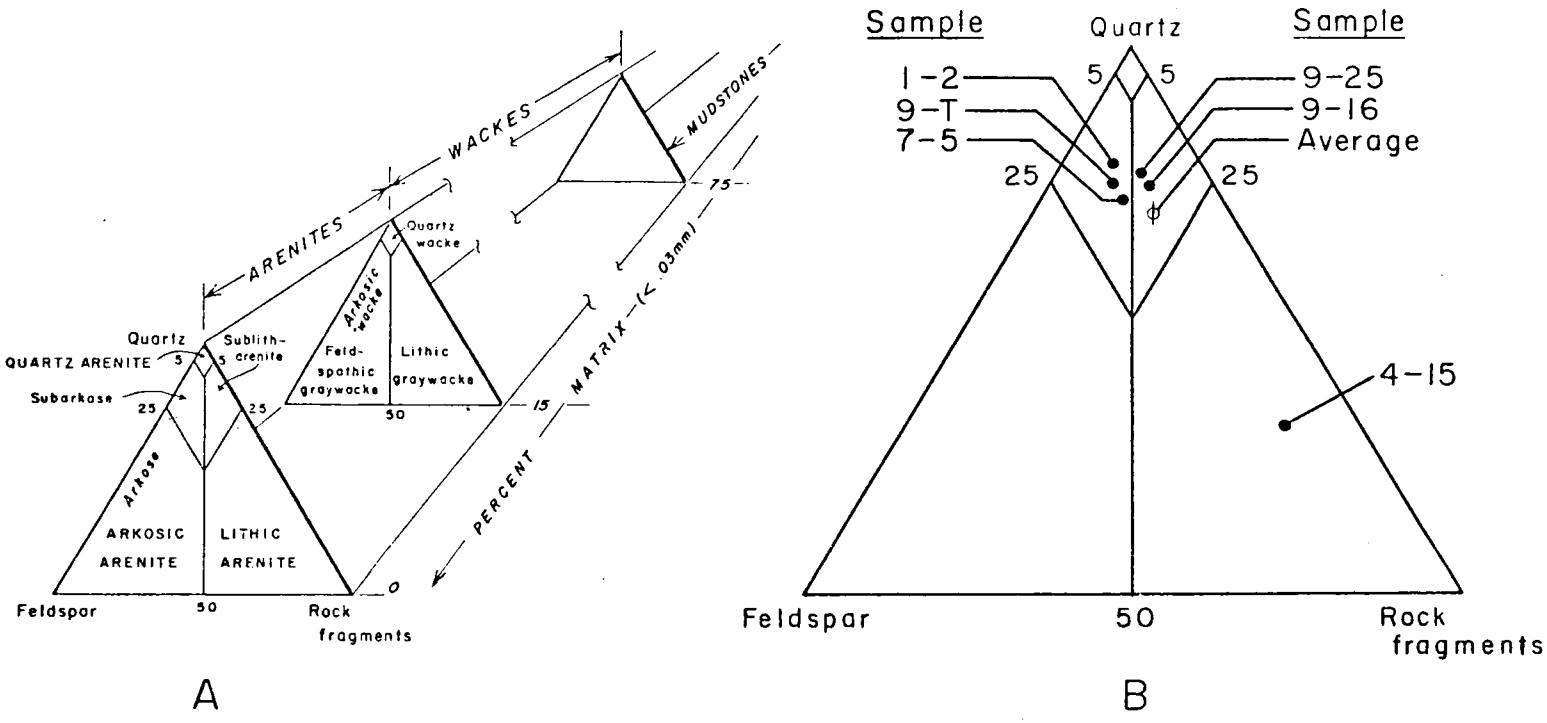

FIGURE 92. - A. Sandstone classification scheme modified from Dott [in Pettijohn (60)].
B. Arenite triangle showing plot of feldspar-quartz-rock fragment components of samples from Table 16, page 189.

assuming that the chert was derived locally together with the lithic fraction.

The resulting array of points is almost equally divided between the categories subarkose and sublitharenite, except for sample 4-15, and are, therefore, transitional. Sample 5-15 is representative of the basal "lag," with over half of the thin-section dominated by siderite pebbles as much as 1.5 mm in diameter, and falls in the lithic arenite category.

The plot of the average percentages for the six samples falls in the sublitharenite category. While the sample site is restricted, this classification is probably representative of the sandstones in the study area. Perhaps a more common term also used for lithic arenites is subgraywacke (60). With increasing matrix content, these rocks would be considered as graywackes (60). In the strict sense, sample 1-2 with 15% matrix (the dividing percentage), would fall in this category.

Thin-Section Textural Studies

Thin-sections were prepared from the core samples and textural studies were made using a total of 27 thin-sections of the sandstone portions of the cores. The purpose of these studies was:

1. To determine both vertically (within a single core) and laterally (between cores) if sandstone grain size changes significantly.

2. To determine the sorting characteristics of the sand-sized fraction (1/16 mm - 2 mm) both vertically and laterally.

3. To relate these textural changes to the roof-fall area in the 004 Section of the Highsplint mine.

4. To use the information in postulating possible geologic depositional conditions that would contribute to unstable ground conditions in the 004 Section.

Procedures Used

Thin-section studies were necessary in order to analyze the texture of sandstone core samples because the major cementing agent of these rocks is silica. Textural studies would have been simpler if the samples could have been disaggregated and sieved. However, various techniques, including boiling with concentrated KOH, failed to disaggregate the sandstones tested. An exception was the upper part of core 7, which was friable and was sieved for comparative purposes.

The method used involved the use of point-counting procedures with a petrographic microscope. The microscope was equipped with a point-counting stage and grain diameters were determined using an ocular micrometer. Grain counts were made according to the Chayes' Method (11). The counting procedure was designed so that the entire slide would be covered. According to similar statistical studies of sandstone thin-sections, at least 100 to 200 grain diameters per slide are desirable for reasonable statistical accuracy (30). In this study, a comparison was made by counting 200 and 300 points using the same slide and it was determined that 200 grains per slide should provide adequate results for comparative purposes. The grid pattern for 200 grains used was 1 mm horizontally and 3 mm vertically determined by click stops on the point-counting stage.

Difficulties

Since the study was comparative in nature, the primary objective was to use consistent methods of analysis from one sample to another. The first consideration was to measure the apparent original long axis of the grains. This was perhaps the most difficult part of the study because most of the sandstones show at least some degree of grain alteration and some interpretation was necessary. Quartz grains commonly displayed sutured contacts together with overgrowth rims. Feldspar and quartz grains often showed varying degrees of alteration, and were often crushed and distorted.

These factors tended to cause some grain diameter measurements to be somewhat subjective. Initial survey studies of the slides indicated, however, that grain diameters differed sufficiently between slides to warrant point-counting. In actual counting practice, original grain boundaries were determined by optical continuity of the grains. In the case of altered grains, as for example feldspar altered to sericite, the original boundaries of the feldspar were often preserved and could be counted.

In this study the matrix was not counted. Most grains were in contact and quartz often displayed interlocking boundaries with sutured contacts, as discussed previously.

Statistical Measures Used

Folk (29) reviewed the essential statistical methods usually considered in the analysis of sediments and disaggregated sandstones.

These methods were used in the thin-section analysis of core samples with the following reservations:

1. The thin-section grain diameters are apparent diameters as seen in the section and do not reflect actual sieve equivalent diameters because the purpose of this study is purely comparative within a single suite of samples.

2. Because of the difficulty in the determination of some original grain boundaries, statistical measures derived from cumulative frequency curves are based on the central 68% of the curves. While the "tails" of the curves often show sample differences in sorting, etc. in the sieved sediments, the difficulty in point-counting because of grain alteration would make the fine fraction especially subject to error.

The results of point-counting procedures are summarized in Table 17. Methods used were as follows:

1. Measurement of the grain diameters for each thin-section was determined by both calculation and graphic methods. The arithmetic mean diameter was initially determined by the following formula.

$$M_a = \frac{\Sigma X}{N}$$

where X = individual grain diameters

N = total number of grains measured

2. A cumulative frequency curve was constructed for each thin-section on arithmetic ordinate paper based on class intervals of 0.25 phi units (the phi unit, or ϕ is defined as the negative logarithm to the

TABLE 17. - Thin-section point-counting data

Core No. & Sample	No. of Grains Counted	Arith. Mean (mm)	Graphic Median (mm)	Percentile 16	Q_3	Grain Q_1	Diameters (ϕ) 84	ϕ_G (ϕ)	Sk_G
10(2)	225	.482	.448	.61	.79	1.43	1.68	.535	-.028
10(7)	215	.308	.250	1.09	1.33	2.61	2.79	.85	-.071
10(Bottom)	215	.452	.448	.70	.89	1.64	1.95	.625	+.264
9(Top)	200	.538	.532	.52	.67	1.11	1.31	.395	+.013
9(16)	220	.523	.518	.56	.66	1.25	1.48	.460	+.152
9(25)	205	.565	.536	.39	.55	1.25	1.40	.505	-.009
8(Top)	210	.483	.466	.52	.69	1.50	1.68	.58	0.0
8(3d)	200	.434	.426	.59	.87	1.58	1.81	.61	-.049
8(7)	215	.430	.392	.71	.89	1.79	2.04	.665	+.038
1(2)	200	.556	.532	.51	.62	1.17	1.28	.385	-.39
1(4)	200	.316	.297	1.10	1.30	2.45	2.70	.80	+.188
1(9)	200	.258	.237	1.32	1.51	2.71	3.20	.94	+.191
2(4)	300	.422	.420	.83	1.0	1.58	1.75	.46	+.087
2(5)	200	.453	.444	.71	.88	1.40	1.56	.425	-.082
3(1)	209	.374	.379	.92	1.09	1.86	2.21	.645	+.256
3(3)	215	.499	.497	.62	.76	1.35	1.57	.425	+.082
3(13)	160	.476	.444	.72	.89	1.46	1.60	.44	-.023
4(2)	210	.493	.473	.68	.84	1.35	1.53	.425	+.059
4(12)	215	.503	.486	.60	.75	1.37	1.55	.475	+.074
5(Top)	214	.315	.252	1.35	1.61	2.49	2.70	.675	+.052
5(1b)	200	.355	.332	1.14	1.29	1.81	1.98	.42	-.071
6(2)	220	.344	.344	1.23	1.34	1.81	1.95	.36	+.139
6(5)	200	.369	.358	1.10	1.24	1.79	1.89	.395	+.040
6(16)	200	.395	.390	.98	1.12	1.60	1.76	.39	+.026
7(4)	205	.346	.332	1.21	1.39	1.85	2.12	.455	+.165
7(5)	210	.330	.321	1.29	1.38	1.93	2.02	.365	+.041

base 2 of the grain size expressed in millimeters). Figure 93 is the cumulative frequency curve for sample 3-13 and illustrates the procedure.

3. Values for the graphic median grain diameters and quartile diameters were taken from the resulting frequency curve.

4. The values derived in step 3 above were used to measure the uniformity of grain size or sorting. The following formula is referred to as the graphic standard deviation (ϕ_G) and is expressed in phi units:

$$\phi_G = \frac{(\phi 84 - \phi 16)}{2}$$

Table 17 shows that the sandstones studied would be classified as well-to moderately-sorted (29).

5. A test for asymmetry of the frequency curve or skewness was based on the following formula for graphic skewness:

$$Sk_G = \frac{\phi 16 + \phi 84 - 2\phi 50}{(\phi 84 - \phi 16)}$$

This formula was used to measure the displacement of the median from the average of the $\phi 16$ and $\phi 84$ points. Positive values indicate skewness toward the fine fraction and negative values indicate skewness toward the coarse fraction. Symmetrical curves would yield a skewness of 0. Table 17 indicates that the skewness for samples studied is very low and that the curves for almost all of the samples are nearly symmetrical. The greatest skewness values are toward the fine fraction.

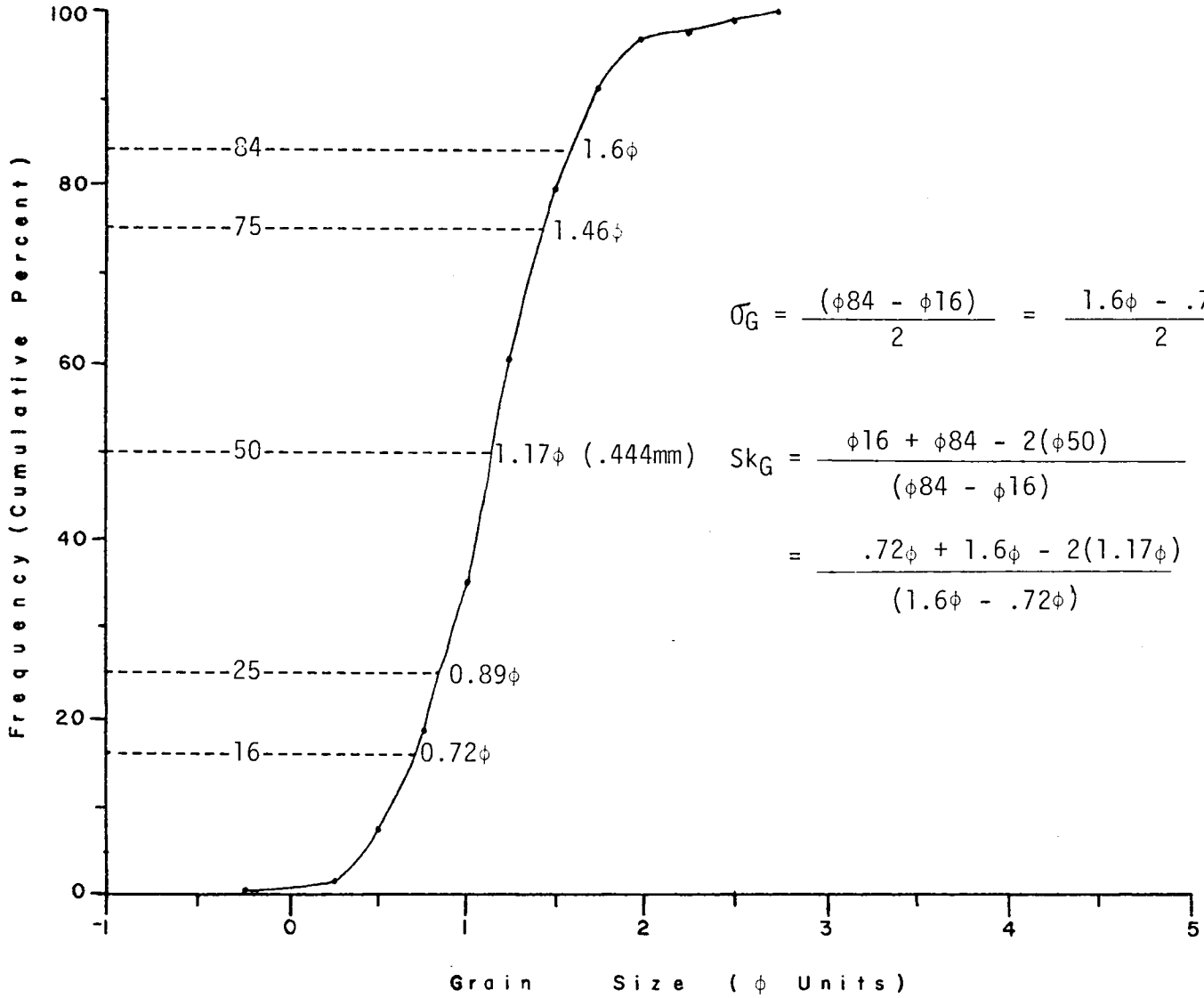

$$\sigma_G = \frac{(\phi 84 - \phi 16)}{2} = \frac{1.6\phi - .72\phi}{2} = .44\phi$$

$$Sk_G = \frac{\phi 16 + \phi 84 - 2(\phi 50)}{(\phi 84 - \phi 16)}$$

$$= \frac{.72\phi + 1.6\phi - 2(1.17\phi)}{(1.6\phi - .72\phi)} = -.023\phi$$

FIGURE 93. - Cumulative frequency curve for sample 3-13 and sample calculations.

Application of Textural Studies to 004 Section

In order to determine if possible trends exist laterally from the roof-fall area in the 004 Section, graphs of averages of values determined from point-counting data have been constructed for each core.

Figure 94 (top) is based on the arithmetic mean grain diameter and shows the relationship of grain diameter averages and corehole sequence away from the roof-fall zone. Maximum grain diameter averages are found in the number 9 and number 4 cores. This trend coincides with possible channel positions shown in Figure 80, page 174. Also, average grain diameters decrease in the number 1 and number 8 cores (Figures 90 and 91, page 192). Rocks in the roof-fall zone, extending from the number 2 core toward the number 8 core, have coarsening-upward textures above the immediate shale roof. Also, they are thin-bedded (0.8 inch to two inches) in the lower eight inches to 16 inches with gradational basal contacts. This evidence suggests that the roof-fall zone corresponds to a position marginal to and between a channel position extending from the number 3 core to the number 5 core, and another channel in the area of the number 9 core. The rocks in the roof-fall area possibly represent "overbank" or splay sands deposited adjacent to channel flow.

Figure 94 (bottom) is a similar plot of average core values. In this case the mean graphic standard deviation indicates increasing standard deviation values in the roof-fall zone, or less uniformity of texture. This aspect might be related to a sudden decrease in transporting energy and/or fluctuating depositional current velocities resulting in a somewhat greater range of sediment diameters being deposited together.

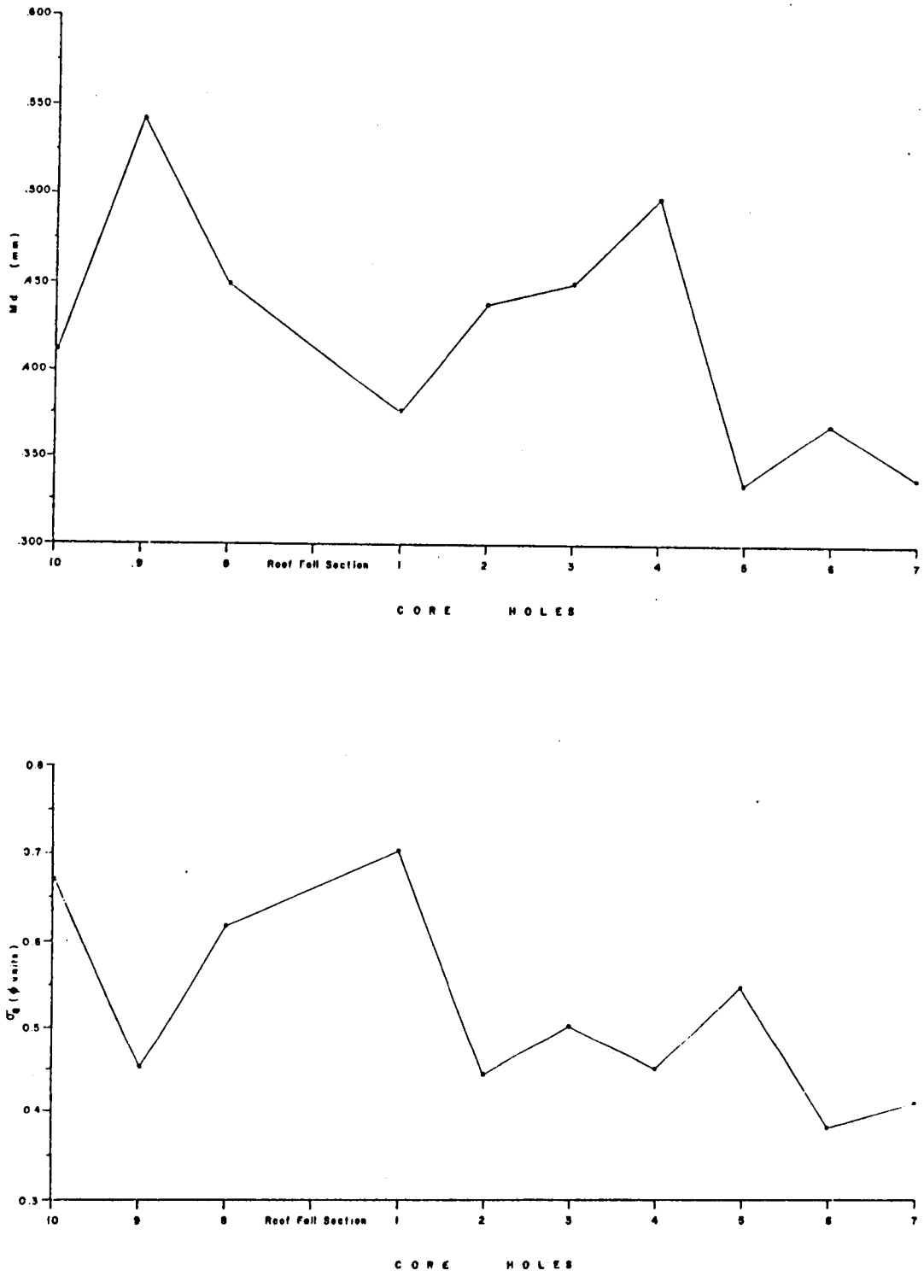

FIGURE 94. - Graph of arithmetic mean grain diameter averages (top) and graph of mean graphic standard deviation averages (bottom) for cores in the 004 Section, Highsplint mine.

Clay Mineralogy

Purpose and Scope

The purpose of clay mineral analysis in this study was aimed specifically at the analysis of clay minerals contained in shale and siltstone samples of the immediate roof rock of the Highsplint mine. Three suites of samples were analyzed. The first suite consisted of 11 samples taken from the rib section at intervals of about 100 feet, extending from the entrance of the mine to the old 004 Section (Figure A1, Appendix A). These samples were used in identification procedures together with another suite of 13 samples taken from the rib sections in the 004 Section drilling site. Analyses of selected peak-height intensities and ratios were done using a suite of 12 core samples leading into a roof-fall zone (Figure 95). These index studies were designed to determine if trends could be delineated that reflected changes in roof stability and to determine if clay minerals in the immediate roof rocks were useful to characterize the main roof.

X-ray Studies

For both identification and index studies, the clay slides were analyzed using a General Electric XL5 diffraction unit with Cu Kα radiatio radiation at 45 kv and 20mu. A scanning speed of 2° 2θ/minute and chart speed of 1°/minute was used.

Core samples were also analyzed using a Phillips (Norelco) x-ray unit at 35 kv and 17 ma. The scanning speed used was 2° 2θ/minute with a chart speed of 30 in/hr.

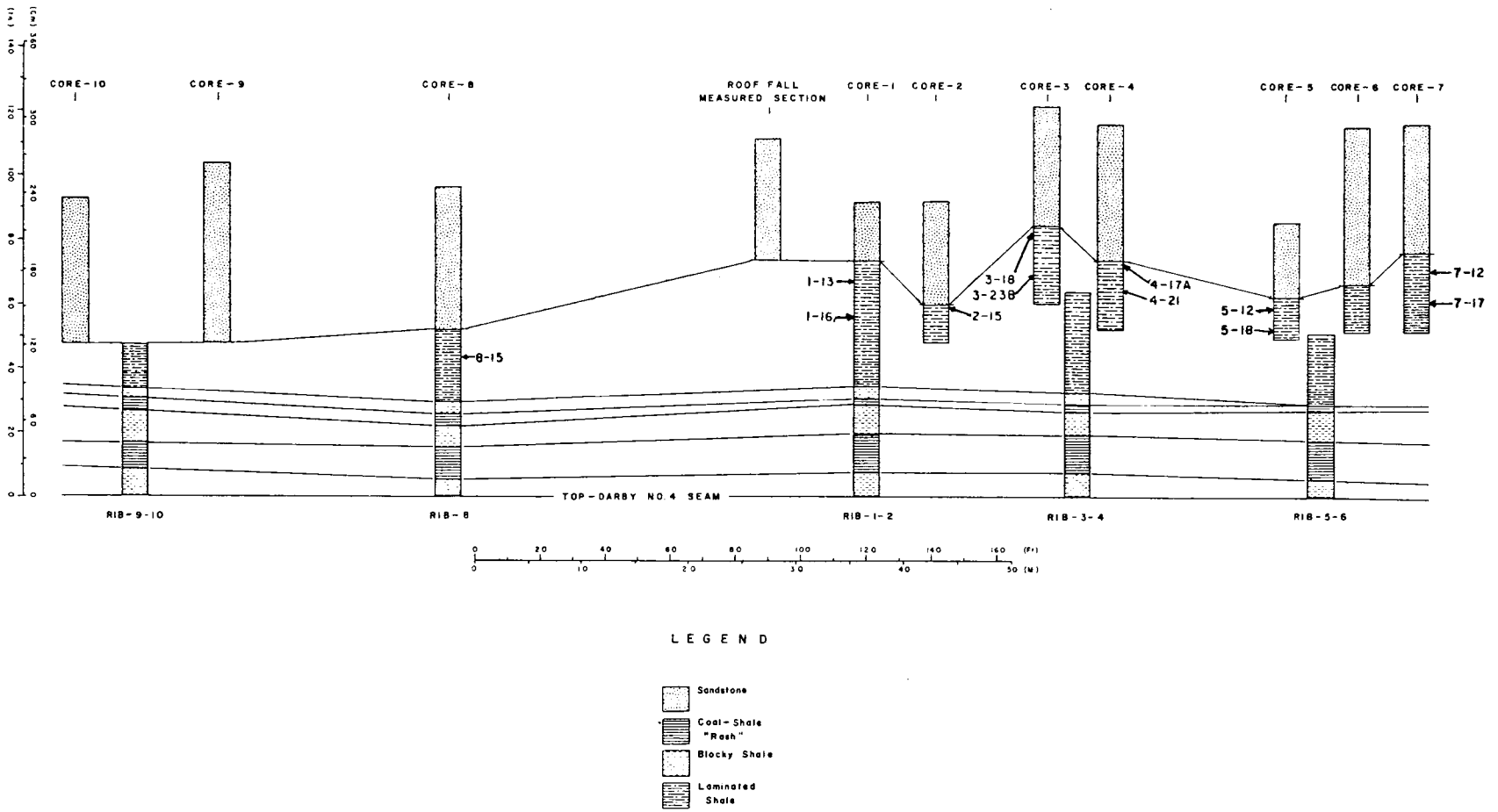

FIGURE 95. - Location of shale and siltstone samples for clay mineral analyses in cores from the 004 Section, Highsplint mine. Uppermost core samples are designated "upper" and lowermost designated "lower" when two samples were taken from the same core.

In all cases, instrument and recorder settings were constant for a particular suite of samples analyzed.

Identification Procedures

Illite, chlorite, kaolinite and a small amount of mixed-layered material were identified in the samples studied. The identification of clays was based exclusively on x-ray diffraction methods (10, 34, 83). Several standard methods of clay preparation and mounting techniques were used (Appendix C).

Illite. Velde and Hower (81) defined illite as a mineral group found in sediments having a primarily dioctahedral muscovite-type structure with less than 10% of expandable layers interlayered in the structures. Used in this sense, these authors concluded that the term illite would possibly include true micas or pure muscovites, and is broad enough to include all 10A layered structure found in sedimentary rocks.

Table 18 shows reflections typical of diffractograms of samples obtained from shales and siltstones in the immediate roof of the Highsplint mine together with chlorite, illite and kaolinite reflections from published sources (34). The relative intensity column (I/I_o) is based on the 10A (001) peak of illite. The height of the 10A peak was taken as 100 on an intensity scale of 0-100 and other peak heights rated in comparison. Other reflections characteristic of illite occur at 4.48A (020,110) and 2.57A (004). The illite (006) reflection at about 3.3A is masked by quartz.

TABLE 18. - Comparison of sample U-2-2 diffraction data with analyzed samples of illite, chlorite and kaolinite

Sample U-2-2[1]			Illite[2]			Chlorite[3]			Kaolinite[4]		
degrees 2θ	d(A)	I/I_o[5]	d(A)	I[6]	hkl	d(A)	I[7]	hkl	d(A)	I[7]	hkl
6.2	14.24	25				14.1	7	001			
8.8	10.00	100	9.98	S	001						
12.4	7.13	85				7.07	9	002	7.16	10+	001
17.8	4.98	35	4.97	M	002						
18.8	4.72	13				4.72	8	003			
19.9	4.45	4	4.47	S	020 110						
21.0	4.22	9							4.18	5	$1\bar{1}1$
25.0	3.56	46				3.54	10	004	3.57	10+	002
26.8	3.32	100	3.31	M	022 003						
27.8	3.21	9									
29.8	2.99	3									
31.7	2.82	6				2.84	5	005			
34.9	2.57	1	2.56	S	200;004	2.53	6	$13\bar{2};20\bar{1}$	2.56	6	$20\bar{1}+$
36.0	2.49	7				2.43	5	$132;20\bar{3}$	2.49	8	200+
37.7	2.38	3	2.38	M	$201;13\bar{2}$				2.37	6	003
39.6	2.27	3							2.28	8	$13\bar{1};131$
40.4	2.23	2									
42.7	2.12	3									
45.4	2.00	23	1.98	M	005	2.00	6	$13\bar{5};204$	1.98	6	$1\bar{3}2$
50.1	1.82	3									

TABLE 18 (Continued)

Sample U-2-2[1]			Illite[2]			Chlorite[3]			Kaolinite[4]		
degrees 2θ	d(A)	I/I_o[5]	d(A)	I[6]	hkl	d(A)	I[7]	hkl	d(A)	I[7]	hkl
60.1	1.54	3				1.53	7	060;33$\bar{1}$	1.54	5	13$\bar{4}$+
61.6	1.50	3	1.50	S	060;33$\bar{1}$				1.49		060

[1]Sample from section U-2, Highsplint mine. Analyzed using Cu Kα radiation at 45 kv and 20 ma.

[2]Illite sample after Grim (34) (only moderate and strong reflections shown).

[3]Data from Shirozu after Grim (34) (reflections <5 omitted).

[4]Data from Brindley and Robinson after Grim (34) (reflections <5 omitted).

[5]I/I_o Intensity determined by setting most intense peak at 100 after background was subtracted. Other peaks are in proportion.

[6]Intensity indicated as strong (S) or moderate (M).

[7]Intensity based on scale from 1 to 10.

The symmetry of the 10A peak has been used to differentiate illite from the true muscovite (10). Samples in this study ranged from only slightly to moderately asymmetrical. Glycolation and heat treating for one hour at 575° tended to sharpen, but not to shift the 10A peak indicating illite.

Confirmation of the dioctahedral nature of illite was indicated by the moderately strong basal reflection at 4.98A and the probable (060) reflection at about 1.50A (34).

Kaolinite. The (001) reflection at about 7A, in addition to the (002) at 3.56A and the (003) at 2.39A were interpreted as belonging to kaolinite. Heat treatment at 575°C for one hour reduced the relative intensity of the 7A peak (Figure 96) and this reduction is due to the destruction of kaolinite. The peak remaining at 7A was attributed to the (002) chlorite peak.

Chlorite. Table 18 shows probable chlorite basal reflections at about 14.2A (001), 7.13A (002), 4.72A (003), 3.56A (004) and 2.82A (005+). However, special treatments were necessary to distinguish chlorite from possible vermiculite or smectite minerals. First, samples were saturated with $MgCl_2$ and treated with ethylene glycol. Figure 96 shows that no noticeable shift in the 14A peak resulted. The slide was then heat treated at 300°C for one hour, again with no change. Heating the slide at 575°C for one hour caused the 14A peak position to remain unchanged (or sharpen slightly), all of which is evidence in favor of chlorite. Vermiculite should become dehydrated with moderate heating

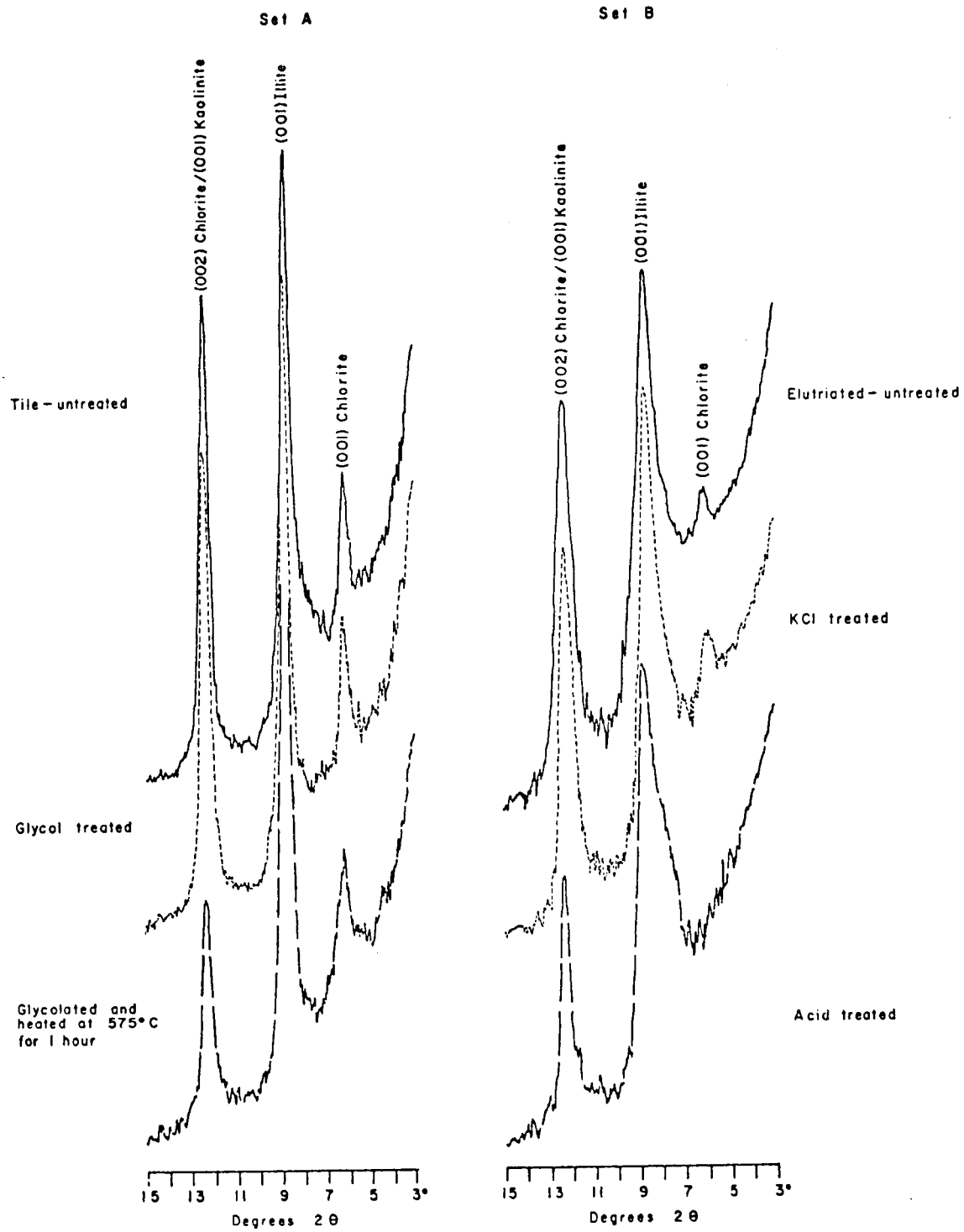

FIGURE 96. - Diffraction patterns of sample U-2-2 showing A. effects of glycolation and heat treatment and B. effects of KCl and acid treatment.

(300°C) and shift from 14A to 9A or 12A. Smectites, however, are affected by glycolation and shift to about 17A. KCl saturation of the sample did not cause a decrease of the d-spacing as might be expected for vermiculite (Figure 96).

Convincing evidence for chlorite resulted from acid treatment. Clays treated with 3N HCl heated to 70°C for 24 hours resulted in the loss of the 14A peak entirely and a reduction in the intensity of the 7A peak (Figure 96). The peak remaining at 7A was attributed to kaolinite.

Most of the chlorite in the samples were iron-rich as evidenced by the relatively stronger (002) and (004) reflections (34).

With the exception of some spalling due to reaction of the shales with the mine atmosphere, the clay minerals identified are compatible with good roof conditions (38, 52, 87).

Clay Mineral Index Studies

In this study, clay minerals were analyzed in order to evaluate their vertical and lateral relationship to the main sandstone roof using peak height indexes. The locations of the samples are shown in Figure 95, page 206, and Table 19 lists sample suites designated as "upper" and those designated as "lower. The "upper" suite includes the uppermost sample in each core. These sample suites were selected to determine if clay-mineral characteristics differed as to proximity to the main-roof contact with the immediate roof rocks.

Indexes Used. The relative abundances of kaolinite, chlorite and illite were not considered useful as possible indicators because of the

TABLE 19. - Shale/siltstone scale of texture

Sample[1]	Suite[2]	Relative[3] Coarseness	Texture Description
8-15	(U,L)	3	Argillaceous siltstone
1-13	(U)	5	Laminated siltstone
1-16	(L)	1	Silty shale; becomes finer upward
2-15	(U,L)	0	Clay (shale)
3-18	(U)	5	Laminated siltstone
3-23B	(L)	1	Silty shale
4-17A	(U)	0	Clay (shale)
4-21	(L)	0	Clay (shale)
5-12	(U)	0	Silty shale; iron-rich bands
5-18	(L)	3	Siltstone; becomes finer upward
7-12	(U)	1	Silty shale
7-17	(L)	1	Silty shale

[1]Sample locations are shown on Figure 95, page 209.

[2]U and L indicate upper or lower sample suites.

[3]Relative coarseness numbers represent an arbitrary "coarseness" from 0 (finest) to 5 (coarsest).

difficulty involved in quantitative clay mineral analysis. Also, to be useful, the method used should have wide-spread applicability not dependent on the presence of a unique clay mineral or combination of clays.

The sharpness ratio of the illite 10A peak was chosen for major consideration because of the widespread occurrence of illite in coal-bearing rocks (84), and because studies have shown that the 10A illite peak may be "responsive" to increasing degrees of diagenesis and incipient metamorphism (45, 85). The sharpness ratio (SR) used in this study is simply the ratio of the height of the 10A illite divided by the width at one-half the peak height (Figure 97).

For comparative purposes, the chlorite 14A peak height was also plotted. The results shown for chlorite are from samples heat treated at 600°C for one hour, because heating sharpened the peak (Figure 98).

Analysis of Sharpness Ratio Values. In order to compare SR values and detect possible trends leading into the roof-fall zone in the old 004 Section, SR values were plotted on graphs. Figure 97 shows SR values of the <4μm smear, <4μm elutriated and <2μm elutriated sample suites for comparative purposes. SR values plotted are from samples prior to heat treatment. However, identical results were obtained after heat treating to 600°C for one hour, except that the SR values were slightly higher for heat treated samples. The corehole locations are drawn to scale and the samples are graphed on the basis of an "upper" and "lower" suite (Figure 95, page 206). No values are indicated for cores 9 and 10 because

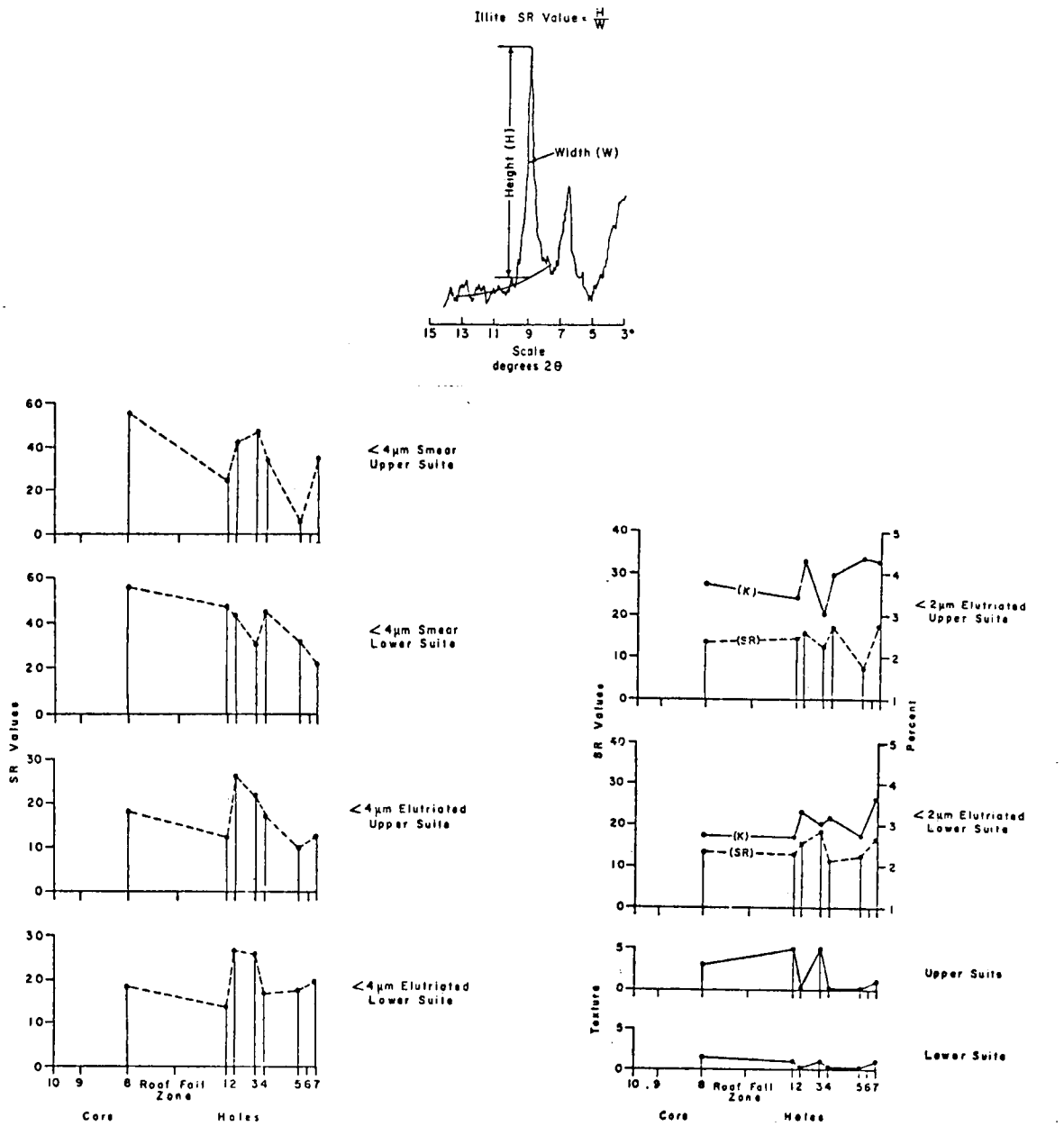

FIGURE 97. - Sharpness ratio values plotted for <4µm smear and elutriated samples (left) and <2µm elutriated samples (right). Relative texture graph (lower right) and method of SR determination (top) also shown.

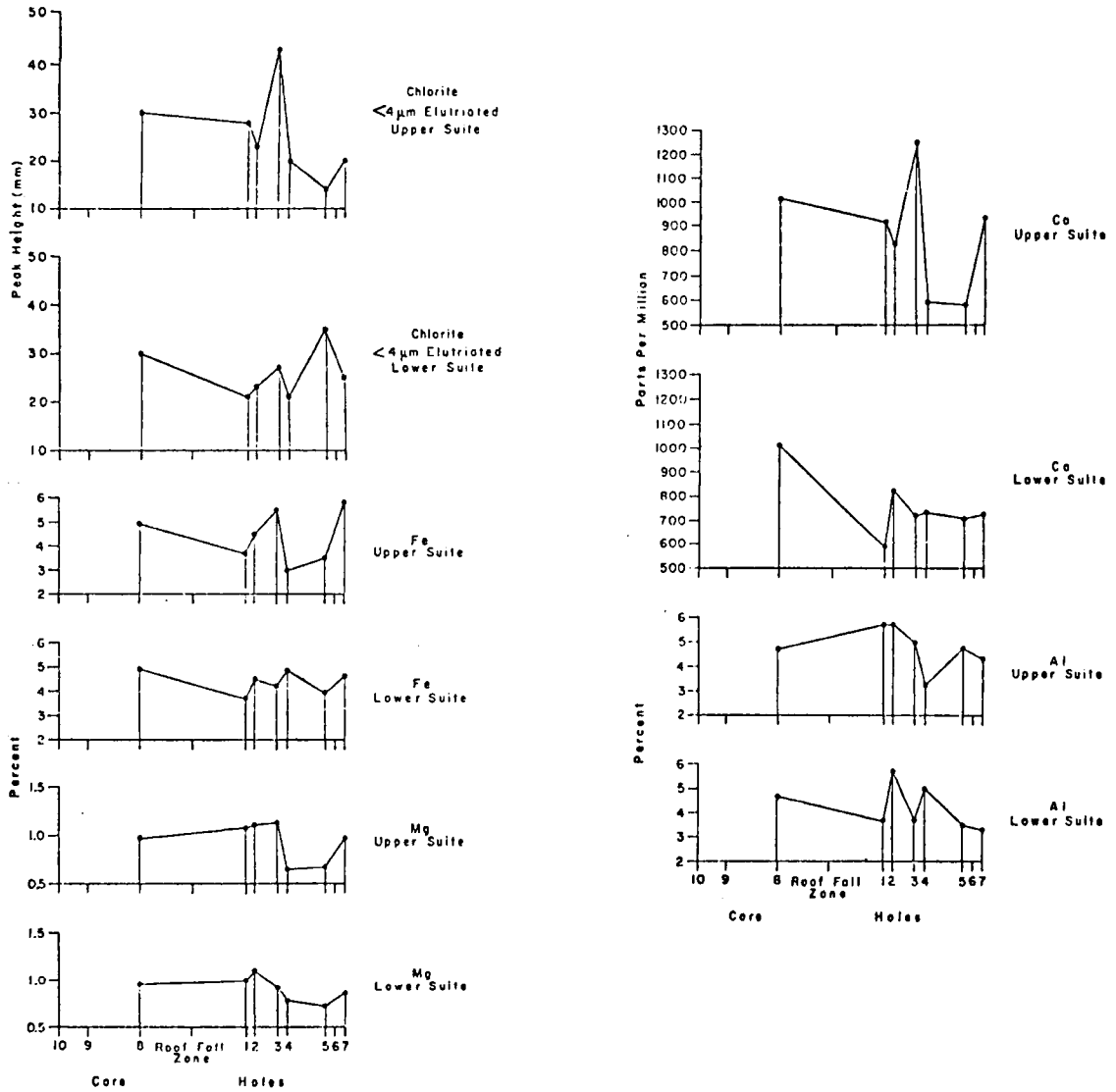

FIGURE 98. - Chlorite 14A peak height plots (upper left) and elemental abundances (lower left and right). Values for elemental abundances from page 218.

no shale or siltstone was present in these cores. Also, nearly all of the shale portion of core 6 was lost during core drilling and was not analyzed.

A comparison of clay mounting techniques in Figure 97 shows some discrepencies between the <4μm smear, <4μm elutriated and <2μm elutriated samples. In order to better evaluate these differences, major element abundances (Figures 97 and 98) were compared with SR values. The major element analysis was done for the study by the U. S. Bureau of Mines. The analyses were made using atomic absorption techniques. The results are shown in Table 20. Assuming that an illite sample with a relatively higher potassium content might result in a higher SR value, potassium content of the sample is shown plotted with the SR value in Figure 97. As indicated, in most cases higher SR values correspond to higher potassium content and vice versa. A comparison of preparation methods indicates that the elutriated samples show a better comparison with potassium than the smear mounts, probably because oriented clays obtained in elutriation enhanced the (001) basal reflections. Also, the <2μm elutriated samples show a closer relationship to the potassium plot than the <4μm size fraction, indicating better results by analyzing the finer fraction.

Texture Comparisons. Oriented thin-sections of the samples used in SR determinations were utilized to compare rock texture to SR values. Because many of the samples were very fine grained, an arbitrary scale of 0 to 5 was used. A value of 0 indicates that the sample is very fine-grained shale, and a value of 5 corresponds to a siltstone (Figure 97).

TABLE 20. - Major element analyses by atomic absorption. Results in weight percent or parts per million as indicated Accuracy reported as ±5 %.

DEPARTMENT OF THE INTERIOR

Bureau of Mines

ANALYTICAL REPORT

Sample of Core Shale

From Noel Moebs Analysis requested for major elements.

Sampled _____ Received at lab. _____ Analyzed 1/23/76

Section or Bureau Roof Support Collector _____

ANALYSIS

Sample No.	Lab No.	Al%	Mg(%)	Fe(%)	K(%)	Ca(ppm)
CORE #8-(15)	75-592	4.75	0.96	4.98	3.78	1013
CORE #1-(13)	75-593	5.75	1.08	3.70	3.43	919
CORE #1-(16)	75-594	3.75	1.00	3.71	3.71	599
CORE #2-(15)	75-595	5.75	1.10	4.56	4.38	821
CORE #3-(18)	75-596	5.00	1.11	5.53	3.05	1237
CORE #3-(23B)	75-597	3.75	0.92	4.22	4.07	720
CORE #4-(17A)	75-598	3.25	0.65	3.00	4.00	590
CORE #4-(21)	75-599	5.00	0.79	4.85	4.20	726
CORE #5 (12)	75-600	4.75	0.68	3.48	4.40	580
CORE #5 (18)	75-601	3.50	0.73	3.98	3.78	718
CORE #7 (12)	75-602	4.25	0.97	5.81	4.31	922
CORE #7 (17)	75-603	3.25	0.87	4.68	4.63	723

For comparative purposes, elemental abundances and texture values were plotted (Figures 97, page 215, and 98, page 216). From these graphs, Tables 21 and 22 were prepared to relate SR values and elemental abundances with textural variations in the samples. Comparisons were made as to increases or decreases in SR values, elemental abundances and chlorite peak height relative to texture from one core to another. In some cases no consistant relationships were evident, especially in the lower suite of core samples where textural differences were less significant.

The most significant apparent relationships are:

1. SR values, Al and K contents are, in general, inversely proportional to texture.

2. Calcium, Mg and Fe contents appear to be directly proportional to coarser texture. The chlorite 14A peak height also appears to be directly proportional.

Even though several of the trends between texture and elemental and index values appear valid, it is important to point out that elemental analysis was done on material that was not entirely clay-sized. The material for elemental analysis was obtained by grinding and dry sieving through a No. 200 mesh sieve (75 μm) whereas clay minerals are <4μm or <2μm. Elemental discrepancies may result from minerals other than clays in the coarser fraction.

Possible Causes of Observed Clay Mineral Trends. The general relationships shown between clay mineral trends and elemental content versus texture suggests that the clays may habe resulted either from

TABLE 21. - Summary of illite sharpness ratios and chlorite peak heights compared with rock texture[1]

	SR Value <2μm elutriated	SR Value <4μm elutriated	SR Value <4μm smear	Chlorite Peak Height
Upper Suite	Inverse (except core 5)	Inverse?	?	Direct
Lower Suite	Inverse?	Inverse?	Inverse? (except core 1)	Direct (except core 5)

[1]Note - underlined proportionality relationship indicates positive correlation with texture, question mark after relationship indicates doubt, and question mark alone indicates no discernable relationship with texture.

TABLE 22. - Summary of elemental abundances compared with rock texture[1]

	Al	K	Ca	Mg	Fe
Upper Suite	?	Inverse	Direct	Direct (Except core 2)	Direct (Except core 2)
Lower Suite	Inverse	Inverse	Direct? (Except core 2)	Direct (Except core 2)	?

[1]Note - underlined proportionality relationship indicates positive correlation with texture, question mark after relationship indicates doubt, and question mark alone indicates no discernable relationship with texture.

sorting of detrital clays during deposition of the sediments or from diagenetic alteration.

Evidence for Detrital Mica:

1. That at least some illite material is a 2M mica polytype is indicated by the presence of the unique 2M peak at about 2.80A in several samples. Also observed at 2.58A was a peak that includes the 2M (131), (116) and (202) reflections and the 1M (131) and (130) reflections. The (130) reflection is also observed in 1Md muscovite (46). The possibility exists, then, that higher SR values are the result of reflections from the 2M polytype because of better crystallinity and perhaps larger crystal size.

2. The muscovites and natural illites exist only in the 1M, 2M and rare 3T form, plus a completely disordered 1Md form. Stability increases in the sequence 1Md→1M→2M, favored by an increase in temperature (81, 91). Because the 2M polytype is formed under relatively higher temperatures and pressures, but has a very slow rate of inversion, muscovites and illites found in sediments that are the 2M polytype are likely detrital (10, 22). Barring the possibility that pressure and temperature conditions were intensive enough to form the 2M polytype in situ, the presence of the 2M polytype indicates a detrital clay.

3. The data listed in Table 23, obtained by heating the clay samples to 600°C for one hour, were used to construct Table 24. A comparison of the peak height and peak width values for each sample shows that heat treating had little effect. These results suggest strongly that very little mixed-layered clays are present, because

TABLE 23. - Sharpness ratio determinations from <2μm elutriated samples (not heat treated)

Core Number	Sample Number	Peak Height (mm)	Peak Width (mm)	SR Value
8	15	96.0	7.0	13.7
1	13	90.0	6.1	14.8
1	16	85.0	6.5	13.0
2	15	103.0	6.5	15.8
3	18	91.5	7.5	12.2
3	23-B	107.5	5.7	18.9
4	17-A	106.0	6.0	17.7
4	21	83.0	7.0	11.9
5	12	45.0	6.0	7.5
5	18	97.0	7.5	12.9
7	12	106.0	6.0	17.7
7	17	109.0	6.5	16.8

TABLE 24. - Sharpness ratio determinations from <2μm elutriated samples (heat treated to 600°C for 1 hour)

Core Number	Sample Number	Peak Height (mm)	Peak Width (mm)	SR Value
8	15	97.0	6.0	16.2
1	13	88.0	4.8	18.3
1	16	85.0	5.5	15.5
2	15	98.0	6.0	16.3
3	18	99.0	5.5	18.0
3	23-B	104.0	5.8	17.9
4	17-A	116.0	5.8	20.0
4	21	84.0	6.5	12.9
5	12	47.0	6.5	7.2
5	18	101.0	6.9	14.6
7	12	108.0	5.5	19.6
7	17	107.0	6.0	17.8

heating should cause a collapse of these layers, and a decrease in peak width (Figure 96, page 211). Also, the peak heights did not increase. This evidence suggests that heat treating did not increase the crystallinity of the clays. This evidence, coupled with a direct relationship with potassium, supports the conclusion that SR values result from detrital micas that are variable in potassium deficiency from sample to sample.

4. The texture of the immediate roof shales and siltstones (Figure 97, page 215) indicates a general increase in coarseness between cores 2 through 4. Also, thin sections of siltstones in the immediate roof rocks show rounded, apparently detrital grains of shale. This same trend is evident in the main sandstone roof rocks (Figure 94 (top), page 204), and may reflect a depositional "low" for detrital sedimentation. Also, the presence of ubiquitous large muscovite flakes on sandstone bedding in the main sandstone roof is certainly detrital.

Evidence for Diagenetic Changes. According to Dunoyer De Segonzac (22) the diagenetic and metamorphic evolution of clays is characterized by the following:

1. Dehydration of the interlayer spaces.

2. Adsorption of potassium and aluminum from the interstitial solutions.

3. Redistribution of ions within the lattices, in particular the passage of aluminum from the octahedra to the tetrahedra.

4. Ordering the lattices, growth of crystals and massive neoformation of illite and chlorite which are stable to burial.

Some evidence to support these diagenetic changes found in this study include:

1. Examination of thin sections of sandstones overlying the immediate roof shales showed alteration of detrital feldspars and solution of quartz grains (Figures 88 and 89, page 191). It would logically follow that the finer-grained immediate roof rocks would also be subject to alteration by interstitial solutions. Increased porosity would favor circulation of fluids, and the main roof sandstones with coarser textures appear to be more strongly altered than finer-grained ones.

2. Since the SR values generally show an inverse relationship to texture (Figure 97, page 215), it is possible that the SR values reflect detrital clays. Dunoyer De Segonzac (22) noted that more crystalline illites should be associated with coarser sediments. His reasoning was that the aggradation of illite by interstitial solutions during early diagenesis proceeds more easily in porous environments, so coarser rocks (sandstones) contain illites more crystalline than those of shales. However, transformations of clay minerals are reversible and successive changes in diagenetic conditions may introduce successively different recrystallizations.

Also, in late diagenesis the relationship between lithology and illite crystallinity becomes less obvious. In late diagenesis, the illites are changed by the adsorption of potassium. This aggradation is favored by compaction which expels the interlayer water, and by increased temperature which produces a reordering of the lattice (22).

This increased crystallinity, which should result in higher SR values, was indicated in the KCl treated samples analyzed in this study. Otherwise untreated clays, when saturated with KCl, had increased SR values compared to the same samples not saturated with KCl. Reconstitution of potassium-deficient clays in the laboratory is rather tenuous. However, Figures 97, page 215 and 98, page 216, show that the core sample SR values are directly proportional to potassium and aluminum abundances.

It may be that instead of being aggraded by the adsorption of potassium, illites may have been originally detrital and not K+ deficient. These clays may be degraded and potassium removed by circulation of interstitial fluids during diagenesis. The low permeability of shales would serve to prohibit such circulation and the illites should have been protected from degradation (69). The result would be relatively higher SR values in shales as observed.

It should be noted that SR values (and chlorite peak heights) were calculated for ten samples obtained from the measured rib sections (Figure 95, page 206). However, the results are not reported here because no significant results were obtained; perhaps because of increased organic content in the rib rocks.

Chlorite Peak Heights. A comparison of chlorite (001) peak height intensities and magnesium, iron and calcium content compared to texture shows that they are generally directly proportional (Figures 97 and 98). Because of these relationships, it would be difficult to separate the detrital origin of chlorite from diagenetic alteration effects through the addition of magnesium and/or iron. However, Dunoyer De Segonzac (22)

noted that diagenetic alteration of mixed-layer clays or degraded three-layer clay minerals by magnesium fixation results in chlorite.

Triplehorn (80) concluded from results very similar to those obtained for chlorite in this study that the increased chlorite content in sandstones resulted from diagenetic effects of interstitial fluids in the Atoka Formation (Pennsylvanian) of Arkansas. His conclusions were based on chemical and x-ray analyses of the <2μm size fraction. Considerable emphasis of the partly diagenetic origin for the clay suites was placed on the alteration of quartz and the presence of authigenic siderite in the sandstones containing the clays. Considerable alteration of original silicate minerals is evident in the main sandstone roof rocks in the Highsplint mine (see discussion, page 188), so a similar diagenetic origin for the chlorites may be postulated.

Conclusions. The identification and possible trends indicated by the clay mineralogy and elemental content of the core shales was based on a limited number of samples representing a relatively small area. However, data suggest that sharpness ratio values are sufficiently sensitive to detect changes in the character of the main sandstone roof, especially the detection of rolling sandstone roof. In order to validate the applicability of results indicated in the old 004 Section, more extensive sampling and analysis would be desirable. However, the practical application of clay mineralogic studies in locating marginal areas of rolling sandstone roof would be overshadowed by the use of sandstone trend projections and isopach data in a mine with the roof rock characteristics present in the Highsplint mine.

IX. SUMMARY AND CONCLUSIONS

Summary of Findings

This research was conducted with the aim of identifying possible geologic conditions that contribute to roof falls in the Bailey Creek and Highsplint mines operated by the Eastover Mining Company in Harlan County, Kentucky. Methods of projecting unstable trends in advance of mining were studied and evaluated.

It is evident that roof falls in the mines have been caused by several interrelated contributing factors of lithology, the geometry of roof rocks and structural features present in the rocks such as joints and "slips."

In order to evaluate the physical features of the Mingo Formation, which includes the Harlan and Darby coal beds, a reference stratigraphic section at Brookside, Kentucky was measured and described. Using this section, together with information gathered at other surface outcrops in the study area, characteristic vertical and lateral stratigraphic sequences were identified. Surface studies were conducted to permit correlations between surface exposures and equivalent roof rocks within the mines which are at the same stratigraphic horizon. Drill core information was not available for correlative purposes. The premise that the character of the roof rocks in such drift mines can be inferred with a reasonable degree of accuracy from outcrop information prior to mining has been verified by underground mapping.

Based on 91 measured rib sections of the immediate roof in the Highsplint mine, together with observations along traverses between section locations, a classification scheme was devised that relates roof stability with lithologic and structural features of the roof. Evaluation of the classification scheme indicates that, even with limited outcrop exposure, roof conditions and lateral trends to be expected underground can be reasonably anticipated from surface exposures at the same stratigraphic level.

Trend analysis techniques that enhance the projection of lithologic and structural features of roof rocks (notably sandstone rolls and joint trends) known to cause unstable roof conditions, were investigated. Correlation of these features was made between surface exposures and within the mines. The analysis of linear sandstone axes and associated cross-bedding, joints and "slips" was supplemented by the use of computer programs developed during this study. These computer programs appear to provide a rapid, systematic means for treating the data. However, the programs need to be tested in several localities before a final determination can be made as to their widespread effectiveness.

In surface studies of structural trends the use of topographic maps and especially geologic quadrangle maps proved to be of considerable value and should be considered a major tool in premining analysis. The computer analysis of drainage patterns on these maps for joint analysis was of more value than areal photographs because shadows and distortion caused by the hilly terrain made linear trends difficult to identify with certainty. Geologic quadrangle maps also provided lithologic

spatial relationships and structural information in the vicinity of the mining sites.

Underground projections of linear sandstone trends in the Highsplint mine were based on several sources of information. In addition to measured rib sections, information such as measured coal sections and mine elevations supplied by the mining company proved useful in projecting trends.

Several studies were conducted in order to investigate in detail the lateral and vertical relationships of roof rocks leading into a known roof-fall zone. A series of ten NX cores, taken from the old 004 Section, Highsplint mine were examined in detail. The immediate roof shales and siltstones showed a general direct relationship between coarser texture, illite clay mineral sharpness ratios, and K and Al elemental content. The clay mineral index trends also showed a correlation between coarser sandstone texture in the overlying main sandstone roof. On the basis of petrographic studies of the main sandstone roof cores, it was concluded that unstable roof conditions occur more frequently marginal to sandstone rolls or channels.

Petrographic studies of the core samples together with megascopic lithologic and biologic features of rocks associated with the Harlan and Darby coal beds lead the author to conclude that deposition of the strata took place in a river-dominated alluvial plain and/or delta lobe environment. The resulting narrow, linear sandstone channels may contribute to roof instability in the mines.

During this study, an important relationship between unstable roof rock trends and the heading direction within the mine was discovered.

Roof instability results when narrow, sand-filled channels or joint trends parallel the heading directions. In most places, the layout of the Highsplint mine is such that both sandstone rolls and frequent joint and "slip" trends cross entries at an angle. However, roof falls in the Bailey Creek mine occur where sand-filled channels parallel the heading directions. Monitoring of the Bailey Creek operations during the six-month period (from April, 1976 to September, 1976) indicated that a change in heading direction to avoid channels has resulted in improved roof conditions.

Recommendations for Future Studies

This study was concerned with the investigation of geologic factors that contribute to roof falls. By necessity, several interrelated studies were conducted to develop methods for predicting unstable ground conditions in advance of mining. Future studies are needed in the following areas:

1. Application of methods developed. The studies reported here were developed in only two mines representing a small geographic area. The methods found useful in these mines should be applied to several mines in eastern Kentucky. These studies ideally would include mines with both "good" and "bad" roof conditions so that an evaluation could be made relative to these conditions. Studies should emphasize an evaluation of the stratigraphic relationships and sequences of the immediate and main roof rocks, both in the mines and on the outcrop. Trend analyses, including rock jointing and sedimentary trends, would

make use of the computer programs developed in this study to further test their use. A comparison of the roof classification scheme developed at the Highsplint mine with other mines should be made to test its applicability, so that its potential use can be further evaluated. It is anticipated that a revision of the classification scheme will be necessary to include different categories of roof conditions in different mines.

2. Refinement of methods. The methods of trend analysis developed to date need further refinement. The computer programs used for joint and sedimentary trend analysis have not provided an entirely satisfactory solution as to the exact number of joint sets present. The development of statistical tests is planned for these programs. Also, the use of space photography and side-scanning radar to substantiate directions of structural weakness in mining areas is planned.

3. Application of new methods. Sedimentary trends studied in the Highsplint and Bailey Creek mines were based on direct observation. Future studies based largely on drill-core information at a mine with a large number of core records would extend the applicability of vertical and lateral stratigraphic relationships established to date.

4. Refinement of compositional studies. Petrographic studies and clay mineral analyses of core samples were conducted in this study to determine possible reasons for roof falls in the Highsplint mine and was based on a limited number of samples. While the value of such studies for trend indicators is limited because of the time-consuming nature of the work, additional studies using greater numbers of samples may provide methods of characterizing the main roof by analysis of the immediate roof.

SELECTED REFERENCES

SELECTED REFERENCES

1. Allen, J. R. L. The Classification of Cross-Stratified Units with Notes on their Origin. Sedimentology, v. 2, 1963b, pp. 93-114.

2. Allen, J. R. L. A Review of the Origin and Characteristics of Recent Alluvial Sediments. Sedimentology, v. 5, 1965, pp. 89-191.

3. Arkle, T. A., Jr. Stratigraphy of the Pennsylvanian and Permian Systems of the Central Appalachians in Carboniferous of the Southeastern United States, ed. by Garrett Briggs. Geol. Soc. America Special Paper 148, 1974, pp. 5-29.

4. Badgley, P. C. Structural and Tectonic Principles. Harper & Row Pub. Co., New York, 1965, 521 pp.

5. Billings, M. P. Structural Geology. Prentice-Hall, Inc., Englewood Cliffs, New Jersey, 3d ed., 1972, 606 pp.

6. Boone, G. M., and E. P. Wheeler. Staining for Cordierite and Feldspars in Thin Section. Am. Mineralogist, v. 53, 1968, pp. 327-331.

7. Butts, Charles. Fensters in the Cumberland Overthrust Block in Southwestern Virginia. Va. Geol. Survey Bull. 28, 1927, 12 pp.

8. Campbell, M. R. Geology of the Big Stone Gap Coal Field of Virginia and Kentucky. U. S. Geol. Survey Bull., v. III, 1893, 106 pp.

9. Carozzi, A. V. Microscopic Sedimentary Petrography. R. E. Krieger Pub. Co., Huntington, N. Y., 1972, 485 pp.

10. Carroll, D. Clay Minerals: A Guide to Their X-ray Identification. Geol. Soc. America Spec. Paper 126, 1970, 80 pp.

11. Chayes, F. A simple Point Counter for Thin-Section Analysis. Am. Mineralogist, v. 34, 1949, pp. 1-11.

12. Cheek, Robert, and Alan Donaldson. Sulfur Facies of the Upper Freeport Coal of Northwestern Preston County, West Virginia. in Some Appalachian Coals and Carbonates: Models of Ancient Shallow-Water Deposition. W. Va. Geol. Survey, Morgantown, 1969, pp. 279-308.

13. Chen, E. H. A Random Normal Number Generator for 32-Bit-Word Computers. Jour. Am. Statistical Assoc. v. 66, No. 34, 1971, pp. 400-403.

14. Coleman, J. M. Brahmaputra River: channel Processes and Sedimentation. Sedimentary Geology, v. 3, No. 2/3, 1968, pp. 129-239.

15. Csejtey, Bela, Jr. Geology of the Nolansburg Quadrangle, Southeastern Kentucky. U. S. Geol. Survey Geol. Quad. GQ-868, 1970.

16. Curray, J. R. The Analysis of Two-Dimensional Orientation Data. Jour. Geol. v. 64, 1965a, pp. 117-131.

17. Davis, J. C. Statistics and Data Analysis in Geology. John Wiley & Sons, Inc., New York, 1973, 550 pp.

18. Dennison, J. M. Analysis of Geologic Structures. W. W. Norton & Co., Inc., New York, 1968, 209 pp.

19. Donaldson, A. C. Pennsylvanian Sedimentation of the Central Appalachians.in Carboniferous of the Southeastern United States, ed. by Garrett Briggs. Geol. Soc. America Special Paper 148, 1974, pp. 47-78.

20. Dott, R. H., Jr. Paleocurrent Analysis of Trough Cross Stratification. Jour. of Sed. Petrology, v. 43, No. 3, 1973, pp. 779-783.

21. Duff, P. M., and others. Cyclic Sedimentation, Elsevier Pub. Co., New York, 1967, 280 pp.

22. Dunoyer De Segonzac, G. The Transformation of Clay Minerals During Diagenesis and Low-Grade Metamorphism: A Review. Sedimentology, v. 15, 1970, pp. 281-346.

23. Elliott, T. Interdistributary Bay Sequences and their Genesis Sedimentology, v. 21, 1974, pp. 611-622.

24. Englund, K. J. Sandstone Distribution Patterns in the Pocahontas Formation of Southwest Virginia and Southern West Virginia. in Carboniferous of the Southeastern United States, ed. by Garrett Briggs. Geol. Soc. America Special Paper 148, 1974, pp. 31-45.

25. Englund, K. J., and others. Geology of the Middlesboro North Quadrangle, Kentucky. U. S. Geol. Survey Geol. Quad. GQ-300, 1964.

26. Ferguson, H. F. Valley Stress Release in the Allegheny Plateau. Assoc. Eng. Geol. Bull., v. 4, No. 1, January,1967, pp. 63-69.

27. Ferm, J. C. Carboniferous Environmental Models in Eastern United States and Their Significance. in Carboniferous of the Southeastern United States, ed. by Garrett Briggs. Geol. Soc. America Special Paper 148, 1974, pp. 79-95.

28. Fisk, H. N. Fine Grained Alluvial Deposits and their Effects on Mississippi River Activity. Mississippi River Commission, Vicksburg, Miss., 1947, 82 pp.

29. Folk, R. L. Petrology of Sedimentary Rocks. The University of Texas, Austin Publication, 1964, 154 pp.

30. Friedman, G. M. Determination of Sieve-Size Distribution From Thin-Section Data for Sedimentary Petrological Studies. J. Geol. v. 66, 1948, pp. 394-416.

31. Friedman, Melvin. Petrofabric Techniques for the determination of Principal Stress Directions in Rocks. in State of Stress in the Earth's Crust. American Elsevier Pub. Co., Inc., New York, 1964, pp. 451-552.

32. Froelich, A. J. Geologic Map of the Louellen Quadrangle, Southeastern Kentucky. U. S. Geol. Survey Geol. Quad. GQ-1060, 1973.

33. Garrels, R. M., and C. L. Christ. Solutions, Minerals and Equalibria. Harper & Row Pub. Co., New York, 1965, 450 pp.

34. Grim, R. E. Clay Mineralogy. McGraw-Hill Book Co., 2nd ed., 1968, 596 pp.

35. Harris, L. D. Details of Thin-Skinned Tectonics in Parts of Valley and Ridge and Cumberland Plateau Provinces of the Southern Appalachians. in Studies of Appalachian Geology: Central and Southern, ed. by G. W. Fisher and others. John Wiley and Sons, Inc., 1970, pp. 161-173.

36. Harris, L. D., and I. Zietz. Development of the Cumberland Overthrust Block in the Vicinity of the Chestnut Ridge Fenster in Southwest Virginia. AAPG Bull., v. 46, No. 12, 1962, pp. 2148-2160.

37. High, L. R., Jr., and M. D. Pecard. Mathematical Treatment of Orientation Data: in Procedures in Sedimentary Petrology, ed. by R. E. Carver. John Wiley and Sons, Inc. New York, 1970, pp. 21-46.

38. Holland, C. T. Mineral Content, a Factor in Weathering of Mine Roof. Min. Cong. J., January, v. 42, No. 1, 1956, pp. 59-53, 67.

39. Hodgson, R. A. Regional Study of Jointing in Comb Ridge-Navajo Mountain Area, Arizona and Utah. AAPG Bull. v. 45, No. 1, 1961, pp. 1-38.

40. Huddle, W. R., and others. Coal Resources of Eastern Kentucky. U. S. Geol. Survey Bull., v. 1120, 1963, 247 pp.

41. Jackson, K. C. Textbook of Lithology. McGraw-Hill Book Co., New York., 1970, 552 pp.

42. Jillson, W. R. The Kendrick Shale - a New Calcareous Fossil Horizon in the Coal Measures of Eastern Kentucky. Ky. Dept. Geology and Forestry, Min. and Forest Resources of Kentucky, series 5, v. 1, No. 2, 1919, pp. 96-104.

43. Jones, D. J. and others. Mountain Bumps in the Coal Fields of Harlan County, Kentucky. Kentucky State Dept. of Mines and Minerals - Geological Division, Ser. VIII, Bull. v. 1, 1934, 25 pp.

44. Kendall, P. F. and H. Briggs. The Formation of Rock Joints and the Cleat of Coal, Proc. Royal Soc., Edinburgh, v. 53, 1933, pp. 164-187.

45. Kopp, O. C., and T. C. Sutton. Effects of Regional Metamorphism on the Clay Minerals of the Valley and Ridge and Blue Ridge Provinces of Southeastern Tennessee. Geol. Soc. America. Abstracts, pt. 4, Southeastern Section, 1969, pp. 42-43.

46. Maxwell, D. T., and John Hower. High-Grade Diagenesis and Low-Grade Metamorphism of Illite in the Precambrian Belt Series. Am. Mineralogist, v. 52, May-June, 1967, pp. 843-857.

47. McColloch, C. M., and others. Cleat in Bituminous Coalbeds. BuMines RI 7910, 1974, 25 pp.

48. _____, and others. Geologic Investigations of Underground Coal Mining Problems. BuMines RI 8022, 1975, 30 pp.

49. McKee, E. D. Significance of Climbing Ripple Structure. U. S. Geol. Survey Prof. Paper, 550-D, 1966, pp. D94-D103.

50. _____ , and G. W. Weir. Terminology for Stratification and Cross-Stratification in Sedimentary Rocks. Geol. Soc. America Bull. v. 64, 1953, pp. 381-390.

51. Meckel, L. D. Paleozoic Alluvial Deposition in the Central Appalachians: A Summary. in Studies of Appalachian Geology: Central and Southern. ed. by G. W. Fisher, and others. John Wiley & Sons Pub. Co., New York, 1970, pp. 49-67.

52. Meyertons, C. T. Mineralogy of Some Coal Mine Roof Shales. VPI Mineral Industries Journal, v. III, No. 1, March 1956, pp. 1-3.

53. Miller, R. L. Pennsylvanian Formations of Southwest Virginia U. S. Geol. Survey Bull., v. 1280, 1969, 62 pp.

54. _____. and W. P. Brosge. Geology and Oil Resources of the Jonesville District, Lee County, Virginia. U. S. Geol. Survey

55. _____, and J. O. Fuller. Geology and Oil Resources of the Rose Hill District - the Fenster Area of the Cumberland Overthrust Block-Lee County, Virginia. Va. Geol. Survey Bull., v. 71, 1954, 383 pp.

56. _____, and J. B. Roen. Geologic Map of the Pennington Gap Quadrangle, Lee County, Virginia and Harlan County, Kentucky. U. S. Geol. Survey Geol. Quad. GQ-1098, 1973.

57. Morse, W. C. The Pennsylvanian Invertebrate Fauna of Kentucky. in Paleontology of Ky. Ky. Geol. Survey, series 6, v. 36, 1931, pp. 293-348.

58. Nickelsen, R. P. and V. N. D. Hough. Jointing in the Appalachian Plateau of Pennsylvania. Geol. Soc. America Bull. v. 78, 1967, pp. 609-630.

59. Overbey, W. K., and others. Predicting Probable Roof Fall Areas in Advance of Mining by Geological analysis. BuMines TPR-70, 1973, 17 pp.

60. Pettijohn, F. J. Sedimentary Rocks. Harper & Row Pub. Co., New York, 3rd ed., 1975, 628 pp.

61. _____, P. E. Potter and R. Siever. Sand and Sandstone. Springer-Verlag Pub. Co., New York, 1972, 618 pp.

62. Potter, P. E. and F. J. Pettijohn. Paleocurrents and Basin Analysis. Springer-Verlag Pub. Co., Berlin, Germany, 1963, 296 pp.

63. Powers, M. C. A New Roundness Scale for Sedimentary Particles. Jour. Sed. Petrology, v. 23, 1953, pp. 117-119.

64. Raistrick, A. and C. E. Marshall. The Nature and Origin of Coal and Coal Seams. The English University Press, Ltd., London, 1939, 282 pp.

65. Reineck, H. E. and I. B. Singh. Depositional Sedimentary Environments. Springer-Verlag Pub. Co., New York, 1975, 439 pp.

66. Rich, J. L. Mechanics of Low-Angle Overthrust Faulting as Illustrated by the Cumberland Thrust Block, Virginia, Kentucky and Tennessee. AAPG bull., v. 18, 1934, pp. 1584-1596.

67. Robinson, M. J. A Deltaic-Back Barrier Model for the Formation of the Beckley Coal Seam in Southern West Virginia. Unpub. MS Thesis, Univ. of South Carolina, 1975, 51 pp.

68. Rodgers, John. Evolution of Thought on Structure of Middle and Southern Appalachians. APPG Bull., v. 33, No. 10, 1949, pp. 1643-1654.

69. Schultz, L. G. Petrology of Underclays. Geol. Soc. America, Bull., v. 69, 1958, pp. 363-402.

70. Secor, D. T. Role of Fluid Pressure in Jointing. Am. J. Sci., v. 263, 1965, pp. 633-646.

71. Selley, R. C. A Classification of Paleocurrent Models. Jour. Geol., v. 76, 1968, pp. 99-110.

72. Smith, Gilbert, and Preston McGrain. Kentucky Coal. in Keystone Coal Industry Manual. McGraw-Hill Book Co., Inc., New York, 1974, pp. 503-507.

73. Smith, N. D. The Braided Stream Depositional Environment: Comparison of the Platte River with Some Silurian Clastic Rocks, North-Central Appalachians. Geol. Soc. America Bull., v. 81, 1970, pp. 2993-3014.

74. Spencer. E. W. Introduction to the Structure of the Earth. McGraw-Hill Book Co., New York, 1969, 597 pp.

75. Stanley, D. J. Graded Bedding-Sole Marking-Graywacke Assemblage and Related Sedimentary Structures in Some carboniferous Flood Deposits, Eastern Massachusetts. in Late Paleozoic and Mesazoic Continental Sedimentation, Northeastern North America, ed. by G. D. Klein, Geol. Soc. America Spec. Paper 106, 1968, pp. 211-239.

76. Stokke, P. R., and B. Carson. Variation in Clay Mineral X-Ray Diffraction Results With the Quantity of Sample Mounted. Jour. Sed. Petrology. v. 43, No. 4, 1973, pp. 957-964.

77. Tazelaar, J. F., and W. L. Newell. Geology of the Evarts and Hubbard Springs Quadrangles, Southeastern Kentucky and Virginia. U. S. Geol. Survey Geol. Quad. GQ-914, 1974.

78. Terry, R. D. and G. V. Chilingar. Summary of "Concerning Some Additional Aids in Studying Sedimentary Formations," by M. S. Shvetsov. Jour. Sed. Petrology, v. 25, 1955, pp. 229-234.

79. Thornbury, W. D. Regional Geomorphology of the United States. John Wiley and Sons, New York, 1965, 609 pp.

80. Triplehorn, D. M. Clay Mineral Diagenesis in Atoka (Pennsylvanian) Sandstones, Crawford County, Arkansas. Jour. Sed. Petrology, v. 40, No. 3, 1970, pp. 838-847.

81. Velde, B. and J. Hower. Petrological Significance of Illite Polymorphism in Paleozoic Sedimentary Rocks. Am. Mineralogist, v. 48, November-December, 1963, pp. 1239-1253.

82. Wang, Fun-Den, and others. Structural Analysis of a Coal Mine Opening in Elastic, Multilayered Material. BuMines RI 7845, 1974, 36 pp.

83. Warshaw, C. M. and R. Roy. Classification and a Scheme for the Identification of Layer Silicates. Geol. Soc. America Bull., v. 72, No. 10, 1961, pp. 1455-1492.

84. Weaver, C. E. Geologic Interpretation of Argillaceous Sediments. Part 1. Origin and Significance of Clay Minerals in Sedimentary Rocks. Part II. Clay Petrology of Upper Mississippian-Lower Pennsylvanian Sediments of Central United States. AAPG Bull., v. 42, 1958, pp. 254-309.

85. _____, Clay Minerals of the Ouachita Structural Belt and Adjacent Foreland: Pub. No. 6120, Bureau of Econ. Geol., University of Texas, 1961, pp. 147-150.

86. Wentworth, C. K. Russell Fork Fault of Southwest Virginia. Jour. Geology, v. 29, 1921, pp. 351-369.

87. White, W. A. Properties of Clay as Related to Coal Mining Problems. Proc. of the Ill. Min. Institute, 1954, pp. 33-38.

88. Wier, C. E. Factors Affecting Coal Roof Rock in Sullivan County, Indiana. Proc. Indiana Acad. Sci. for 1969, Indianapolis, Ind., v. 79, 1970, pp. 263-269.

89. Williamson, I. A. Coal Mining Geology. Oxford University Press, New York, 1967, 266 pp.

90. Yarbrough, R. E. A Geographical Study of a Micro-region in Appalachia—The Clover Fork River Valley of Harlan County, Kentucky. Univ. of Tennessee, Unpublished Doctoral Dissertation, 1972.

91. Yoder, H. S., and H. P. Eugster. Synthetic and Natural Muscovites. Geochem. Cosmochim. Acta. v. 8, 1955, pp. 225-280.

APPENDIXES

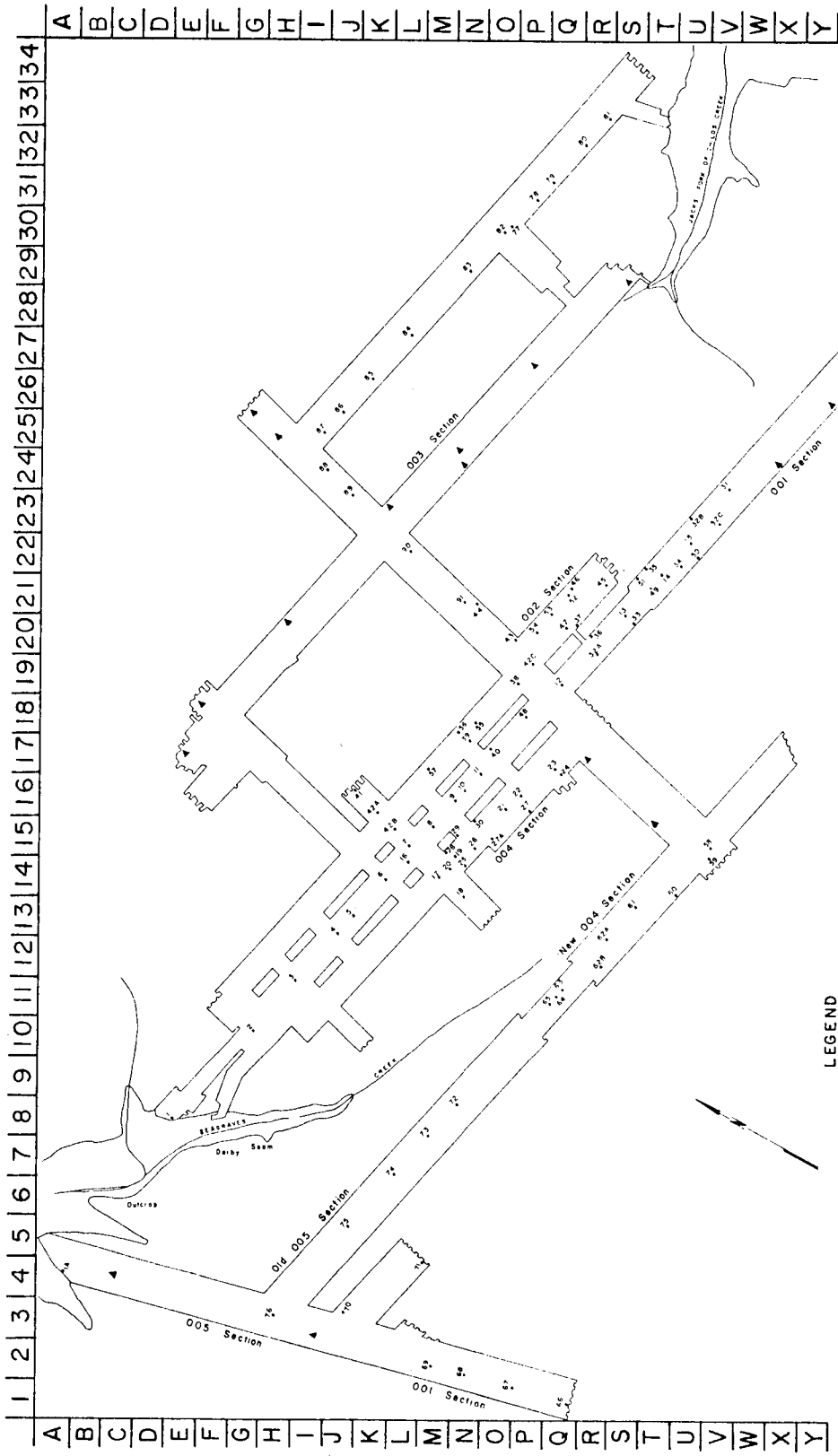

FIGURE A1. - Location map of Highsplint mine showing coordinate system for rib sections and coal sections.

APPENDIX B

TABLE B1. - English-metric length conversion

1 mile = 1.609 kilometers
1 foot = 30.480 centimeters
1 inch = 2.540 centimeters
1 micron (μ) = 1 micrometer (μm) = 10^{-6} meter = 3.937 x 10^{-7} inches

TABLE B2. - Comparison of quantitative terms for layered rocks

Terms to describe stratification		Terms to describe cross-stratification		Thickness
Very thick-bedded	Beds	Very thick cross-bedded	Cross-beds	Greater than 120 cm.
Thick-bedded		Thickly cross-bedded		120 cm. (about 4 ft.) to
Thin-bedded		Thinly cross-bedded		60 cm. (about 2 ft.) to
Very thin-bedded		Very thinly cross-bedded		5 cm. (about 2 in.) to
Laminated	Laminae	Cross-laminated	Cross-Laminae	1 cm. (about 1/2 in.) to
Thinly laminated		Thinly cross-laminated		2 mm. (about .08 in.) or less

[after McKee and Weir (50)].

TABLE B3. - Measured rib sections - Highsplint mine

Station Number	Location Coordinates	Total Thickness (inches)	Total Shale Thickness (inches)	Roof Composition	
				Sandstone	Shale Roof and Estimated Thickness to Sandstone (inches)
1	E - 8	60.5	44.5	X	
1A	A - 4	61	47	X	
2	G - 10	45	35	X	
3	H - 11	62	33		X - 12
4	J - 13	49	26		X - 6
5	J - 13	51	25.5		X - 4
6	K - 14	49	28	X	
7	L - 15	40	20	X	
8	M - 15	24.5	11	X	
9	M - 16	33.5	14.6	X	
10	N - 16	45.5	19	X	
11	N - 17	55	43	X	
12	Q - 19	50	31	X	
13	S - 20	92	74		X - 24
14	T - 21	72.5	57.5		X - 24
15	U - 22	69	58		X - 24
16	L - 14	55	25		X - 12
17	M - 14	128	107		X - 60
18	N - 14	26	15	X	
19	M - 15	51.5	27.5	X	
20	M - 14	43.5	27.5	X	
21	O - 16	43	28	X	
22	O - 16	49	27	X	
23	P - 17	105	87	X	
24	Q - 17	59	43		X - 24
25	N - 14	58	46	X	
26	N - 15	87	65		X - 24
27	P - 16	97	81		X - 24
27A	O - 15	96	84	X	
28	M - 15	36.5	19	X	
29	M - 15	54.5	33	X	
30	N - 15	61	45	X	
31	V - 24	53.5	35.5		X - 12
32A	R - 20	84	73	X	
32B	U - 23	54.5	25.5	X	
32C	V - 23	43.5	25	X	
33	S - 20	78	78		X - 12
34	T - 22	72	61		X - 24
35	S - 22	92	77		X - 24
36	R - 20	53.5	39	X	
37	Q - 20	67	49		X - 12
38	O - 19	45	26	X	
39	N - 17	29	15	X	

TABLE B3 (Continued)

Station Number	Location Coordinates	Total Thickness (inches)	Total Shale Thickness (inches)	Roof Composition	
				Sandstone	Shale Roof and Estimated Thickness to Sandstone (inches)
40	N - 17	33.5	22	X	
41	J - 16	66.5	40.5	X	
42A	K - 16	50	18	X	
42B	K - 15	48.5	23		X - 8
42C	P - 19	72.5	52.5		X - 12
43	Q - 20	70.5	52.5		X - 12
44	N - 21	69	54		X - 12
45	R - 21	74	62		X - 12
46	Q - 21	38	29	X	
47	Q - 20	71.5	51.5		X - 18
48	P - 18	59.5	23.5	X	
49	S - 21	119.5	104.5		X - 48
50	U - 22	111	95		X -
51	S - 21	85	71		X - 24
52	Q - 21	34	19	X	
53	P - 20	48	35	X	
54	P - 20	82.5	68.5		X - 24
55	M - 18	29.5	17.5	X	
56	M - 18	44	30	X	
57	L - 17	59	39		X - 12
58	U - 15	36	19	X	
59	U - 15	58	35	X	
60	T - 14	44	27	X	
61	S - 13	72.5	54	X	
62A	R - 12	76.5	67.5		X - 60
62B	R - 12	64	52		X - 48
63	Q - 11	75	61		X - 48
64	Q - 11	15	15	X	
65	P - 11	21.5	8.5	X	
66	Q - 1	56	34	X	
67	O - 1	58	42	X	
68	N - 2	48	34	X	
69	M - 2	30	19	X	
70	J - 3	33	18.5	X	
71	L - 4	43	23	X	
72	M - 8	50	29		X
73	M - 8	50.5	32.5	X	
74	J - 7	46.5	30	X	
75	J - 5	30	29	X	
76	H - 3	6	2	X	
77	O - 30	38	32		X - 18
78	P - 31	99	85		X
79	P - 31	94	73		X
80	Q - 32	40	30	X	

TABLE B4. - Underground mapping - checklist

Mapping party _____ Date _____

I. Station (section) location - spad no. ____ pillar no. ___ other___

II. Type of section - roof-fall area____ intersection ____ other _____

III. Floor conditions - flat ____ rolling ____ trends w/entries _____
heaving _____

IV. Estimation of roof strata - immediate _____ main ____
If immediate roof - composition _____ est. thick. to main roof - flat _____ rolling _____

V. Roof conditions - stable ____ sags ____ cutters ____ spalling _____
blocks falling ____ other _____

VI. Rib conditions - stable ____ crushed ____ other _____

A. Composition of Immediate Roof

1. Measured rib section for unit thicknesses and composition. In general, laminated shale, siltstone, claystone, coal/shale rash, coal, etc.

Rib Section

Thickness	Description

2. Secondary Features
   a. Fossils _____
   b. Water Seepage _____
   c. Mineralization _____
   d. Veins/dikes _____
   e. Other _____

B. Structure of Immediate Roof

1. Faults - strike ____ dip ____ stratigraphic displacement hor. ____ vert. ____

2. Coal cleat - Face cleat - strike ____ dip ____ frequency _____
   Butt cleat - strike ____ dip ____ frequency _____

3. Slips - Strike ____ dip ____ frequency ____ continuity _____
   relationship to other structures _____

TABLE B4. - Underground mapping - checklist (continued)

I. Station (section) Location - spad no. ____ pillar no.____ other____

4. Joints - Strike ____ dip ____ frequency ____ continuity _____
relationship to other structures _____

5. Chemical structures - unit ____ ironstone ____ banded _____
nodules ____ concretionary structures ____ other ____

6. Soft-sediment structure - slumping ____ folding ____
load casts ____

C. Composition and Structure - Main Roof

1. Flat or rolling _____ If rolling, est. of relief _____

2. Linear trends? _____ bearing of axes _____
_____

3. Composition _____ Special - lag gravel, etc. _____

4. Bedding characteristics:
a. Plane-beds? Thickness _____
b. Cross-beds? Type _____ strike and dip _____
c. Change in bedding - horizontal (lenses, etc.) _____
d. Change in bedding - vertically (cycles, etc.) _____

5. Linear bedding structure:
a. Plant fossils (logs, carbonized debris) - directional?____
_____ contributes to instability?_____

b. Paleocurrent indicators:
ripple marks _____ flute casts _____ other ____

6. Discontinuities in Main Roof:
Rider seams, joints, veins, etc. Describe.

APPENDIX C

Clay Mineral Preparation Procedures

Several methods of sample preparation were tested and utilized in clay mineral analysis. The laboratory techniques used for each suite of samples, however, were kept constant so that deviations in sample preparation methods would not influence results within a suite.

Separation of the Clay-Sized Fraction

Two methods were used in obtaining the clay-sized fraction from shale samples. The first method consisted of breaking the shale into approximate 1/4-inch square pieces using a hammer, after which the pieces were ground by hand using an iron mortar and pestle. Fifty grams of the sample were then placed in flasks with 500 ml of distilled water and agitated using a wrist-action shaker for two hours. No dispersing agent was used in the process. After shaking, the suspended clays were siphoned and placed in large beakers and/or graduated cylinders and distilled water added to make a total volume of one liter. After mixing, the clay-fractions (<4μm and <2μm) were obtained using settling times according to Stoke's Law. The clay-sized fraction of the suspension was then separated by siphoning the upper 10 cm of the clay-water suspension. The clay suspension was then concentrated by centrifuging at 1000 rpm for 20 minutes and allowed to partly or entirely air dry in evaporating dishes, depending on the mounting procedure to be used.

A second method of clay preparation was used for most of the samples because it required less time and yielded comparable results. In this case, after breaking the shale into 1/4 inch squares 20 grams of chips were dry ground for one minute in a CRC micro-mill grinder. More extensive grinding was avoided because of the danger of damaging the clay minerals (34). The material was then placed in a Hamilton-Beach blender with 500 ml of distilled water and agitated for one minute at low speed. An additional 500 ml of water was then added and blending continued for one minute. The 1000 ml of sediment in distilled water was then transferred to cylinders for gravity separation and centrifuging as in the first method.

Mounting Techniques

Four mounting techniques were investigated including: pipette on glass slide (elutriated), suction on ceramic tile, smear on glass slide and pressed pellet.

1. Pipette on glass slide. The elutriated slides were prepared by placing the clay suspension on frosted glass slides using a pipette and allowing to air dry.

2. Suction on ceramic tile. The tiles were prepared by pipetting the suspensions onto the tiles at about 1 cm depth. The liquid was then drawn through one unglazed tile by vacuum, leaving a smooth clay film on the tile. The tiles were then allowed to air dry.

3. Smear on glass slide. In this technique, the clay suspension was allowed to air dry to a thick paste. The glass slides were first

frosted by grinding with silicon carbide, and a thin, uniform layer of clay was spread onto the slides using one inch wide strips of acetate. The slides were then air dried.

4. Pressed pellet. The clay was prepared for the pressed pellets by grinding and sieving through a 200 mesh (75 micron) sieve. The powdered sample was placed in a 1-3/16 inch diameter aluminum cup (Spex-Cup) and placed in a cylindrical die and pressed at five tons total pressure for five minutes.

A comparison of diffractograms resulting from each of the four mounting techniques indicated very little apparent differences in results. The pressed-pellet technique appeared to give more higher order reflections due to a lesser degree of clay orientation, whereas the elutriated slides enhanced the basal (001) reflections because of preferred orientation of the clays. According to Stokke and Carson (76), the suction on ceramic tile and smear on glass techniques avoid variations in results due to the quantity of sample mounted. While they did not include the pressed-pellet method in their study, that technique would also avoid gravity segregation of clay species. In fact, evaluation of clay minerals observed (chlorite, illite and kaolinite) indicated that segregation effects of species due to gravity settling techniques would not be a serious consideration in this study. As a result of this preliminary study, pressed-pellet and ceramic tile methods were used for identification purposes, whereas smears and elutriation on glass slides were used for clay mineral index studies.

APPENDIX D

Unimodal and Bimodal Programs

The following section describes the general procedures used in unimodal and bimodal analyses of rock jointing, cross-bedding and paleocurrent directional data. The computer programs are written in Fortran IV language for input into an I.B.M. 370 computer, and are filed with the Department of Physical Sciences, Morehead State University.

Description of the Program - Unimodal Output

Ordering of Observations. The program is designed to read a variable number of observations and order these observations from smallest to largest in order to simplify the generation of frequency distributions of sample results for unimodal distributions. For bidirectional data such as rock joints, coal cleats and trough axes, bearings in the northwest quadrant are recorded through the range 0° (north) through -90° (west); whereas bearings in the northeast quadrant are recorded through the range 0° (north) through +90° (east). For 360° data such as cross-bedding, the observations are ordered from 0° through +359°.

Frequency Distribution. Using the ordered observations, a frequency distribution is generated with K, the number of classes, being determined by the following formula:

$$K = 1 + 3.3(N), \text{ where } N \text{ is the sample size.}$$

The starting boundary (left-most or westerly) and ending boundary (right-most or easterly) for each class interval is somewhat arbitrary. In this case, the left-most boundary is 0.5 units less than the smallest (left-most) observation and the right-most boundary is 0.5 units larger than the largest observation. Then, the range of each class interval is given by:

$$\text{(Right-most boundary value--left-most boundary value)} \div K$$

The number of observations or frequency distribution in each class is then recorded.

Test for Uniform Randomness - Class Range. In addition to providing an indication of the distribution of the data, the frequency distribution is used as a basis for testing the uniform randomness of the data within the range in which the data are observed. This test is based on the Chi-square (χ^2) statistic:

$$\chi^2 = \sum_{\substack{\text{all} \\ \text{classes}}} \frac{(\text{observed count} - \text{expected count})^2}{\text{expected count}}$$

with the number of degrees of freedom equal to the number of classes minus one. The expected count per class is given by:

$$\text{Expected count} = \frac{\text{Sample size}}{\text{Number of classes}}$$

Test for Uniform Randomness - 360° and 180° Basis. Next, Tukey's Chi-square is calculated as a means of testing the hypothesis of complete uniform randomness on a 360° basis (37).

Tukey's Chi-square is computed according to the following formulas:

$$C = \frac{\Sigma N \cos \theta_i}{(\Sigma \cos^2 \theta_i)^{1/2}}$$

$$S = \frac{\Sigma N \sin \theta_i}{(\sin^2 \theta_i)^{1/2}}$$

$$N = \frac{n_o - n_e}{n_e}$$

Where θ_i equals the midpoint of the ith interval in degrees.

n_o equals the number of observations per interval.

n_e equals the expected number of observations per interval.

Then

$\chi^2 = C^2 + S^2$ may be viewed as an observation from an approximate Chi-square distribution having 2° of freedom. This result was tested at the .05 level of significance.

For data measured on a 0° to 180° scale, the procedure calls for doubling each θ_i value.

Vector Information

The vector azimuth is calculated using the following formulas:

$$\tan \theta = \frac{\Sigma \sin \theta_i}{\Sigma \cos \theta_i}$$

Where θ equals the azimuth of the vector resultant.

θ_i equals individual observations

If $\Sigma \cos \theta_i < 0$, then θ is replaced with $\theta + 180°$.

The vector magnitude (R) is given by:

$$R = \sqrt{(\Sigma \cos \theta_i)^2 + (\Sigma \sin \theta_i)^2}$$

The calculations for vector magnitude are based on the individual observations and not grouped data.

Raleigh Significance Level. The Raleigh significance level is given by $e^{-R2/n}$, which gives the probability of an R-value this large or larger. The larger the R-value, the more consistent the data. Also, the larger the R-value, the smaller the significance level.

Variance About Azimuth of Vector Resultant. The variance about the azimuth of the vector resultant is computed for two reasons:

1. It provides an indication of the effectiveness of the azimuth as a measure of the center of the data.

2. It provides a basis for comparisons with the mean azimuth having minimum variance.

If θ_i denotes the ith observation and θ^* denotes the azimuth of the vector resultant, then the formula for the associated veriance (Var.) is:

$$\text{Var.} = \frac{\Sigma(\theta_i - \theta^*)^2}{n - 1}$$

The calculating formula is:

$$\text{Var.} = \frac{\Sigma\theta_i^2 - 2\theta^* \Sigma \theta_i + n\,\theta^{*2}}{n - 1}$$

Calculation of the Mean Azimuth. In calculating the mean azimuth, the objective is to determine a mean $\bar{\theta}$ such that the variance (Var.) is minimized:

$$\text{Var.} = \frac{\Sigma(\theta_i - \bar{\theta})^2}{n - 1} \quad \text{or} \quad \frac{n\Sigma\theta_i^2 - (\Sigma\theta_i)^2}{n(n-1)}$$

If the data is bidirectional (0° - 180°) then $\bar{\theta}$ is the usual sample average. However, if the data is azimuthal data (0° - 360°), then $\bar{\theta}$ must be computed using a minimum variance procedure indicated by the following formula:

$$\bar{\theta} = \frac{\Sigma\theta_i}{n} + \frac{360}{n}K$$

$$\text{Where } K = 0, 1, 2\ldots\ldots, n - 1$$

This follows from the fact that θ_i, $\theta_i - 360°$, and $\theta_i + 360°$ each denote the same azimuth. The program is designed to determine the value such that the absolute difference between the angle and $\bar{\theta}$ is minimized. For each angle in which θ_i is not used, $\Sigma\theta_i/n$ is changed by the amount $360°/n$ either clockwise or counter-clockwise. The program allows for K changes when $0 \leq K \leq n-1$. In order to determine the appropriate K, the variance is computed for each value of K. The K value yielding minimum variance is then used to determine $\bar{\theta}$, or the mean azimuth.

Normal Goodness of Fit

The normalty assumption of data is explored using the normal goodness of fit statistic based on intervals of equal probability. The statistic utilizes estimates for the mean ($\bar{\theta}$) and variance (Var.) of the

distribution taken from the mean azimuth procedure section. These values are used to determine approximate intervals of equal probability as follows:

	Intervals
	$\bar{\theta}$ - .967 $\sqrt{\text{Var}}$ or less
	$\bar{\theta}$ - .967 $\sqrt{\text{Var}}$ to $\bar{\theta}$ - .431 $\sqrt{\text{Var}}$
	$\bar{\theta}$ - .431 $\sqrt{\text{Var}}$ to $\bar{\theta}$
	$\bar{\theta}$ to $\bar{\theta}$ + .431 $\sqrt{\text{Var}}$
Where	$\bar{\theta}$ + .431 $\sqrt{\text{Var}}$ to $\bar{\theta}$ + .967 $\sqrt{\text{Var}}$
	$\bar{\theta}$ + .976 $\sqrt{\text{Var}}$ or more

With six classes of equal probability established, the expected number of observations per class interval is determined by:

$$n_e = \frac{\text{Total observation}}{\text{Number of class intervals}}$$

Next the χ^2 (Chi-square) statistic was computed by:

$$\chi^2 = \Sigma \frac{(n_o - n_e)^2}{n_e}$$

The results are then tested using the .05 level of significance.

Description of the Program - Bimodal Output

The bimodal output section of the program is designed to provide a minimum variance solution to the bimodal characterization problem. The procedure provides for optimal splitting of the sample so as to obtain a sample mean for each subsample such that the overall variance is minimized.

The procedure depends upon the specification of the ith and the jth observation between which the sample should be divided. The overall variance is calculated for each sample division point from the ith through the jth observation with the division point being determined when the minimum variation is achieved. The overall variation is defined by the formula:

$$\text{Overall variation} = \Sigma(\theta_i - \overline{\theta}_1)^2 + (\theta_i - \overline{\theta}_2)^2$$

Where θ_i equals individual observations

$\overline{\theta}_1$ and $\overline{\theta}_2$ equals the first and second subsample means.

After the range and means for each subsample has been determined, the variance is computed for each subsample according to methods described for unimodal output.

Strain Model Program

The following describes the general procedures used in the Strain Model Program of rock jointing analysis. The computer programs are written in Fortran IV language for input into an I.B.M. 370 computer, and are filed with the Department of Physical Sciences, Morehead State University.

Description of the Program

The Strain Model Program is designed to analyze joints according to the strain ellipsoid concept. The program is written to analyze joints based essentially on minimum variance criteria and will accommodate the

four models shown in Figure 70, page 148. Similar procedures are used to analyze joints in each of the four models, but major differences may be noted as follows:

Models A and B (Figure 70, page 148) group joints into four sets, whereas models C and D permit a six-set grouping.

In order to test the strain ellipsoid model, several restrictions are placed on the analysis. For models A and B, directions (joint means) 1 and 2 are perpendicular to each other; and for models C and D, directions 1 and 2, 3 and 5, and 4 and 6 are perpendicular.

Finally, models A and C differ from models B and D in that models B and D require angle θ_1 to equal θ_2.

The computer program also permits output for models which are the mirror image of the above models. For example, in models A and B, directions 1 and 3 are westerly and 4 and 2 are easterly. For models C and D, directions 1, 6, and 3 are westerly and 2, 4, and 5 are easterly.

The computer program is designed to provide data analysis following any of the above models using analogous procedures. The following description for model C will illustrate the method.

Direction Designation. The first step in the procedure is to assign directions - i.e. d_1, d_2, d_3, d_4, d_5, and d_6 (Figure 70, page 148).

The direction d_1 is determined at the beginning of the computer run by preliminary analysis of the joint distribution and may be set at any desired bearing. The resulting directions will coincide with joint-set means.

Region Determination. Next, a region (See Figure 70, page 148), for observations associated with each of the six directions is determined as follows:

TABLE D1. - Region Determination

Direction	Region Number	Region
d_1	1	(east) +90° through $\frac{d_1 + d_6}{2}$
d_2	2	$\frac{d_3 + d_2}{2}$ through $\frac{d_2 + d_4}{2}$
d_3	3	$\frac{d_6 + d_3}{2}$ through $\frac{d_3 + d_2}{2}$
d_4	4	$\frac{d_2 + d_4}{2}$ through $\frac{d_4 + d_5}{2}$
d_5	5	$\frac{d_4 + d_5}{2}$ through (west) -90°
d_6	6	$\frac{d_1 + d_6}{2}$ through $\frac{d_6 + d_3}{2}$

Ordering of Observations. In order to effectively analyze the data, the observations are ordered as follows:

$$-90° \text{ (west) } x_1 \leq x_2 \leq x_3 \ldots\ldots x_{n-1} \leq x_n + 90° \text{ (east)}$$

Where: x_1 through x_n are individual observations.

Regional and Overall Variation. Based on the preceding directions, regions and observations the variation for individual regions is computed by:

$$\text{Regional variation} = \sum_{\substack{\text{all obs.} \\ \text{in region}}} (x_i - \text{regional dir.})^2$$

The overall variation is then computed by:

$$\text{Overall variation} = \sum_{\text{reg. 1}} (x_i - d_1)^2 + \sum_{\text{reg. 2}} (x_i - d_2)^2 + \sum_{\text{reg. 3}} (x_i - d_3)^2 + \sum_{\text{reg. 4}} (x_i - d_4)^2 + \sum_{\text{reg. 5}} (x_i - d_5)^2 + \sum_{\text{reg. 6}} (x_i - d_6)^2$$

For each choice of θ_1 and θ_2, the overall variation is computed. If the result is smaller than the previous smallest overall variation, then the overall variation, regional directions, regional variations and sample sizes are saved for subsequent comparisons involving the remaining values of θ_1 and θ_2. After all values of θ_1 and θ_2 have been examined, results for the θ_1 and θ_2 combination having the smallest overall variation are utilized to compute regional and overall variance.

Regional and Overall Variance. The regional variance (Var.) is computed as follows:

$$\text{Regional Var.} = \frac{\text{regional variation}}{n_i}$$

Where n_i is the number of observations found in the region of a joint set.

The overall variance (Var.) is computed by:

$$\text{Overall Var.} = \frac{\text{overall variation}}{n}$$

Where n is the total sample size.

Independent Mean Program

An additional computer program for rock joint analysis was written in Fortran IV language for input into an I.B.M. 370 computer. The program is herein designated the Independent Mean Program or I. M. Program, and is filed with the Department of Physical Sciences, Morehead State University.

Description of the Program

Comparison with the Strain Model. The I. M. Program differs from the preceding strain program in that the joint-set means are established with no angular restrictions. The program can accommodate the establishment of either four or six sets of joints, and in this respect is similar to the four-or six-set Strain Model Program.

Since the six-set and four-set I. M. programs are quite similar, a description of the six-set program will illustrate the procedure.

Region Determination. It is assumed that there are definitely six major directions present in the data. Therefore six regions are

established, each of which contains at least one observation (identical observations are grouped within the same region). The procedure is the same as that used to establish regions in the Strain Model Program (Table D1, page 261).

Ordering of Observations. The sample of size n is ordered as follows:

$$-90^\circ \text{ (west) } x_1 \leq x_2 \leq x_3 \ldots . x_{n-1} \leq x_n + 90^\circ \text{ (east)}$$

Where x_1 through x_n are individual observations.

The objective is to divide the resulting chain of ordered observations in five places so as to obtain six groups, or regions, of data such that the overall variation is minimized.

Regional and Overall Variation. Calculation of the regional variation in each of the six regions is done using the following formula:

$$\text{Regional variation} = (x_i - \bar{x}_i)^2$$

Where: x_i equals the ith region.

$\bar{x}_i$ equals the average direction in region i.

The overall variation is then computed as follows:

$$\text{Overall variation} = \sum_{\text{reg. 1}} (X_i - \bar{X}_1)^2 + \sum_{\text{reg. 2}} (X_i - \bar{X}_2)^2$$

$$+ \sum_{\text{reg. 3}} (X_i - \bar{X}_3)^2 + \sum_{\text{reg. 4}} (X_i - \bar{X}_4)^2 + \sum_{\text{reg. 5}} (X_i - \bar{X}_5)^2 + \sum_{\text{reg. 6}} (X_i - \bar{X}_6)^2$$

Where X_i equals the ith observation within the region.

$\bar{X}_j$ equals the average direction (in region j).

The computation of the overall variation is made more efficient by the fact that:

$$\text{Overall variation} = \Sigma X_i^2 - \frac{(\Sigma X_i)^2}{\underset{1}{\text{reg.}}\ n_i} + \frac{(\Sigma X_i)^2}{\underset{2}{\text{reg.}}\ n_2}$$

$$+ \frac{(\Sigma X_i)^2}{\underset{3}{\text{reg.}}\ n_3} + \frac{(\Sigma X_i)^2}{\underset{4}{\text{reg.}}\ n_4} + \frac{(\Sigma X_i)^2}{\underset{5}{\text{reg.}}\ n_5} + \frac{(\Sigma X_i)^2}{\underset{6}{\text{reg.}}\ n_6}$$

Since ΣX_i^2 is constant for a given sample, the problem is to determine the region so as to maximize the second part.

Partitioning of Data. The program then examines each possible partition involving six occupied regions (with identical observations belonging in the same region) and selects the partition having the smallest overall variation. As each partition is examined the information associated with the smallest overall variation, which includes the overall variation and the regional sample size, is used.

Regional and Overall Variance. After the examination of all possible partitions is complete, the results associated with the "best" partition are used to calculate variance (Var.) as follows:

$$\text{Regional Var.} = \frac{\text{regional variation}}{n_i}$$

Where: n_i equals the total observations within the region.

The overall variance (Var.) is computed by:

$$\text{Overall Var.} = \frac{\text{overall variation}}{n}$$

Where: n equals the total observations.

Generation of Simulated Data

According to the procedure described by Chen (13), a set of simulated data was generated using the I. B. M. 370 computer at the University of Kentucky. The Simulated Data Program was written by Dr. David Muse in Fortran IV language with the following objectives:

1. First, to generate an "ideal" set of linear data with controlled variances that increase at predetermined values around established means according to a 6-mode set.

2. Using the generated data, it was then possible to provide "ideal" data input for all computer programs used in this study. These programs include the 4-mode and 6-mode Independent Mean Programs, and 4-mode and 6-mode Strain Programs.

By an analysis of results obtained from the simulated data by each of the computer programs, it was possible to compare the following:

1. The comparison between means and variances determined by the 6-mode Independent Mean Program and 6-mode Strain Program.

2. A comparison between results obtained by analyzing a known 6-mode data set using both the 4-mode I. M. Program and 4-mode Strain Program.

Description of the Program

Assumptions. Several assumptions were made in the generation of simulated data as follows:

1. For each direction of the 6-model, the observations about this direction were normally distributed with an assumed mean direction and an assumed variance.

2. The assumed mean directions were N70°E, N30°E, N20°E, N20°W, N60°W, and N70°W. These assumed mean directions are designed to simulate means for the following system of orthogonal joint sets: N70°E - N20°W, N30°E - N60°W, and N20°E - N70°W.

3. The variances associated with the distribution for each direction was assumed to be the same. Data sets were generated for each of the following variances: 1, 2, 4, 8, 16, 32, and 64.

4. Data sets generated were of sample size 54 with nine observations per direction.

Possible Modifications. The program was designed to be generally applicable under the assumptions listed above. However, it could be easily modified to generate any number of observations if desired. Also, the program permits the introduction of 6-mode sets in any desired direction within the -90°(west) to +90°(east) range, together with any desired variance for the 6-mode program.

Generation of the Data. According to the procedure proposed by Chen (13), the following series of formulas may be used to generate

the ith pair of random numbers (R_{xi}) from (i-1)th pair of random numbers:

1. In order to minimize serial correlation, the following dual type of generator was used to produce random numbers for sequence.

$$R_{1,i} = R_{1,i-1}\,(2^{P1} + 3) \quad (\text{modulo } 2^{31}) \qquad \ldots\ldots 1$$

$$R_{2,i} = R_{2,i-1}\,(2^{P2} + 3) \quad (\text{modulo } 2^{31})$$

Where P is a positive integer greater than 2 and less than 31 and R_o, the starting number, is a randomly chosen odd integer. If either $R_{1,i}$ is negative the result is made positive by adding $(2^{31} + 1)$.

2. The production of independent standard uniform numbers ($U_{1,i}$, $U_{2,i}$) then utilized the formulas:

$$U_{1,i} = R_{1,i}/(2^{31} - 1)$$

$$U_{2,i} = R_{2,i}/(2^{31} - 1)$$

3. Finally, two independent standard normal numbers ($X_{1,i}$, $X_{2,i}$) were derived from:

$$X_{1,i} = (-2 \log_e U_{1,i})\,(\cos\,(2\,U_{2,i}))$$

$$X_{2,i} = (-2 \log_e U_{1,i})\,(\sin\,(2\,U_{2,i}))$$

Observations for the 6-mode program were then produced by transformation:

$$d_{1,i} = (\text{mean direction} + X_{1,i} \text{ (variance)}$$

and

$$d_{2,i} = (\text{next mean direction}) + X_{2,i} \text{ (variance)}$$

For a given 6-mode sample, the following values of $d_{1,i}$ were used:

+70°	+30°	+20°	-20°	-60°	-70°
$d_{1,1}$	$d_{2,1}$	$d_{1,2}$	$d_{2,2}$	$d_{1,3}$	$d_{2,3}$
$d_{1,4}$	$d_{2,4}$	$d_{1,5}$	$d_{2,5}$	$d_{1,6}$	$d_{2,6}$
$d_{1,7}$	$d_{2,7}$	$d_{1,8}$	$d_{2,8}$	$d_{1,9}$	$d_{2,9}$, etc.

After each pair of values ($d_{1,i}$, $d_{2,i}$) was generated, the $R_{1,i}$, $R_{2,i}$ values previously generated were used to repeat the process with formula set 1 to generate additional values.

VITA

David Kent Hylbert was born in Fayetteville, West Virginia in 1938. He attended elementary schools in Zanesville, Ohio and was graduated from Zanesville High School in 1956. The following September he entered Ohio University and was graduated in 1960 with a Bachelor of Science degree in Geology. In 1961 he accepted a teaching assistantship at Ohio University and received a Master of Science degree in Geology in 1968. He has been employed by the Geoscience Department, Morehead State University, Morehead, Kentucky, since 1963.

In September, 1969 he took a two-year leave of absence from Morehead State University and entered the Graduate School at the University of Tennessee. He completed the course work for the Doctorate in Geology in 1971.

He is a member of the American Mineralogical Society, Society of Economic Paleontologists and Mineralogists, Sigma Xi, Geological Society of Kentucky and Kentucky Academy of Science.

He is married to the former Shirley Ann Shrigley of Zanesville, Ohio.